

Bangor University

DOCTOR OF PHILOSOPHY

Characterisation of a novel role for the cancer-associated protein Translin in the regulation of genome stability

Althagafi, Hussam

Award date:
2020

Awarding institution:
Bangor University

[Link to publication](#)

General rights

Copyright and moral rights for the publications made accessible in the public portal are retained by the authors and/or other copyright owners and it is a condition of accessing publications that users recognise and abide by the legal requirements associated with these rights.

- Users may download and print one copy of any publication from the public portal for the purpose of private study or research.
- You may not further distribute the material or use it for any profit-making activity or commercial gain
- You may freely distribute the URL identifying the publication in the public portal ?

Take down policy

If you believe that this document breaches copyright please contact us providing details, and we will remove access to the work immediately and investigate your claim.

P R I F Y S G O L
BANGOR
U N I V E R S I T Y



**Characterisation of a novel role for the cancer-associated protein
Translin in the regulation of genome stability**

Hussam Awwadh Eidh Althagafi

Banner ID/ 500332662

School of Biological Science

University of Bangor

United Kingdom

July, 2020

Declaration and Consent

Details of the Work

I hereby agree to deposit the following item in the digital repository maintained by Bangor University and/or in any other repository authorized for use by Bangor University.

Author Name:

.....

Title:

Supervisor/Department:

Funding body (if any):

Qualification/Degree obtained:

This item is a product of my own research endeavours and is covered by the agreement below in which the item is referred to as “the Work”. It is identical in content to that deposited in the Library, subject to point 4 below.

Non-exclusive Rights

Rights granted to the digital repository through this agreement are entirely non-exclusive. I am free to publish the Work in its present version or future versions elsewhere.

I agree that Bangor University may electronically store, copy or translate the Work to any approved medium or format for the purpose of future preservation and accessibility. Bangor University is not under any obligation to reproduce or display the Work in the same formats or resolutions in which it was originally deposited.

Bangor University Digital Repository

I understand that work deposited in the digital repository will be accessible to a wide variety of people and institutions, including automated agents and search engines via the World Wide Web.

I understand that once the Work is deposited, the item and its metadata may be incorporated into public access catalogues or services, national databases of electronic theses and Dissertations such as the British Library’s EThOS or any service provided by the National Library of Wales.

I understand that the Work may be made available via the National Library of Wales Online Electronic Theses Service under the declared terms and conditions of use (<http://www.llgc.org.uk/index.php?id=4676>). I agree that as part of this service the National

Library of Wales may electronically store, copy or convert the Work to any approved medium or format for the purpose of future preservation and accessibility. The National Library of Wales is not under any obligation to reproduce or display the Work in the same formats or resolutions in which it was originally deposited

Statement 1:

This work has not previously been accepted in substance for any degree and is not being concurrently submitted in candidature for any degree unless as agreed by the University for approved dual awards.

Signed (candidate)

Date

Statement 2:

This thesis is the result of my own investigations, except where otherwise stated. Where correction services have been used, the extent and nature of the correction is clearly marked in a footnote(s).

All other sources are acknowledged by footnotes and/or a bibliography.

Signed (candidate)

Date

Statement 3:

I hereby give consent for my thesis, if accepted, to be available for photocopying, for inter-library loan and for electronic storage (subject to any constraints as defined in statement 4), and for the title and summary to be made available to outside organisations.

Signed (candidate)

Date

NB: Candidates on whose behalf a bar on access has been approved by the Academic Registry should use the following version of **Statement 3:**

Statement 3 (bar):

I hereby give consent for my thesis, if accepted, to be available for photocopying, for inter-library loans and for electronic storage (subject to any constraints as defined in statement 4), after expiry of a bar on access.

Signed (candidate)

Date

Statement 4:

Choose **one** of the following options

a)	I agree to deposit an electronic copy of my thesis (the Work) in the Bangor University (BU) Institutional Digital Repository, the British Library ETHOS system, and/or in any other repository authorized for use by Bangor University and where necessary have gained the Required permissions for the use of third party material.	
b)	I agree to deposit an electronic copy of my thesis (the Work) in the Bangor University (BU) Institutional Digital Repository, the British Library ETHOS system, and/or in any other repository authorized for use by Bangor University when the approved bar on access has been lifted.	
c)	I agree to submit my thesis (the Work) electronically via Bangor University's e-submission system, however I opt-out of the electronic deposit to the Bangor University (BU) Institutional Digital Repository, the British Library ETHOS system, and/or in any other Repository authorized for use by Bangor University, due to lack of permissions for use of third party material.	

In addition to the above I also agree to the following:

1. That I am the author or have the authority of the author(s) to make this agreement and do hereby give Bangor University the right to make available the Work in the way described above.
2. That the electronic copy of the Work deposited in the digital repository and covered by this agreement, is identical in content to the paper copy of the Work deposited in the Bangor University Library, subject to point 4 below.
3. That I have exercised reasonable care to ensure that the Work is original and, to the best of my knowledge, does not breach any laws – including those relating to defamation, libel and copyright.
4. That I have, in instances where the intellectual property of other authors or copyright holders is included in the Work, and where appropriate, gained explicit permission for the inclusion of that material in the Work, and in the electronic form of the Work as accessed through the open access digital repository, *or* that I have identified and removed that material for which adequate and appropriate permission has not been obtained and which will be inaccessible via the digital repository.
5. That Bangor University does not hold any obligation to take legal action on behalf of the Depositor, or other rights holders, in the event of a breach of intellectual property rights, or any other right, in the material deposited.
6. That I will indemnify and keep indemnified Bangor University and the National Library of Wales from and against any loss, liability, claim or damage, including without limitation any related legal fees and court costs (on a full indemnity bases), related to any breach by myself of any term of this agreement.

Signature: Date:

Abstract

Translin and Trax are a pair of highly conserved proteins that are functionally linked with each other. They are nucleic acid binding proteins associated with in chromosome translocations in cancers. They have subsequently been demonstrated to function in a broad spectrum of biological process, including tRNA processing, mRNA regulation in neuronal cells, spermatogenesis function and in microRNA degradation in oncogenesis, the latter leading to the suggestion that they might be a drug target for a number of cancers. Given this, and the proposal that Translin is associated with the DNA damage response, set out to address whether Translin and/or Trax have a functional role in preserving genome stability. In this study, the biological role of Translin and Trax was explored using the facile experimental model system, *Schizosaccharomyces pombe*. A previous study had shown that both Tsn1 (Translin) and Tfx1 (Trax) did not exhibit any significant function role in *S. pombe*. Recently, a Translin-Trax hetero-octamer complex (C3PO) has been found to be essential in the regulation of RNA interference (RNAi). Additionally, the RNAi component Dicer (Dcr1) has been demonstrated to function in an RNAi-independent role to prevent genome instability. In order to ask whether Tsn1 and/or Tfx1 have redundant role with Dcr1, *tsn1* Δ , *tfx1* Δ and *dcr1* Δ single and double mutants were generated and assessed for genome stability phenotypes. We find that Tsn1, but not Tfx1, plays a redundant role in controlling genome stability in the absence of Dcr1. We propose that in the absence of Dcr1, Tsn1 acts by suppressing the transcription-DNA replication-associated recombination. Given that Dcr1 has been proposed to regulate and maintain genome stability, we extend this investigation to assess if Tsn1 and/or Tfx1 have primary roles associated with the RNases H activity. This study indicates that Tsn1 functions in one of two pathway RNase H pathways. Taken together, the data represented here demonstrate a new role for Tsn1 in maintain genome stability in a pathway could be associated with RNA:DNA hybrids control so, more invistagations are required to prove that. These data offer the basis for understanding how Translin might influence oncogenic chromosomes translocations, addressing a long-standing question in chromosome biology.

Acknowledgment



In the name of Allah (God), the Most Beneficial, the Most Merciful All praise and thanks are only for Allah Almighty, through whom perfected goodness / good works are achieved by His grace and favour. The encouragement and power which God has given me is the secret behind the completion of my life project (Ph.D.). Upon the support and help of God. I appreciate profoundly the support and patience of those whose names may not all be mentioned, enabling my vision to become real.

When I start writing my PhD thesis, I really faced extremely academic challenges. I have believe that I would not be able to do all this hard work without the support, guidance and diligence of following individuals. I am so happy and grateful to have this kind of people in my life.

I would like to show appreciation my supervisor, Dr Ramsay McFarlane, who offered his valuable experience, understanding and patience which added substantially to my graduate knowledge. I am in appreciation of the immense knowledge and skills that he has in various fields (e.g. vision and ethics). His experience, wisdom and commitment empowered and encouraged me greatly.

I wish as well to express thanks to Dr Natalia Gomez-Escobar for her support during the different stages of the research project and for her assistance in writing the thesis.

I would also like to take this opportunity to thank Dr David Pryce of the Biological and Molecular Biology with Genetics Department for making important suggestions and giving the text resources examined in this study.

My parent efforts have also been very important. First of all, my dad, Awwadh was the one who established my habit of learning and instilled the love of education into me from my childhood days. My mom who showed great care and love throughout my childhood. My parents made numerous sacrifices for me and gave unrestrained love and care. I have a lot of affection for them, and know that without their support it would not be possible to achieve this aim. I consider them

as my best friends and I love them very much. I wish to express to them my deepest gratitude for their unwavering support and guidance. While I was away, I am thankful for their support, prayers and wishes for me.

It is important to mention my lovely wife Rawiyah, whose guidance, reassurance, unwavering compassion and devotion played an important role in helping me to get through these difficult times. Without her help, I couldn't have completed this work and achieved my dreams. Moreover, I can't forget to share my sincere gratitude to my gorgeous children, Tameem and Ameer for sticking together and loving me throughout the most difficult time of my life.

Moreover, I wish to thank my brothers and sisters who encouraged me in all my efforts and inspired me to follow my dreams. My family always receives extra gratitude for giving me financial and emotional support. I was always mindful that they trusted in my talents, and wished me the best. I am deeply grateful to them for communicating to me that my goal in life should be to continue learning, to be content, to know myself better and to accept myself. I would only be able to get to know and appreciate other individuals as I learned to do so.

Last but not least, I would appreciate to extend my honest acknowledgment to a few special people. I am unable to fully express my gratitude for Fahad Alharthi who gave me a huge amount of support, genuine treatment and a feeling of being at home in Bangor. He was with me at all times, during happy and hard times, where his motivation and encouragement was precious. Because of his support and suggestions on organising the entire thesis my research was able to take up the current structure. One's journey becomes easier when you have the right friendship. I believe that interdependence is certainly more worthwhile as compared to independence. Furthermore I want to show my honest thanks to Mohammad Althagafi, Fahad Algahtani Ahmad Althomali and Sulaiman who stick up with me at all times.

It doesn't seem adequate to just say thank you, but I do this with great gratitude and respect to all of your support, inspiration too.

List of Abbreviations

3': Three prime end of DNA.

5': Five prime end of DNA.

ATM: Ataxia telangiectasia mutated.

ATP : Adenosine Triphosphate

BDNF: Brain-derived neurotrophic factor.

BIR: break-induced replication.

bp: base pair.

cDNA: complementary DNA.

CDGS: Chromatin-dependent gene silencing.

CDKs: cyclin-dependent kinases.

CLRC: cryptic loci regulator complex.

Clr4: Histone methyltransferase

CML: -chronic myelogenous leukaemia.

cnt: central core

CPT: camptothecin.

C3PO: component 3 promoter of RISC.

DAPI: 4', 6-diaminino-2-phenylindole.

DDK: Cdc7-Dbf4 kinases.

DDR: DNA damage responses.

dH₂O: Distilled water.

dHJ: double Holliday junction.

D-loop: Displacement loop.

DMSO: Dimethyl sulphoxide.

DNA: Deoxyribonucleic acid.

DNA-PK: DNA-dependent protein kinase.

dNTP: deoxyribonucleotide triphosphate.

DRIP: DNA: RNA immunoprecipitation.

dsDNA: double-stranded DNA.

dsRNA: double-stranded RNA.

DSBs: double strand breaks.

DSBR: double strand break repair.

g: Gram.

GADD: growth arrest and DNA damage.

EDTA: ethylenediamine tetraacetic acid.

FL: follicular lymphoma.

FPC: fork protection complex

HP1: heterochromatin protein 1.

HDAC: histone deacetylase.

HJ: Holliday junction.

HR: homologous recombination.

IR: ionizing radiation.

kb: kilobase.

kDa: kilo Dalton.

L: Litre.

LB: Luria-Bertani media.

LiAC: Lithium acetate.

LOH: loss of heterozygosity

MCM: mini chromosome maintenance.

MEFs: mice embryotic fibroblasts.

MMC: mitomycin C.

MMS: methyl methane sulfonate.

MRN: MRE11-RAD50-NBS1 complex.

mg: Milligram.

miRNA: micro-RNAs.

µg: Microgram.

µl: Microliter.

ml: Millilitre.

mM: Millimolar.

mRNA: messenger RNA.

NB: nitrogen base.

NBL: nitrogen base liquid.

NE: nuclear envelope.

NHEJ: non-homologous end joining.

ng: Nanogram.

NLS: nuclear localization signal.

ORF: open reading frame.

PCNA: proliferating cell nuclear antigen.

PCR: polymerase chain reaction.

pmol: picomole.

PEG: polyethylene glycol.

RC: replicative complex.

rDNA: ribosomal DNA.

RDRP: RNA-dependent RNA polymerase.

PTGS: post-transcriptional gene silencing.

piRNA: PIWI-interaction RNAs.

RFB: replication fork barriers.

RFC: replication factor clamp loader.

rDNA: ribosomal DNA.

RISC: RNA-induced silencing complex.

RITSC: RNAi-induced transcriptional silencing complex.

RLC: RISC loading complex.

RER : ribonucleotide excision repair

RNA Ribonucleic acid.

RNAi: RNA interference.

RNase P : ribonuclease P

RT-PCR: Reverse transcriptase PCR.

q-RT-PCR: Quantitative real-time PCR.

RPA: replication protein A.

rNMPs: ribonucleotide monophosphate

RNA Pol: RNA polymerase.

SDS: Sodium Dodecyl Sulfate.

SDSA: synthesis-dependent strand annealing.

siRNA: small interference RNA.

ssDNA: Single-stranded DNA.

TB-BPB: testis-brain RNA-binding protein.

TCA: Trichloroacetic acid

TGS: transcriptional gene silencing.

TK: tyrosine kinase.

TFs: transcription factors.

TRAX: Translin-associated factor X.

TRC: transcription-replication conflicts

tRNA: transfer RNA.

TBZ: thiabendazole.

UTR: untranslated region.

UV: ultra-violet.

V(D)J: variable (V), diversity (D) and joining (J) coding segments.

YE: yeast extract.

YEA: yeast extract agar.

YEL: yeast extract liquid.

Table of Contents

Declaration and Consent	II
Abstract	V
Acknowledgment	VI
List of Abbreviations	VIII
Table of contents	XIII
List of Figures	XVII
List of Tables	XXI
Chapter 1: Introduction	1
1.1 Types of DNA damage	
1.2 DNA repair	
1.3 Gnomonic instability	
1.4 DNA Replication	6
1.5 Replication fork progression	10
1.6 The DNA double-strand break (DSB) repair pathways	14
1.6.1 The non-homologous DNA end- joining (NHEJ) repair pathway	15
1.6.2 The homologues recombination repair pathway	17
1.7 The Chromosomal translocations	21
1.8 Replication fork barriers and recombination	24
1.9 Role of Dicer in controlling genome stability	26
1.10 RNA-DNA hybrids (R-loops)	27
1.11 RNA interference (RNAi)	31
1.12 Translin and Trax	35
1.13 Biochemical Characteristics of Translin and TRAX	36
1.14 Translin and Trax: RNAi interference	40
1.15 Evidence roles of Translin and Trax in DNA Repair	42
1.16 The Role of Translin and Trax in Oncogenesis	43

1.17	<i>S. pombe</i> as a model organism for this project	45
1.18	Aims of this Study	45
Chapter 2: Materials and Methods		46
2.1	Media and strains utilized in this project.	47
2.2	Plasmid extraction procedure from <i>E. coli</i> .	47
2.3	<i>S. pombe</i> gene deletions	49
2.4	Phenol/Chloroform purification of <i>S. pombe</i> genomic DNA.	58
2.5	Transformation of <i>S. pombe</i> by using lithium acetate (LiAC).	58
2.5.1	Transformation of <i>S. pombe</i> strains using a DNA knockout cassette.	58
2.5.2	Transformation of plasmid.	59
2.6	<i>S. pombe</i> Genomic DNA Extraction.	59
2.7	Confirmation of successfully gene deletion by PCR screening.	60
2.8	Drop Tests for Drug Sensitivity.	62
2.9	Storage of <i>S. pombe</i> Strains.	65
2.10	Ultraviolet (UV) irradiation of <i>S. pombe</i> .	65
2.11	Yeast meiotic crosses.	66
2.12	Whole-cell protein extraction <i>S. pombe</i> .	66
2.13	Western blotting for <i>S. pombe</i> .	67
2.14	Determination of Recombination Frequency (Fluctuation test):	68
Chapter 3: Results		69
3.1	Introduction	70
3.2	Results	72
3.2.1	<i>tfx1Δ</i> mutation suppresses the <i>ago1Δ</i> chromosomal phenotypic instability in a <i>tsn1</i> -dependent fashion	Error! Bookmark not defined.
3.2.2	Spot Test for TBZ sensitivity	Error! Bookmark not defined.
3.2.3	Colony growth assay	Error! Bookmark not defined.
3.2.4	Construction of relevant mutant strains	72
3.2.5	Spot Assay of TBZ sensitivity for <i>dcr1Δ tfx1Δ</i> and <i>dcr1Δ tsn1Δ</i> .	81

3.2.6 Determination of <i>tfx1</i> Δ and <i>tsn1</i> Δ mutant responses to DNA damage in Dcr1 absence	82
3.3 Discussion	90
3.3.1 Mutation of <i>tfx1</i> Δ suppresses the chromosome instability of the <i>ago1</i> Δ mutant.	90
3.3.2 Loss of Tsn1 Increases Chromosome Instability in a <i>dcr1</i> Δ background	91
3.3.3 Tsn1, but not Tfx1, is required in the DNA damage response of Dcr1-Defective Cells	92
Chapter 4: Results	94
4.1 Introduction	95
4.1.1 The genetic test summary used in this study	96
4.2 Results	98
4.2.1. Construction of <i>tsn1</i> Δ , <i>dcr1</i> Δ single mutants and <i>tsn1</i> Δ <i>dcr1</i> Δ double mutants	98
4.2.2. Sensitivity assay of TBZ and DNA damaging agent for <i>tsn1</i> Δ , <i>dcr1</i> Δ single mutant and <i>tsn1</i> Δ <i>dcr1</i> Δ double mutants.	103
4.2.3. Recombination frequency analysis for the <i>tsn1</i> Δ , <i>dcr1</i> Δ single mutants and the <i>tsn1</i> Δ <i>dcr1</i> Δ double mutants at tRNA genes.	107
4.2.4. Construction of <i>tfx1</i> , <i>dcr1</i> single mutants and <i>tfx1</i> <i>dcr1</i> double mutants.	109
4.2.5. Sensitivity assay of TBZ and DNA damaging agent for <i>tfx1</i> Δ , <i>dcr1</i> Δ single mutant and <i>dcr1</i> Δ <i>tfx1</i> Δ double mutants.	112
4.2.6. Recombination frequencies analysis for the <i>tfx1</i> Δ , <i>dcr1</i> Δ single mutants and the <i>tfx1</i> Δ <i>dcr1</i> Δ double mutants at tRNA genes.	116
4.3 Discussion	119
4.3.1 Tsn1, but not Tfx1, suppress recombination in the absence of Dcr1	119
Chapter 5: Results	123
5.1 Introduction	124
5.1.2 An overview of the induction of using 1-PpoII in specific DSB system.	126
5.2 Results	128
5.2.1 Construction of <i>tsn1</i> Δ and <i>tfx1</i> Δ single mutants in the I-PpoI background.	128

5.2.2. Sensitivity assay of DNA damaging agent for <i>tsn1Δ</i> and <i>tfx1Δ</i> single mutants in the I-PpoI background.	131
5.2.2 Analysis of I-PpoI induction.	135
5.2.3 RNase H activity, but not Tsn1 or Tfx1 are needed for DSB repair.	140
5.3 Discussion	145
Chapter 6: Results	147
6.1 Introduction	148
6.2 Results	150
6.2.1 Determination of <i>tsn1Δ</i> mutant responses to DNA damage in absence of RNase H activity.	150
6.2.2 Determination of <i>tfx1Δ</i> mutant responses to DNA damage in absence of RNase H activity	153
6.3 Discussion	162
Chapter 7: Final Discussion	164
7.1 Introduction	165
7.2 Tsn1, but not Tfx1, suppress recombination in the Dcr1 deficient.	167
7.3 Tsn1, but not Tfx1, functions in the RNases H pathways	169
7.4 Closing remarks	170
8. References:	172

List of Figures

Figure 1.1 Genome Instability: Pathway to Disease	4
Figure 1.2 Mechanistic Diagram depicting the Early Stages of the DNA Replication Process in an Eukaryotic Cell	5
Figure 1.3 Schematic of a DNA replication fork	8
Figure 1.4 The basic graphic of eukaryotic replisome complex	9
Figure 1.5 summary of the NHEJ repair mechanism.....	12
Figure 1.6 Graphic models of the Homologous Recombination (HR) pathways	16
Figure 1.7 Schematic showing examples of chromosome rearrangement (including translocation) and their consequences	19
Figure 1.8 <i>S. pombe</i> approach resolving the transcription/replication-collision to protect integrity of the genome	24
Figure 1.9 R-loop structure	26
Figure 1.10 RNAi model for Heterochromatin assembly at the <i>S. pombe</i> centromere.	30
Figure 1.11 Diagram showing the role of the Translin and Trax (C3PO) in <i>Drosophila</i> . RNAi pathway.	36
Figure 1.12 Complex of Translin and Trax (TN/TX), a possible therapy-target for Dicer-deficient tumours	39
Figure 2.1 Design order of a square Petri dish for spot essay.....	58
Figure 3.2 Extent of <i>ago1Δ</i> growth is more increased by <i>tfx1Δ</i> mutant	68
Figure 3.3 Illustration of target gene knockout process.....	70
Figure 3.4 Description of the position of primers in confirming the appropriate deletion of the interest gene	71
Figure 3.5 PCR screening for the efficient construction of <i>tfx1Δ</i> mutant.....	72
Figure 3.6 PCR screening for the efficient construction of <i>tsn1Δ</i> mutant	73
Figure 3.7 PCR screening for the efficient construction of <i>dcr1Δ</i> mutants	74
Figure 3.8 PCR screening for the efficient construction of <i>dcr1Δ tfx1Δ</i> mutants.....	75
Figure 3.9 PCR screening for the efficient construction of <i>dcr1Δ tsn1Δ</i> candidates.....	76
Figure 3.10 Single <i>tsn1Δ</i> , but not <i>tfx1Δ</i> , mutations increase TBZ sensitivity in <i>dcr1Δ</i> mutations.....	77
Figure 3.11 <i>tsn1Δ</i> Mutation but not <i>tfx1Δ</i> in the <i>dcr1Δ</i> Background increased phleomycin sensitivity.	79

Figure 3.12 <i>tsn1Δ</i> Mutation but not <i>tfx1Δ</i> in the <i>dcr1Δ</i> background increased belomycin sensitivity.	80
Figure 3.13 Mutation of <i>dcr1Δ tsn1Δ</i> , but not <i>tfx1Δ dcr1Δ</i> is more sensitive to hydroxyurea (HU) sensitivity.	81
Figure 3.14 The <i>dcr1Δ tsn1Δ</i> double mutant, but not <i>dcr1Δ tfx1Δ</i> , is enhanced sensitive to ultraviolet (UV).	82
Figure 3.15 Sensitivity spot test of Camptothecin (CPT) for several of <i>S. pombe</i> strains.	83
Figure 3.16 Sensitivity spot test of Methyl methane sulfonate (MMS) for several of <i>S. pombe</i> mutants.	84
Figure 3.17 Sensitivity spot test of Mitomycin C (MMC) for several of <i>S. pombe</i> mutants.	85
Figure 4.1 Graphic model of the recombination system utilized for plasmid-by-chromosome to determine the frequency of a recombination at <i>ade6::tRNA^{GLU}</i>	93
Figure 4.2 PCR screening for the efficient construction of <i>tsn1Δ</i> mutants.	95
Figure 4.3 PCR screening for the efficient construction of <i>dcr1Δ</i> mutants.	96
Figure 4.4 PCR screening for the efficient construction of <i>dcr1Δ</i> mutants.	97
Figure 4.5 PCR screening for the efficient construction of <i>dcr1Δ tsn1Δ</i> mutant.	98
Figure 4.6 Spot essay of TBZ sensitivity that confirms that <i>dcr1Δ tsn1Δ</i> double mutant is hypersensitivity in both <i>tRNA^{GLU}</i> orientations (1 and 2).	100
Figure 4.7 Spot essay of Phleomycin sensitivity that confirms that the <i>dcr1Δ tsn1Δ</i> cells are enhanced sensitivity.	101
Figure 4.8 Spot assay of HU sensitivity spot assay that confirms the <i>dcr1Δ tsn1Δ</i> double mutants are hypersensitivity.	102
Figure 4.9 Recombination test for the <i>ade6::tRNA^{GLU}</i> –orientation 1 strains.	104
Figure 4.10 Recombination test for the <i>ade6::tRNA^{GLU}</i> –orientation 2 strains.	105
Figure 4.11 PCR screening for the efficient construction of <i>tfx1Δ</i> mutant. A.	107
Figure 4.12 PCR screening for the efficient construction of <i>dcr1Δ tfx1Δ</i> mutants.	108
Figure 4.13 Mutation of <i>dcr1Δ</i> produces in equal suppression of <i>dcr1Δ tfx1Δ</i> double mutant of TBZ sensitivity in both <i>tRNA^{GLU}</i> orientations.	110
Figure 4.14 Mutation of <i>dcr1Δ tfx1Δ</i> genes in both <i>tRNA^{GLU}</i> orientations results in phelomycin sensitivity to have the same levels observed in the <i>dcr1Δ</i> single mutant.	111
Figure 4.15 Mutation of the <i>dcr1Δ</i> results in a similar suppression of <i>dcr1Δ tfx1Δ</i> double mutant of HU sensitivity in both <i>tRNA^{GLU}</i> orientations.	112
Figure 4.16 Recombination test for the <i>ade6::tRNA^{GLU}</i> –orientation 1 strains.	114

Figure 4.17 Recombination test for the <i>ade6::tRNA^{GLU}</i> –orientation 2 strains.	115
Figure 5.1 Schematic diagram depicting the I-PpoI cleavage sites within the <i>S. pombe</i> genome indicated by the red lines.....	124
Figure 5.2 PCR screening for the efficient construction of <i>tsn1Δ</i> mutants in I-PpoI background. A.....	126
Figure 5.3 PCR screening for the efficient construction of <i>tfx1Δ</i> mutant mutants in I-PpoI background. A.....	127
Figure 5.4 Mutation of <i>tsn1Δ</i> and <i>tfx1Δ</i> genes in both BP90 and I-PpoI backgrounds results in phelomycin sensitivity similar the WT.	129
Figure 5.5 Mutation of <i>tsn1Δ</i> and <i>tfx1Δ</i> genes in both BP90 and I-PpoI backgrounds results distinct to belomycin response.....	130
Figure 5.6 Mutation of the <i>tsn1Δ</i> and <i>tfx1Δ</i> result in a similar response to HU in both BP90 and I-PpoI backgrounds.	131
Figure 5.7 Western blotting showing the detection of I-PpoI protein levels in WT.....	133
Figure 5.8 Western blotting showing the detection of I-PpoI protein levels in <i>rnh1Δ rnh201Δ</i>	134
Figure 5.9 Western blotting showing the detection of I-PpoI protein levels in <i>tsn1Δ</i>	135
Figure 5.10 Western blotting showing the detection of I-PpoI protein levels in <i>tfx1Δ</i>	136
Figure 5.11 Bar graph showing qPCR analysis of the break site in the WT strain.	138
Figure 5.12 Bar graph showing qPCR analysis at the break site in the <i>rnh1Δ rnh201Δ</i> double mutant strain.....	139
Figure 5.13 Bar graph showing qPCR analysis of the break site in the <i>tsn1Δ</i> single mutant strain.....	140
Figure 5.14 Bar graph showing qPCR analysis of the break site in the <i>tfx1Δ</i> single mutant strain.....	141
Figure 6. 1 The <i>tsn1Δ rnh201Δ</i> mutant showed mild, elevated sensitivity to Phleomycin.	148
Figure 6.2 The <i>tsn1Δ rnh201Δ</i> mutant exhibits hypersensitivity to hydroxyurea (HU) sensitivity	149
Figure 6.3 Sensitivity spot test of ultraviolet (UV) for several of <i>S. pombe</i> mutants.....	150
Figure 6.4 The <i>tsn1Δ rnh201Δ</i> double mutant is not sensitive to camptothecin (CPT).....	151
Figure 6.5 Sensitivity spot test of Methyl methane sulfonate (MMS) for several of <i>S. pombe</i> mutants.....	152
Figure 6.6 Mutation of <i>tfx1Δ rnh1Δ</i> and <i>tfx1Δ rnh201Δ</i> double mutants exhibit no elevated sensitivity to phelomycin.	154

Figure 6.7 Tfx1 is not required from HU in the absence of RNase H activity.	155
Figure 6.8 Sensitivity spot test of ultraviolet (UV) for several of <i>S. pombe</i> mutants.....	156
Figure 6.9 Sensitivity spot test of to camptothecin (CPT) for several of <i>S. pombe</i> mutants....	157
Figure 6.10 Sensitivity spot test of Methyl methane sulfonate (MMS) for several of <i>S. pombe</i> mutants.....	158

List of tables

Chapter 2

Table 2.1 Yeast and bacterial media used.....	43
Table 2.2 <i>S. pombe</i> strains used in this project.....	45
Table 2.3 <i>E. coli</i> used in this study	50
Table 2.4 PCR primers used to delete target gene	51
Table 2.5 Sequence of PCR primers utilized for gene deletion assessment	55
Table 2.6 Drugs used in this study.....	57

Chapter 1: Introduction

1.1 Types of DNA damage

Endogenous DNA damage can occur through metabolic or hydrolytic processes, and results in chemical abnormalities in the DNA molecule as opposed to sequence errors that might be caused by mutations. Often, endogenous damage can be repaired through native systems, although these repair mechanisms are not always perfect, so some DNA damage can accumulate in non-replicating cells (Tubbs and Nussenzweig, 2017).

Metabolic processes within the cell can produce reactive oxygen species, which in turn can induce oxidative damage in DNA. Such damage can result in chemical alteration of bases, and can even result in single strand breaks (Yu *et al.*, 2016). The oxidative degradation of lipids can also result in DNA damage, largely as this is a free radical mediated process that produces further reactive oxygen species. In particular, reactive electrophilic compounds such as alpha and beta-unsaturated aldehydes, which react with DNA bases to form epoxy aldehydes (Medeiros and Medeiros, 2019). These aldehydes are more reactive with DNA than their parent forms, demonstrating genotoxic and mutagenic effects.

There is also an inherent chemical instability in the DNA molecule, which can result in several types of DNA damage, including depurination, depyrimidations, and cytosine deamination. In essence, the glycosidic bonds between the DNA backbone and the nucleotide base can be hydrolysed, resulting in loss of individual bases (Chatterjee and Walker, 2017). Oxidative damage is inflicted on DNA many thousands of times per day in the human body, and there are innate mechanisms in place that are able to accommodate the vast majority of these (Tudek *et al.*, 2010).

DNA damage can also come from exogenous sources such as drugs, poisons, or various forms of radiation, and the inherent DNA repair mechanisms are also able to correct many of these forms. As an example, hydroxyurea, is used therapeutically for several hyperproliferative disorders, including various cancers. It functions via the inhibition of ribonucleotide reductase by quenching the tyrosyl radical found in the active site of the M2 protein subunit, thereby severely impacting upon DNA replication (Platt, 2008). Once the tyrosyl radical is quenched, it no longer stabilises the nearby iron centre, thereby increasing its vulnerability to chelation.

Chapter 1: Introduction

There has been some dispute over whether hydroxyurea depletes cells of their pool of deoxyribose nucleoside triphosphate (dNTP), however the incorporation of dNTP into new DNA strands is inhibited, arresting synthesis with stalled replication forks (Koç *et al.*, 2004; Petermann *et al.*, 2010).

Another example is found in the peptide antibiotic phleomycin, originally isolated from the *Streptomyces* species, which can induce mutations in the genome through the introduction of double stranded breaks (Peer *et al.*, 2009). Given that oxygen is required for phleomycin-induced DNA breakage, which is converted into hydrogen peroxide in the process, a secondary oxidative threat is also present (Sleigh, 1976).

Replication forks are also known to stall if they collide with transcription complexes (Pomerantz and O'Donnell, 2010). This can lead to considerable instability in the affected region, which may ultimately lead to cell death. Consequently, mechanism that can allow recovery from such collisions and allow the progression of the replication fork are crucial for not only continued stability and survival of the cell, but also the propagation of the genome. A set of auxiliary DNA helicases have been found to promote the continuation of replication through barriers such as transcription complexes (Pomerantz and O'Donnell, 2010).

1.2 DNA repair

There are several mechanisms through which DNA repair can be undertaken within the cell. These vary based upon the type of DNA damage present and the stage of the cell cycle in which the damage is detected. Nucleotide damage as a result of oxidation or other forms of metabolic processes and even single strand breaks can be addressed using base excision repair in which the damaged single-stranded region is cleaved from the double helix, allowing fresh nucleotides and polymerase to reconstruct the section from the template provided by the other strand (Beard *et al.*, 2019). In situations that involve oxidative damage to the bases themselves, such as thymine dimers, nucleotide excision repair can take place. Nucleotide excision repair (NER) fills a useful role between base excision repair and the larger DNA mismatch repair mechanisms, allowing restoration of DNA damaged by ultraviolet light, for example.

Chapter 1: Introduction

This process must be carefully regulated and accurately performed to ensure lesions are corrected rather than exacerbated. The xeroderma pigmentosum group C (XPC) protein complex is central to the damage detection process, and is able to detect the presence of the usual oscillating pattern of DNA bases in the double helix (Sugasawa, 2016). With the addition of UV-damaged DNA-binding protein (UV-DDB), which is able to detect more subtle photolesions, XPC can bind to DNA at regions that are suspected of damage. XPA and helicases then co-operate to identify chemical abnormalities in the DNA (Sugitani *et al.*, 2016). Damage recognition is followed by similar backbone cleavage, nucleotide removal, and free nucleotide polymerase reactions as seen with base excision repair; the difference between these two mechanisms bring the length of the damaged region (Hiller *et al.*, 2018).

More serious damage such as double-strand breaks can be repaired to some extent by non-homologous end joining or microhomology-mediated end joining, depending upon the stage of the cell cycle in which the damage is detected. Microhomology-mediated end joining takes place in the S phase and is often inaccurate, while non-homologous end joining takes place in G0, G1, or G2 stages and is marginally more accurate (Ceccaldi, Rondinelli and D'Andrea, 2016). This usually takes place through a micro-homology-mediated base-pairing process in which single strands come together, followed by trimming of any excess DNA flaps and filling of any gaps. This can be an error-prone process resulting in loss of DNA information, leading further errors such as telomere fusion, a finding consistent with many forms of cancer (Seol, Shim and Lee, 2018).

Sometimes nucleotide bases become methylated, which can be corrected at any stage of the cell cycle through a direct reversal mechanism that involves the enzymatic cleavage of the methyl group, restoring the base to its native form (Kunkel and Erie, 2005). This process is generally very accurate. Base substitution mismatches or insertion-deletion errors that have occurred during DNA replication can be accurately corrected during a process known as DNA mismatch repair (Kunkel and Erie, 2005).

Chapter 1: Introduction

In situations where the DNA either cannot be repaired or the normal repair mechanisms have yet to identify the lesions, DNA replication can still sometimes take place regardless using the process of translesion synthesis, in which the replication process allows for a DNA polymerase with a higher tolerance (lower stringency requirement) in the DNA reading which allows the cellular machinery to move over lesioned areas. This, naturally, has the potential to be inaccurate (Lehmann, 2005).

1.3 Gnomonic instability

Genomic instability is a hallmark of cancer and defined as a high tendency towards mutations and genetic change within a genome (Tubbs & Nussenzweig, 2017; Fragkos & Naim, 2017; Choi & Lee, 2013; Hanahan & Weinberg, 2011). Genome instability is crucial for the cells to maintain genomic stability for their appropriate functioning (Felipe-Abrio, et al, 2015; Yao & Dai, 2014; Aguilera & García-Muse, 2013; Faggioli, Vijg & Montagna, 2011). Genomic instability exists in several different types, such as chromosomal rearrangements, point mutations and gain/loss of whole chromosomes due to chromosomes number change and deletion (He, et al, 2018; Ferguson, et al. 2015; Aguilera & Gómez-González, 2008). Another major factor in genomic instability comprise of epigenetic aberrations, which not only alter the assembly of chromatin but are also regulate in DNA methylation and histone modifications (Choi & Lee, 2013; Katto & Mahlknecht, 2011). Epigenetic aberrations and genetic change are present in most tumour cells and are the main drivers of carcinogenesis—the initiation, promotion and progression of cancer (Aronica, et al, 2015; Lord & Ashworth, 2012; Gordon, Resio & Pellman, 2012; Geigl, et al, 2008). Genomic instability is a result of defects in the regular cell-processes. A number of defects which may lead to genome instability can for example occur in all of the following processes: chromosome segregation, replication of DNA and DNA damage repair processes (Fragkos & Naim, 2017; Felipe-Abrio, et al, 2015; Sirbu & Cortez, 2013; Choi & Lee, 2013).

There are two types of stresses that can cause damage: exogenous stresses (for example ionising radiation) and endogenous stresses (for example DNA replication stress) which can cause DNA lesions, which threaten the stability of the genome (Bouwman & Crosetto, 2018, Tubbs & Nussenzweig, 2017; Fragkos & Naim, 2017; Li, J. & Xu, 2016). Therefore, the cell is equipped with a range of response-mechanisms to correct the damages caused by these stresses. These

Chapter 1: Introduction

different pathways are sometimes grouped together under the term “DNA damage response” (DDR). Included in the DDR are: checkpoint activation of DNA damage, repair of DNA and also Apoptosis (programmed cell death) if the damage to the DNA is irreparable (Tubbs & Nussenzweig, 2017; Fragkos & Naim, 2017; Jeggo, Pearl & Carr, 2016; Choi & Lee, 2013).

Any defect in these protective systems can lead to genetic instability, which can cause cancer development as well as many diseases related to aging (Figure 1.1) (Knijnenburg, et al, 2018; So, et al, 2017a; Yang, K., Guo & Xu, 2016; Ohle, et al, 2016; Ferguson, et al. 2015). The high fidelity replication of DNA is extremely important for faithful transmission of the genetic code, and failures in this process can result in chromosomal abnormalities, with one example being translocations. These undesired genetic alterations lead to abnormal cell behaviour, causing the development of cancer and other diseases. Therefore, all the processes of DNA replication should be properly synchronised with others process (such as transcription) in order to avoid any genomic instability (Burgers & Kunkel, 2017; Labib & Hodgson, 2007; Lord & Ashworth, 2012).

1.4 DNA Replication

Cancer can be considered a cell cycle disease. A regular cell that is completing its cell cycle passes through four phases: a first Gap phase (known as “G1”), the Synthesis or “S” phase, a second Gap phase (“G2”) and finally the Mitosis or “M” phase. In the S phase, DNA is duplicated and completed prior to cell division. High fidelity in DNA replication is fundamental so that the correct genetic information is transformed and genomic instability is avoided (Bouwman & Crosetto, 2018; Kang, S., et al, 2018; Parker, Botchan & Berger, 2017a; Li & Xu, 2016; Gelot & Lopez, 2015). In eukaryotes, the genome replication starts at specific orgine sites, enriched in AT content, DNA replication is initiated from several origins on one chromosome (Fragkos & Naim, 2017; Parker, Botchan & Berger, 2017; Kang, et al, 2018). A complex known as the origin recognition complex (ORC) recognises the origins during the early G1 phase. Once the ORC has bounded at replication origins, it then functions as a foundation which supports the formation of multiple proteins into the pre-replicative complex (pre-RC). This occurs in the later stages of the G1 phase (Kang, et al, 2018; Duzdevich, et al, 2015). One of the major components of pre-RC is the mini-chromosome maintenance (MCM) protein complex.

Chapter 1: Introduction

MCM not only unwinds double-strand DNA (dsDNA), but also inhibits DNA replication from occurring more than once per cell cycle. Of course, the integrity of DNA, both from the perspective of genetic sequence and as a chemical structure, must be ensured because discrepancies or other errors being passed on to new cells have the potential to induce oncogenic mutations. One of the key regulators of DNA replication is the minichromosome maintenance (MCM) protein complex, which carries out a process of replication licencing, thereby ensuring that only a single copy of the genome, or any of its component parts, is produced during cellular replication (Li *et al.*, 2015). This heterohexameric complex provides a crucial checkpoint in the replicative cycle, disruption of which can lead to carcinomas (Shima *et al.*, 2007). Subunits MCM4/6/7 have helicase activity and are therefore capable of unwinding double-stranded DNA, while MCM2/3/5 carry out a regulatory function. Despite the complex as a whole not having helicase activity, all six subunits are required for DNA unwinding *in vivo* (Neves and Kwok, 2017). The atomic-level mechanism for the MCM-mediated DNA translocation has been elucidated recently, involving a double hexamer that encircles double stranded DNA, dissociating into single hexamers, each of which encircles a single strand (Meagher, Epling and Enemark, 2019).

To form each bidirectional replication fork, two MCM complexes are load at pre-RC and establish the fork (Kang, et al, 2018; Burgers & Kunkel, 2017; Chang, E. & Stirling, 2017; Lei, 2005). Several protein kinases – such as Cdc7-Dbf4 kinases (DDKs) and S-phase cyclin-dependent kinases (CDKs) – are crucial for the activation of the MCM proteins and support both the initiation of the DNA replication process, as well its progression (Bouwman & Crosetto, 2018; Burgers & Kunkel, 2017; Parker, Botchan & Berger, 2017; Duzdevich, et al, 2015) (Figure 1.2).

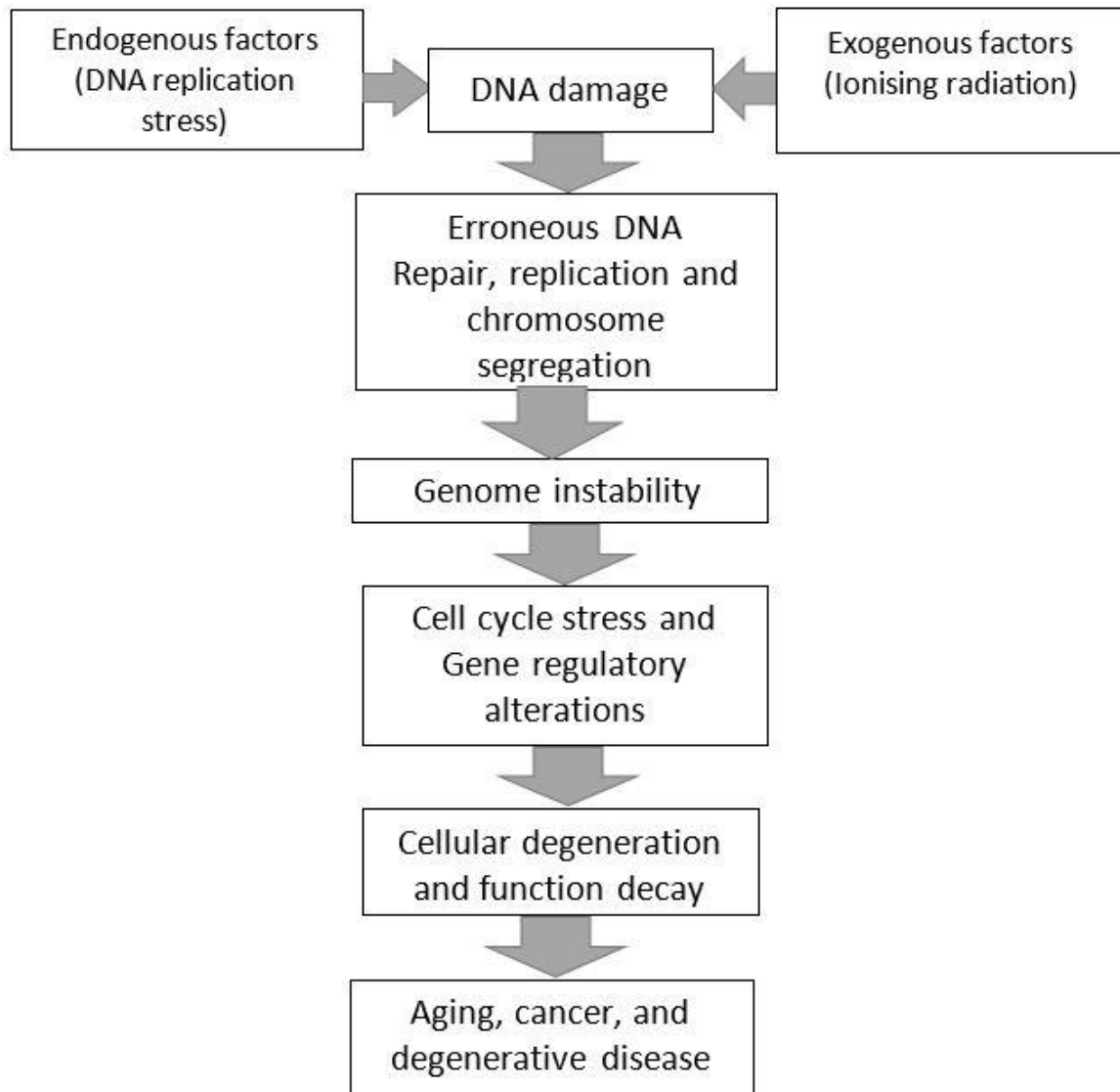


Figure 1.1 Genome Instability: Pathway to Disease. Graphic flow chart indicating how DNA damage can lead to cancer and other diseases. Failure to counter DNA damage by the cellular response system causes genomic instability, which may lead to cancer development. Checkpoint of DNA damage arrest cell division, allowing the DNA repair pathways to repair the damaged genome in a timely manner. However, if the defence mechanisms are unable to correct the damage, then genome instability follows. This can cause the development of cancer and other diseases (adapted from Vijg & Montagna, 2017).

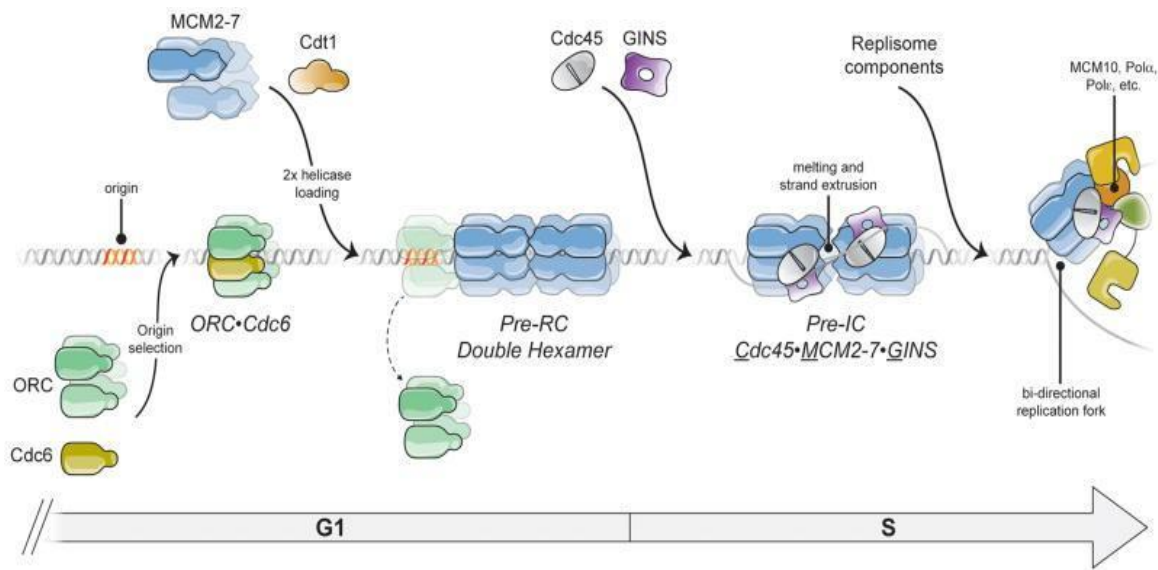


Figure 1.2 Mechanistic Diagram depicting the Early Stages of the DNA Replication Process in an Eukaryotic Cell. During the early stage of the G1 phase, ORC with Cdc6 complex are linked to the replication origins. The ORC are foundation for multiple proteins to assemble into MCM2-7 complexes in the form of stable double hexamer. The hexamer then encircles the duplex DNA pre-replicative complex (pre-RC). The helicase is activated during the S phase leading to origin unwinding. To form each bidirectional replication fork, two MCM proteins and additional activators such as (Cdc45 and GINS) are required to form the pre-initiation complex. This complex, in conjunction with ribosome components such as DNA polymerase, ultimately forms the replication fork (Parker, Botchan & Berger, 2017).

1.5 Replication fork progression

The point from where the dsDNA unwinds and becomes single-strand DNA (ssDNA) is called a replication fork. The process uses ATP hydrolysis to drive denaturation and creates a Y-shaped fork structure (Figure 1.3). Replication protein A (RPA) is a complex of heterotrimeric proteins that preserves the stability of ssDNA at the fork (Kang, et al, 2018; Branzei & Foiani, 2007; Stillman, 2008).

During the replication process, the two strands of DNA unwinding and act as templates on which DNA polymerases build nucleotides and create new daughter strands. One of the strands is known as the leading strand and the other as the lagging strand (Figure 1.3). Leading and lagging strands are synthesised in the opposite direction, which means that the direction of replication of both strands are opposite to each other (Figure 1.3). The replication at the leading strand is continuous since its direction is the same as the direction of the replication fork. Replication starts when the enzyme primase adds a short RNA strand at the 3' end (Arezi & Kuchta, 2000).

This short RNA strand is called a primer, which synthesises the daughter strand by serving as the initiation point for polymerase ϵ (Figure 1.4). Because the lagging strand is opposite to the direction of synthesis by DNA polymerases, loops are created on the lagging strand template and so the replication at the lagging strand occurs in a fragmented and not a continuous fashion (Figure 1.4) thus, many short primers of RNA are added at several regions on this strand to form short RNA:DNA fragments, the so-called Okazaki fragments. These fragments are joined with RNA primers by the enzyme polymerase δ (Figure 1.4).

Finally, once the strands are complete, exonuclease enzymes remove the primers, and their place is filled by deoxyribonucleotide. Next, the new strands need to be proofread so that any mistakes and mismatches can be corrected. On the lagging strand, the Okazaki fragments are linked via DNA ligase (Burgers & Kunkel, 2017; Lujan, Williams & Kunkel, 2016; Pellegrini & Costa, 2016; Berti & Vindigni, 2016; Leman & Noguchi, 2013; Stillman, 2008).

Chapter 1: Introduction

There are several other proteins which also play a part in initiating and supporting the formation of replication forks, including the clamp loader, the proliferation cell nuclear antigen (PCNA), the replication factor C (RFC) and fork protection complex (FPC). Together, these components are referred to as the replisome (Leman & Noguchi, 2013) (Figure 1.4). Furthermore, various checkpoint proteins that attach to the replisome act as protective factors in DNA replication and preserve genome stability (Leman & Noguchi, 2013). It is essential for cells to continuously monitor and regulate the replication forks to protect genomic stability. Interference in the replication with the replisome can lead to arrested replication forks, which are recombinogenic in nature and can be subject to the unscheduled induction homologous recombination (HR) and chromosomal translocation which might result in the development of cancer (So, et al, 2017; Gadaleta & Noguchi, 2017; Brambati, et al, 2015a; Castel, et al, 2014; Pryce, et al, 2009).

Multiple internal and external factors cause DNA lesions that affect the replication fork (Jones & Petermann, 2012; Berti & Vindigni, 2016). Furthermore, natural genomic loci can act as replication fork barriers (RFBs) and block/delay the progression of replication (Berti & Vindigni, 2016; Gadaleta & Noguchi, 2017). RFBs can result in replication fork collapse and HR promotion, which can result in genome instability unless it is corrected in a timely manner (Gadaleta & Noguchi, 2017; Lin & Pasero, 2012; Pryce, et al, 2009).

The conflict between replication and transcription machineries is an example of a natural impediment that might block and stall the DNA replication fork which can ultimately result in genomic instability (Chang & Stirling, 2017; Aguilera & García-Muse, 2013; Fragkos & Naim, 2017; Ren, Castel & Martienssen, 2015; Brambati, et al, 2015). In terms of natural impediments, other factors, such as a response to drugs, can also cause stalled DNA replication forks. For example, ribonucleotide reductase inhibitor hydroxyurea (HU) inhibits deoxyribonucleotide triphosphate (dNTP) synthesis and impairs DNA synthesis. However, it does not stop the replicative helicase from unwinding the parental DNA duplex, which can lead to collapse of the replication fork and the formation of DNA double-strand breaks (DSBs) (Saada, Lambert & Carr, 2018; Aguilera & García-Muse, 2013; Petermann, et al, 2010).

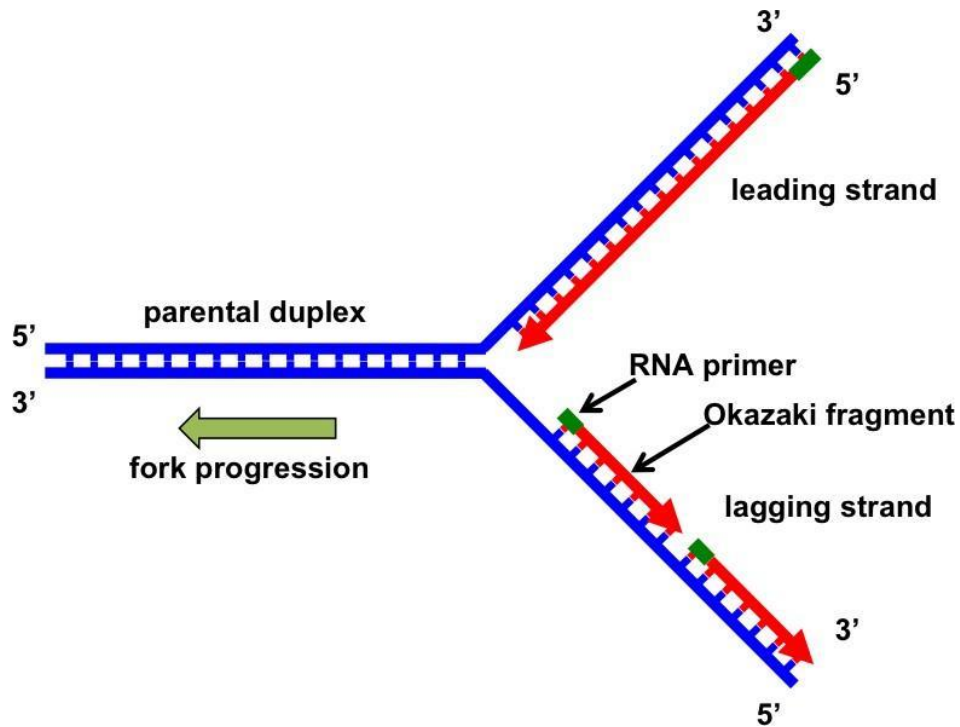


Figure 1.3 Schematic of a DNA replication fork At the leading strand, DNA replication is carried out in the 5 to 3-direction, but at the lagging strand, replication occurs in the opposite direction and in a discontinuous manner, leading to the formation of short Okazaki fragments. Both the leading and lagging strands require RNA primers to initiate the replication (taken from Leman & Noguchi, 2013).

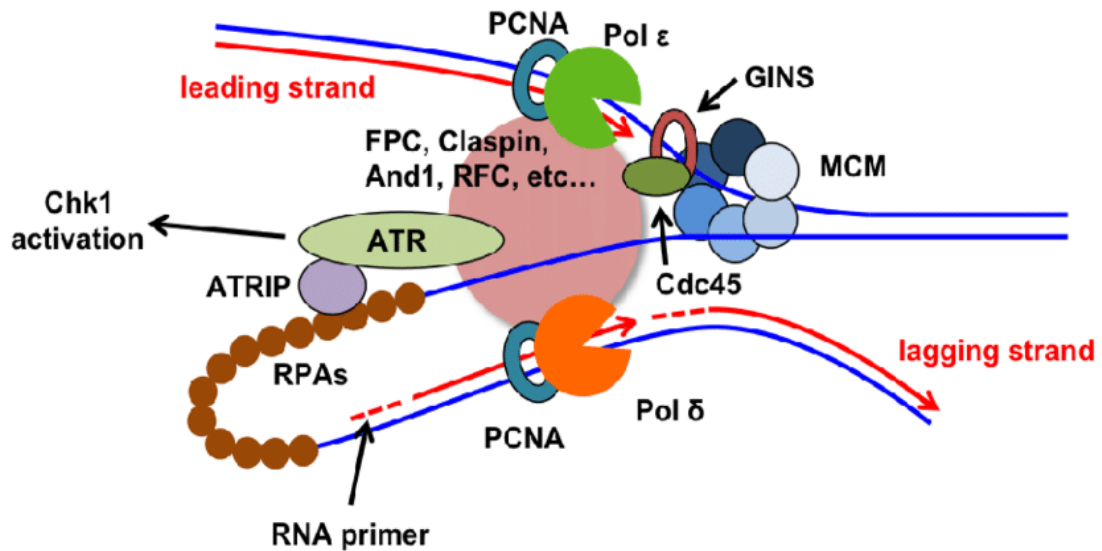


Figure 1.4 The basic graphic of eukaryotic replisome complex

The replication on leading and lagging strand is carried out by Pol ϵ and Pol δ . Several replisome components, including fork protection complex (FPC) and replication factor clamp loader (RFC), are charged with coordinating polymerase activities and regulating DNA synthesis with unwinding of dsDNA by GINS [go-ichi-ni-san] and Cdc45- mini-chromosome maintenance MCM (taken from Leman & Noguchi, 2013).

1.6 The DNA double-strand break (DSB) repair pathways

Numerous internal and external factors damage the genome, creating thousands of DNA lesions and leading to genomic instability (Tian, H., et al, 2015; Takagi, 2017). It is highly important for the cells to effectively repair any DNA damage in time to avoid further mutations and genomic rearrangements, which can lead to cancer development (Davis & Chen, 2013; Uckelmann & Sixma, 2017). The most hazardous type of DNA lesion are double-strand breaks (DSBs), in which both DNA strands are broken and which can result in chromosomal rearrangements (Chang & Stirling, 2017; Ohle, et al, 2016; Mladenov & Iliakis, 2011a). There are several external factors that can cause DSBs, such X-rays and gamma rays. Nevertheless, programmed DSBs can be generated naturally during the recombination process – for instance, during meiosis and immune cell development (Takagi, 2017; Tian, et al, 2015; Brugmans, Kanaar & Essers, 2007). Furthermore, damage to the DNA template through the normal S phase could cause stalling of the replication fork, which results in non-programmed DSBs that in turn restart the replication fork (Gadaleta & Noguchi, 2017; Davis & Chen, 2013; Lieber, 2010). Eukaryotic organisms have highly developed and specialised DNA repair mechanisms for chromosome DSBs repair repairing, such as non- homologous DNA end joining (NHEJ) and homologous recombination (HR) (Zhao, X., et al, 2017; Ohle, et al, 2016; Davis & Chen, 2013; Lieber, 2010). Both the recombination pathways are controlled via the cell cycle, and if the cell fails to select the correct pathway for repair, cancer can develop. For instance, the HR pathway performs the DNA lesion in specific phases, namely the S and G2 phases, since a homologous sequence (sister chromatid) is available and is also needed to repair the template. In contrast, repair via the NHEJ pathway is also able to be carried out during the S or G2-phases when an intact DNA sequence is not sufficiently available or and near a DSB. In this case, NHEJ repair is predominant during the G1 phase, in which the broken ends of the DNA-end are directly re-joined without the need for a homologous sequence (Zhao, et al, 2017; Takagi, 2017b, Davis & Chen, 2013; Lieber, 2010; Brugmans, Kanaar & Essers, 2007).

Chapter 1: Introduction

1.6.1 The non-homologous DNA end- joining (NHEJ) repair pathway

In the NHEJ pathway, the repair of two DNA ends occurs directly: the two ends are directly re-joined, and there is no need for a homologous sequence in this mechanism (Sishc & Davis, 2017; Mladenov, et al. 2016; Fell & Schild-Poulter, 2015; Peng & Lin, 2011; Mladenov & Iliakis, 2011). Nevertheless, it is an error-prone repair mechanism because small-scale mutations and chromosomal rearrangements can occur during this process. In contrast with HR, the activation of NHEJ is not restricted to particular phase of cells (Zaboikin, et al, 2017; Ohle, et al, 2016; Peng & Lin, 2011; Daley, et al, 2005). The steps of repair pathway of NHEJ are recognition, resection, polymerisation and ligation of the broken DNA ends; various proteins are used in these steps. Any fault during the process leads to translocation and telomere fusion. Important proteins involved in the process include the Ku which is heterodimer consisting of both (Ku70 and Ku80 subunits), DNA dependent protein kinase catalytic subunit (DNA-PKcs), DNA ligase IV (LigIV), X-ray repair cross-complementing protein 4 and XRCC4 like factor XLF (Chang & Stirling, 2017; Boboila, Alt & Schwer, 2012; Espejel, et al, 2002).

In eukaryotes, the repair process starts when a Ku heterodimer composed of two subunits, namely, the Ku70-Ku80 heterodimer recognises and binds to the free end of the DSB DNA formation. Protecting DNA ends is one function of the Ku heterodimer. First, a ring-shaped structure is formed by the protein, which can encircle the DNA ends by acting as platform to bind NHEJ machinery's core factors to target damage site, including DNA-PKcs (DNA-dependent protein kinase, catalytic subunit). An active complex of Ku70-Ku80 subunit- (DNA-PKcs) is formed once DNA-PKcs has been recruited to the ends of broken DNA; in this step, phosphorylation occurs, and the endonuclease Artemis is recruited to the site. Then, overhangs at the DNA ends are cleaved, making them appropriate for the re-ligation process (He, et al, 2018; Li & Xu, 2016; Mladenov & Iliakis, 2011; Davis & Chen, 2013; Khalil, Tummala & Zhelev, 2012). It has been suggested that in different organisms, the MRE11 -RAD50 -NBS1 complex (MRN complex), that not only facilitates the HR pathway (see below) but is also involved in the functioning of DNA polymerase and addition nucleases, is necessary to complete the process ends prior ligation. Finally, the complex of XRCC4-DNA Ligase IV is involved in ligating the DNA ends, which then leads DNA integrity being restored (Fell & Schild-Poulter, 2015; Liu, P., et al, 2015; Boboila, Alt & Schwer, 2012).

Chapter 1: Introduction

Both XRCC4 and XLF are needed for ligase IV, but the precise function of XLF in NHEJ pathway is still unclear. However, it could be used to stimulate XRCC4-ligaseIV ligation activity (Figure 1.5) (Davis & Chen, 2013; Boboila, Alt & Schwer, 2012; Mladenov & Iliakis, 2011)

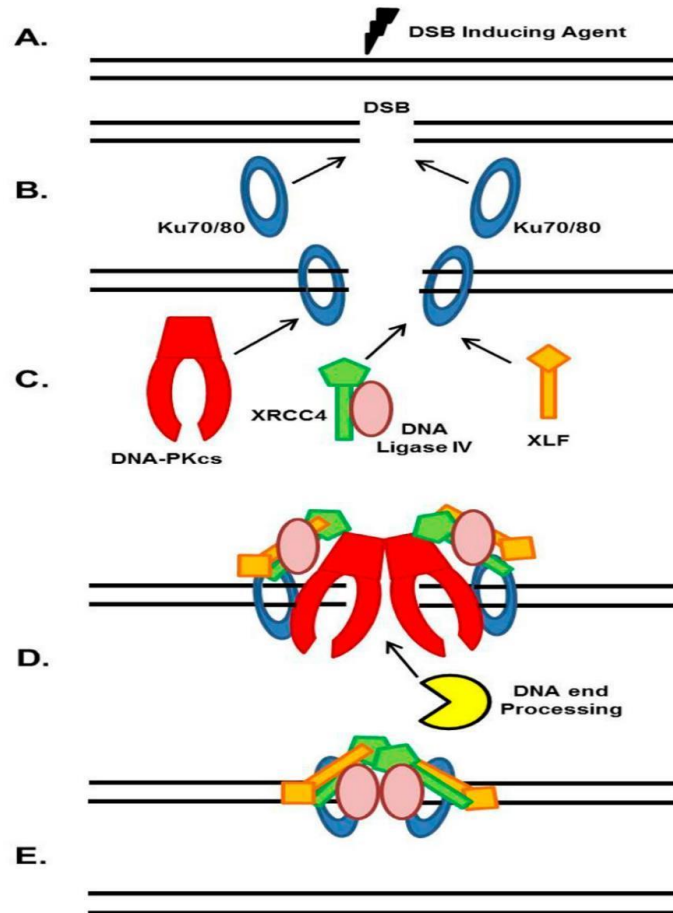


Figure 1.5 Summary of the NHEJ repair mechanism Both A and B.: First, a DNA double strand break (DSB) is created. The Ku heterodimer is quickly bound (C). The Ku70-Ku80 complex recognises and binds to the broken DNA end, leading to the recruitment of DNA-PKcs, which then stimulates the end processing via Artemis nuclease (D). The role of Artemis is processing the DNA ends to make them compatible for the step of ligation' (E). As the last step, the LigIV/XRCC4/XLF complex ligates the DNA broken ends (taken from Sishc & Davis, 2017).

Chapter 1: Introduction

1.6.2 The homologues recombination repair pathway

HR requires a homologous sequence (sister chromatid) to repair DSBs, and it is considered a high-fidelity repair pathway. In contrast to the NHEJ pathway, HR is recognised to be generally error-free (Sishc & Davis, 2017; Sakofsky & Malkova, 2017a; Zhao, et al, 2017; Essani, Glieder & Geier, 2015). HR is fundamental in maintaining genomic stability. It does so through the repair of DSBs which were damaged through exogenous factors. It is further essential in repairing DNA replication forks and also the maintenance of telomeres in when telomerase is absent. In addition, HR is involved in chromosomal pairing and exchanging during meiosis, resulting in genetic diversity and reductional segregation (McFarlane, Al-Zeer & Dalgaard, 2011; Li, X. & Heyer, 2008; Kolesar, et al, 2012).

DSB repair (DSBR), synthesis-dependent strand annealing (SDSA) and break-induced replication (BIR) are the main HR repair pathways for repairing DSBs (Rodrick et al., 2018). These three pathways are initiated when the conserved MRN-complex detects the formation of DSBs (Khalil, Tummala & Zhelev, 2012; Llorente, Smith & Symington, 2008; Lieber, 2010), resulting in recruitment of the kinase ataxia telangiectasia mutated (ATM), a checkpoint kinase which has the function of phosphorylating and activating several DNA repair elements, such as all MRN complex members. The MRN complex interacts with either the Dna2-Sgs1/BLM complex or with exonuclease Exo1 to mediate (5'→3') resection at the ends of DSB, and these interactions create overhangs of single-strand DNA (ssDNA) with 3'OH ends (Talens, et al, 2017, Ohle, et al, 2016). DNA replication protein A (RPA) binds to the tails of nascent ssDNA, where the formation of a secondary structure is potentially prevented by RAD51 (Khalil, Tummala & Zhelev, 2012; Heyer, Ehmsen & Liu, 2010a). The two functions of RAD51 and BRCA2 are both able to act as a replacement for the RPA complex by using RAD51 (an essential HR protein) which creates a filament of nucleoprotein on the ssDNA (Zhao, et al, 2017; Ohle, et al, 2016; Barlow & Rothstein, 2010).

Chapter 1: Introduction

The RAD51-recombinase form a displacement loop (D-loop) by searching and invading homologous intact duplex DNA (Suwaki, Klare and Tarsounas. 2011; Llorente, Smith & Symington, 2008; So, et al, 2017) Then, the DNA polymerases extend the invading strand 3' end in the D-loop. After invading strand extension, HR can take any of the three proposed pathways (Figure 1.6).

The first pathway is the DSBR. In this pathway, an extended invading strand is annealed to the DSB's other ends. This results in a double Holliday junction (dHJ) (Lord & Ashworth, 2016; Zhao, et al, 2017). It is possible to process a dHJ into two products, either via the separation of the two sets of strands generating a non-crossover product or alternatively allowing for the facilitation of the endonucleolytic cleavage to occur, by having resolvases lead to a crossover event (Figure 1.6). Furthermore, the dHJ can also be dissolved via TOPOIII α and BLM-promoted branch migration, leading to non-crossover event (Zhao, et al, 2017; Essani, Glieder & Geier, 2015; Li & Heyer, 2008). The second pathway is SDSA, during which the D-loop unwinds and the extended re-anneals of invading strand with DSB second end, resulting in repair using the strand which has been reannealed as a template.

There is a decrease in the likelihood of chromosomal rearrangements occurring in the SDSA-pathway, because contrary to the DSBR-pathway, the SDSA-pathway only generates non-crossover events (Figure 1.6) (Heyer, Ehmsen & Liu, 2010; Sugiyama, et al, 2006; Barlow & Rothstein, 2010). The third pathway, BIR, emerges when the replication fork are collapsed or telomere length occurs, but it may also take place under some circumstances as a backup or alternative to DSBR or SDSA when telomerase is absent (Kramara, Osia & Malkova, 2018). The formed D-loop can turn into a replication fork in this pathway and is then able to copy the distal of DNA sequence to the donor molecular site until the end of the chromosome. In order for BIR to be possible, the synthesis of both strands (leading and lagging) need to have completed the DNA replication process (Figure 1.6) (Sakofsky & Malkova, 2017; Llorente, Smith & Symington, 2008; Malkova & Ira, 2013).

Chapter 1: Introduction

It has been proposed that BIR mediates alternative telomere lengthening (ALT), a pathway that be used by which compromised tumour cell maintain the length of their telomere (Kramara, Osia & Malkova, 2018; Roumelioti et al., 2016). Furthermore, studies have indicated that BIR repairs DSBs in sub-telomare regions (Batte et al., 2017). Furthermore, research has indicated that the accumulation of R-loops at DNA damage sites (often in rDNA) leads to a slow repair of the DNA-damage via BIR in *Saccharomyces cerevisiae* (Amon & Koshland, 2016).

Moreover, BIR is essential to restart the stalled replication fork and to protect telomere however; it also considered induce chromosome instability because it can cause an extensive heterozygosity loss (LOH). In yeast, BIR has been linked with large-scale LOH, followed by the creation of non-reciprocal translocation and complex chromosome rearrangement (e.g. when the end of a DSB does not invade a sister chromatid molecule, but a homologue) (Sakofsky & Malkova, 2017b; Mladenov, et al. 2016; Hastings, et al, 2009).

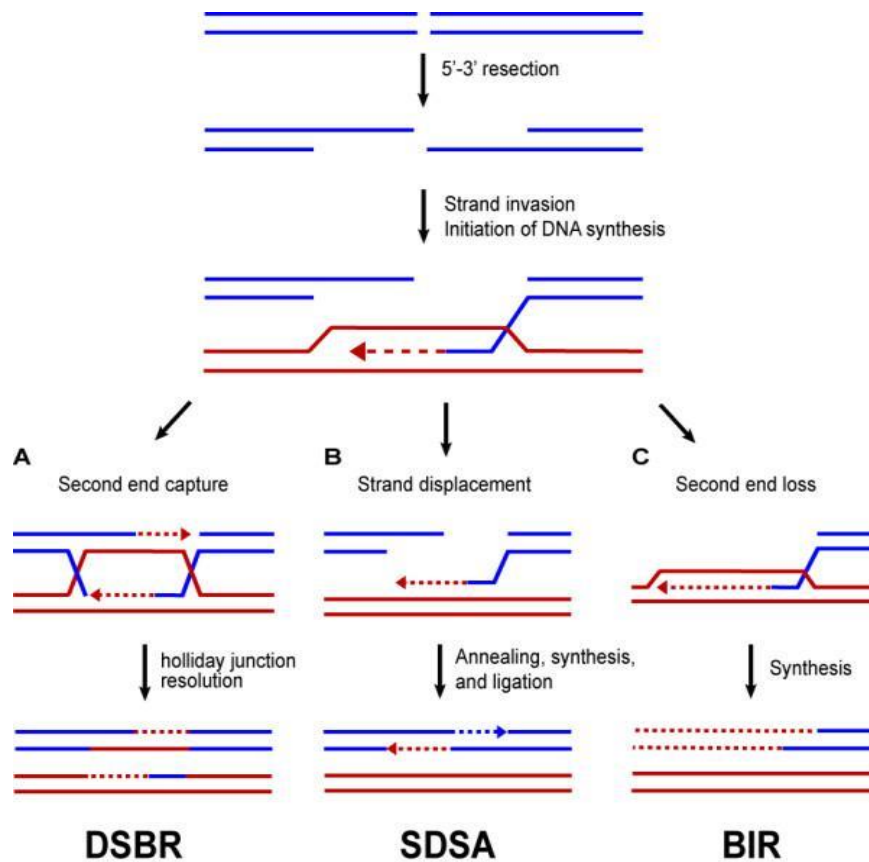


Figure 1.6 Graphic models of the Homologous Recombination (HR) pathways Homologues recombination can be repaired DSBs In three pathways. The DNA ends are initially processed to 3' ssDNA tails. These tails invade homologous template redline with new synthesis of DNA crossed line. They are three possible result of this invasion are displayed. **A)** in DSBR pathway, the start invading strand can be annealed to capture second end anneal after priming DNA synthesis. That leads to form a double holliday junction dhj. Double holliday junction could be fixed by a non-crossover recombination product or crossover recombination product. **B)** As alternative, following invades the homologous template by the single ssDNA tail, DNA synthesis round is produced from the 3' end. Synthesis- dependent strand annealing (SDSA pathway) can take place by unwinding and re-annealing to the other DSB end. **C)** In the case of a break-induced replication (BIR), the one end of DSB is missing and the remaining ends invades the homologous DNA synthesis priming template at the chromosome end. Arrowheads show 3' ends and dashed lines represent newly synthesised DNA adapted from (Barlow & Rothstein, 2010).

1.7 The Chromosomal translocations

Deletions, inversions and translocations alter the original structure of chromosomes and result in new arrangements (Figure 1.7.A) (Harewood & Fraser, 2014). Regarding the causes for genome instability, the principal type of chromosome translocation is chromosome rearrangement (Nambiar & Raghavan, 2011). A translocation is defined as an abnormal breakage and attachment of a complete or a part of a chromosome to another; it occurs when non-homologue chromosomes suffer an abnormal recombination (Figure 1.7.B) (Roukos & Misteli, 2014; Harewood & Fraser, 2014; Tucker, 2010; Nambiar & Raghavan, 2011). Translocations are major contributors in the initiation and progression of cancers, and are the main drivers in lymphoma and leukaemia cases (Zheng, 2013a; Nambiar & Raghavan, 2011).

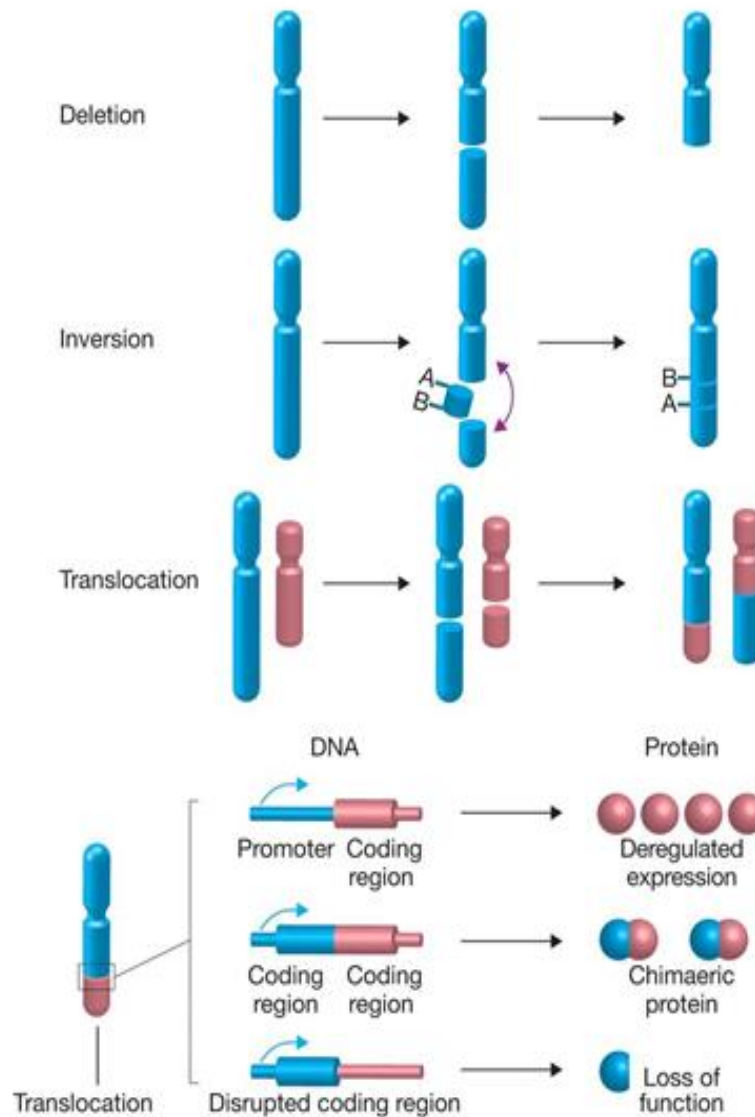
Translocations come in two different types: reciprocal and non-reciprocal. One speaks of a reciprocal translocation if a pair of non homologous chromosomes exchange segments. Reciprocal translocations are usually balanced and are found in different cancers, including leukaemia and lymphoma (Gollin, 2007; Lieber, 2016). Non-reciprocal translocations, on the other hand, are one-way transfers of one chromosome arm to another non-homologous chromosome, without the reciprocal transfer. If they fuse close to the region of centromere and the short arm is lost, then this type of translocation is also possible between two acrocentric chromosomes (Zhang, Y., et al, 2010; Nussenzweig & Nussenzweig, 2010; Ly, et al, 2019). If no chromosomes are gained or lost during translocation between two non-homologous chromosomes, it is a balanced translocation. In contrast, an unequal translocation is a transfer that results in a gain or loss of genetic material and is thus unbalanced (Harewood & Fraser, 2014; Zheng, 2013).

During translocation, chromosome segments break from different points and, depending on where these breakpoint are located, can interrupt the tumour suppressor genes or fuse different genes or activate protooncogenes by bringing active promoters adjacent to the oncogene open reading frame; all these outcomes can lead to cancer initiation (Figure 1.8.B) (Roukos & Misteli, 2014; Harewood & Fraser, 2014; Zheng, 2013b; Nambiar & Raghavan, 2011; Zheng, 2013).

Chapter 1: Introduction

One cause of translocation is alteration in DNA damage repair genes, such as DNA double-strand break (DSB) repair processes. DSBs are a fundamental element in initiating a translocation, and both external factors (e.g. ionising radiation (IR)) or internal factors (e.g. a blocked replication fork) can induce DSBs (Bouwman & Crosetto, 2018; So, et al, 2017; Vijg & Montagna, 2017). To mend DSBs, cells initiate DNA repair mechanisms such the homologous recombination (HR) mechanism. However, a failure on part of the cells to repair DSBs can result in a rearrangement of the chromosomes (So, et al, 2017; Roukos & Misteli, 2014; Gelot & Lopez, 2015). Thus any faulty chromosome replication can potentially cause translocations in chromosomes (Labib & Hodgson, 2007). Normal repair of DSBs in S-phase or G2 is via an inter-sister chromatid pathway. Translocations can occur when this HR partner choice is faulty and HR occurs between non-homologous chromatids. Moreover, break-induced replication (BIR) can ensue when a broken end invades a non-homologous chromatid and generates a new DNA replication fork (Llorente, Smith & Symington, 2008; Sakofsky & Malkova, 2017).

A well-studied example of a chromosomal translocation is the Philadelphia chromosome. It is generated by a translocation between chromosomes 22 and 9 [t (9:22)] that creates a fusion gene from the *BCR* and *ABL1* genes. The ABL/BCR fusion gene is translated into a non-standard ABL1 protein with abnormal, oncogenic tyrosine kinase (TK) activity causing chronic myelogenous leukaemia (CML) (Nambiar & Raghavan, 2011; Kang, Z., et al, 2016; Druker, 2008; Tabarestani & Movafagh, 2016). Another well documented translocation is the translocation between chromosomes 14 and 18 [t (14; 18)], which results in overproduction of the anti-apoptotic protein (BCL2) due to a highly active promoter being positioned in front of the *BCL2* gene. Increased production of BCL2 creates more chances for mutations that have survival benefits for cells, however, there is also an increased possibility for mutations and alterations which lead to follicular lymphoma (FL) (Kang, et al, 2016; Druker, 2008; Nambiar & Raghavan, 2011; Raghavan & Lieber, 2006). A great example of breakpoint junctions binding protein is Translin, which was first found in chromosomal translocations in human lymphoid neoplasms (see Section 1.10) (Aoki, et al, 1995; Kasai, et al, 1997a). Although researchers hypothesise that Translin functions as a mediator on the chromosomal rearrangement breakpoints (Gajecka, et al, 2006) mechanism behind Translin binding to breakpoint junctions in malignancies has yet to be found out.



Figur 1.7 Schematic showing examples of chromosome rearrangement including translocation] and their consequences]. Chromosomal rearrangements come in three main types: deletion, where chromosomes break and a DNA segment is removed; inversion, where a DNA segment breaks, inverts at a 180° position and is replaced at the same position; and translocation, where two DNA segments swap between two non-homologous chromosomes. There are two ways in which translocation produces oncogenes: 1) - interrupting and inactivating the tumour suppressor gene, which results in chimeric fusion protein, or 2) - inactivating the tumour suppressor gene (taken from Roukos and Misteli, 2014).

1.8 Replication fork barriers and recombination

During S phase the replication and transcription mechanisms use the same DNA template (Gómez-González & Aguilera, 2019; Belotserkovskii et al., 2018; Brambati et al., 2015; Hamperl & Cimprich, 2016) leading to potential conflict between the two processes. A collision between replication and transcription activities can stall the replication fork and collapse the replicative process if it is not resolved properly (Belotserkovskii, et al, 2018; Hamperl, Stephan, et al, 2017; Fragkos & Naim, 2017; Cerritelli & Crouch, 2016; Lin & Pasero, 2012). Furthermore, the replication fork collapse may lead to DSB formation, requiring an HR-mediated repair of the collapsed replication fork. (Gómez-González & Aguilera, 2019; Belotserkovskii, et al, 2018; Hamperl, S. & Cimprich, 2016; Brambati, et al, 2015b) Aberration in this HR repair process can lead to chromosomal rearrangements, such as translocations (Gadaleta & Noguchi, 2017; Castel, et al, 2014; Felipe-Abrio, et al, 2015; Lin & Pasero, 2012).

Two potential types of collision can occur between transcription and replication. The first type occurs when the replisome and the RNA polymerase collide head-to-head with each other, which is caused due to DNA and RNA synthesis having the same directional polarity and is associated with the lagging strand of DNA synthesis. The second type, which occurs on the template of the leading strand, is the head-to-tail (or co-directional) collision between the transcription and replication (Bermejo, Lai & Foiani, 2012; Brambati, et al, 2015; Hamperl & Cimprich, 2016). Head-to-head collision is considered more harmful than head-to-tail collision in both prokaryotic and eukaryotic cells (Gómez-González & Aguilera, 2019; Chang & Stirling, 2017; Brambati, et al, 2015; Bermejo, Lai & Foiani, 2012; Prado & Aguilera, 2005) as recombination rates are found to be higher in head-to-head collisions compared to head-to-tail events (Hamperl, et al, 2017)

Various types of organisms, such as yeast and bacteria, have been used to study transcription–replication conflicts and there appears to be a number of different mechanisms involved in regulating the coordination between the two processes and helping initiate recombinogenic lesions (Oestergaard & Lisby, 2017; Gadaleta & Noguchi, 2017; Felipe-Abrio, et al, 2015; Ren, Castel & Martienssen, 2015; Bermejo, Lai & Foiani, 2012).

Chapter 1: Introduction

There is a number of further mechanisms in bacteria that either avoid or resolve replication/transcription-collisions. In replisome, DNA helicases remove proteins and/or RNA-DNA hybrids (R-loops) that are created if the nascent transcript pairs up with its ssDNA template. Transcription regulators also play a critical role via backtracked RNA polymerases or rescuing stalled (Brambati et al., 2015; Merrih et al., 2012), such as the several helicase (including Pif1 and Sen1) which are involved in the maintenance of replication forks, help the removal of RNA:DNA hybrids and prevent replication–transcription interference in vitro (Brambati, et al, 2015; Grierson, et al, 2011; Kassavetis & Kadonaga, 2014). Members of the Pif1 helicase family help fork progress through various types of natural barriers including transcription blocks (Paeschke, Capra & Zakian, 2011). Meanwhile, Sen 1 in particular is required to prevent RNA:DNA hybrids from accumulating at the fork in head with RNA Pol II transcribed genes (Cohen, et al, 2018; Brambati, et al, 2015; Alzu, et al, 2012).

Replication/transcription-collisions in eukaryotes occur at separate genomic loci, such as tDNA (encode tRNA) and rDNA loci, as well as RNA Pol II transcribed genes (Merrih et al., 2012). In eukaryotes, the number of tDNA genes are located throughout the genome, such as 186 tDNA loci in *S. pombe*. *S. pombe* -tDNA, which is transcribed by RNA polymerase III, can slow down the DNA replication process as well as function as chromatin barriers in the centromeres (McFarlane & Whitehall, 2009; Gadaleta & Noguchi, 2017). In organisms such as *S. pombe*, the centromere is between 35 kb and 110 kb in size and consists of three different regions. First is the central core (*cnt*), which is where the kinetochore is assembled. The two regions flanking the *cnt* are referred to as the ‘innermost repeats’ (*imr*) and ‘outer repeats’ (*otr*). Two inverted repeats also surround the *cnt*, which contains tDNA that acts as a barrier between the *cnt* and heterochromatic regions of the centromeres (Mutazono et al., 2017, Jaendling & McFarlane, 2010).

When DNA replication encounters tDNAs it can be slowed and/or paused, which can cause genome instability. This effect was later established when *S. pombe* tDNAs were inserted with the *ade6⁺* gene where they slowed replication fork progression and it was further established that they supply strong replication fork barrier (RFB) activity (Labib & Hodgson, 2007; Pryce, et al, 2009). However, in the presence of a normally functioning DNA replisome, these RFBs did not form measurable recombinogenic lesions, indicating that tDNAs within the genome are not recombinogenic under non-stressed conditions (Pryces et al., 2009). However, when the replisome

Chapter 1: Introduction

becomes compromised (e.g., under replicative stress conditions, or loss of replisomal function) it is proposed that when the replication machinery and RNA polymerase III collide head-to-head with each other, then this can give rise to DNA instability (Lin & Pasero, 2012; Bermejo, Lai & Foiani, 2012; Pryce, et al, 2009). Additionally, in *S. cerevisiae*, the DNA replication-associated fragile sites are enriched for tDNA and as a result these genes are then involved in the development of recombination (Durkin & Glover, 2007; Cha & Kleckner, 2002, Keeney & Neale, 2006). DNA helicase is fundamental to the replication process in Eukaryotes as the helicase resolve issues that could prevent that the DNA replication process can be completed successfully. As in *S. cerevisiae*, DNA helicase Rrm3 is necessary to resolve replication/transcription-collisions (Felipe-Abrio, et al, 2015; Castel et al., 2014).

1.9 Role of Dicer in controlling genome stability

The role for Dcr1 has been shown to be independent of the RNAi pathway. Dcr1 is essential to release stalled RNA Pol II in the pericentromeric heterochromatin *S. pombe*. If the RNAi fails to remove Pol II, it will lead to stalled replication forks, resulting in the induction of genome stability (Ren, Castel & Martienssen, 2015; Castel & Martienssen, 2013; Castel et al., 2014).

Pol II accumulation is polymerase collision hallmark observed in the outside pericentromeric regions of *S. pombe* that resolves replication–transcription collisions. During this process, Dcr1 is an RNAi component that ceases transcription at collision sites, resulting in the preservation of genome integrity (Castel & Martienssen, 2013; Ren, Castel & Martienssen, 2015). Double-strand RNA (dsRNA) molecules are cleaved into approximately between 20–25 nucleotide siRNA duplexes by the Dicer enzyme's endonuclease activity and then processed by other constituents of RNAi mechanism leading to transcriptional silencing (see Section below).

Dicer has been found to be a gene that functions as a haploinsufficient tumour suppressor (Castel, et al, 2014) Dicer mutation gene is related to cancer development (see Section below). (Castel, et al, 2014) further found that Dcr1 is required in *S. pombe* to promote the release of RNA Pol II from both the 3' end of the greatly transcribed genes of RNA Pol II, which leads to the transcription's termination and rDNA-antisense transcription and tDNA being normally transcribed via RNA polymerase I and RNA polymerase III leading to promote replication site

stress and DNA damage. HR is essential if RNA Pol II and the replisome need to be resolved; in the absence of Dcr1, the replication fork is resumed, causing chromosome rearrangements such as translocations and chromosome instability which ultimately leads to the development of cancer (Figure 1.8)(Brambati, et al, 2015; Ren, Castel & Martienssen, 2015; Castel, et al, 2014). Furthermore, Dcr1 mutation leads to build-up of RNA:DNA-hybrids at the locus of rDNA. The reason for this are transcription/replication-mechanism collisions (Castel, et al, 2014).

1.10 RNA-DNA hybrids (R-loops)

When nascent RNA transcripts are re-annealed to their template DNA strand, then RNA:DNA hybrids and R-loops form (Figure 1.9). Initially, R-loops occur naturally during the transcription and replication processes (Gómez-González & Aguilera, 2019; Belotserkovskii, et al, 2018b; Crossley, Bocek & Cimprich, 2019; Belotserkovskii, et al, 2018; Kojima, et al, 2018, Zhao, H., et al, 2018; Ohle, et al, 2016; Fragkos & Naim, 2017). However, many studies on both prokaryotes and eukaryotes demonstrated that the main internal source of DNA damage is the accumulation of hybrid RNA:DNA as they influence the functioning of cells which then has the potential to result in genome instability (Gómez-González & Aguilera, 2019; Belotserkovskii, et al, 2018; Ohle, et al, 2016; Brambati, et al, 2015; Felipe-Abrio, et al, 2015). RNA:DNA hybrids are also main components in blocking transcription elongation and the replication fork's progression, causing stress and leading to the formation of DSBs (Zhao, et al, 2017; Kojima, et al, 2018, Ohle, et al, 2016; Castel, et al, 2014). Moreover, highly recombinogenic accrued at specific replication-transcription collision site accumulates hybrids, that results in recruitment RAD52 (HR factors) and demonstrates that the R-loops misregulation potentially promotes cancer initiation and progression (Crossley, Bocek & Cimprich, 2019; Belotserkovskii, et al, 2018; Brambati, et al, 2015; Castel, et al, 2014; Crossley, Bocek & Cimprich, 2019; Lin & Pasero, 2012).

Therefore, Dcr1 is the key element for the removal of RNA:DNA hybrids that help to solve replication-transcription collision in *S. pombe*. Dicer's new function role could be characterised as acting as tumour suppressor gene (Castel, et al, 2014; Kumar, et al, 2009). Interestingly, several components of pathways that avoid and replication-transcription conflicts are tumour suppressors, such as RAD52 (Mazina, et al, 2017; Ren, Castel & Martienssen, 2015)

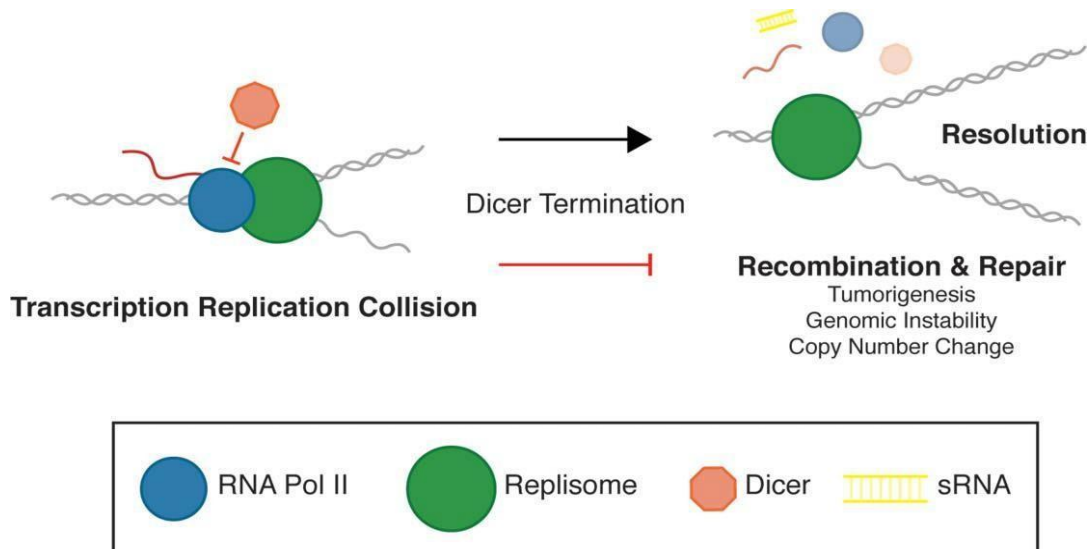


Figure 1.8 *S. pombe* approach resolving the transcription/replication-collision to protect integrity of the genome. Transcription is mediated by RNA Pol II (blue). The collision between RNA Pol II and replisome (green) stalls the replication fork which in turn results in Pol II accumulation. Dcr1 (orange) terminates transcription and leads to replication completion and small RNA (sRNA) inhibition (yellow). If Dcr1 is absent, HR will resolve the collision and restart the replication fork. This may also cause genome instability and change to copy numbers (taken from Ren, Castel & Martienssen, 2015).

Chapter 1: Introduction

To prevent unscheduled RNA:DNA hybrid generation, many mechanisms have been developed in eukaryotic cells to eliminate these hybrids, such as RNase H1 and RNase H201, which are part of a specific group of protein enzymes that remove the RNA moiety of RNA:DNA hybrids, which in turn stalls replication stress and maintains genome stability (Kojima, et al, 2018; Zhao, et al, 2018; Fragkos & Naim, 2017; Brambati, et al, 2015; Ohle, et al, 2016). However, in *S. cerevisiae*, RNA:DNA hybrids also degraded via Sen1—an RNA-DNA helicase that unwinds RNA:DNA hybrids (Santos-Pereira & Aguilera, 2015)

A recent finding has demonstrated that *S. pombe* is required to both generate and remove RNA:DNA hybrids to obtain complete homologues recombination efficiency. This suggests that RNA:DNA hybrids have an unpredicted positive role in the DNA repair process to maintain genome instability. Too little RNase H will lead hybrids to inhibit HR completion, whereas too much RNase H will lead hybrids to allow earlier steps of HR, so a small quantity of RNA:DNA is actually needed (Ohle, et al, 2016). This indicates that both these hybrids must be generated and remove processes that depend primarily on RNase H1 (Rnh1) and RNase H2 (Rnh201). In addition, extensive research on unexpected *S. pombe* observations should be verified to identify additional factors that are involved in RNA:DNA hybrid creation at breaks as well as investigations into additional roles played to protect genome stability by both hybrids (Plosky, 2016; Ohle, et al, 2016) .

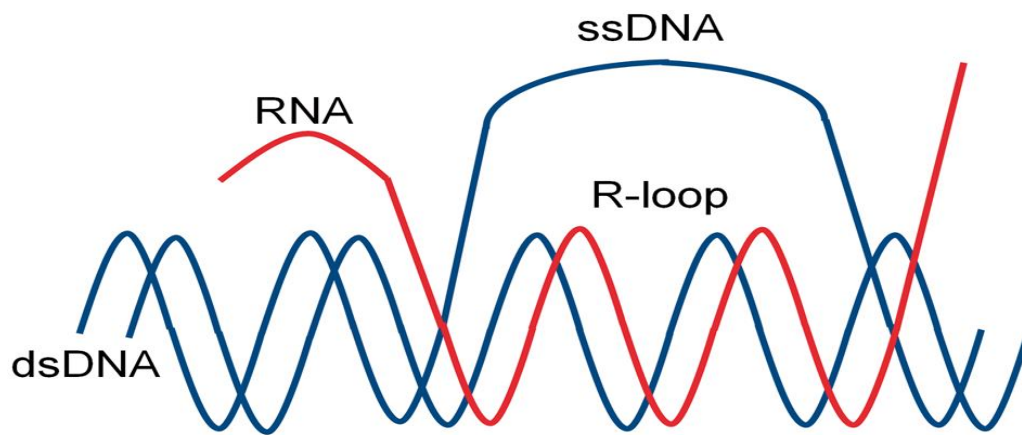


Figure 1.9 R-loop structure. An R-loop is defined as a three-stranded structure that consists of a single-stranded DNA and an RNA/DNA hybrid. The latter is created through annealing of the nascent mRNA to the complementary DNA strand's template (taken from Kojima et al., 2018).

1.11 RNA interference (RNAi)

RNAi is an essential mechanism regarding the regulation of gene expression (both transcriptional and the post-transcriptional) in a wide range of eukaryotes (Son, et al, 2017; Nicolás & Ruiz-Vázquez, 2013; Kalantari, Chiang & Corey, 2015; Chang, Y., et al, 2013; Cottenet, 2017). For this purpose, RNAi utilises small non-coding RNA molecules with an approximate length of 20 to 30 nucleotides (Meng & Lu, 2017; Cottenet, 2017; Castel & Martienssen, 2013; Patil, Zhou & Rana, 2014; Holoch & Moazed, 2015; Kalantari, Chiang & Corey, 2015). There are two main pathways for gene expression regulation by RNAi, the first pathway being known as post-transcriptional gene silencing (PTGS). PTGS inhibits the translation of mRNA in the cytoplasm by directly targeting the mRNA. The other pathway is referred to as chromatin-dependent gene silencing (CDGS), which involves promoting the generation of heterochromatin to repress specific genes by inhibiting transcription (Moazed, 2009; Tatiparti, et al, 2017).

Several different short regulatory RNAs exist, including the first small interfering RNAs (siRNAs) as well as the microRNAs (miRNAs). These are involved in initiating transcriptional repression. A third type is the PIWI-interacting RNAs (piRNAs), which are involved in the transcriptional repression of transposons in the germlines of animals (Son, et al, 2017; Holoch & Moazed, 2015; Moazed, 2009; Castel & Martienssen, 2013). It is important to note that both siRNAs and miRNAs (as main RNAi mediators) participate in both CDGS and PTGS (Chen, et al, 2018; Son, et al, 2017; Moazed, 2009; Holoch & Moazed, 2015; Castel & Martienssen, 2013). When the RNAi PTGS process is first started, long double-strand molecules of RNA (dsRNA) are produced through various pathways that become processed into siRNA. dsRNA can be generated by transcripts from opposite strands; long-hairpin RNAs can form intra-strand dsRNA. These dsRNA are a substrate for a type RNase III enzyme called Dicer.

Dicer has an endoribonuclease activity, and cleaves the dsRNA molecules into small dsRNA with 20–25 nucleotide (nt) in length. Following that, the siRNA from the previous step is assembled into the RNA-induced silencing complex (RISC). RISC possesses endoribonuclease activity via a subunit termed Argonaute. In this process, the duplex siRNA is loaded onto the Argonaute protein with two strands, one of which stays bound to the RISC, while the second strand (the so-called

Chapter 1: Introduction

‘passenger’) is removed so. This exposes the guide strand sequence. The RISC complex, with the help of the guide strand, is then directed to the target mRNA so that cleavage and silencing can take place through the Argonaute component.

It is necessary that sequence-specific base-pairing between siRNA and mRNA occurs for this process to be carried out, as the siRNA is perfectly complementary to its mRNA target, which can cause transcriptional degradation (Chen, et al, 2018; Son, et al, 2017; Bartel, 2004; Kalantari, Chiang & Corey, 2015; Swarts, et al, 2014; Volpe & Martienssen, 2011).

Translin/Trax is a complex of two proteins. It is considered a component-3-promoter of RISC (C3PO) (see Section 1.10) and acts as an endoribonuclease, and aids the cleaving of the siRNA’s passenger strand as well as the binding of the duplex siRNA onto the Argonaute protein (RISC). It is possible to observe this process particularly well in *Drosophila melanogaster* and also human cells (see Section 1.12) (Jaendling, et al, 2008; Wang, et al, 2016; Tian, Y., et al, 2011; Ye, et al, 2011). New RNA-strand RNAi processes can have an effect on gene expression at an individual gene level via CDGS. This is mediated via localised epigenetic modification of chromatin. This potentially causes the repression of the transcription and the development of heterochromatin. The process, referred to as transcriptional gene silencing (TGS), involves targeting histones and DNA methyltransferases (Castel & Martienssen, 2013; Holoch & Moazed, 2015). Currently, we have the most understanding of how the processes of RNAi pathways function in the formation of heterochromatin in *S. pombe*.

In *S. pombe*, nuclear siRNA drives the formation of heterochromatin (Woolcock & Bühler, 2013; Alper, Lowe & Partridge, 2012; Reyes-Turcu & Grewal, 2012; Castel & Martienssen, 2013; Holoch & Moazed, 2015). This is achieved by siRNA targeting nascent centromeric RNA molecules, a product of RNA polymerase II. It is of note that *S. pombe* possesses a single copy of genes from the RNAi pathway; this includes Argonaute (*ago1*), Dicer (*dcr1*) and also RNA-dependent RNA polymerase (*rdp1*). A mutation in these genes leads to a loss of the heterochromatin at the centromere; this is measured by the loss of histone 3 lysine 9 methylation

Chapter 1: Introduction

and Swi6 (HP1) localization to areas of heterochromatin (Alper, Lowe & Partridge, 2012; Holoch & Moazed, 2015). In *S. pombe*, RNA polymerase II (RNA Pol II) initiates the process. RNA polymerase II generates nascent RNA transcription, which are used as template for RNA-dependent RNA polymerase complex (RDRC) to transcribe the pericentromeric RNA repeat. Transcription into dsRNA (Figure A 1.10). What then follows is their assembly into an RNA-induced transcriptional silencing (RITS) complex. This complex contains Chp1 and Ago1 to feedback targeting RITS to the nascent RNA and stop translation.

This leads to the recruitment of a complex consisting of Clr4-Rik1-Cul4 (CLRC). The Histone methyltransferase (Clr4) that is contained in this complex methylates methylated histone (H3K9). H3K9me is needed for both the assembly and the spreading of heterochromatin; it is a binding site for Swi6, which is necessary for the formation of heterochromatin protein. Lastly, Chp1 signals to the RDRC complex (Rdp1) to increase the number of dsRNAs, which in turn are cleaved by Dcr1. This is necessary for the process to continue (Figure 1.10) (Castel & Martienssen, 2013; Tadeo, et al, 2013; Holoch & Moazed, 2015; Kalantari, Chiang & Corey, 2015b, Zocco, et al, 2016; Matsui & Corey, 2017). RNAi (RITS) is further essential for the formation of heterochromatin at a number of genomic loci, for example transposon long terminal repeats (Woolcock et al., 2011). It should be noted that to date, there is no evidence that *S. pombe* C3PO orthologues [Tsn1 (translin)/Tfx1 (Trax)] are required for centromeric or heterochromatin silencing. Indeed, Tsn1 and Tfx1 mutants do exhibit any overt phenotype and no centromeric or heterochromatic defective (Gomez-Escobar et al., 2016; Jaendling et al., 2008).

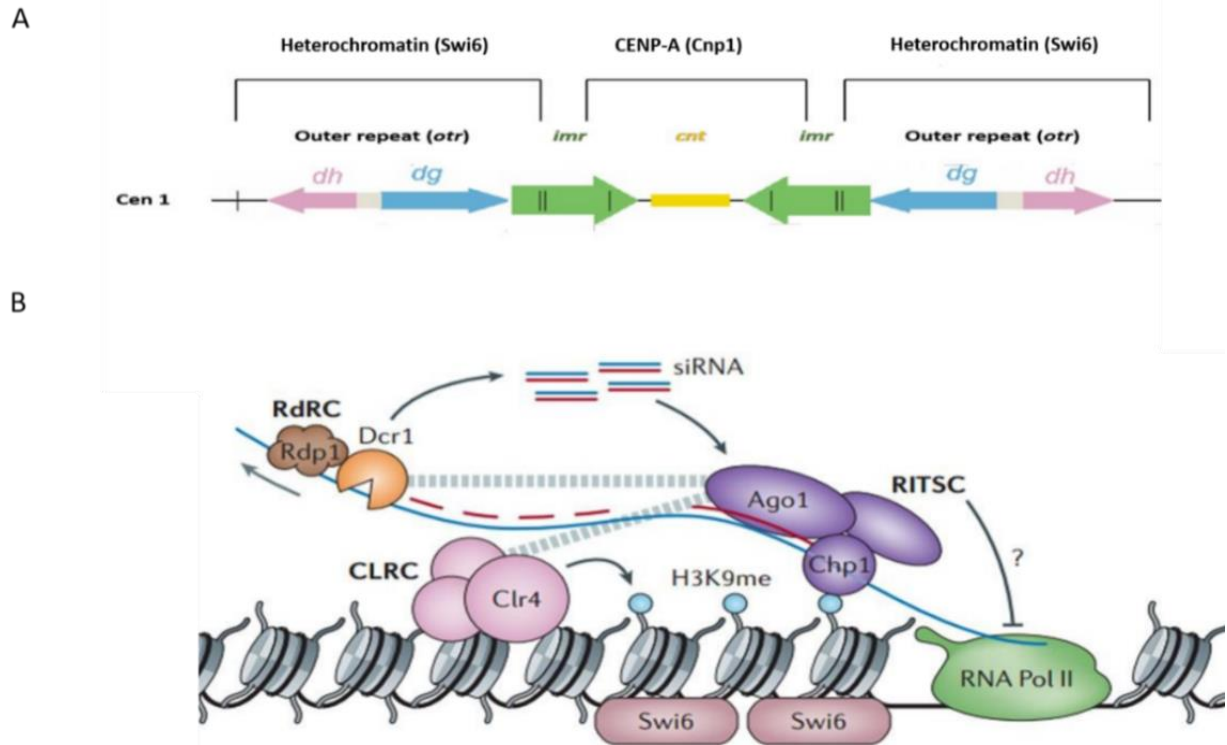


Figure 1.10 RNAi model for heterochromatin assembly at the *S. pombe* centromere. (A) Centromeric core regions in *S. pombe* consist of two different regions, *imr* (green) and *cnt* (yellow). Surrounding these two regions is the region otr (light blue/purple). This consists of two repetitive sequences: *dg* (light blue) and *dh* (purple). The vertical lines of the *imr* region depict the boundary elements (tRNA genes). (B) The RITS complex, consisting of Ago1, Chp1 and siRNA, plays a role in targeting nascent transcripts (shown in the model in blue) through siRNA base pairing. This in turn leads to RNA Polymerase II transcription being inhibited, though the exact process is currently not known (hence it is symbolised by a question mark). Chp1 and H3K9 interaction then leads to Clr4 recruitment to methylate histone H3K9, which is then used as a binding site for. The result is a double-stranded RNA (dsRNA) which consists of siRNA and the nascent strand. The RdRC complex (Rdp1) then uses the nascent strand to produce more dsRNAs. Dcr1 cleaves them into siRNAs. Both the RNA- and the H3K9me-cycle are heavily linked via an RITS complex. This is to promote the efficient assembly of heterochromatin (adapted from Castel & Martienssen, 2013).

1.12 Translin and Trax

Translin is a novel nucleic acid binding protein which was discovered through an analysis of the factors that bind to the breakpoint junctions of chromosomal translocation in lymphoid tumours in humans (Aoki et al., 1995). Translin has been found to show specific strong binding to single-stranded DNA and consensus sequence motifs 5'-ATGCAG-3' and 5'-GCCC (A/T) (G/C) (G/C) (A/T)-3' at chromosome translocation breakpoint junctions in several cases of lymphoid malignancies (Aoki, et al, 1995, Kasai, et al, 1997). Translin displayed particular binding to the breakpoint junction of chromosome in a patient diagnosed with Chronic Myeloid Leukaemia (CML) carrying t(9;22)(q34;q11) (Martinelli et al., 2000) and another patient diagnosed with Acute Myeloid Leukaemia (AML) carrying t(9;11)(p22;q23) (Atlas, et al, 1998, Martinelli, et al, 2000). It is also believed to be a factor in a type of sarcoma known as liposarcoma, as Translin binding sequences have been identified at the reciprocal translocations breakpoints between fused in sarcoma (FUS) on chromosome 16 (short arm) and CHOP on chromosome 12 (long arm) (Hosaka, et al, 2000, Kanoe, et al, 1999). Other chromosomal translocation breakpoints that are associated with cancer development have also been identified as Translin DNA binding sites; notably, hot spots of human male meiotic recombination also feature Translin sites (Abeyasinghe, et al, 2003; Visser, et al, 2005; Wei, et al, 2003; Gajecka, et al, 2006b). It can be argued, however, that a mechanistic role showing Translin functions directly in chromosome translocation is still unproven. Furthermore, Translin-null mutants did not show any notable defect in recombination processes such as meiotic recombination and recovery of DNA damage in eukaryotes such as mice, *Drosophila* and *S. pombe* (Yang, S. & Hecht, 2004; Jaendling & McFarlane, 2010; Jaendling, et al, 2008; Claußen, et al, 2006).

The name 'Translin' is derived from the word 'translocation'. Translin is a protein with an approximate molecular weight of 26 kDa. Human Translin consists of 228 amino acids (Lluis, et al, 2010; Jaendling & McFarlane, 2010). Research found that in the case of mice, Translin is the gene that encodes the testis–brain RNA-binding protein (TB-RBP) (Wu, et al, 1997). Additionally, TB-RBP plays a role in mRNA regulation in both spermatogenesis as well as neurons (Moazed, 2009; Li, Z., Wu & Baraban, 2008; Jaendling & McFarlane, 2010). Keeping this role in mind, Translin-deficient drosophila and mice have displayed behavioural abnormalities (Stein, et al, 2006; Suseendranathan, et al, 2007; Jaendling, et al, 2008).

Chapter 1: Introduction

Using Translin as ‘bait’, a yeast two-hybrid screen was carried out and another protein called Translin-associated factor X (Trax) was recognised. The molecular weight of Trax is approximately 33 KDa and its amino acid sequence is paralogous to Translin’s amino acid sequence (Aoki et al., 1997). This suggests a possible association between Trax and Translin proteins. In addition, Trax stability depends on the stability and Translin existence (Yang & Hecht, 2004; Jaendling, et al, 2008). This phenomenon highlights the close functional association between the two binding partners. Moreover, it has been demonstrated that both Translin and Trax orthologs should be found together in all kind of eukaryotic (Chennathukuzhi, et al, 2003; Claßen, et al, 2006; Jaendling, et al, 2008; Jaendling & McFarlane, 2010).

Translin appears controls to levels of Trax at a post-transcriptional level. This observation was identified by mutation of *Tsn1* gene encoding for both in *S. pombe* and mice after that compare the level of *tfx1* mRNA and protein. The deletion resulted in a significant reduction on level of Trax but no alteration mRNA level (Kasai, et al, 2018). However, despite the close association, the Translin stability has not been commanded by Trax (Claßen, et al, 2006). Translin and Trax are highly-conserved proteins across humans to fission yeast. This indicates that they are likely to play a crucial biological role (Jaendling & McFarlane, 2010; Laufman, et al, 2005; Martienssen, Zaratiegui & Goto, 2005). Since their discoveries, Translin and Trax have been postulated to be involved in several biological processes, including genome stability, response to DNA damage, cell growth, RNAi, mRNA transport and translation, and the microRNA degradation in the process of oncogenesis, the latter resulting in the suggestion that both proteins Translin/Trax could be druggable oncology targets (Gomez-Escobar, et al, 2016).

1.13 Biochemical Characteristics of Translin and TRAX

The Translin found in mice and the Translin found in human cells each only have three distinct amino acids, while the remaining ones are identical. Translin in fission yeast consist of 236 amino acids and has 36% identity with the human Translin. Translin and TRAX are highly evolutionarily conserved, with considerable primary sequence homology between several species, including humans, fruit flies, zebrafish, thale cress, and even mould (*Neurospora crassa*) (Parizotto, Lowe and Parker, 2013). Example sequence comparisons are shown in Figure 1.11

Chapter 1: Introduction

Translin and TRAX have been considered as potential therapeutic agents in oncology as various cancers have been shown to display degradation of precursors for tumour-suppressing miRNAs that is largely the result of translin-TRAX activity (McFarlane and Wakeman, 2020). However, given the range of functions of this protein complex, therapeutic intervention that affects translin-TRAX function may have further repercussions beyond the pharmacological intentions.

One of the key model systems that has allowed greater understanding of the translin-TRAX systems is *Schizosaccharomyces pombe*. The genes for both proteins have been identified in the yeast, and in the first study of the *S. pombe* homologs, deletion of the genes slightly increased cell proliferation, demonstrating that these genes were not essential for replication in fission yeast, however the yeast form of translin has much higher binding affinity for RNA (Laufman *et al.*, 2005). More recently, specific amino acids within the translin protein structure have been identified (Y85, R86, H88, R92 and K193) which provide a substantial portion of the RNA binding affinity (Gupta, Pillai and Chittela, 2019). It has been discovered that conserving Translin leads to the formation of octameric rings; a similar change in structure also occurs in the family of helicase enzymes, which are associated with DNA repair as well as recombination and replication (Kasai, et al, 1997b; VanLoock, et al, 2001; Ishida, et al, 2002; Fukuda, et al, 2008; Jaendling, et al, 2008; Jaendling & McFarlane, 2010).

Translin binds ssDNA and ss/dsRNA (Kasai, et al, 1997; Eliahoo, et al, 2014). Crystallographic studies have found that Trax and Translin form a 2:6 barrel-like octamer that was recently recognized as C3PO (Ye, et al, 2011; Parizotto, Lowe & Parker, 2013; Zhang, J., et al, 2016; Park, et al, 2017). Translin and Trax create a heterooctamer complex can act as an RNase, the activity of which depends on the Trax subunit (Chennathukuzhi et al., 2003; Yang & Hecht, 2004; Jaendling & Mcfarlane, 2008). The heterooctamer has the ability to bind to ssDNA sequences and to a lesser degree, it can also bind to ssRNA sequences, though this ability is less developed. Translin homooctomer can bind to both single-stranded RNA (ssRNA) as well as double-stranded-RNA (dsRNA) (Liu, Y., et al, 2009; Jaendling & McFarlane, 2010; Parizotto, Lowe & Parker, 2013; Fu, Shah & Baraban, 2016). It has been found that Translin can act as an RNase in vitro. However, a similar DNase activity was not found (Wang et al., 2004).

Chapter 1: Introduction

While Trax is also usually found in the cytoplasm, Translin is localised in the nucleus as well as in the regions of the cytoplasm (Yang, S., et al, 2004; Li, Wu & Baraban, 2008; Eliahoo, et al, 2014). Moreover, studies on mice have shown that the binding of Translin (TB-RBP) to RNA is inhibited by Trax and that the binding activity of Translin to ssDNA sequences is enhanced (Chennathukuzhi, et al, 2003; Gupta, G. D. & Kumar, 2012; Park, et al, 2017; Wang, et al, 2016b).

The Translin found in humans is more likely to bind to single-stranded microsatellite (d(GT)_n) repeats as well as G-strand telomeric repeats (d(TTAGGG)_n), which is an indication that Translin has a function in either microsatellite repeat function or telomere functions (Jacob, et al, 2004; Jaendling, et al, 2008; Laufman, et al, 2005). In addition, when *S. pombe* and human Translin are compared, we see that human Translin has a preference for G-rich ssRNA, rather than G-rich ssDNA. It appears that Translin has a function within the metabolism of RNA, rather than the metabolism of DNA (Hecht, 2008; Jaendling & McFarlane, 2010).

Previous studies have proven that both Translin- and Trax complexes play a part in regulating mRNA, in particular in processes involving neuronal dynamics. In both the testis and the brain cells of mice, Translin protein supports both the transport of mRNA and also the stabilisation of mRNA. Studies have suggested that Translin binds to specific RNA sequences at the end of 3'-UTRs untranslated regions of target mRNAs (Han, Gu & Hecht, 1995). It is further believed that Translin is involved in stabilising a specific miRNA found in germ cells, a phenomenon which suggests that Translin could also be involved in regulating the posttranscriptional gene expression in male germ cells (Yu & Hecht, 2008).

It is believed that in cells of mammalian origin, the Translin and Trax-complex controls the targeting of brain-derived neurotrophic factor (*BDNF*) mRNA to neuronal dendrites. In addition, human neurological disorders have been observed in cases where the binding regions of Translin and Trax within *BDNF* mRNA are affected by mutation (Gupta, A., Pillai & Chittela, 2019; Chiaruttini, et al, 2009), which implies that Translin and Trax are potentially supporting normal functioning of the nervous system (Jaendling & McFarlane, 2010; Gomez-Escobar, et al, 2016).

Chapter 1: Introduction

Again in mammalian cells, Translin and Trax potentially also control some aspects of mitotic cell proliferation function (Yang & Hecht, 2004; Yang, et al, 2004). Research on the base-line expression levels of various proteins noted that when cells divide mitotically, the expressions indicate a relationship between the Translin-level and the rate of cell proliferation. Any overproduction of Translin can result in increased cell proliferation (Ishida, et al, 2002). Studies have additionally proven that the expression of *Tsn*-gene occurs in particular periods during the cell cycle. It starts in the S-phase and while reaching its optimum in G2/M phase. It is therefore possible that Translin influences the replication of DNA and might also have the ability to lead to an increased cell division rate.

Microscopic analysis has furthermore proven that Translin also helps in speeding up the microtubule-arrangement as well as chromosome-segregation during mitosis (Ishida et al., 2002). In a study on *S. pombe*, it has additionally been observed that in the case of loss of Tsn1 and Tfx1, the rate of cell proliferation increases slightly (Laufman et al., 2005).

Translin	
D.melanogaster	QRLIFIIALVIYL [29] EDYLLGILQLASELSR
H.sapiens	QRLVFLAAFVVYL [29] EDYLSGVLILASELSR
D.rerio	QRLAFLAAFVVYL [29] EDYLAGVLILASELSR
A.thaliana	QAVVSQALAFMHWL [26] EDYLTGICFMSNDLPR
N.crassa	QDAIATVLLHAWL [41] EYLLALISVVEDLSR
Trax	
D.melanogaster	QEFIEAYTYMEYL [61] TEYILGLSDLTGELMR
H.sapiens	QEYVEAVSFQHFI [47] VDYLLGVADLTGELMR
D.rerio	QEYVEAVSFHHFI [42] TDYLLGVADLTGELMR
T.adhaerens	EEFVEAMTYYYL [24] YDFAAGIADLSGELMR
A.thaliana	QEYVEAATFYKFC [30] LDYILGLADLTGELMR
N.crassa	EELAEALTFAHYL [79] DDYFYGVFDLSGEMMR

Figure 1:11 Sections from the primary structures of translin and TRAX in humans, fruit flies, zebrafish, thale cress, and neurospora mould, indicating similarities and conserved amino acids at various points across creatures in these kingdoms (Liu et al., 2009).

1.14 Translin and Trax: RNAi interference

In human cells as well as in *Drosophila*, a Translin-Trax hetero-octamer complex (C3PO) has been found to be essential in the regulation of RNA interference (RNAi) (Liu, et al, 2009; Ye, et al, 2011; Zhang, et al, 2016). It was further proven that the Trax-subunits in these hetero-octamers are fundamental in regards to the ribonuclease activity of this complex (Parizotto, Lowe & Parker, 2013; Weng, et al, 2018; Kasai, et al, 2018). When point mutation occurs in the catalytic sub-units in Trax, the RNase activity of C3PO is affected (Tian, et al, 2011; Kasai, et al, 2018; Baraban, Shah & Fu, 2018). Small interfering RNAs (siRNAs) mediate RNA interference and function together with the RNA-induced silencing complex (RISC) (more details see previous Section 1.10). In order to activate the RISC, which is necessary for the silencing activity, the transformation of the RLC (RISC loading complex) to the RISC is required (Chen, et al, 2018; Son, et al, 2017; Castel & Martienssen, 2013; Holoch & Moazed, 2015).

In recent studies, C3PO was shown to carry out endoribonuclease activity, cleaving off the passenger strand from the siRNA precursor duplex. This permits the guidance of the strand towards RISC (Ago2) in order to cleave and silence the targeted mRNAs (Figure 1.12). However, the exact mechanism associated with removal of the passenger strand has not quite been identified (Liu, et al, 2009; Ye, et al, 2011).

The yeast *S. cerevisiae* contains neither Translin/Trax orthologues nor any RNAi pathways (Laufman, et al, 2005; Jaendling & McFarlane, 2010). In addition, the function of C3PO in RNAi may be restricted to certain eukaryotic species only; for instance, C3PO does not participate in RNAi in the filamentous fungus *Neurospora crassa*. However, *N. crassa* C3PO does act as a ribonuclease in the processing of tRNA, specifically in the maturation-process of pre-tRNAs to tRNAs (Li, L., et al, 2012). After pre-tRNA processing by ribonuclease P (RNase P), C3PO removes the fragments of pre-tRNA at the 5' end. Furthermore, Li et al. (2012) found C3PO also potentially participates in tRNA-processing in mouse embryonic fibroblast cells.

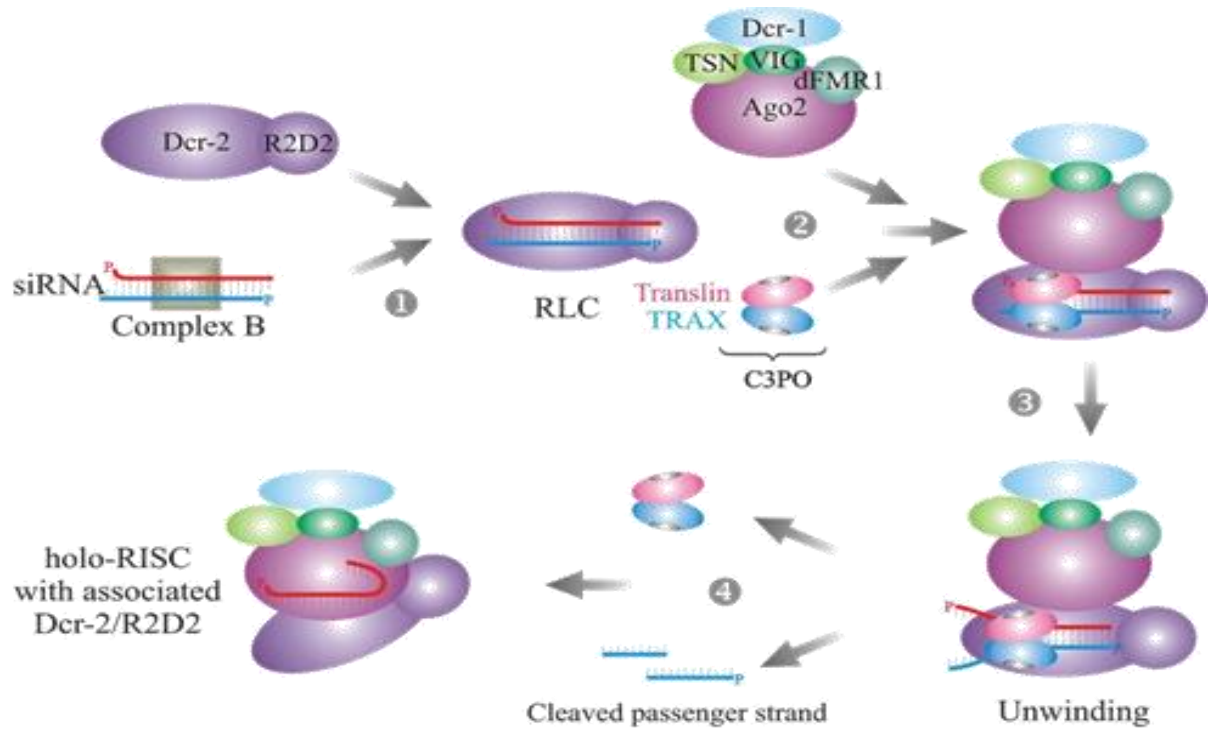


Figure 1.12 Diagram showing the role of the Translin and Trax)C3PO(in *Drosophila* RNAi pathway. The figure depicts the four steps for C3PO in the RNAi pathway. Step 1: Transfer of the small interfering RNA (siRNA) duplex (which consists of the passenger and the guide strands) from complex B to RLC (RISC loading complex) that contains both Dcr-2 and R2D2. Step 2: Joining together of the C3PO (Translin and Trax) with the RLC complex, then the RISC complex, which contains particular components, including Dcr-1 and Ago2. This generates holoRISC through a Dcr-2–Ago2 interaction. Step 3: Removal of the passenger strand from the siRNA duplex, which is induced by the endonuclease activity of C3PO. Step 4: The holoRISC complex associates and then targets the selected mRNA (taken from Jaendling & McFarlane, 2010).

1.15 Evidence roles of Translin and Trax in DNA Repair

Research indicates that both Translin and Trax play an important role in DNA repair processes. After treating HeLa cells with either etoposide or mitomycin C, Translin could be observed to translocate from the cytoplasm to the nucleus (Kasai, et al, 1997; Jaendling & McFarlane, 2010). When DNA in mouse cell lines was treated with damaging agents (ionising irradiation or mitomycin C), Translin was translocated in the nucleus, whereas longer incubation resulted in the reduction in Translin on the nuclear level (Fukuda, et al, 2008). This finding suggests that damage to cells leads to a signalling mechanism being activated (Kasai, et al, 1997; Jaendling & McFarlane, 2010). Moreover, after being exposed to X-rays, the formation of hematopoietic colonies in Translin knockout mice was delayed compared to their wild types. This leads to the assumption that there is a tissue specific role for Translin in DNA damage recovery (Fukuda, et al, 2008; Jaendling & McFarlane, 2010). This is because Translin does not have a nuclear localisation signal (NLS). This leads to the postulate that the nuclear transport in Translin depends on it directly interacting with additional proteins which carry a nuclear localization signal (NLS). There is a possibility that one of these is Trax (Kasai, et al, 1997; Laufman, et al, 2005).

Trax and Translin bind to a number of other proteins that are a part of the processes involved in DNA damage response. Use of a yeast-two hybrid system revealed that murine Translin binds to factor GADD34 (growth-arrest and DNA-damage-inducible Protein) (HASEGAWA, et al, 2000; Jaendling & McFarlane, 2010). GADD34 is involved in initiating the translation (Patterson, et al, 2006) which leads to the hypothesis that Translin, in conjunction with apoptosis inhibitor protein GADD34, could be associated with an RNA-processing/binding activity rather than being directly involved in DNA damage repair (Jaendling & McFarlane, 2010).

However, it has also been proposed that GADD34 may support the transport of Translin from the cytoplasm to the nucleus as part of the response to any damage detected in the DNA (HASEGAWA, et al, 2000). Moreover, when cells are exposed to gamma radiation, Trax interacts with C1D protein, an activator for the DNA-dependent protein kinase (DNA-PK). This prevents the association of Trax with Translin (Erdemir, et al, 2002). In both the HR and NHEJ pathways, C1D protein is essential for DNA repair (Li & Heyer, 2008; Erdemir, et al, 2002).

Chapter 1: Introduction

Currently, the direct function of Trax in repairing DNA damage has not been entirely understood. However, it is possible that Trax plays an essential role in DNA damage repair through its interaction with Ataxia Telangiectasia Mutated (ATM)-mediated pathway, which is essential for the MRN complex at DSBs (Chern, et al, 2019; Wang, et al, 2016). It was further shown that a dysfunctional Trax can lead to ATM-inactivation (Wang et al., 2016). While studies have indicated that Translin and Trax react to DNA damage, the mutants of *S. pombe* *tsn1* and *tfx1* have shown no sensitivity for several damaging agents – including Mitomycin C, Phelomycine, HU hydroxyurea, MMS methylmethanesulphonate and UV – has been detected (Jaendling & McFarlane, 2008). Moreover, various genetic assays which investigated their possible involvement in recombination or genome stability failed to demonstrate that Translin and Trax (Tsn/Tfx) have such a function in *S. pombe* model organisms (Jaendling, et al, 2008).

1.16 The Role of Translin and Trax in Oncogenesis

The most widely known function of Dicer is its role as a ribonuclease enzyme within RNA interference (RNAi), where it causes the generation of small RNAs (Moazed, 2009; Castel & Martienssen, 2013; Kasai, et al, 2018; Holoch & Moazed, 2015; Son, et al., 2017). Dicer is critical for the regulation of biogenesis and also aids the process of maturation of most miRNAs. The RNaseIII Dicer transforms precursor miRNAs (pre-miRNA) to mature miRNAs (Asada, et al, 2014; Svobodova, Kubikova & Svoboda, 2016; Mei, Kehui & Wenming, 2016; Song & Rossi, 2017; Kasai, et al, 2018). This in turn signals Argonaute to function as a translational suppressor of specific mRNAs. miRNAs are essential when it comes to the modulation and the regulation of approximately 30% of human gene expression. In numerous types of human cancers, it can be observed that the small non-coding RNAs fail to function as intended. Additionally, miRNAs also help to reduce activity of several tumour-suppressive and oncogenic mRNAs. It is therefore possible to conclude that these small RNAs can have both an oncogenic as well as a tumour-suppressing function (Kumar, et al, 2009; Hata & Kashima, 2016; Gurtner, et al, 2016; Voglova, Bezakova & Herichova, 2016). The Reduction of mature miRNAs and accumulation of pre-miRNAs have been identified in many human cancer tissues (Gurtner et al., 2016; Kasai, et al, 2018). Moreover, the complete loss of the miRNA- generating enzyme Dicer is fatal for cells and leads to tumour formation and progression (Kumar, et al, 2009; Asada, Canestrari & Paroo, 2016).

Chapter 1: Introduction

However, typically, 40% of cancers show Dicer1 haploinsufficiency. Studies have shown that deficiency of Dicer can directly cause miRNA depletion, with their tumour suppressor activities being also lost as a result (Asada et al., 2014; Fu et al., 2016; Hata & Kashima, 2016; Asada, Canestrari & Paroo, 2016). It has been discovered that the Translin and Trax (TN/TX) complex functions as an RNase enzyme by degrading pre-miRNAs in Dicer1 haploinsufficiency (Figure 1.13). Inhibition of (TN/TX) activity in Dicer haploinsufficiency tumours lead to both miRNA and tumour suppression restoration (Fu et al., 2016; Hata & Kashima, 2016; Kasai, et al., 2018). This has led to the hypothesis that these two proteins can act as therapeutic targets for proper functioning of the miRNA (Asada, et al, 2014; Asada, Canestrari & Paroo, 2016).

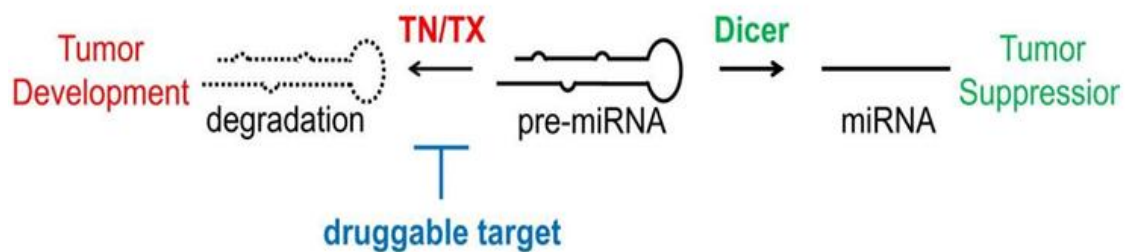


Figure 1.13 Complex of Translin and Trax (TN/TX) a -possible therapy-target for Dicer deficient tumours. The Translin and Trax (TN/TX) complex has been proposed as a possible useful therapeutic target in the aim to restore tumour suppression-function miRNA. Normal levels of Dicer lead to formation of mature miRNA from pre-miRNA, which in turn leads to tumour suppression. However, in haploinsufficiency of Dicer the ribonuclease complex of (TN/TX) causes the pre-mRNAs to degrade, which subsequently results in the development of a tumour. For this reason, it can be hypothesised that inhibition of (TN/TX) prevents miRNA-loss to suppress the development of tumours and Dicer-deficiency (taken from Asada et al., 2016).

Chapter 1: Introduction

1.17 *S. pombe* as a model organism for this project

The fission yeast, also known as *S. pombe*, was first isolated in Africa. It is primarily used for brewing purposes. The yeast was taken out from millet beer by Paul Linder who named it ‘*Pombe*’, meaning ‘beer’ in Swahili. From 1950s onwards, the yeast began to be widely used for research purposes (Nurse, 2002). The size of the complete genetic content of this yeast is around 13.8 Mb and it consists of three chromosomes of varying size, namely 3.5, 4.6 and 5.7 Mb, respectively (Wood et al., 2002; Koyama et al., 2017). 2002 saw the completion of the whole genome sequence, which revealed that the *S. pombe* genome contains around 5000 genes (Wood et al., 2002). Several genes are conserved in both *S. pombe* and humans; these genes are missing in other model organisms, for example in the budding yeast *S. cerevisiae* (Koyama et al., 2017). Recently *S. pombe* has been used as a tool for RNAi and cellular epigenetics exploration (Laufman, et al, 2005). Buhler & Gasser, 2009; Zhang et al., 2016; Koyama et al., 2017). The RNAi pathway in *S. pombe* has single copy RNAi genes such as *ago1* and *dcr1* (Martienssen et al., 2005; Zhang, et al., 2016). All these mentioned features, and the facile nature tractability/ genetics make *S. pombe* an excellent laboratory model organism for this present project.

1.18 Aims of this Study

The overarching aim of this research is to investigate the function of Trax (Tfx1) and Translin (Tsn1) in the genome stability regulation.

- To assess the relationship between the RNAi gene Dcr1, Tfx1 and Tsn1 in genome instability regulation. Several DNA damaging drugs were used to find out the effect of Tfx1 and Tsn1 with RNAi factors on the DNA repair.
- To determine whether Tsn1 and/or Tfx1 have role in recombination regulation by using recombination system that monitors the frequency of recombination at tRNA gene. In order to monitor recombination a plasmid-by-chromosome recombination system was developed at the *ade6* locus. This recombination system has been previously used to show tRNA genes slow DNA replication fork progression thus acting as a replication fork barrier (RFB) and stimulating recombination. This system works by introducing a single tRNA gene, separately in both orientations (orientation 1 and orientation 2) into the unique *Bst*XI site in the *S. pombe* genomic *ade6* locus; this causes the strains to become auxotrophic for adenine.

Chapter 2: Materials and Methods

Chapter 2: Materials and Methods

2.1 Media and strains utilized in this project.

The Media used in this project are shown in (Table 2.1). *Schizosaccharomyces pombe* strains used in this project are listed in (Table 2.2). *Escherichia coli* strains used in this project are shown in (Table 2.3). The required nucleotides, amino acid as well as other supplements for fission yeast media were added to special media as required with the final concentration equivalent to 200 mg/L. Antibiotics like ampicillin (Sigma), geneticin (G418) (Sigma), nourseothiricin (Werner BioAgents) used as the concentration of 100 µg/mL.

2.2 Plasmid extraction procedure from *E. coli*.

The process of plasmid extraction from *E. coli* strains have been developed via using the QIAGEN miniprep kit. For this, *E. coli* stocks at (from -80°C storage) was inoculated in 5 mL broth of Luria Bertani (LB), consisting of ampicillin (100 µg/L). The culture was incubated in orbital incubator overnight at 37°C. Following incubation, the cells were spun at 3,000 g for 5 minutes. The pellet was resuspended in 250 µL P1 buffer (at 4°C) containing RNase A (ribonuclease), ensuring no visible clumps are formed after resuspending the pellet. This was followed by transferring the mixture to sterile Eppendorf tube, then 250 µL lysis buffer (P2) was added to kill and lyse the cells. This procedure involved, gentle mixing of the content in the tube, by inverting the tubes 5-6 times; this facilitates shearing of genomic DNA. The lysis reaction was not left more than 5 minutes. After thorough mixing, 350 µL neutralising/binding buffer (N3) was added, the tubes were immediately inverted for gentle mixing at least for 5-6 times. The tube was spun for 12,000 r.p.m for 10 minutes in a table-top microfuge. The pellet was thrown out, while the supernatant was collected and transferred to new QIAprep spin column (QIAGEN). The tubes were spun at 12,000 r.p.m for 30-60 seconds, pellet was bathed and washed in 0.5 mL PB buffer (washing buffer) after rejection all supernatant. This step was followed by centrifugation maximum at 13,000 r.p.m for about 30-60 seconds table-top microfuge, after discarding the supernatant, the QIAprep tube was rinsed with 750µL PE buffer, again followed by centrifugation maximum at 12,000 r.p.m for 30-60 seconds in table-top microfuge. The supernatant was discarded and then centrifuged for 1 minute to eliminate residual wash buffer, to avoid residual alcohol hindering. Further steps and interfere with enzymatic activities. The total DNA of cells were eluted by taking 50 µL buffer EB containing 10 mM Tris-Cl with (pH 8.5) to allow the reaction time of 1 minute and after that 1 minute centrifuge.

Chapter 2: Materials and Methods

Table 2.1 Yeast and bacterial media used

YEA	(1 litre)
Glucose	30 g
Yeast extract	5 g
Agar	14 g
YEL	(1 litre)
Glucose	30 g
Yeast extract	5 g
SPA	(1 litre)
Agar	30 g
Potassium dihydrogen orthophosphate	1 g
Glucose	10 g
Vitamins (x1000)	1 ml (added after media autoclaved)
NBA	(1 litre)
Nitrogen base	1.7 g
Ammonium sulphate (NH ₄) ₂ SO ₄	5 g
Agar	10 g
Glucose	5 g
EMM2	(1 litre)
Potassium hydrogen phthalate	3 g
Minerals (x10000)	0.1 ml
Ammonium chloride NH ₄ Cl	5 g
Glucose	20 g
Vitamins (x1000)	1 ml

Chapter 2: Materials and Methods

Di-sodium hydrogen phosphate (NH ₄) ₂ SO ₄	2.2 g
Agar	14 g
Salt (x50)	20 ml
LBA	(1 litre)
Yeast extract	5 g
Tryptone	10 g
Agar	14 g
Sodium chloride	10 g
Ampicillin (50 mg/ml)	2 ml
Vitamins (x1000)	(1 litre)
myo-inositol	10 g
Biotin	10 mg
Pantothenic acid	1 g
Nicotinic acid	10 g

2.3 *S. pombe* gene deletions

The Bähler used for gene deletion was amplified in this study (Bähler et al. 1998). The present study involves pFA6a-natMX6 and pFA6a-kanMX6 plasmids that are utilized as template DNAs for PCR amplification of deletion cassettes. By integrating the right antibiotic-resistant marker, 70-100 bps homologous sequences (the knockout cassette primers of the PCR) are present in the upstream and downstream of the target gene to be deleted, this also comprise 20 bp homologous sequence at the DNA flanking region of the precise selected marker cassette. Most of the primers used to carry out this study were designed with the aid of software of the Bähler lab. Used primers are shown in table 2.4.

Chapter 2: Materials and Methods

The primers and the plasmids were diluted 10-times using 1x TE buffer [1.0 M Tris-HCl (pH7.5) and 1.0 M EDTA] prior to performing PCR, All the 50 Ml PCR reactions encompassed: 1 μ L DNA template (equivalent to 20 ng of plasmid DNA), 1 μ L 10x dNTPs, 1 μ l high FINNZYMES (fidelity Phusion polymerase), 10 μ L 5x Phusion™ HF buffer, 1 μ L each of forward and reverse primers with the final strength of 20 ng/ μ L, 2.5 μ L of DMSO and lastly 32 μ L sterile dH₂O. With the help of the following programme, the select marker cassettes were amplified- foremost step involve 98°C for 1 minute following 35 cycles for 20 seconds at 98°C, then 30 seconds at 59°C, followed by 1 minute and 50 seconds at 72°C, and the concluding extension was performed for 5 minutes at 72°C. All the PCR yields were pooled to carry out the purification process using phenol/chloroform procedure.

Chapter 2: Materials and Methods

Table 2.2 *S. pombe* strains used in this project

Strain number	Genotype	Source
BP90	<i>h⁻ ade6-M26 ura4-D18 leu1-32</i>	McFarlane, Bangor University
BP91	<i>h⁺ ade6-52 ura4-D18 leu1-32</i>	McFarlane, Bangor University
BP743	<i>h⁻ rad3-136</i>	McFarlane, Bangor University
BP1079	<i>h⁻ ade6-M26 ura4-D18 leu1-32 tsn1::kanMX6</i>	McFarlane, Bangor University
BP1080	<i>h⁻ ade6-M26 ura4-D18 leu1-32 tsn1::kanMX6</i>	McFarlane, Bangor University
BP1089	<i>h⁻ ade6-M26 ura4-D18 leu1-32 tfx1::kanMX6</i>	McFarlane, Bangor University
BP1090	<i>h⁻ ade6-M26 ura4-D18 leu1-32 tfx1::kanMX6</i>	McFarlane, Bangor University
BP1478	<i>h⁻ ade6::tRNAGLU (1) his3-D1 ura4-18 lys1-37 leu1-32</i>	McFarlane, Bangor University
BP1508	<i>h⁻ ade6::tRNAGLU (2) his3-D1 ura4-18 lys1-37 leu1-32</i>	McFarlane, Bangor University
BP1534	<i>h⁻ ade6::tRNAGLU (1) his3-D1 ura4-18 lys1-37 leu1-32(pSRS5)</i>	McFarlane, Bangor University
BP1535	<i>h⁻ ade6::tRNAGLU (2) his3-D1 ura4-18 lys1-37 leu1-32(pSRS5)</i>	McFarlane, Bangor University
BP1685	<i>h⁻ ade6::tRNAGLU (1) his3-D1 ura4-18 lys1-37 leu1-32 swi1::ura4 (pSRS5)</i>	McFarlane, Bangor University
BP1687	<i>h⁻ ade6::tRNAGLU (2) his3-D1 ura4-18 lys1-37 leu1-32 swi1::ura4 (pSRS5)</i>	McFarlane, Bangor University
BP2746	<i>h⁻ ade6-M26 ura4-D18 leu1-32 dcr1::ura4⁺</i>	McFarlane, Bangor University
BP2748	<i>h⁻ ade6-M26 ura4-D18 leu1-32 tsn1::kanMX6 dcr1::ura4⁺</i>	McFarlane, Bangor University
BP2749	<i>h⁻ ade6-M26 ura4-D18 leu1-32 tsn1::kanMX6 dcr1::ura4⁺</i>	McFarlane, Bangor University

Chapter 2: Materials and Methods

BP2750	<i>h⁻ ade6-M26 ura4-D18 leu1-32 tfx1:: kanMX6 dcr1:: ura4⁺</i>	McFarlane, Bangor University
BP2757	<i>h⁻ ade6-M26 ura4-D18 leu1-32 ago1:: ura4⁺</i>	McFarlane, Bangor University
BP2758	<i>h⁻ ade6-M26 ura4-D18 leu1-32 ago1:: ura4⁺</i>	McFarlane, Bangor University
BP2759	<i>h⁻ ade6-M26 ura4-D18 leu1-32 tsn1::kanMX6 ago1:: ura4⁺</i>	McFarlane, Bangor University
BP2761	<i>h⁻ ade6-M26 ura4-D18 leu1-32 tfx1:: kanMX6 ago1:: ura4⁺</i>	McFarlane, Bangor University
BP2762	<i>h⁻ ade6-M26 ura4-D18 leu1-32 tfx1:: kanMX6 ago1:: ura4⁺</i>	McFarlane, Bangor University
BP3246	<i>h⁻ ade6-M26 ura4-D18 leu1-32 tfx1:: kanMX6 ago1:: ura4⁺ tsn1::kanMX6</i>	McFarlane, Bangor University
BP3247	<i>h⁻ ade6-M26 ura4-D18 leu1-32 tfx1:: kanMX6 ago1:: ura4⁺ tsn1::kanMX6</i>	McFarlane, Bangor University
BP3248	<i>h⁻ ade6-M26 ura4-D18 leu1-32 tfx1:: kanMX6 tsn1::natMX6</i>	This study
BP3249	<i>h⁻ ade6-M26 ura4-D18 leu1-32 tfx1:: kanMX6 tsn1::natMX6</i>	This study
BP3250	<i>h⁻ ade6-M26 ura4-D18 leu1-32 tsn1::kanMX6 dcr1:: ura4⁺</i>	This study
BP3313	<i>h⁻ ade6::tRNAGLU (1) his3-D1 ura4-18 lys1-37 leu1-32 dcr1::natMX6</i>	This study
BP3314	<i>h⁻ ade6::tRNAGLU (1) his3-D1 ura4-18 lys1-37 leu1-32 dcr1::natMX6 tsn1::kanMX6</i>	This study
BP3322	<i>h⁻ ade6::tRNAGLU (1) his3-D1 ura4-18 lys1-37 leu1-32 tsn1::kanMX6 (pSRS5)</i>	This study
BP3324	<i>h⁻ ade6::tRNAGLU (1) his3-D1 ura4-18 lys1-37 leu1-32 dcr1::natMX6 (pSRS5)</i>	This study
BP3325	<i>h⁻ ade6::tRNAGLU (1) his3-D1 ura4-18 lys1-37 leu1-32 dcr1::natMX6 (pSRS5)</i>	This study
BP3326	<i>h⁻ ade6::tRNAGLU (1) his3-D1 ura4-18 lys1-37 leu1-32 dcr1::natMX6 tsn1::kanMX6 (pSRS5)</i>	This study
BP3327	<i>h⁻ ade6::tRNAGLU (1) his3-D1 ura4-18 lys1-37 leu1-32 dcr1::natMX6 tsn1::kanMX6 (pSRS5)</i>	This study

Chapter 2: Materials and Methods

BP3328	<i>h⁻ ade6::tRNAGLU (1) his3-D1 ura4-18 lys1-37 leu1-32 tsn1::kanMX6 (pSRS5)</i>	This study
BP3335	<i>h⁻ ade6::tRNAGLU (2) his3-D1 ura4-18 lys1-37 leu1-32 tsn1::kanMX6</i>	This study
BP3336	<i>h⁻ ade6::tRNAGLU (2) his3-D1 ura4-18 lys1-37 leu1-32 tsn1::kanMX6</i>	This study
BP3343	<i>h⁻ ade6::tRNAGLU (2) his3-D1 ura4-18 lys1-37 leu1-32 dcr1:: kanMX6</i>	This study
BP3344	<i>h⁻ ade6::tRNAGLU (2) his3-D1 ura4-18 lys1-37 leu1-32 tsn1::kanMX6 (pSRS5)</i>	This study
BP3345	<i>h⁻ ade6::tRNAGLU (2) his3-D1 ura4-18 lys1-37 leu1-32 tsn1::kanMX6 (pSRS5)</i>	This study
BP3348	<i>h⁻ ade6::tRNAGLU (2) his3-D1 ura4-18 lys1-37 leu1-32 dcr1:: kanMX6 (pSRS5)</i>	This study
BP3349	<i>h⁻ ade6::tRNAGLU (2) his3-D1 ura4-18 lys1-37 leu1-32 dcr1:: kanMX6 (pSRS5)</i>	This study
BP3362	<i>h⁻ ade6::tRNAGLU (2) his3-D1 ura4-18 lys1-37 leu1-32 tsn1::kanMX6 dcr1:: kanMX6</i>	This study
BP3364	<i>h⁻ ade6::tRNAGLU (2) his3-D1 ura4-18 lys1-37 leu1-32 tsn1::kanMX6 dcr1:: natMX6 (pSRS5)</i>	This study
BP3365	<i>h⁻ ade6::tRNAGLU (2) his3-D1 ura4-18 lys1-37 leu1-32 tsn1::kanMX6 dcr1:: natMX6 (pSRS5)</i>	This study
BP3376	<i>h- ade6-M210 leu1-32 ura4-D18 mat1Msmt0 his2 tetR-tup11D70::ura4 ura5::I-PpolCS-hph+ lys1::kanmx6-TATAcyc1-tetO7-spo5DSR leu1::pDUAL-TATAcyc1-tetO7-3xFlag-I-Ppol-4xDSR tsn1::natmx6</i>	This study
BP3378	<i>h- ade6-M210 leu-32 ura4-D18 mat1Msmt0 his2 tetR-tup11D70::ura4 ura5::I-PpolCS-hph+ lys1::kanmx6-TATAcyc1-tetO7-spo5DSR leu1::pDUAL-TATAcyc1-tetO7-3xFlag-I-Ppol-4xDSR tsn1::natmx6</i>	This study
BP3379	<i>h- ade6-M210 leu-32 ura4-D18 mat1Msmt0 his2 tetR-tup11D70::ura4 ura5::I-PpolCS-hph+ lys1::kanmx6-TATAcyc1-tetO7-spo5DSR leu1::pDUAL-TATAcyc1-tetO7-Flag-I-Ppol-4xDSR tsn1::natmx6</i>	This study

Chapter 2: Materials and Methods

BP3380	<i>Mat1Msm0 his2 tetR-tup11D70::ura4 ura5::I-PpolCS-hph+ lys1::kanmx6-TATAcyc1-tetO7-spo5DSR Leu1::pDUAL-TATAcyc1-tetO7-3xFlag-I-Ppol-4xDSR trax::natmx6</i>	This study
BP3385	<i>h⁻ ade6::tRNAGLU (1) his3-D1 ura4-18 lys1-37 leu1-32 dcr1::natMX6</i>	This study
BP3386	<i>h⁻ ade6::tRNAGLU (2) his3-D1 ura4-18 lys1-37 leu1-32 dcr1:: kanMX6</i>	This study
BP3387	<i>h⁻ ade6::tRNAGLU (1) his3-D1 ura4-18 lys1-37 leu1-32 dcr1::natMX6 (pSRS5)</i>	This study
BP3388	<i>h⁻ ade6::tRNAGLU (2) his3-D1 ura4-18 lys1-37 leu1-32 dcr1::natMX6 (pSRS5)</i>	This study
BP3389	<i>h⁻ ade6::tRNAGLU (2) his3-D1 ura4-18 lys1-37 leu1-32 tfx1:: kanMX6</i>	This study
BP3390	<i>h⁻ ade6::tRNAGLU (2) his3-D1 ura4-18 lys1-37 leu1-32 tfx1:: kanMX6</i>	This study
BP3391	<i>h⁻ ade6::tRNAGLU (2) his3-D1 ura4-18 lys1-37 leu1-32 tfx1:: kanMX6</i>	This study
BP3392	<i>h⁻ ade6::tRNAGLU (1) his3-D1 ura4-18 lys1-37 leu1-32 tfx1:: kanMX6</i>	This study
BP3393	<i>h⁻ ade6::tRNAGLU (1) his3-D1 ura4-18 lys1-37 leu1-32 tfx1:: kanMX6</i>	This study
BP3395	<i>h⁻ ade6::tRNAGLU (1) his3-D1 ura4-18 lys1-37 leu1-32 dcr1::natMX6 tfx1:: kanMX6</i>	This study
BP3397	<i>h⁻ ade6::tRNAGLU (2) his3-D1 ura4-18 lys1-37 leu1-32 dcr1::natMX6 tfx1:: kanMX6</i>	This study
BP3399	<i>h⁻ ade6::tRNAGLU (2) his3-D1 ura4-18 lys1-37 leu1-32 tfx1:: kanMX6</i>	This study
BP3400	<i>h⁻ ade6::tRNAGLU (2) his3-D1 ura4-18 lys1-37 leu1-32 tfx1:: kanMX6</i>	This study
BP3401	<i>h⁻ ade6-M26 ura4-D18 leu1-32 rnh1:: kanMX6</i>	McFarlane, Bangor University
BP3402	<i>h⁻ ade6-M26 ura4-D18 leu1-32 rnh1:: kanMX6</i>	McFarlane, Bangor University
BP33405	<i>h⁻ ade6-M26 ura4-D18 leu1-32 rnh201::kanMX6</i>	McFarlane, Bangor University

Chapter 2: Materials and Methods

BP33406	<i>h⁻ ade6-M26 ura4-D18 leu1-32 rnh201:: kanMX6</i>	McFarlane, Bangor University
BP3410	<i>h⁻ ade6-M26 ura4-D18 leu1-32 rnh1:: kanMX6 rnh201::hphMX6</i>	McFarlane, Bangor University
BP3412	<i>h⁻ ade6-M26 ura4-D18 leu1-32 rnh1:: kanMX6 tfx1::natMX6</i>	McFarlane, Bangor University
BP3413	<i>h⁻ ade6-M26 ura4-D18 leu1-32 rnh201:: kanMX6 tfx1::natMX6</i>	McFarlane, Bangor University
BP3417	<i>h⁻ ade6-M26 ura4-D18 leu1-32 rnh201:: kanMX6 tsn1::natMX6</i>	McFarlane, Bangor University
BP3419	<i>h⁻ ade6-M26 ura4-D18 leu1-32 rnh201:: kanMX6 rnh1::natMX6</i>	McFarlane, Bangor University
BP3424	<i>h⁻ ade6-M26 ura4-D18 leu1-32 trax1::natMX6 rnh1:: kanMX6</i>	McFarlane, Bangor University
BP3426	<i>h⁻ ade6-M26 ura4-D18 leu1-32 tsn1:: kanMX6 rnh1::natMX6</i>	McFarlane, Bangor University
BP3428	<i>h⁻ ade6::tRNAGLU (1) his3-D1 ura4-18 lys1-37 leu1-32 tfx1:: kanMX6 (pSRS5)</i>	This study
BP3431	<i>h⁻ ade6::tRNAGLU (2) his3-D1 ura4-18 lys1-37 leu1-32 tfx1:: kanMX6 (pSRS5)</i>	This study
BP3433	<i>h⁻ ade6::tRNAGLU (1) his3-D1 ura4-18 lys1-37 leu1-32 dcr1:: natMX6 tfx1:: kanMX6 (pSRS5)</i>	This study
BP3435	<i>h⁻ ade6::tRNAGLU (2) his3-D1 ura4-18 lys1-37 leu1-32 dcr1:: natMX6 tfx1:: kanMX6 (pSRS5)</i>	This study
BP3463	<i>h⁺ ade6-M26 ura4-D18 leu1-32 tsn1::kanMX6</i>	This study
BP3464	<i>h⁺ ade6-M26 ura4-D18 leu1-32 tsn1::kanMX6</i>	This study
BP3465	<i>h⁺ ade6-M26 ura4-D18 leu1-32 tsn1::kanMX6</i>	This study
BP3466	<i>h⁺ ade6-M26 ura4-D18 leu1-32 tsn1::kanMX6</i>	This study
BP3467	<i>h⁺ ade6-M26 ura4-D18 leu1-32 tsn1::kanMX6</i>	This study

Chapter 2: Materials and Methods

Table 2.3 *E. coli* used in this study

Bangor Strain Number	<i>E. coli</i> strain	Source
BE09	DH5 α (Parc782)	McFarlane, Bangor University
BE122	DH5 α (pSRS5)	McFarlane, Bangor University
BE183	DH5 α (PYL16)	Hartsuiker collection , Bangor University
BE193	DH5 α (pFA6a)	Oliver Fleck collection , Bangor University

Chapter 2: Materials and Methods

Table 2.4 PCR primers used to delete target gene

Primer name	Primer Sequence	Purpose
Tfx1 NatMX6-F	5' TATAGACTTATACATTTATACCTTCCACACGGCT TTGCTGAATTGAGGATATTATAAACTTTAACCGA ATTTGCCAA ATCGGATCCCCGGGTAAATTA-3'	Reverse primer for the Nourseothricin ^R cassette for tfx1 replacement
Tfx1 NatMX6-R	5'ATTATGATTTTCAAAAGCTGCAAAACAGAAAAA CTTTTAATAAACTAGTAAGTGTCTGTCGAGAGCTG TCGATCATATATGAA TTCGAGCTCGTTTAAAC -3'	Forward primer for the Nourseothricin ^R cassette for tfx1 replacement
Dcr1-Kan-F	5'-ATA GCT TAG GAT TCATTA TTTTTAAGAGA CAAATT TCTCGT CAATTG AAT GAAACC TCGCCTT TAT TTT CTT TTT GACGGA TCCCCGGGT TAA TTA A- 3'	Forward primer for the Kanamycin cassette for dcr1 replacement
Tsn1-Kan-F	5'-TTA TTTGCA TAC TGA AAA CATCAT TCG AAT ATC AAC ACT ACTCAA CAG CAT ACA TTA CAG ATTAAG TCG ACG GAT CCC CGG CGT TTA AAC-3	Forward primer for the Kanamycin cassette for tsn1 replacement
Tsn1-Kan-R	5'ATA TTA AAA AAG CAATTT TATCGG CTC AAT TTTAGTCAAGCGTACAGCTGGCAAATAAATTGTTAG CAA TGA ATT CGA CGT TTA AAC-3	Reverse primer for the Kanamycin cassette for tsn1 replacement
Dcr1NatMX6- F	5'-ACA TAT GCA TGT TTA TTT GAA TAG CTT AGG ATT CAT TAT TTT TTA AGA GAC AAA TTT CTC GTC AAT TGA ATG AAA CCT TCC GCC TTT ATT TTC TTT TTG ACG GAT CCC CGG GTT AAT TAA-3'	Forward primer for the Nourseothricin cassette for dcr1 replacement
Dcr1NatMX6- F	5'-AAT ATC ACG AAA GGA TCC GTG CTT TGG AGA CCC AAA TTG AAA GTT TGA AAA GTT ACA AGG GCC GCG GTC ATA AAA AAT GAAATACTGTATATT TCAGT CGA GCC GCG GTC ATA AAA AAT GAA ATA CTG TAT ATT TCA AGT CGA ATT CGA GCT CGT TTA AAC-3'	Forward primer for the Nourseothricin cassette for dcr1 replacement
Dcr1-Kan-R	5'-ATA GCT TAG GAT TCATTA TTTTTAAGAGA CAAATT TCTCGT CAATTG AAT GAAACC TCGCCTT TAT TTT CTT TTT GACGGA TCCCCGGGT TAA TTA A- 3'	Reverse primer for the Kanamycin cassette for dcr1 replacement

Chapter 2: Materials and Methods

2.4 Phenol/Chloroform purification of *S. pombe* genomic DNA.

The DNA to be purified was added to the mixture containing same amount of phenol/chloroform along with 0.1 M NaCl (with ratio 1:1) in a sterile Eppendorf tube. The mixture was centrifuged at 12,000 r.p.m in round number of 14 minutes in a table-top microfuge. The supernatant was collected in another A sterile Eppendorf tube comprising 3-times by volume of 100% ethanol (absolute alcohol C₂H₅OH). The mixture was mixed slowly and carefully then, placed at -80°C for 2 hours to facilitate the precipitate the DNA. The step was followed by centrifugation of the precipitated DNA at 12,000 g for 45 minutes at specific temperature 4°C. Before centrifugation, the rest of the supernatant was rejected, while the DNA pellet was gently washed with 70% ethanol and spun at 12,000 g for 15 minutes. The supernatant was thrown out, and pellets were air dried for 10 minutes at the room temperature. The procedure was followed by resuspension of the pellet in 40 µL of 1x TE buffer with (pH 8.0). The final step involved collection of the DNA cassette, which was then stored at -20°C.

2.5 Transformation of *S. pombe* by using lithium acetate (LiAC).

2.5.1 Transformation of *S. pombe* strains using a DNA knockout cassette.

For the transformation procedure, A single colony of the appropriate *S. pombe* strain was taken and grown at 30°C overnight in 5 mL YEL containing adenine (200 mg/L) as a supplement. After appropriate growth, on the second day, 100-200 µL of overnight culture was inoculated into 100 mL of YEL, containing supplemental adenine (200 mg/L) overnight. When the growth was attained to the final density of 1×10^7 cells/mL, the cells were centrifuged at 3,000 g for 5 minutes at room temperature. Thereafter procedure, the cells were washed with an equal volume of sterile dH₂O. The process of washing centrifugation was repeated. The procedure was followed by resuspension of the cells in 1 mL sterile dH₂O followed by transferring them to a sterile 1.5 mL Eppendorf tubes.

Chapter 2: Materials and Methods

The procedure was followed by washing the cells with 1 mL 0.1 M LiAc/ 1X TE, following this, the cells were resuspended in 0.1 M LiAc/TE so as to retain the cellular concentration of 2×10^9 cells/mL. After obtaining the desired cellular density, 100 μ L by volume was transferred to sterile Eppendorf tubes and 2 μ L of sheared herring testis DNA (10 mg/mL Invitrogen) were taken to mix together with 10-20 μ g of the appropriate DNA cassette solution, which is to be utilised for the gene knockout. The suspensions obtained were incubated at normal room temperature for approximately 10 minutes, following this, 260 μ L of 40% PEG/LiAc/TE was added. The mixture was slowly and carefully mixed, then incubated at 30 °C in a water bath for 1 hour (approximately), this step was followed by addition of 43 μ L DMSO and the cells were instantly shocked by the heat for at least 5 minutes in different water bath set at 42°C. The tubes were cool down to room temperature for 10 minutes. The cells should rinsed with 1 mL sterile dH₂O and then centrifuged at 3,000 g for 3 minutes. After discarding the supernatant, the pellet were resuspended in 500 μ L of sterile dH₂O. The procedure was followed by plating 100 μ L of the aliquots onto YEA media plates followed by incubation for 18 hours at 30°C. On appearance of growth on the plates, the cells were replicated on YEA plates (incorporated with selective antibiotics) and then incubated at 30°C for approximately 3 days.

2.5.2 Transformation of plasmid.

The lithium acetate (LiAc) procedure was applied to carry out transformation of *S. pombe* strains using 1 μ g plasmid DNA, the procedure was followed by inoculation of cells on the selective NBA and incubated for 3-4 days at 30°C.

2.6 *S. pombe* Genomic DNA Extraction.

One colony of the appropriate *S. pombe* was picked into 5 mL YEL supplemented with adenine (200 mg/L) and incubated overnight at 30°C in orbital incubator. The cells were harvested by centrifugation at 4,000 g for 5 minutes; the cells were then washed with sterile distilled water and transferred to sterile 1.5 mL screw-cap tubes, followed by centrifugation for 1 minute. This step was followed by addition of 200 μ L lysis buffer (comprising 5 mL 10% SDS, 0.5 mL TE 100X, 1 mL Triton X-100 and 5 mL 1M NaCl) together with 200 μ L phenol-chloroform and 0.3 g acid-washed beads were added to each tube. For 30 seconds, Bead-Beater (FastPrep120, ThermoSavant) was used to disrupt the cells, the process was followed by centrifugation at 12,000

Chapter 2: Materials and Methods

r.p.m. for 15 minutes. Top aqueous layer was collected and transferred to sterile new Eppendorf tubes, to this, adding 1 mL 100% ethanol (absolute alcohol). The mixture was then left at -80°C for 2 hours followed by centrifugation at 13,000 r.p.m for 12 minutes. The supernatant was discarded, and pellet collected was washed gently by 1 mL 70% ethanol and then air-dried for a short duration and then resuspended in 100 µL of 1x TE buffer (pH 7.5).

2.7 Confirmation of successfully gene deletion by PCR screening.

Once the genomic DNA was collected from for new knockout strains, several suitable primers were designed aimed at the deletion cassettes as well as the target genes. A 25 µL PCR reaction mixture was created from the following: 10.5 µL of sterile dH₂O, 12.5 µL MyTaq™ Red Mix (BioLine), 0.5 µL of 20 ng/µL of forward and reverse primers plus 1 µL extracted genomic DNA (10% dilution). The programme for PCR samples was fixed as follows: denaturation process was initiated at 98°C for 1 minute with subsequently 40 cycles of 1:40 minute set at 96°C and at 58°C for 30 seconds followed by 72°C for 30 seconds.

The concluding step involved an extension for 5 minutes at 72°C. The annealing temperature (X) was fixed according to the primer sequence. Finally, the PCR-amplified yields were visualised by running on 1% agarose gel to estimate the size of the DNA fragment using DNA ladder sequence for reference. The PCR primers used to confirm gene deletion are shown in table 2.5.

Chapter 2: Materials and Methods

Table 2.5 Sequence of PCR primers utilized for gene deletion assessment

Primer name	primer Sequence	Notes
Tfx1check-F	5'-CAAATAGTCATCTTGATTTGC -3'	Upstream of <i>tfx1</i> Open Reading Frame
Tfx1check-R	5'-TCTAACATATAGAAAGCAGCG-3'	Downstream of <i>tfx1</i> Open Reading Frame
Tfx1-int- F	5'-ATAAGAGGGAGAAAATTATTCG-3'	Forward primer inside <i>tfx1</i>
Tfx1-int- R	5'-CTCCTCGGGAGGAGTTGC-3'	Reverse primer inside <i>tfx1</i>
KanMX6- F	5'-CGGATGTGATGTGAGAACTG-3'	Forward primer inside Kan R cassette
KanMX6- R	5'-CAGTTCTCACATCACATCCG-3'	Reverse primer inside Kan R cassette
Tsn1check-F	5'-GATCTAAACAACCCAAGCG-3'	Upstream of <i>tsn1</i> Open Reading Frame
Tsn1check-R	5'-GCATTCATCATAGGACTGCC-3'	Downstream of <i>tsn1</i> Open Reading Frame
Tsn1-int- R	5'-GAACACAGAGATAGTACTGC-3'	Reverse primer inside <i>tsn1</i>
Tsn1-int- F	5'-AAACTGACTGCAGAGGTC-3'	Forward primer inside <i>tsn1</i>
NatMX6- R	5'-CTCAGTGGAAATCCTAACC-3'	Reverse primer inside Nourseothricin cassette
Ago1check-F	5'-ACTTATGTTGCGTTTGCGTGC-3'	Upstream of <i>ago1</i> Open Reading Frame
Ago1check-R	5'-AGCTATCAACAGTGGATAGAGC-3	Downstream of <i>ago1</i> Open Reading Frame

Chapter 2: Materials and Methods

Ago1-int- F	5'-AGGTACTTGTTAGCTTCATTCG-3'	Forward primer inside <i>ago1</i>
Dcr1check- F	5'-AGTATTCTGCTCGTGTGATTG-3	Upstream of <i>dcr1</i> Open Reading Frame
Dcr1check- R	5'-TGATTGAAACTCGAGATGCTTTG-3'	Downstream of <i>dcr1</i> Open Reading Frame
Dcr1-int- F	5'-ATTCGACGAATGTCATCATGC-3'	Forward primer inside <i>dcr1</i>
Dcr1-int- R	5'-AGACGATATCATCAGTCACACG-3'	Reverse primer inside <i>dcr1</i>

2.8 Drop Tests for Drug Sensitivity.

A colony of the appropriate *S. pombe* strain was selected and inoculated into 5 mL YEL media supplemented with adenine (200 mg/L) followed by overnight incubation at 30°C on the shaker in order to get cell saturation. The second day, 10 µL of the sample was taken and fixed on 25 square haemocytometer, with the help of coverslip and observed under light microscope (40X). The procedure was followed by resuspension of the cells in 1 mL of sterile dH₂O to a concentration of 5 x 10⁶ cells/mL. This was followed by preparation of serial dilution of cells with a dilution factor of 1:10. after this, each dilution ,10 µL was taken and spotted onto YEA plates having supplemented with adenine (200 mg/L) (see Figure 2.1) along with the recommended concentration of the antibiotics or other drugs to be tested (drug concentrations details are listed in Table 2.6). Correctly, labelled plates were incubated for approximately 3 to 4 days at 30°C.

Chapter 2: Materials and Methods

Table 2.6 Drugs used in this study

Drug	Concentrations
Thiabendazole (TBZ) (Sigma)	(12, 14 , 15, 16, µg/ml)
Methyl Methanesulfonate (MMS) (Sigma)	(0.005, 0.0075%)
Mitomycin C (Sigma)	(0.15 mM)
Phleomycin (Sigma)	(2.5, 3 , 4, 5, 6 µg/ml)
Hydroxyurea (HU) (Sigma)	(8, 9, 10 mM)
Camptothecin (Sigma)	(1, 1.6 µg/ml)
Belomycin (Sigma)	(2.5, 3 , 4, 5, 6 µg/ml)

Chapter 2: Materials and Methods

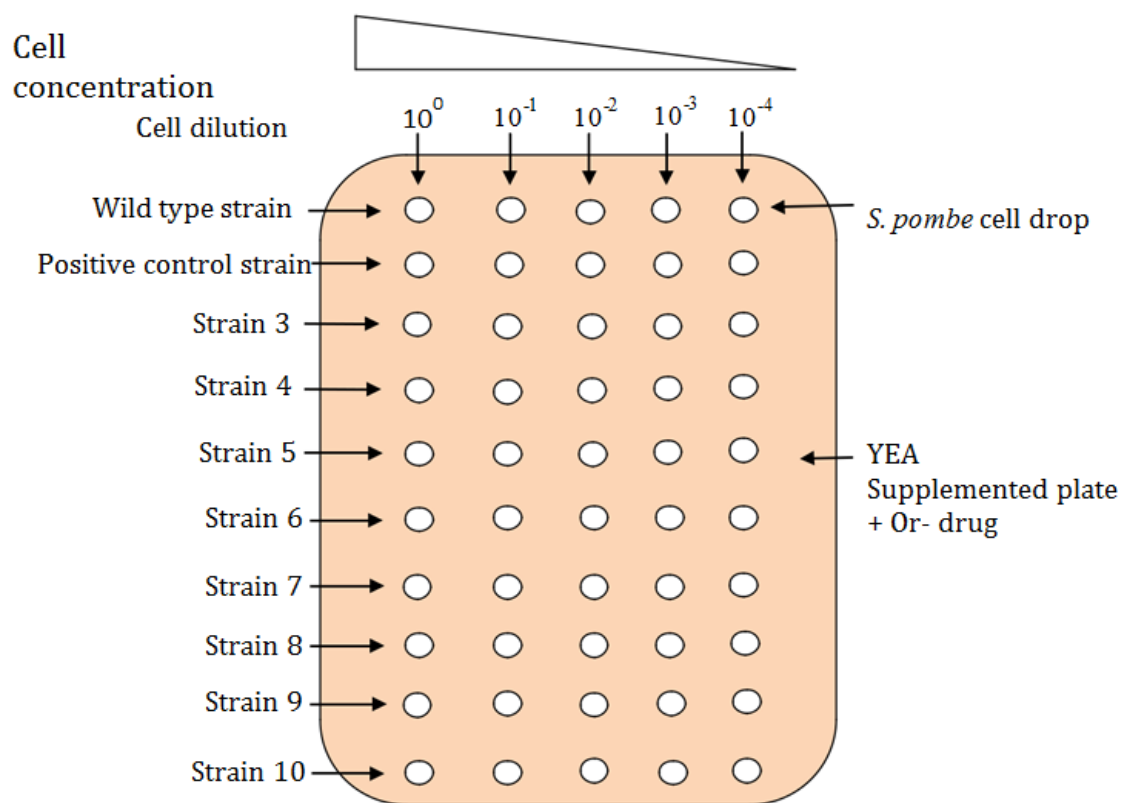


Figure 2.1 design order of a square Petri dish for spot essay. Figure shows serial dilutions drops of indicate *S. pombe* strains in a square Petri dish. Different concentration of drop tests were managed to figure out the influence of several DNA damaging drugs into target strains.

Chapter 2: Materials and Methods

2.9 Storage of *S. pombe* Strains.

For long-term storage, single colony was inoculated in 5 mL YEL supplemented with adenine (200 mg/L) followed by overnight incubation at 30°C in orbital incubator in order to get the cell saturation. To 700 µL of culture, 300 µL of the final concentration of 30% was added and the mixture was then stored at -80 °C.

2.10 Ultraviolet (UV) irradiation of *S. pombe*.

The inoculum was taken and serially diluted to 1:10 concentration. 10 µL of each different strains dilution was spotted on YEA plates supplemented with adenine (200 mg/L), the spots were permitted to dry. UV irradiation (CL1-1021UV cross-linker) was used to expose all plates. Different range of exposure was provided including 60, 70, 80 and 90 J/m². These plates with right label were incubated for approximately 3-4 days at 30°C.

Chapter 2: Materials and Methods

2.11 Yeast meiotic crosses.

S. pombe strains were inoculated in YEL to a concentration of 2.5×10^7 cells/mL, cells of opposite mating type (h^+/h^-) were mixed in 1.5 mL sterile Eppendorf tube in similar proportion of 750 μ L for each indicated strain. The process was followed by centrifugation at 6,000 r.p.m for 30-60 seconds, the supernatant was rejected, and the pellet collected was rinsed with 1 mL sterile dH₂O followed by centrifugation. The wash process was repeated for three times, then the pellet was resuspended in 100 μ L of sterile distilled water. This was followed by inoculation on SPA supplemented with 200 μ g/mL lysine, histone, leucine, uracil and adenine, the culture was incubated for 2 days at 25°C. After 2 days of incubation with shaking, the cells were examined microscopically to count the number of asci (with four spores).

The unmated cells and the asci were carefully scrapped off the SPA plate and inoculated into a sterile Eppendorf containing 1 mL 0.6% β -glucuronidase (Sigma) solution. After thorough mixing the culture was incubated at 25-30°C for 18 hours in order to release spores from asci. This step was followed by addition of ethanol for 5 minutes to kill vegetative cells. The spores were spin at 6,000 r.p.m for 1 minute in an Eppendorf tube. Subsequently rejected all supernatant, the pellet was washed 3 times in 1 mL sterile distilled water and, lastly resuspended 1 mL sterile dH₂O. 20 μ L sample from each dilution was dropped on YEA to permit viable spores to grow. The plates were incubated 30°C for maximum 3 days and viable colonies were assessed.

2.12 Whole-cell protein extraction *S. pombe*.

A single colony from each strain was incubated around 18 hours in 5 ml YEL. The second day, 25 μ L from individual cultures was grown in 25 ml YEL at 30 °C. The cells at 4 °C were then harvested via centrifuging for 5 minutes at 4,000 g. The pellet was resuspend in 250 μ L of 20% final concentration of Trichloroacetic acid (TCA) with 400 μ L acid glass beads. The cells were vortexed three times at max speed with one minute on ice between. The bottom of the Eppendorf was pierced carefully with red-hot needle and placed to new Eppendorf. The mixture were spun for 2 minutes at 6,000 g. After that, the cells were washed by adding 300 μ L of 5% Trichloroacetic acid (TCA). Again, the mixture was spun at 6,000 g for 2 minutes at 4°C. All supernatant was removed from top of the tube and 700 μ L of 5% Trichloroacetic acid (TCA) was added.

Chapter 2: Materials and Methods

The resuspension was centrifuged for ten minutes at 14,000 g at 4 °C. The top liquid was removed and pellets were washed by adding 750 µl of 100% ethanol. The resuspension was spun at 14,000 g for 10 minutes at 4 °C. Finally the pellet was resuspend in 40 µl (1 M Tris Cl in PH 8.0). The cell lysate was stored at -80°C until required.

2.13 Western blotting for *S. pombe*.

The primary antibody was Anti-flag antibody (Abcam #AB49763). The primary antibody for western blotting was diluted 1:1000. The (Santa Cruz Biotechnology, sc-2348) secondary antibody mouse was diluted at 1:3000. The samples were boiled for a maximum 5 minutes at 94 °C and loaded gently in NuPAGE Novex 4-12% Bis-Tris Gel (Invitrogen # NP0322). The gel was run approximately one hour at 100 V. Four equal sheets of mini-size Transfer Stacks (7 x 8.5 cm for Blot mini gel tank) was cut plus one sheet of PVDF membrane (Millipore; #IPVH00010). Transfer buffer was used to wet the filter papers which developed by composing 600 ml of water , 200 mL of 5x transfer buffer (Bio – Rad #10026938) and 200 ml of ethanol.

The membrane was wetted in methanol then water for a maximum of 5 minutes. The protein was fully transferred to PVDF membrane within 7 minutes by using a Trans-Blot® Turbo™ Transfer System for fast transfer with high quality. A blot sandwich was constructed as follows order: two filter paper sheets, the gel, the membrane and two filter paper sheets. After that, blocking the membrane overnight on a shaker in dark room with 1x PBS including 10% skimmed powder milk without TWEEN (sigma-Aldrich; #P1379). The membrane was probed for one hour with 10 ml of 10% skimmed milk powder and 10 µl primary antibody with TWEEN. The membrane was washed triple times in 1x PBS and 0.5% TWEEN each for 10 minutes. Then probing the membrane with 10 ml of 10% skimmed milk powder and 4 µl secondary antibody then it was washed 3 times for 10 minutes. Wetted whole membrane in exactly amount of chemiluminescence (ECL, ThermoFisher Scientific; #32132) solutions at room temperature for 5 minutes. Finally, In a dark room, The membrane was exposed to X-Ray films (Thermo Fisher #34091) within optimal time of exposure to detect protein signal, The membrane was rinse and stored in 1x PBS in fridge.

Chapter 2: Materials and Methods

2.14 Determination of Recombination Frequency (Fluctuation test):

For determine Recombination frequency fluctuation analysis was used. The plasmid-by-chromosome recombination frequency (Fluctuation test) was assessed utilising the pSRS5 plasmid, which particularly carries (*ade6-ΔG1483*), a recombination marker *ade6* mutant allele that was generated by deleting a guanine at nucleotide site 1482 in the *ade6* ORF (Pryce et al., 2009). One separate colony of appropriate *S. pombe* strain to be tested for recombination frequency was grown independently in 5 mL of suitable selective liquid medium (in order to retain plasmid) followed by overnight incubation at 30°C on the shaker. Serial dilutions of suspensions was plated on selective NBA solid medium (in order to retain plasmid) and incubated for around 3-4 days at 30°C till tiny-colonies were observed. For individual experiment, completely seven tiny-colonies were cultured independently into 5 mL of a suitable selective liquid NBL media and incubated at 30°C on a shaker between 2-3 days, until saturated. Following for each culture five dilutions were made. 100 µL was plated out into (YEA) and YEA with 20 mg/ml guanine (final concentration of guanine; soluble/ dissolved in 0.35 M NaOH/ddH₂O stock, pH was adjusted to 6.5 with 1 M HCl). In this experiment Lower dilution of indicate strain (10^{-1} to 10^{-2}) was pleated out into YEA with 20 mg/ml guanine to prevents to uptake the adenine from YEA media and the adenine prototroph was assessed (Ade⁺ recombinant totals). Furthermore, 100 µL higher dilution of indicate strain (10^{-3} to 10^{-5}) were plated onto YEA plates to measure the number of viable cells. After 3 days incubation at 30°C, all plates with over 50 colonies, where calculated and used on average to identify the total viable colony. Three biological repeat was performed for each strain and Student's t test was used to determine the mean value of at least three independent median values (adenine prototrophs/viable cell).

Chapter 3: Results

The function of Tsn1 and Tfx1 in the absence of Dcr1

3.1 Introduction

Accurate segregation of chromosomes in eukaryotic cells ensures precise transmission of genetic materials to daughter cells (Bouwman & Crosetto, 2018, Kang, et al, 2018, Brouwers, Martinez & Vernos, 2017, Li & Xu, 2016). Genetic disorders like cancer contribute significantly to abnormalities of the eukaryotic cell division cycle (Potapova & Gorbsky, 2017; Santaguida & Amon, 2015). Centromeres are eukaryotic chromosomal loci that ensure kinetochore formation and sister chromatid segregation (Moreno-Moreno et al., 2017; Steiner & Heinkoff, 2015; Jain & Cooper, 2010; Fennell et al., 2015). Therefore, genomic integrity can only be maintained with effective maintenance of centromere function (Harland et al., 2014). Lack of preserving the function of centromeres and/or structure can cause chromosomes mis-segregation, and potential oncogenic outcomes linked with cancer (He, et al, 2018; Santaguida & Amon, 2015; Lee et al., 2013; Carmichael et al., 2004; Volpe et al., 2002). The heterochromatin nature of centromere regions is marked by histone H3K9 methylation, and binding of heterochromatin protein 1 (Swi6 in *S. pombe* binding) (Zocco et al., 2016; Wang et al., 2016 ; Buhler & Gasser, 2009; Tadeo et al., 2013; Chan & Wong, 2012; Stimpson & Sullivan, 2010). Heterochromatin formation at the centromeres is vital for the functionality of kinetochores in ensuring proper chromosome segregation (Mutazono et al., 2017; Schmidt & Cech, 2015; Stimpson & Sullivan, 2010; Schoeftner & Blasco, 2009).

The RNAi machinery facilitates the formation and maintenance of heterochromatin and centromeres in eukaryotes with complex centromeres, including *S. pombe*. Deleting major RNAi regulatory genes, for instance, *ago1*, influences of the centromeric function via decreasing methylation of H3K9, Swi6 corporation and results in chromosomal missegregation leading to cell with defective mitosis and increase sensitivity to TBZ (microtubule disrupting agent) (Shimada et al., 2016; Sadeghi et al., 2015; Holoch & Moazed, 2015; Tadeo et al., 2013; Buhler & Gasser, 2009; Volpe et al., 2003).

The complex of Translin-TRAX (C3PO) plays a key role in RNAi pathways in humans and *Drosophila melanogaster* by removing passenger strands from siRNAs, contributing to RISC complex-mediated silencing (Holoch & Moazed, 2015; Tian et al., 2011; Ye et al., 2011; Liu et al., 2009; Jaendling McFarlane, 2010).

Chapter 3: Results

Past research conducted on null mutants of *tsn1* and *tfx1*, in *S. pombe*, showed no significant phenotypic change indicating that *tsn1* and *tfx1*, are not essential for fission yeast (Jaendling & McFarlane, 2010; Laufman et al., 2005; Jaendling et al., 2008). This suggested that *tsn1* Δ and *tfx1* Δ mutants in *S. pombe* are not defective in RNAi mediated centromere maintenance of *S. pombe* centromeric transcripts heterochromatin silencing remains intact (Gomez-Escobar et al., 2016).

Recently, Wang et al. (2016) found that DSB repair via the ATM-mediated pathway was associated with murine Trax serving as an ATM scaffold protein. In addition, it has been found that the Dcr1 but not the Ago1 being necessary for DNA damage response by Castel et al. (2014). Results obtained during this study indicate that the instability of chromosome noticed in the case of *dcr1* Δ *tsn1* Δ double mutants could be caused by the inability of the cell to repair or respond to DNA damage. These results also show that it is the Tsn1, and not Tfx1, which is needed by the cells to respond to DNA damages when Dcr1 is not present which indicates a separation of function between these Tsn1 and Tfx1. It is important to note that the results of sensitivity tests also indicated that increased sensitivity to different DNA damaging agents demonstrated by the *dcr1* Δ *tsn1* Δ double mutants is related to damage associated with DNA replication by using phleomycin and hydroxyurea (HU) sensitivity.

Interestingly, a study in the McFarlane's team demonstrated that *tfx1* mutation but not *tsn1* suppresses sensitivity of an *ago1* Δ mutant to TBZ (Gomez-Escobar et al., 2016). This suppression was postulated to be related to altered telomere function, and not related to centromere heterochromatin per se. Indeed, suppression was not apparent in another RNAi mutant, *dcr1* Δ (McFarlane, unpublished data). Indeed, *dcr1* Δ *tsn1* Δ double mutant appears to show increased TBZ sensitivity (McFarlane, unpublished data). Recent work by Castel and co-workers (2014) demonstrated an RNAi –independent function for Dcr1, which is thought to be associated with accumulation of genotoxic RNA:DNA hybrids. Given this, and the proposal that Translin is associated with genome stability regulation, we wanted to ask whether *tsn1* and/or *tfx1* had a function role in preserving genome stability when Dcr1 is lost.

3.2 Results

3.2.1 Construction of relevant mutant strains

Construction of relevant mutant strains in this study was done *de novo* (also referred to as direct gene mutation). No genetic crossing was involved in the construction of strains. A recent study by the McFarlane's group of researchers found that *tsn1* Δ mutations were responsible for the non-Mendelian fashion of segregation after mating, an indication of yet an undefined haploinsufficiency for *tsn1* in meiosis or a meiotic driven role in poison-antidote (Shropshire et al., 2017; Hu et al., 2017; Nuckolls et al., 2017). Moreover, recent studies targeting the identification of non-essential *S. pombe* mutants that are defective in sporulation and mating, discovered *tsn1* Δ mutants as having defects in sporulation (Dudin et al., 2017). The observed outcomes are indications of *tsn1* Δ mutants possessing a post-meiotic defect, therefore, we resorted to constructing *de novo* knockout mutants in duplicate, from mitotically dividing cells.

Generating single mutants required the deletion of *tfx1* Δ , *tsn1* Δ , and *dcr1* Δ from the parent strain (BP90). In generating double mutants, *dcr1* Δ candidate *has* been removed from a newly constructed single *tfx1* Δ or *tsn1* Δ mutants using a PCR-based gene targeting technique (Bähler et al., 1998) (note: each mutant has two isolates as minimum). Plasmids with antibiotic-resistant selectable markers were derived from *Escherichia coli* (Table 2.3). The *kanMX6* (kanomycin-resistance) gene and *natMX6* (nourseothricin-resistance) genes have been used as replacement cassettes in deleting *tsn1*, *tfx1* and *dcr1*. Thereafter, they (replacement cassettes) have been amplified using PCR primers of 80 and 20 base pairs homologous sequences. The former was directly flanking the upstream and downstream sequences as well as the *dcr1*, *tsn1* and *tfx1* ORFs, while the latter, had the antibiotic resistance genes of a template plasmid (Figure. 3.1). The purified PCR product was transformed chemically into the indicated *S. pombe* strains (Section 2.5.1) To verify the deletion of gene *tfx1* Δ , *tsn1* Δ , and *dcr1* Δ candidates have been checked by PCR (Figure. 3.1 and 3.2) utilizing three sets of primers (Figure. 3.2).

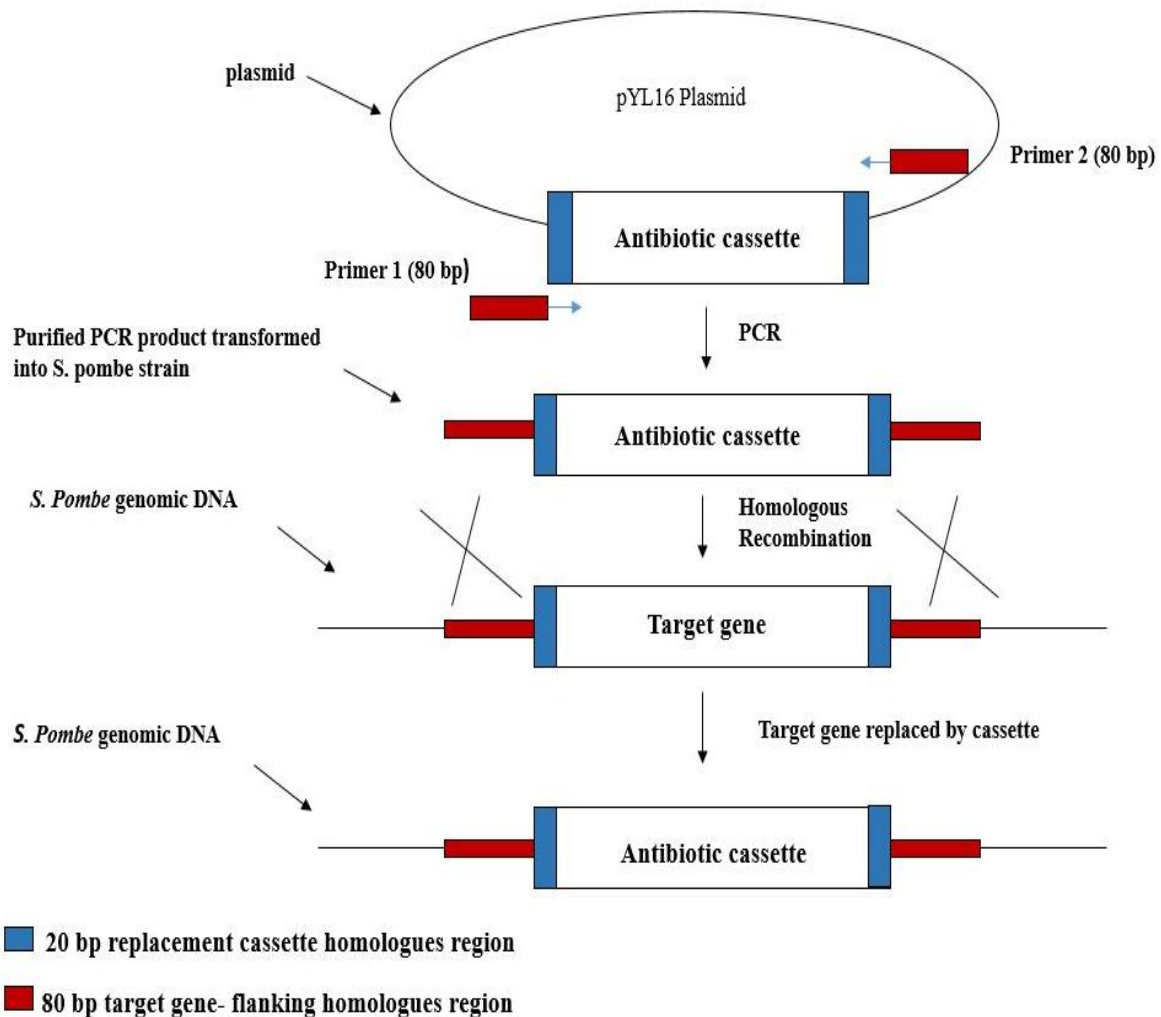


Figure 3.1 Illustration of target gene knockout process. Utilization of various plasmids as templates during selectable antibiotic-resistant amplification markers was done via PCR with primers of 80 bp homologous sequence flanking directly to the upstream and downstream, target gene and Open Reading Frame for delating (red box), as well as, 20 bp sequence of homologous to the plasmid containing a target antibiotic-resistant marker (blue box). A chemical transformation of purified PCR products to strains of *S. pombe* followed by replacement of the target gene via a replacement cassette.

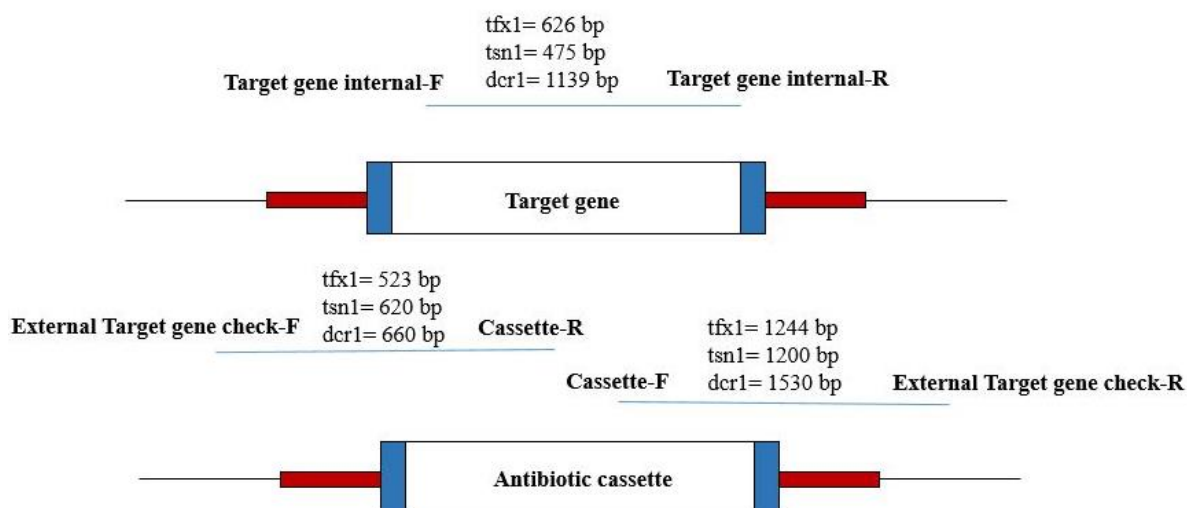


Figure 3.2 Description of the position of primers in confirming the appropriate deletion of the interest gene. The deletion of the target gene was followed by replacement with antibiotic-resistant cassettes as illustrated by Bahler et al. (1998) (See details in Figure. 3.1). Checking primers are in three sets at their strategic location and were used to validate if cassette replacements have successfully transformed and deleted the target genes. No PCR product will be generated by using internal-F/target gene and internal-R/target gene, however. The deleted genes should be provided with the expect size of PCR products due to availability of Cassettes originating from Cassette-F/External target gene check-R primer and External target gene check-F/Cassette-R

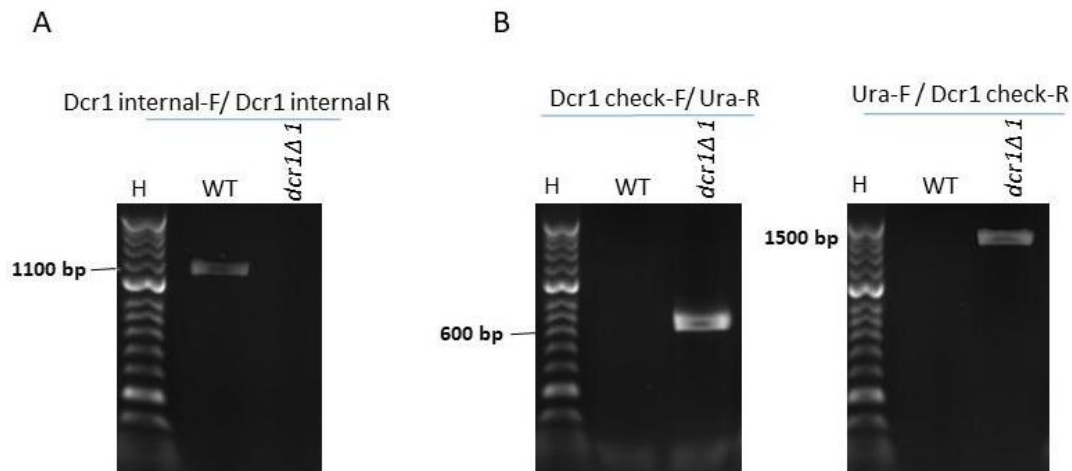


Figure 3.3 PCR screening for the efficient construction of *dcr1Δ* mutants. **A.** Agarose gel image shows products of PCR for the WT and *dcr1Δ* using the Dcr1-int-F and Dcr1-int-R primers. The *dcr1* gene was seen in expected Band sizes of 1139. The gel image does not show PCR products for correct deletion of *dcr1Δ* strains. **B.** products of PCR for the *dcr1Δ* and WT candidate strains were obtained using primers dcr1 check-F and ura4-R primers. The *dcr1Δ* strains were seen in expected sizes of 660 bp, but not in WT (the *dcr1*⁺ strains). In addition, the *dcr1Δ* and WT candidate strains were amplified by using ura4-F and dcr1 check-R primers. The *dcr1Δ* strains were present in expected sizes of 1530 bp. However, nothing was seen in the *dcr1*⁺ strains (WT). H = Hyper ladder.

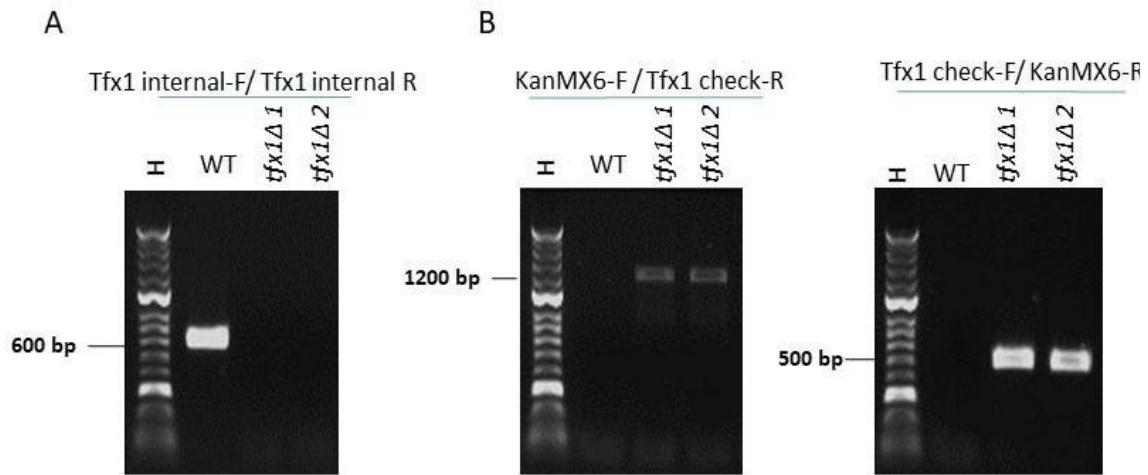


Figure 3.4 PCR screening for the efficient construction of *dcr1Δ tfx1Δ* mutants.

A. Agarose gel image shows products of PCR for the WT and *tfx1Δ1* and *tfx1Δ2* using the the Tfx1-int-F and Tfx1-int-R primers. The *tfx1* gene was seen in expected Band sizes of 627 bp. The gel image does not show PCR products for correct deletion of *tfx1Δ* strains. **B.** products of PCR for the *tfx1Δ* and WT candidate strains were obtained using primers Tfx1 check-F and KanMX6-R. The *tfx1Δ* strains were seen in expected sizes of 523 bp, but not in the WT (*tfx1*⁺ strains) and the *tfx1Δ* and WT candidate strains were amplified by using KanMX6-F and Tfx1 check-R primers. The *tfx1Δ* strains were present in expected sizes of 1244 bp. However; nothing was seen in the *tfx1*⁺ strains (WT). H = Hyper ladder.

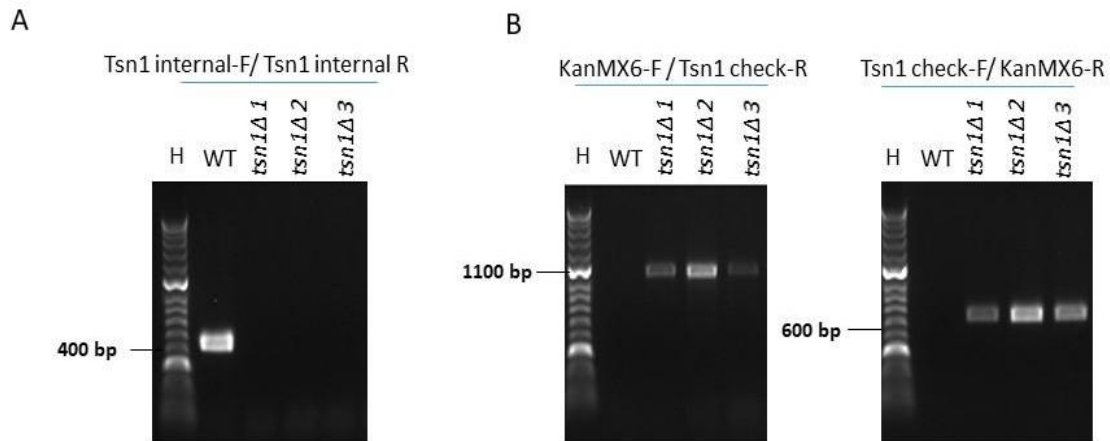


Figure 3.5 PCR screening for the efficient construction of *dcr1Δ tsn1Δ* candidates. **A.** Agarose gel image shows products of PCR for the WT, *tsn1Δ1*, *tsn1Δ2* and using *tsn1Δ3* the the Tsn1-int-F and Tsn1-int-R primers. The *tsn1* gene was seen in expected Band sizes of 475 bp. The gel image does not show PCR products for correct deletion of *tsn1Δ* strains. **B.** products of PCR for the *tsn1Δ* and WT candidate strains were obtained using primers Tsn1 check-F and KanMX6-R. The *tsn1Δ* strains were seen in expected sizes of 620 bp, but not in WT (the *tsn1*⁺ strains). In addition, the *tsn1Δ* and WT candidate strains were amplified by using KanMX6-F and Tsn1 check-R primers. The *tsn1Δ* strains were present in expected sizes of 1200 bp. However, nothing was seen in the *tsn1*⁺ strains (WT). H = Hyper ladder.

3.2.2 *tfx1Δ* mutation suppresses the *ago1Δ* chromosomal phenotypic instability in a *tsn1Δ*-dependent fashion

Here we wished to validate the previous findings that mutation of *tfx1Δ* is a suppressor to the defective chromosomal instability of *ago1Δ* cells (all indicated strain containing with *tsn1Δ* and *tfx1Δ* single mutations, as well *ago1Δ* mutations were generated by individuals in McFarlane group although they were confirmed here by using PCR before using).

3.2.3 Spot Test for TBZ sensitivity

Cells defective cells in chromosome segregation due to aberrant centromeres like the *ago1Δ* mutant, display high TBZ sensitivity (Sadeghi et al., 2015; Lee et al., 2013; Buhler & Gasser, 2009; Volpe et al., 2003). Single *tsn1Δ*, *tfx1Δ*, *ago1Δ*) and double mutants (*ago1Δ tsn1Δ* and *ago1Δ tfx1Δ*) strains were exposed to different concentration to TBZ drug and both single *tfx1Δ* and *tsn1Δ* mutants were not exhibited any sensitivity to TBZ compared to the negative control WT, as shown in (Figure 3.1.A). This result is exactly consistent with pervious research of Jeandling et al. (2008). High increased sensitivity of the *ago1Δ* mutant to TBZ drug was observed and was partially suppressed via mutation of *tfx1Δ* but not *tsn1Δ* mutant as in (Figure 3.1A). Interestingly, the *ago1Δ tsn1Δ* double mutants and the triple mutant *ago1Δ tfx1Δ tsn1Δ* to TBZ were supersensitive to TBZ compared to the *ago1Δ* single mutant in Figure.3.1B. Conspicuously, the high TBZ sensitivity was being suppressed by a few colonies at 33°C in background strains of *ago1Δ tsn1Δ* and *ago1Δ tfx1Δ tsn1Δ* Figure.3.1B

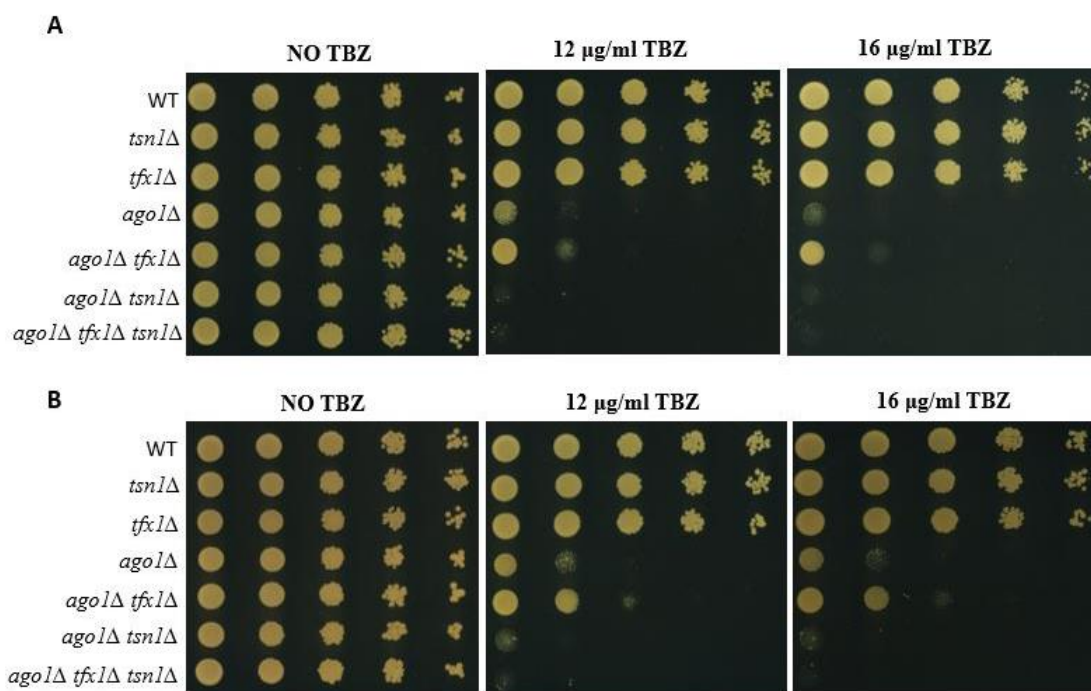


Figure 3.6 *tfx1Δ* mutation, but not *tsn1Δ* partial suppresses the TBZ sensitivity of single a *ago1Δ* mutation 10-fold serial dilution of *S. pombe* mutant strains were spotted onto YAE and exposed to TBZ drug in several range of concentration. The plates have been incubated for approximately 3 days at 30°C (A) and 33°C (B). **A.** single mutant of *tsn1Δ* and *tfx1Δ* were not displayed any sensitivity to TBZ in relative to the negative control WT. The positive control was *ago1Δ* strain, which showed high sensitivity to TBZ. **B.** significant suppressed sensitivity has been shown in the *ago1Δ tfx1Δ* double mutant relative to the *ago1Δ* single mutant, whereas the *ago1Δ tsn1Δ* double mutants and *ago1Δ tfx1Δ tsn1Δ* triple mutants shows high increased TBZ sensitivity in comparison to the *ago1Δ* single mutant.

3.2.4 Colony growth assay

Defects emanating from *ago1Δ* chromosomal instability can be monitored by streaking single colonies of *ago1Δ* cells on YEA (Yeast Extract Agar). It is found that WT growth was higher than of *ago1* (Figure.3.7). Moreover, we found that the *ago1Δ tfx1Δ* double mutant growth was sensitivity stronger compared to the *ago1Δ* single mutant (Figure. 3.7), however, the growth of *ago1Δ tsn1Δ* double mutant has been lower relative to WT. These data are partly consistent with the sensitivity pattern of the TBZ (Figure.3.7). In addition, the results support the fact that there is partial restoration of genomic stability by *tfx1Δ* mutation in an *ago1Δ* background which relies on the availability of *tsn1* in a *tfx1*-free context.

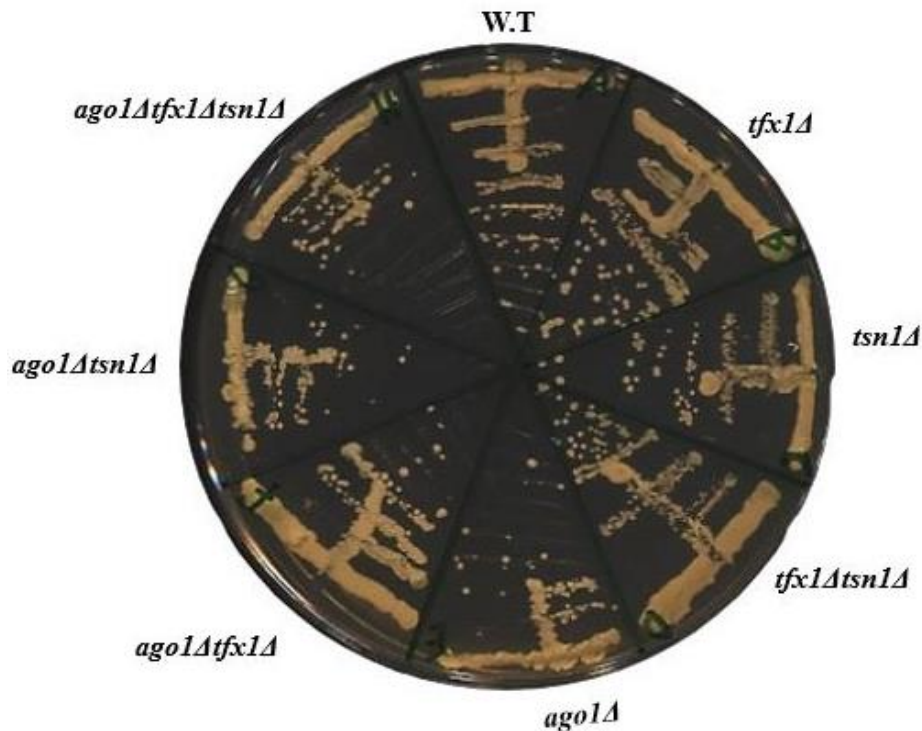


Figure 3.7 Extent of *ago1Δ* growth is more increased by *tfx1Δ* mutant. All appropriate strains of *S. pombe* have been streaked onto YEA Petri plates and incubated for 3 days at temperatures of 30°C. *tfx1Δ* and *tsn1Δ* mutants growth phenotype is similar to the WT. However, the *ago1Δ* single mutant has lower growth than WT, while the growth of *ago1Δ tfx1Δ* double mutant was slightly better than the *ago1Δ* single mutant. Defects in growth phenotypes of the *ago1Δ* single mutants were similarly observed in *ago1Δ tfx1Δ tsn1Δ* triple mutant as well as *ago1Δ tsn1Δ* double mutants.

3.2.5 Spot Assay of TBZ sensitivity for *dcr1Δ tfx1Δ* and *dcr1Δ tsn1Δ*.

TBZ is a drug that disrupts microtubules. Cells defective in function of centromere like *dcr1Δ* single mutants are sensitive to it TBZ (Sadeghi et al., 2015; Lee et al., 2013; Buhler & Gasser, 2009; Volpe et al., 2002). To address whether the *tfx1* and *tsn1* had redundant function with the *dcr1* which is RNAi regulatory gene, double mutants were analyzed for their TBZ responding (Figure 3.8). It was showed that the *dcr1Δ* single mutant was sensitive to the TBZ compared to the negative control WT strain. Moreover, TBZ sensitivity of the *dcr1Δ tsn1Δ* double mutant was found to be higher in comparison to the *dcr1Δ* single mutant (Figure. 3.8). Finally, *dcr1Δ tfx1Δ* double mutants exhibited no additional sensitivity in comparison with *dcr1Δ* single mutant but was sensitive compared to the WT.

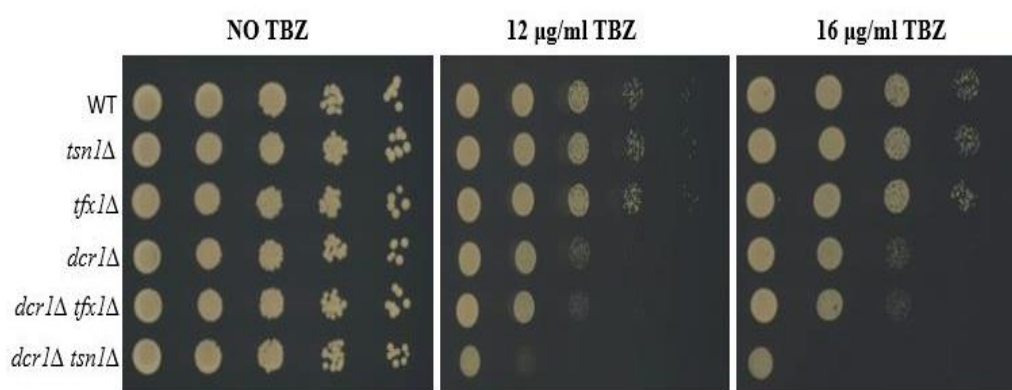


Figure 3.8 Single *tsn1Δ*, but not *tfx1Δ*, mutations increase TBZ sensitivity in *dcr1Δ* mutations. 10-fold serial dilutions of all appropriated *S. pombe* strains were spotted onto YAE and exposed to the TBZ in two different range of concentration (12-16). The *dcr1Δ* single mutant exhibited high-enhanced sensitivity to TBZ compared to the WT. Similar TBZ sensitivity was shown in the *dcr1Δ tfx1Δ* double mutants. Moreover, the *dcr1Δ tsn1Δ* double mutant strains displayed supersensitive to TBZ, compared with WT strain and much greater sensitivity than *dcr1Δ tfx1Δ* double mutant and the *dcr1Δ* single mutant strain.

3.2.6 Determination of *tfx1* Δ and *tsn1* Δ mutant responses to DNA damage in Dcr1 absence

Relative to the observations from the *ago1* Δ background (more details in section 3.2.1), analysis of the roles of both *tsn1* and *tfx1* function in the background of *dcr1* Δ showed that *tsn1* Δ but not *tfx1* Δ mutation enhanced chromosomal instability in the absence of Dcr1. This was as analyzed by TBZ drug sensitivity in (Figure 3.10). These outcomes supported the fact that *tsn1* but not *tfx1* are essential for preserving chromosomal stability in the *dcr1* Δ mutant background. The Trax and Translin have been postulated to play role in DNA repair response, however, there is limited evidence to support the assertion. Recently, Wang et al. (2016) found that DSB repair via the ATM-mediated pathway was associated with murine Trax serving as an ATM scaffold protein. In addition, it has been found that the Dcr1 but not the Ago1 being necessary for DNA damage response by Castel et al. (2014), let us to examine whether *tsn1* and *tfx1* are necessary or have redundant role for the pathway of DNA damage response in a *dcr1* Δ background. To address this question, the appropriate mutant strains of *S. pombe* have been assessed and exposed to several DNA-damaging drugs with analyzed for their corresponding response to various pathways of repairing DNA damage. The DNA damaging agents include phleomycin (Figure 3.9), belomycine (Figure 3.10), hydroxyurea (HU; Figure 3.11), ultraviolet irradiation (UV; Figure 3.12), camptothecin (CPT; Figure 3.13) and methyl methane sulfonate (MMS Figure 3.14). Mitomycin C (MMC Figure 3.15). Remarkably, our finding observed that the *dcr1* Δ *tsn1* Δ double mutant was hypersensitivity when compared to the *dcr1* Δ single mutant to some DNA damaging agents, include Phleomycin, Belomycine, HU and UV. Also, it has been shown that *dcr1* Δ *tfx1* Δ has similar sensitivity in comparison of single *dcr1* Δ mutant to these agents such as Camptothecin agents (CPT). Notably, neither of the double mutants (*dcr1* Δ *tsn1* Δ or *dcr1* Δ *tfx1* Δ) displayed no increased sensitivity when exposed to response to MMC or MMS when relative to the *dcr1* Δ . Altogether, these analyses are sufficient to indicate the involvement of *tsn1* but not *tfx1* for recovery process of DNA damage in the Dcr1 absence, a discovery that unveils a novel function of the *tsn1* in response to pathway of DNA damage.

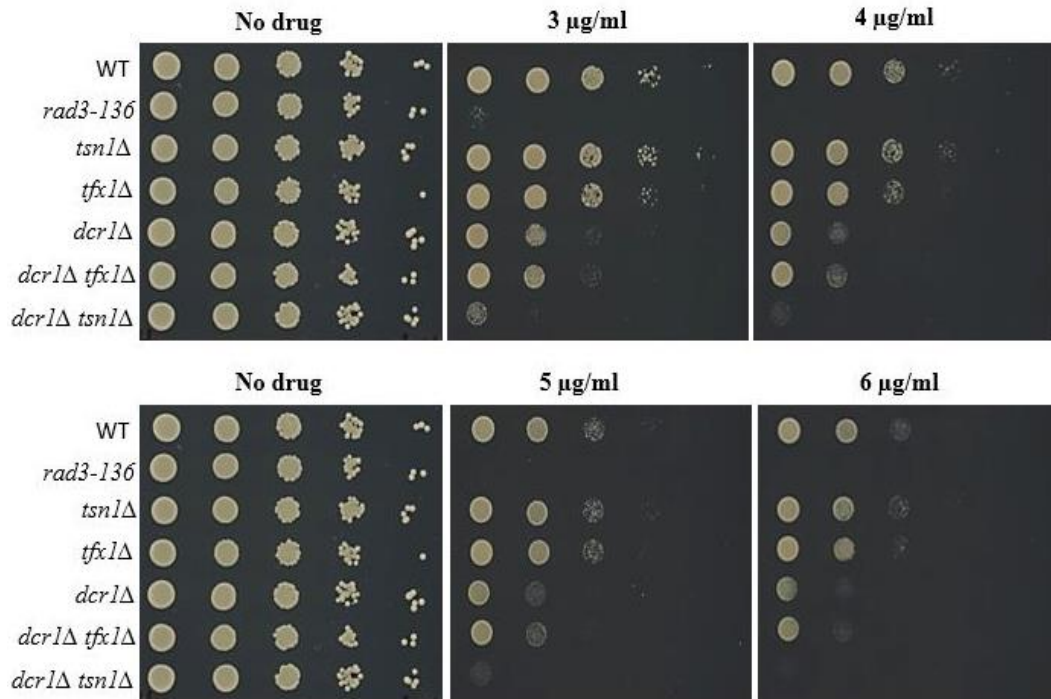


Figure 3.9 *tsn1*Δ Mutation but not *tfx1*Δ in the *dcr1*Δ Background increased phleomycin sensitivity. 10-fold serial dilutions of all appropriated *S. pombe* strains were spotted onto YAE. Strains have been exposed to phleomycin in different range of concentration. The plates have been incubated for approximately 3 days at 30°C. The positive control was *rad3-136* cells which is checkpoint control genes in this spot assay. The data displayed that the *dcr1*Δ *tsn1*Δ double mutant is hypersensitive but not the *dcr1*Δ *tfx1*Δ, showed partially suppress to phleomycin when compared to the *dcr1*Δ single mutant.

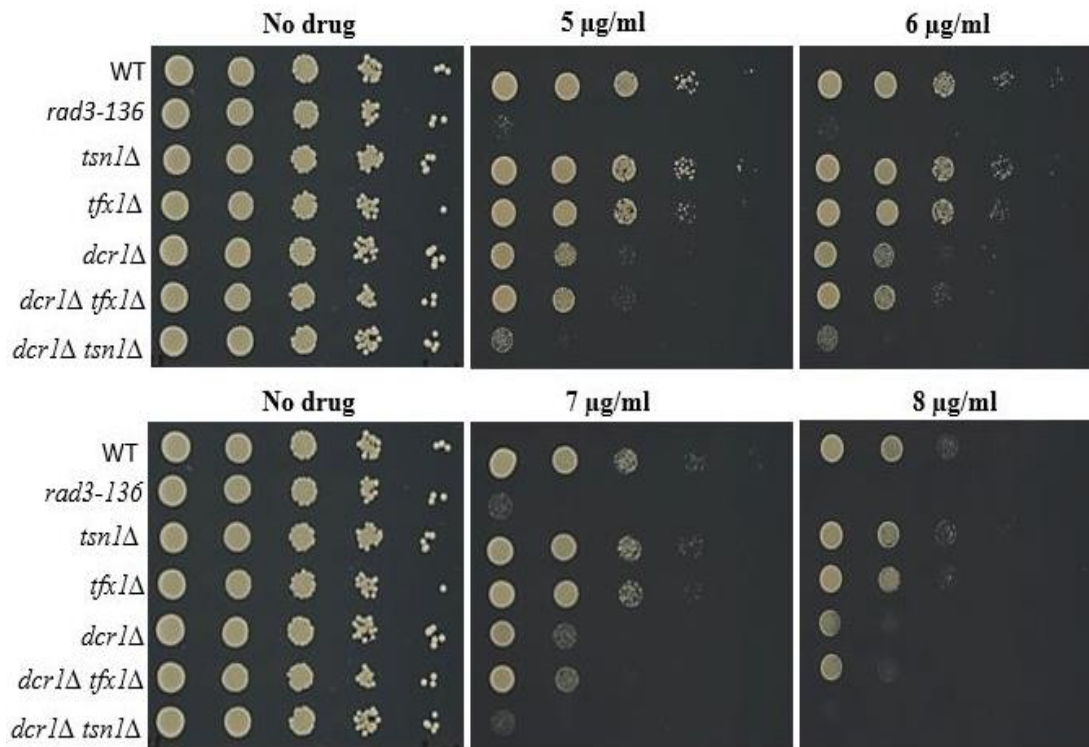


Figure 3.10 *tsn1Δ* Mutation but not *tfx1Δ* in the *dcr1Δ* background increased belomycin sensitivity. 10-fold serial dilutions of all appropriated *S. pombe* strains were spotted onto YAE. Mutant Strains have been exposed to phleomycin in different range of concentration. The positive control was *rad3-136* cells which is checkpoint control genes in this spot assay. The data displayed that the *dcr1Δ tsn1Δ* double mutant is hypersensitive to belomycin but not the *dcr1Δ tfx1Δ*, when compared to the *dcr1Δ* mutant.

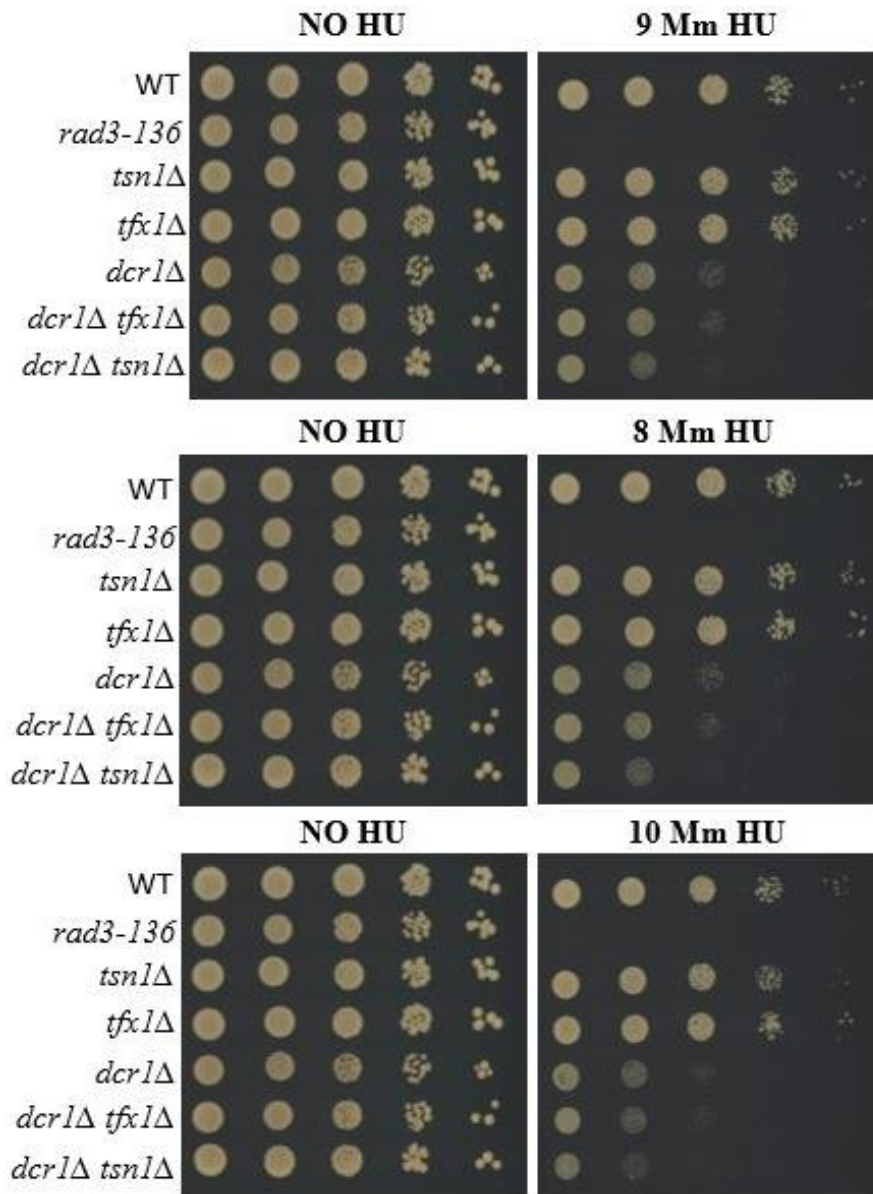


Figure 3.11 *dcr1*Δ *tsn1*Δ deletion strains are hydroxyurea (HU) sensitivity. 10-fold serial dilutions of *S. pombe* cultures were spotted onto YAE plates supplemented with hydroxyurea at concentrations indicated. *rad3-136* cells serve as positive control for HU sensitivity. *tsn1*Δ *dcr1*Δ strains show increased sensitivity whereas a *tfx1*Δ mutation show partially suppression relative to *dcr1*Δ.

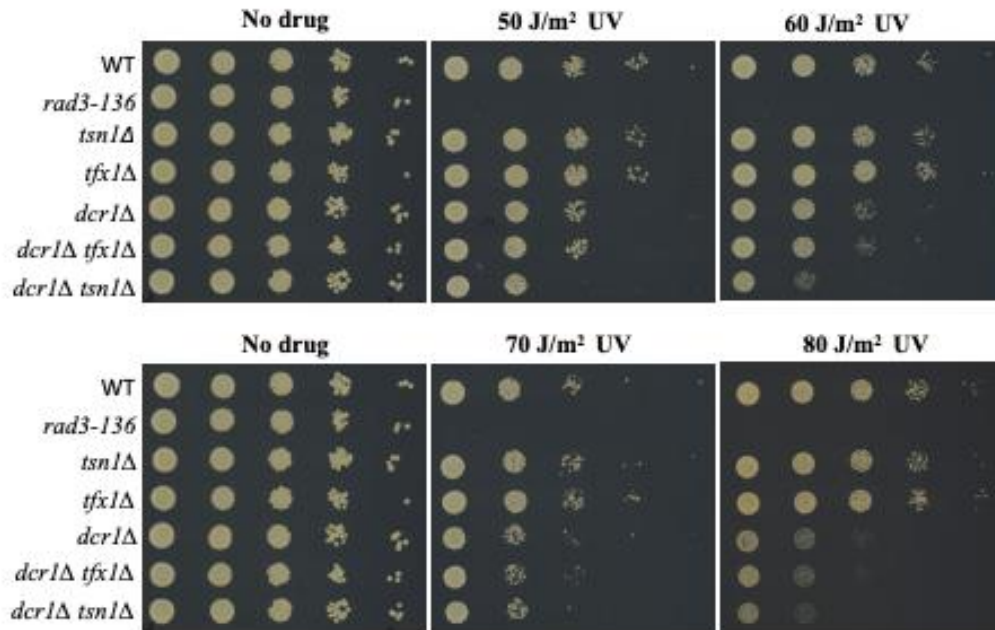


Figure 3.12 The *dcr1Δ tsn1Δ* double mutant, but not *dcr1Δ tfx1Δ*, is enhanced sensitive to ultraviolet (UV). 10-fold serial dilutions of the indicated *S. pombe* strains were spotted onto YAE. Mutant Strains have been exposed to different doses of ultraviolet (UV). The plates were then incubated for approximately 3 days at 30°C. The positive control was *rad3-136* cells which is checkpoint control genes in this spot assay. The result shows that the *dcr1Δ tsn1Δ* double mutant displayed a mild increase sensitivity in UV, but not *dcr1Δ tfx1Δ* mutants, relative to the *dcr1Δ* mutant.

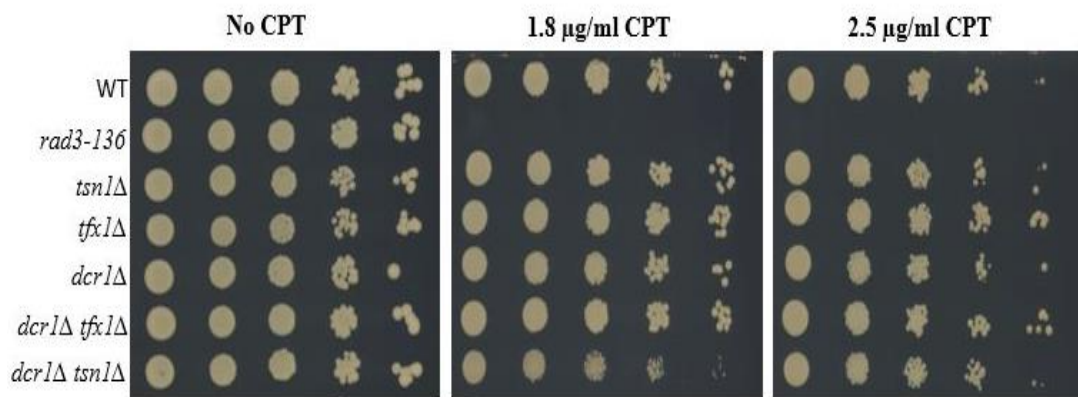


Figure 3.13 Sensitivity spot test of Camptothecin (CPT) for several of *S. pombe* strains. 10-fold serial dilutions of the indicated *S. pombe* strains were spotted onto YAE. Mutant Strains have been exposed to different concentration of camptothecin (CPT). The plates were then incubated for approximately 3 days at 30°C. The positive control was *rad3-136* cells which is checkpoint control genes in this spot assay. The result show that the *dcr1Δ tsn1Δ* and *dcr1Δ tfx1Δ* double mutant exhibited no increase sensitivity in CPT, in relative to the WT and *dcr1Δ* single mutant.

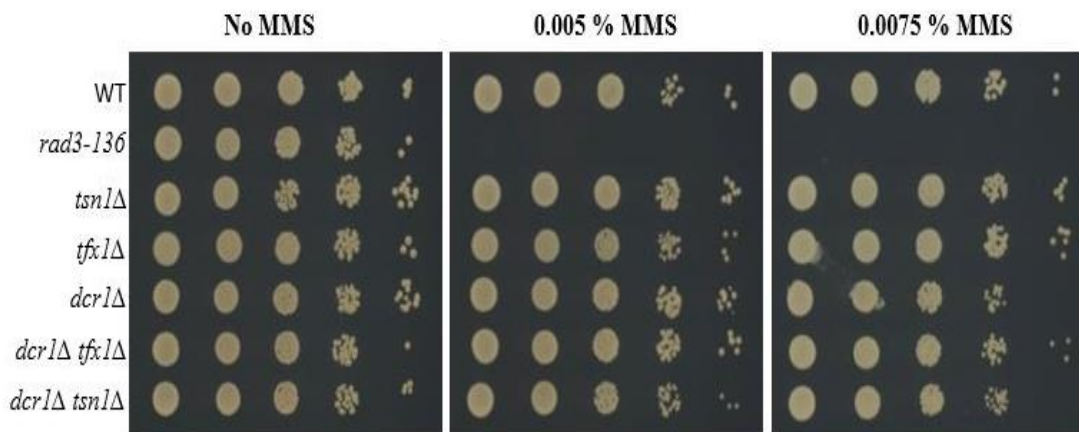


Figure 3.14 Sensitivity spot test of Methylmethane sulfonate (MMS) for several of *S. pombe* mutants. 10-fold serial dilutions of the indicated *S. pombe* strains were spotted onto YAE. Mutant strains have been exposed to different doses of Methyl methane sulfonate (MMS). The plates were then incubated for approximately 3 days at 30°C. The positive control was *rad3-136* cells which is checkpoint control genes in this spot assay. No sensitivity has been shown in the *dcr1Δ tfx1Δ* or *dcr1Δ tsn1Δ* double mutants to MMS in comparison of WT or the *dcr1Δ* single strain.

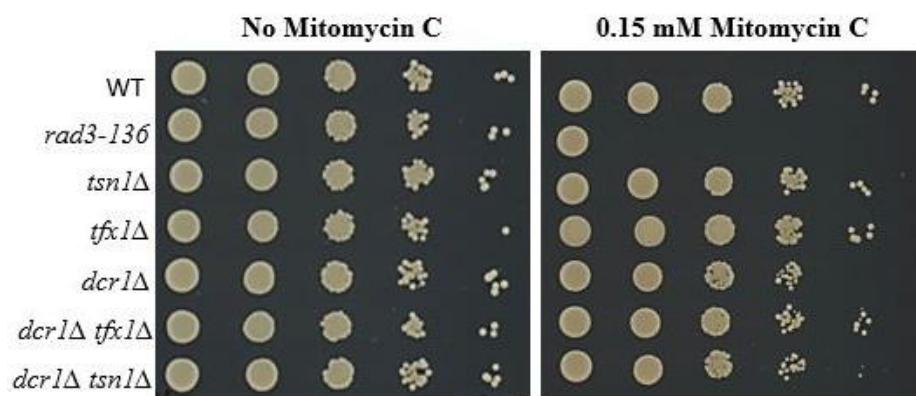


Figure 3.15 Sensitivity spot test of Mitomycin C (MMC) for several of *S. pombe* mutants. 10-fold serial dilutions of the indicated *S. pombe* strains were spotted onto YAE. Mutant strains have been exposed to different concentration of Methyl methane sulfonate (MMS). The plates were then incubated for approximately 3 days at 30°C. The positive control was *rad3-136* cells which is checkpoint control genes in this spot assay. No sensitivity has been shown in the *dcr1Δ tfx1Δ* or *dcr1Δ tsn1Δ* double mutants to MMC in comparison of WT or the *dcr1Δ* single strain.

3.2 Discussion

3.3.1 Mutation of *tfx1Δ* suppresses the chromosome instability of the *ago1Δ* mutant.

The heterochromatic nature of the centromeres contributes to their functional role in linking chromosomes and spindle microtubules. Centromeres ensure faithful chromosomal segregation in the meiosis and mitosis (Forsburg & Shen, 2017; Moreno-Moreno et al., 2017; Thakur et al., 2015; Fennell et al., 2015; Westhorpe & Straight, 2014; Buhler & Gasser, 2009). In *S. pombe*, the process of heterochromatic development in the centromeres requires the RNAi machinery (Mutazono et al., 2017; Shimada et al., 2016; Tadeo et al., 2013). As a result, chromosomal missegregation occurs due to *ago1Δ* and other RNAi gene mutations that interfere with the centromere function. The effects of chromosomal segregation in the cells are shown in the increased sensitivity to TBZ as a microtubule-destabilizing agent (Sadeghi et al., 2015; Buhler & Gasser, 2009; Lee et al., 2013). In the RNAi regulation system, C3PO consist of the Translin and Trax complex, which required to remove the siRNA- passenger strands in human cells and *D. melanogaster* (Holoch & Moazed, 2015; Ye et al., 2011; Tian et al., 2011; Liu et al., 2009). According to previous studies on the null mutations of the *tsn1* and *tfx1* genes in *S. pombe*, no observed change in the stability of genome was observed (Laufman et al., 2005; Jaendling et al., 2008). This implies that the *tfx1* and *tsn1* genes do not play major role in the functioning of fission yeast RNAi pathway, though they could probably function in a redundant fashion (Jaendling & McFarlane, 2010). According to this and previous studies, the chromosomal instability defect of *ago1Δ* cells is partially and fully suppressed by *tfx1Δ* but not *tsn1Δ* (N. Al-mobadel, Ph.D. thesis, Bangor University). One of the approaches used to confirm the results of the present study is using TBZ sensitivity tests to confirm the consistency of the data. The tests revealed that the *ago1Δ* mutant was partially suppressed by the *tfx1Δ* mutation, but not by the *tsn1Δ* mutant. The triple mutant *ago1Δ tfx1Δ tsn1Δ* was highly TBZ sensitive as shown in (Figure 3.1).

Additionally, the McFarlane group evaluated the segregation of endogenous chromosome by monitoring the level of anaphase deficiencies. The results indicated that the chromosomal missegregation of the *ago1* single mutant were significantly reduced by an additional *tfx1Δ* mutation. However, additional *tsn1Δ* mutation did not suppress the chromosome defect of in the *ago1Δ* mutants (Othman Alzaharani PhD thesis, Bangor University). Taken together, the data demonstrate that *ago1Δ* mutant defect is suppressed by *tfx1Δ* mutation.

Chapter 3: Results

Interestingly, the suppression of the *ago1* Δ phenotype by mutating *tfx1* appears to be dependent on *tsn1*. As additional, loss of Tsn1 result in a genom stability phenotype similar to the *ago1* Δ single mutant. One explanation for this is that mutation of Tfx1 releases Tsn1 from being bound to *tfx1* freeing it to act to suppress for loss of Ago1. Tsn1 does not function to suppress the *ago1* Δ phenotype by re-establishing centeromeric hetrochromatine, as this is not restored in the *ago1* Δ *tfx1* Δ double mutant (Gomez-Escobar et al., 2016). The mechanism driving the suppression requires further investigation.

Previously, it has been shown that the stability/levels of *tfx1* are dependent on *tsn1* in *S. pombe* (Jaendling et al., 2008). In addition, in a *tsn1* Δ mutant Tfx1 levels are almost undetectable, but there is some low level Tfx1. The fact that a *tfx1* Δ mutation suppresses *ago1* Δ defects, but *tsn1* Δ does not (when Tfx1 levels are very low) suggests that the very low levels s of Tfx1 in *tsn1* Δ mutant are sufficient for function or alternatively, the *ago1* Δ *tsn1* Δ phenotype is similar to the *ago1* Δ *tfx1* Δ *tsn1* Δ triple mutant, phenotype.

3.3.2 Loss of Tsn1 Increases Chromosome Instability in a *dcr1* Δ background

As discussed, proper segregation of chromosomes during mitotic and meiotic divisions requires the development of centromeric heterochromatin (Mutazono et al., 2017; Schmidt & Cech, 2015; Zeng et al., 2010; Buhler & Gasser, 2009; Stimpson & Sullivan, 2010). Development of heterochromatin and its sustenance in centromeres occurs through the RNAi pathway in *S. pombe* (Mutazono et al., 2017; Shimada et al., 2016; Sadeghi et al., 2015; Holoch & Moazed, 2015; Buhler & Gasser, 2009; Volpe et al., 2003). Since it has been observed that greater TBZ sensitivity is exhibited by the *dcr1* Δ *tsn1* Δ double mutants relative to the *dcr1* Δ single and *dcr1* Δ *tfx1* Δ double mutants (Figure 3.10). It can be suggested that Tsn1 becomes functionally important when Dcr1 is not present.

Our results showed that the instability of chromosomes demonstrated by *dcr1* Δ cells is increased by *tsn1* Δ but not the *tfx1* Δ mutation. In addition to this, this observation points towards the fact rescue of Ago1 defects through Tfx1 loss is peculiar and can be a sign of quite distinct mechanistic defect. It has also been reported by co-workers in the McFarlane group that *tsn1* Δ mutation, not the *tfx1* Δ mutation, increased mini-chromosome instability in *dcr1* Δ background. This is in accordance with the observation that *tsn1* loss augments the instability of chromosome in *dcr1* Δ

cells (Z. Al-shehri, PhD thesis, Bangor University; N. Al-mobadel, PhD thesis, Bangor University). These findings support the hypothesis that Tsn1 contributes to maintaining genome stability when Dcr1 is not present, but Tfx1 does not.

3.3.3 Tsn1, but not Tfx1, is required in the DNA damage response of Dcr1-Defective Cells

The DNA repair response has been shown to involve Trax (Chien et al., 2018; Wang et al., 2016) but a role for Translin is less clear (Jaendling & McFarlane, 2010). Moreover, recent reports indicate that the DNA damage response in *S. pombe* also involves Dcr1 through an RNAi-independent Ago1-independent mechanism (Ren et al., 2015; Castel et al., 2014). Considering these reports, this research aimed to determine if the increase in chromosomal instability demonstrated by the *dcr1Δ tsn1Δ* double mutants is due to DNA repair pathway defects.

Results obtained during this study indicate that the instability of chromosome noticed in the case of *dcr1Δ tsn1Δ* double mutants could be caused by the inability of the cell to repair or respond to DNA damage. These results also show that it is the Tsn1, and not Tfx1, which is needed by the cells to respond to DNA damages when Dcr1 is not present which indicates a separation of function between these Tsn1/and Tfx1. It is important to note that the results of sensitivity tests also indicated that increased sensitivity to different DNA damaging agents demonstrated by the *dcr1Δ tsn1Δ* double mutants is related to damage associated with DNA replication so it could infer a function for Tsn1 linked to S-phase.

This idea is further complemented by the observation that the agents, which are less related to S-phase, such as MMS (uses mismatch repair type mechanism), were unable to show significant change sensitivity between *dcr1Δ* single mutant and *dcr1Δ tsn1Δ* (for example Figure 3.15). The findings of Castel et al. (2014) support to these findings, since they reported that Dcr1 is needed for inhibition of transcription mediated by RNA Pol II from areas where transcription may collide with replication. This leads to maintain the genomic stability (Ren et al., 2015). When the Dcr1 is not present, collisions between RNA-DNA hybrids mediated by RNA Pol II and the DNA replication machinery occur. The DNA replication fork can collapse and DSBs can be formed that may drive chromosomal rearrangements and instability (Castel et al., 2014; Brambati et al., 2015).

Chapter 3: Results

A strong affinity of Translin for controlling RNA species has long been known (Jaendling & McFarlane, 2010). Hence, it is possible that Tsn1 is involved in decreasing the stability of RNA-DNA hybrids when Dcr1 is absent leading to suppression of recombination and preserving genome stability. For that reason, *tsn1* Δ mutation with the *dcr1* Δ background could stimulate the recombination to occur which leads to chromosomal translocations.

Considering all these results, it can be proposed that in the absence of Dcr1, Tsn1 acts by suppressing the transcription-DNA replication-associated recombination and this can explain the speculated function for Translin in mediating chromosomal translocations (Aoki et al., 1995). The role of Dcr1 in this particular mechanism has been distinguished from the RNAi regulation pathway (Castel et al., 2014). This suggests a function of Tsn1 in RNA regulation of DNA damage response.

Phleomycine and belomycine agent proposed to cause formation of DSBs. The indicated increased sensitivity of the *dcr1* Δ *tsn1* Δ double mutants in comparison to the *dcr1* Δ mutant to phleomycin and belomycine as shown in (Figures 3.11 and 3.12) could indicate role for Tsn1 in repairing DSBs in the absence of Dcr1. Interstand crosslinks are formed by the MMC agent. This leads to blockage of the replication fork which becomes unable to proceed further. In contrast to HU, MMC causes collapse of the replication fork and the structures formed are distinct from those induced by HU. Removal of RNA-DNA hybrids during the HU-mediated stalling of replication fork requires Dcr1 and potentially Tsn1. It can be suggested that the varying phenotype responses demonstrated by these mutant cells to DNA damage reagents serve as a evidence supporting the proposition that Tsn1 function is linked with the mechanism of transcription replication collision, which is consistent with our hypothesis that Tsn1 can participate in removal of RNA-DNA hybrids in absence of Dcr1 leading to suppression of recombination.

The work described in the next chapter explores the hypothesis that increased recombination results in respond loss of *tsn1*, but not *tfx1*, in a Dcr1-deficient background.

Chapter 4: Results

Tsn1, but not Tfx1, is required for suppressing recombination in the deficient of Dcr1

4.1 Introduction

The initiation of cancer and its progression is caused by genetic alteration including chromosomal translocations. Chromosomal translocation can occur due to abnormal recombination between nonhomologous chromosomes (Nambiar & Raghavan, 2011; Roukos & Misteli, 2014; Harewood & Fraser, 2014; Zheng, 2013; Nambiar & Raghavan, 2011). Initially, Translin was identified by the ability to bind to chromosomal translocation break point in human lymphoid cells (Aoki et al., 1995). It was later found that Translin is also implicated for controlling different RNA processes (Gomez-Escobar et al., 2016; Asada et al., 2014; Li et al., 2012; Liu et al., 2009; Wu et al., 1997). However, the linkage between these processes have not been clarified. In an analysis of the *tsn1Δ* and *tfx1Δ* null mutants in *S. pombe*, the works of Jaendling et al. (2008) showed no detectable defects in DNA repair processes such as chromosomal recombination. Before this particular study, the role of Translin as a redundant factor in DNA repair processes and recombination had not been tested which might account for a potential cancer-initiation and progression activity (Jaendling & McFarlane, 2010).

In this present study we have shown that in the *Dcr1* mutation, *Tsn1* is required in the DNA damage response (see in Chapter 3). *Dcr1* is required for removing RNA Pol II-mediated RNA:DNA hybrids from DNA replication sites, such as tRNA genes and rDNA to prevent collisions between two mechanisms transcription and replication fork (Gadaleta & Noguchi, 2017; Ren et al., 2015; Loya & Reines, 2016; Castel et al., 2014; Molla-Herman et al., 2015). Due to the high recombinogenicity of RNA:DNA hybrids at sites (Aguilera & Gómez-González, 2017; Castel et al., 2014; Loya & Reines, 2016). We hypothesised that the hypersensitivity to HU of the *dcr1Δ tsn1Δ* double mutant but not the *dcr1Δ tfx1Δ* double mutant, could lead to an increase in recombination creation inducing lesions in the *dcr1Δ tsn1Δ* cells but not in the *dcr1Δ tfx1Δ* cells.

This suggests the role of *Tsn1*, but not *Tfx1*, is needed to suppress DNA transcription, replication collisions and subsequent recombination when *Dcr1* is absent. This chapter attempts to investigate the possibility of this hypothesis, to determine if *Tfx1* and/or *Tsn1* have role in recombination regulation at a tRNA gene (tDNA), a known DNA replication slow zone, in the *dcr1Δ* single mutant, the *dcr1Δ tsn1Δ* double mutant and *dcr1Δ tfx1Δ* double mutant.

4.1.1 The genetic test summary used in this study

Castel et al. (2014) demonstrated that RNA polymerase II transcribes Anti-sense strands at tRNA genes, and tRNA genes have RNA Pol II accumulated in the *dcr1Δ* cells relative to the control WT. This unexpected finding from (Castel et al., 2014), indicates that the transcription of RNA Pol II antisense occurs in the at tRNA genes. Previously, the McFarlane group set up a recombination system that monitors the frequency of recombination at tRNA gene (Pryce et al., 2009). In order to monitor recombination a plasmid-by-chromosome recombination system was developed at the *ade6* locus (Figure 4.1). This recombination system has been previously used to show tRNA genes slow DNA replication fork progression thus acting as a replication fork barrier (RFB) and stimulating recombination (Pryce et al., 2009). The recombination system works by introducing a single tRNA gene, separately in both orientations (orientation 1 and orientation 2) into the unique *Bst*XI site in the *S. pombe* genomic *ade6* locus; this causes the strains to become auxotrophic for adenine as shown in (Figure 4.1.A). In addition, a plasmid called pSRS5 was manufactured that carries a mutant allele for *ade6* known as *ade6-ΔG1483*. This mutant allele has a point mutation at the position distal to the site the tRNA gene was introduced into the *ade6*⁺ locus as shown in (Figure 4.1.B). Recombination of the *S. pombe* plasmid-borne *ade6-ΔG1483* allele and chromosome-borne *ade6::tRNA^{GLU}* allele leads to the production of adenine prototrophs (Ade⁺) that can be used to genetically measure recombination frequency.

Regarding to the findings of Castel et al. (2014), we speculated that either RNA Pol II and/or RNA Pol III mediated RNA:DNA hybrids could be produced at the *ade6::tRNA^{GLU}* locus. One or both could cause transcription-replication collision. Since it is known that the tRNA gene acts as RFB it would be useful to monitor the frequency of replication here, in order to monitor the frequency of recombination *tsn1Δ*, *dcr1Δ* and *tfx1Δ* mutants including *ade6::tRNA^{GLU}*, which have been described in Section 4.2.1 (Figures 4.2 - 4.5/ 4.11- 4.12). Following this, these mutated strains have been transformed using the pSRS5 plasmid then recombination frequency was monitored using a process of fluctuating analyses as described in Section 2.14 (Figures 4.9, 4.10, 4.16 and 4.17).

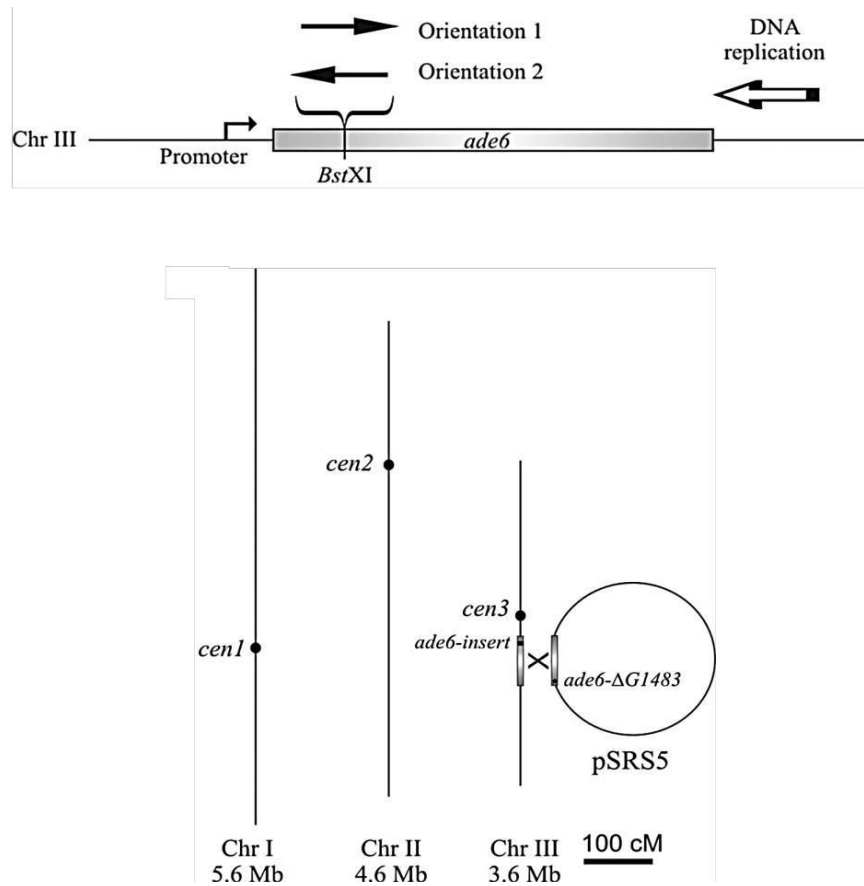


Figure 4.1 graphic model of the recombination system utilized for plasmid-by-chromosome to determine the frequency of a recombination at *ade6::tRNA^{GLU}*.

(A) *tRNA^{GLU}* was independently inserted in both orientations 1 and 2, (black arrows above the site of *Bst*XI) into the *ade6* gene at the *Bst*XI site. The large arrow towards the right of the image shows the direction of the replication on the *ade6* gene. The *ade6* gene is expressed in a left to right direction while the promoter is present next to the *Bst*XI site as shown by the angular arrow. Collision between DNA replication and RNA Pol III machinery is predicted to occur head-to-head in orientation 1 and head-to-tail in orientation 2. Conversely, in orientation 1 could create a head-to-head collision between the replication fork and RNA Pol II. On the other hand, in orientation 2 could create a head-to-tail collision between RNA Pol II and the replication fork. (B). Shows three vertical lines, each one of them represents a chromosome of *S. pombe* below. As shown in the figure, on the smallest chromosome *ade6* locus is located, labelled Chr III. This is the site where the *tRNA^{GLU}* (showcased in A) is inserted. Plasmid pSRS5 is depicted as a large open circle right next to Chr III, it is shown to carry the second *ade6* allele (*ade6-ΔG1483*). The *ade6* allele has a point mutation at the 3' end of *ade6*, this position is distal to where the *tRNA^{GLU}* was placed. Due to the mutations in chromosome and the plasmid carrying the allele, prototroph (Ade⁺) will be generated, which will then be utilized to quantify and measure the frequency of DNA recombination (taken from Pryce et al., 2009).

4.2 Results

4.2.1. Construction of *tsn1*Δ, *dcr1*Δ single mutants and *tsn1*Δ *dcr1*Δ double mutants

As mentioned previously, the *S. pombe* strains were generated using methods for targeting gene based on PCR, whereby they were replaced with antibiotic-resistant cassettes (See Section 2.3). In order to explore the hypothesis Tsn1/ functions to control recombination in the absence of Dcr1, the parent *ade6::tRNA^{GLU}* strains were used to delete both *tsn1* and *dcr1* (BP1478 and BP1508). These were then replaced by single mutant *tsn1*Δ in *tRNA^{GLU}* orientation 1 (BP3335), *tsn1*Δ in *tRNA^{GLU}* orientation 2 (BP3336), *dcr1*Δ in *tRNA^{GLU}* orientation 1 (BP3385) and *dcr1*Δ in *tRNA^{GLU}* orientation 2 (BP3386; Figures 4.2, 4.3, and 4.4). In generating *tsn1*Δ *dcr1*Δ double mutants in *tRNA^{GLU}* orientation 1, *dcr1*Δ single mutant was deleted from *tsn1* single mutants (BP3362; Figure 4.5) mutants and to generate *dcr1*Δ *tsn1*Δ double mutants in *tRNA^{GLU}* orientation 2 (BP3364) *tsn1*Δ background single mutant was used to delete *dcr1* (note: each mutant has two isolates as minimum). Plasmids with antibiotic-resistant selectable markers were derived from *Escherichia coli* (Section 2.3). The *kanMX6* (kanomycin-resistance) gene and *natMX6* (nourseothricin-resistance) genes have been used as replacement cassettes in deleting *tsn1* and *dcr1*. For example, the kanomycin-resistance (*kanMX6*) has been used for the *tsn1*Δ mutants and nourseothricin-resistance (*natMX6*) has been used for the *dcr1*Δ.

Thereafter, they replaced cassettes with PCR primers of 80 and 20 base pairs homologous sequences were amplified. The former was directly flanking the upstream and downstream sequences as well as the *dcr1* and *tsn1* ORFs, while the latter, had the antibiotic resistance genes of a template plasmid (Figure 3.3). The purified PCR product has been transformed chemically into the indicated *S. pombe* strains. To verify the gene deletion *tsn1*Δ, *dcr1*Δ and *dcr1*Δ *tsn1*Δ candidates were checked by PCR (Figure. 4.2, 4.3, 4.4 and 4.5) using three primer sets as shown in (Chapter 3 Figure. 3.4).

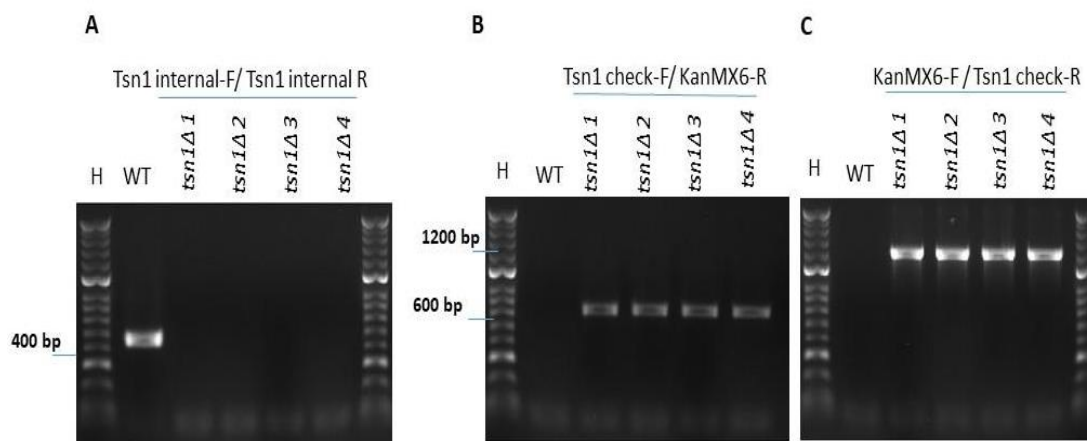


Figure 4.2 PCR screening for the efficient construction of *tsn1Δ* mutants. **A.** Agarose gel image shows products of PCR for the WT and *tsn1Δ1* along with *tsn1Δ 2* in *tRNA^{GLU}* orientation 1 and *tsn1Δ3* and *tsn1Δ 4* in *tRNA^{GLU}* orientation 2 using the the Tsn1-int-F and Tsn1-int-R primers. The *tsn1* PCR products was seen close to the expected sizes of 476 bp. The gel image does not show band for correct deletion of *tsn1Δ* strains. **B.** products of PCR for the *tsn1Δ* and WT candidate strains were obtained using primers Tsn1 check-F and KanMX6-R. The *tsn1Δ* strains give PCR products close to the expected sizes of 620 bp, but not in the WT (the *tsn1⁺* strains) **C.** the *tsn1Δ* and WT candidate strains were amplified by using KanMX6-F and Tsn1 check-R primers. The *tsn1Δ* strains give PCR products close to the expected sizes of 1200 bp. However, nothing was seen in the *tsn1⁺* strains (WT). H = Hyper ladder

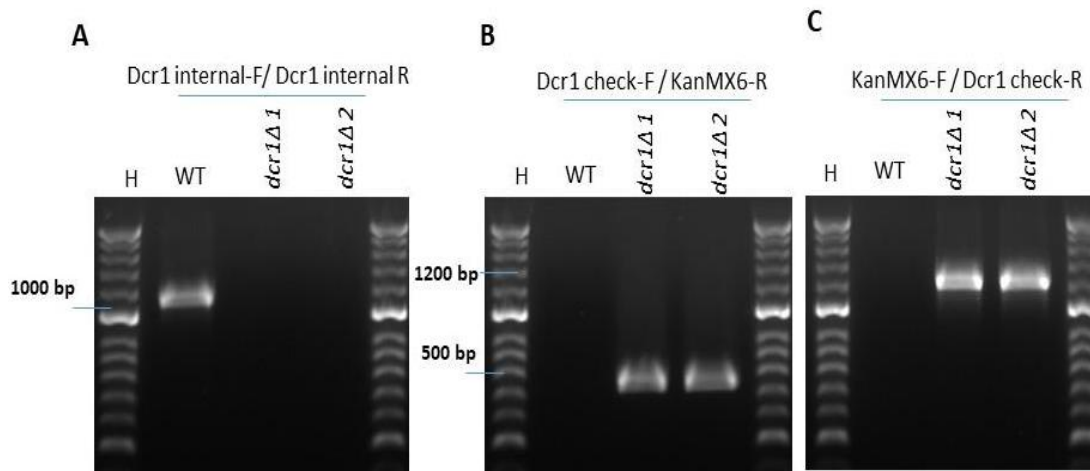


Figure 4.3 PCR screening for the efficient construction of *dcr1Δ* mutants. **A.** Agarose gel image shows products of PCR for the wild-type along with *dcr1Δ1* and *dcr1Δ2* in *tRNA^{GLU}* orientation 1 utilizing Dcr1-int-F and Dcr1-int-R primers. The *dcr1* PCR product had PCR product close to the expected the sizes of 1139 bp. The gel image does not show bands for correct deletion of *dcr1Δ* strains. **B.** products of PCR for the WT and *dcr1Δ* candidate strains were obtained utilizing Dcr1 check-F and KanMX6-R primers. The *dcr1Δ* strains gives PCR products close to the expected sizes of 550 bp, but not in the *dcr1⁺* strains (WT). **C.** the *dcr1Δ* and WT candidate strains were amplified by using KanMX6-F and Dcr1 check-R primers. The *dcr1Δ* strains had PCR product close to the expected sizes of 1297 bp. However, nothing was seen in the *dcr1⁺* strains (WT). H = Hyper ladder

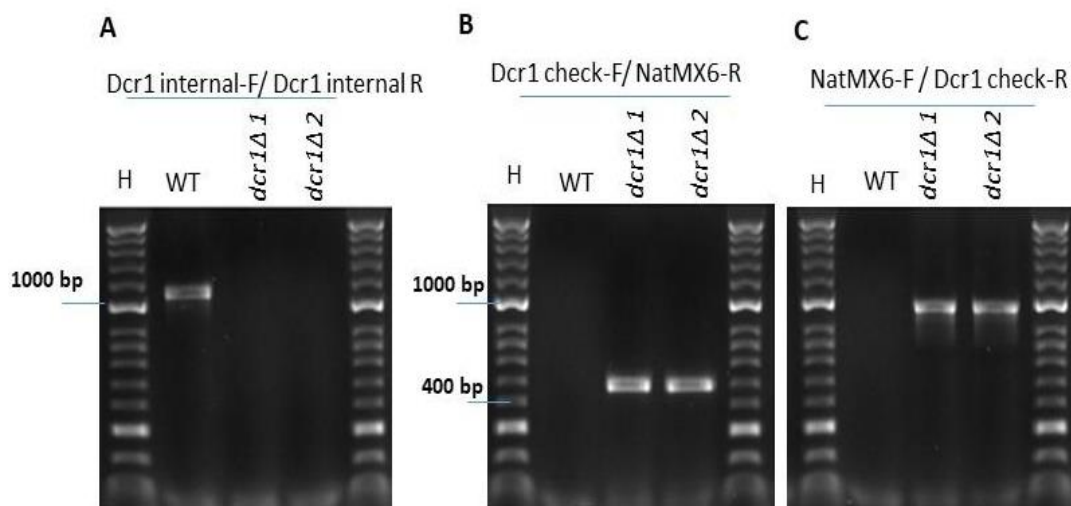


Figure 4.4 PCR screening for the efficient construction of *dcr1Δ* mutants. **A.** Agarose gel image shows products of PCR for the wild-type along with *dcr1Δ1* and *dcr1Δ2* in *tRNA^{GLU}* orientation 2 using the the Dcr1-int-F and Dcr1-int-R primers. The *dcr1* PCR product had PCR products close to the expected sizes of 1139 bp. The gel image does not show bands for correct deletion of *dcr1Δ* strains. **B.** products of PCR for the WT and *dcr1Δ* candidate strains were obtained using Dcr1 check-F and NatMX6-R primers. The *dcr1Δ* strains give PCR products close to the expected sizes of 478bp, but not in the *dcr1⁺* strains (WT). **C.** the *dcr1Δ* and WT candidate strains were amplified by using NatMX6-F and Dcr1 check-R primers. The *dcr1Δ* strains had PCR products close to the expected sizes of 969 bp, however, nothing was seen in the *dcr1⁺* strains (WT). H = Hyper ladder

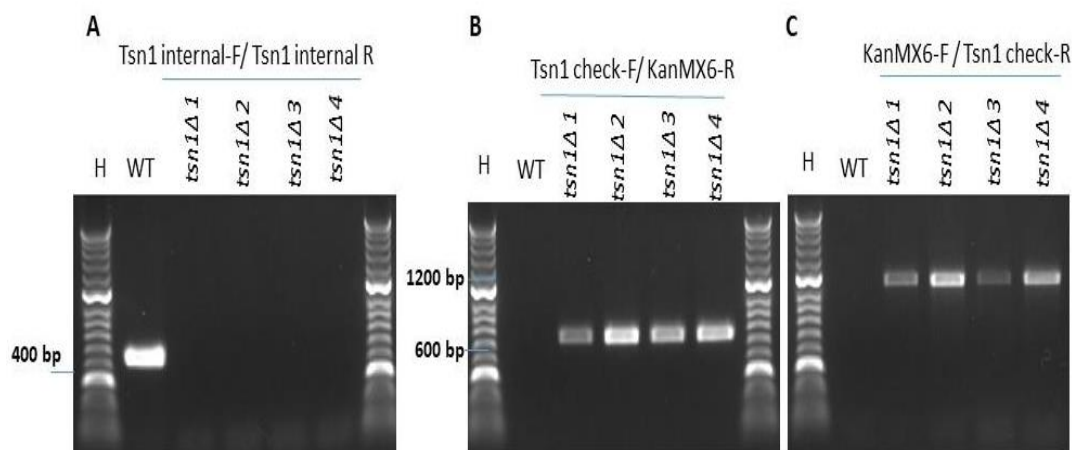


Figure 4.5 PCR screening for the efficient construction of *dcr1Δ tsn1Δ* mutant.

A. Agarose gel image shows products of PCR for the wild-type along with *tsn1Δ 1* and *tsn1Δ 2* in *tRNA^{GLU}* orientation 1 and *tsn1Δ 3* and *tsn1Δ 4* in *tRNA^{GLU}* orientation 2 using the the Tsn1-int-F and Tsn1-int-R primers. The *tsn1* PCR product is close to 475 bp expected sizes. The gel image does not show PCR products for correct deletion of *tsn1Δ* strains. **B.** products of PCR for the WT and *tsn1Δ* candidate strains were obtained using Tsn1 check-F and KanMX6-R primers. The *tsn1Δ* strains give PCR products close to expected sizes of 620 bp, but not in the *tsn1⁺* strains (WT). **C.** the *tsn1Δ* and WT candidate strains were amplified by using KanMX6-F and Tsn1 check-R primers. The *tsn1Δ* strains had PCR products close to the expected sizes of 1200 bp. However, nothing was seen in the *tsn1⁺* strains (WT). H = Hyper ladder

4.2.2. Sensitivity essay of TBZ and DNA damaging agent for *tsn1Δ*, *dcr1Δ* single mutant and *tsn1Δ dcr1Δ* double mutants.

In Chapter 3 it was found that the *dcr1Δ tsn1Δ* double mutant exhibited increased sensitivity when exposed to the microtubule destabilizing drug TBZ, and DNA damaging agent such as phleomycin and HU, in comparison to the *dcr1Δ* single mutant. We repeat the experiment here with the newly constructed strains with mutations of the *ade6::tRNA^{GLU}* strains. The results from this experiment corroborated the findings of the previous experiment, that mutation of *tsn1* alone did not result in any sensitivity in comparison to WT. the *dcr1Δ tsn1Δ* double mutants showed hypersensitivity to drugs like TBZ and other DNA damaging agents such as phleomycin and HU relative to the *dcr1Δ* single mutants and WT (Figure 4.6- 4.8). Interestingly, the *dcr1Δ tsn1Δ* double mutant in *tRNA^{GLU}* orientation 2 has been hypersensitive relative to the *dcr1Δ tsn1Δ* double mutant in orientation 1 for all used drugs. Together these findings reconfirm the notion that in the deficient of Dcr1, it is important to have Tsn1 in response of the DNA damage recovery.

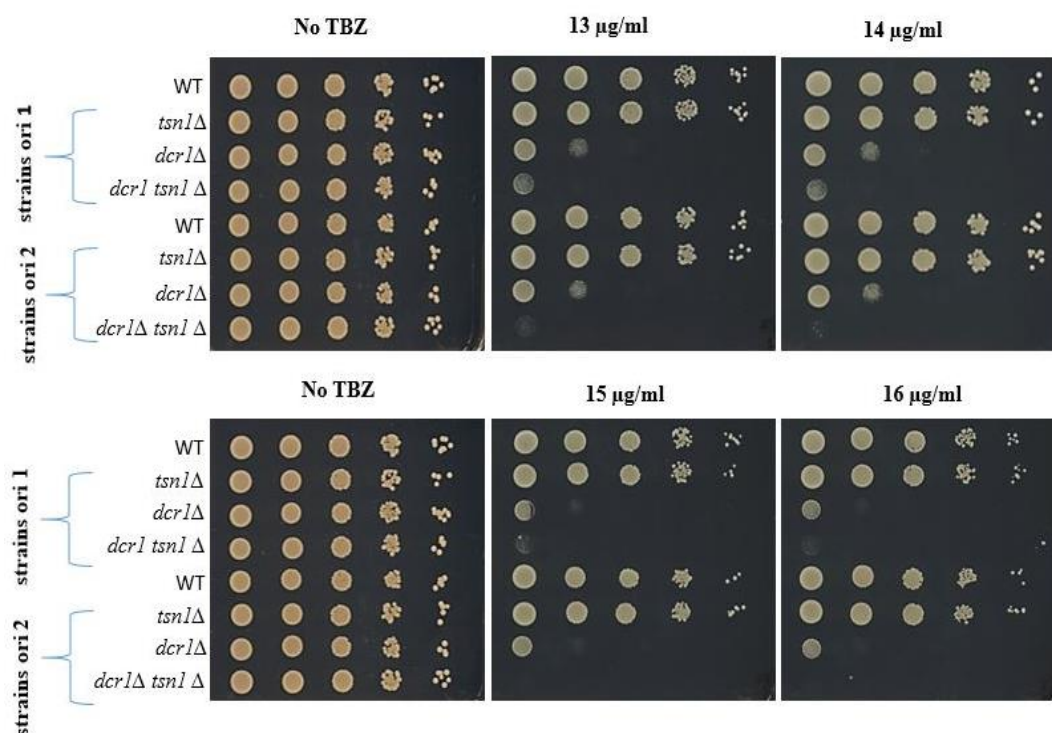


Figure 4.6 Spot assay of TBZ sensitivity that confirms that *dcr1*Δ *tsn1*Δ double mutant is hypersensitivity in both *tRNA*^{GLU} orientations (1 and 2). 10-fold serial dilutions of all appropriate *S. pombe* strains were spotted onto YEA. Mutant strains were exposed to TBZ in different range of concentration. The plates have been incubated for roughly 3 days at 30°C. Both *dcr1*Δ *tsn1*Δ double mutants in both *tRNA*^{GLU} orientations (1 and 2) showed greater increased sensitivity to TBZ, compared with the *dcr1*Δ single mutant.

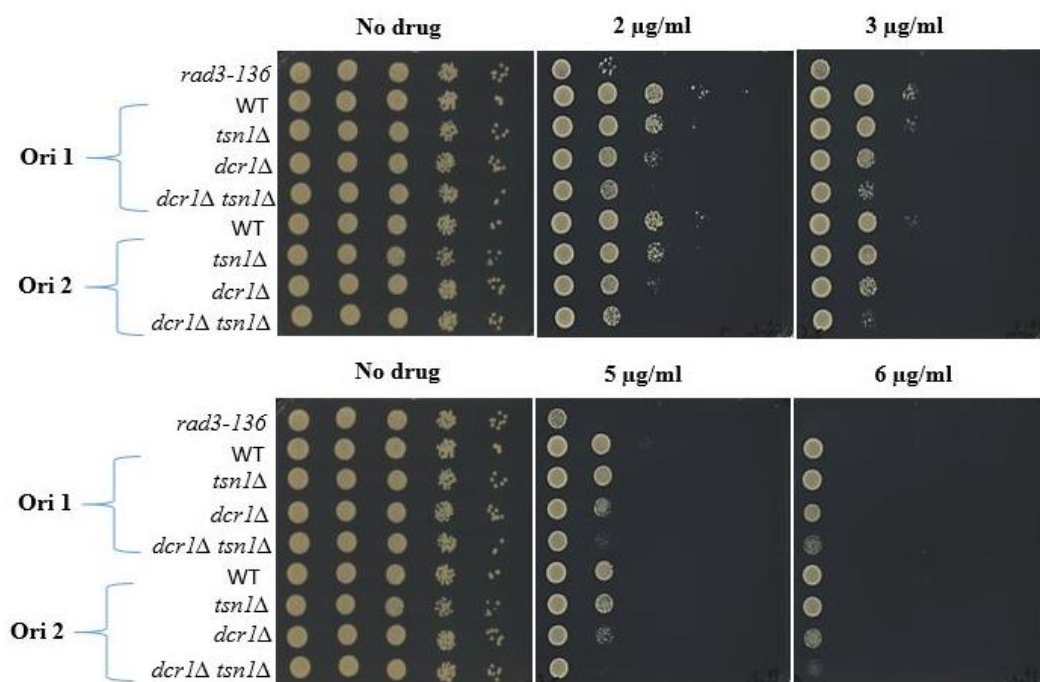


Figure 4.7 Spot assay of Phleomycin sensitivity that confirms that the *dcr1Δ tsn1Δ* cells are enhanced sensitivity. 10-fold serial dilutions of all appropriate *S. pombe* strains were spotted onto YEA. Mutant strains exposed to phleomycin in different range of concentration. The plates have been incubated for around 3 days at 30°C. The positive control was *rad3-136* cells, which is a checkpoint control gene. in both *tRNA^{GLU}* orientations (1 and 2) displayed less sensitivity to Phleomycin in *dcr1Δ tsn1Δ* background.

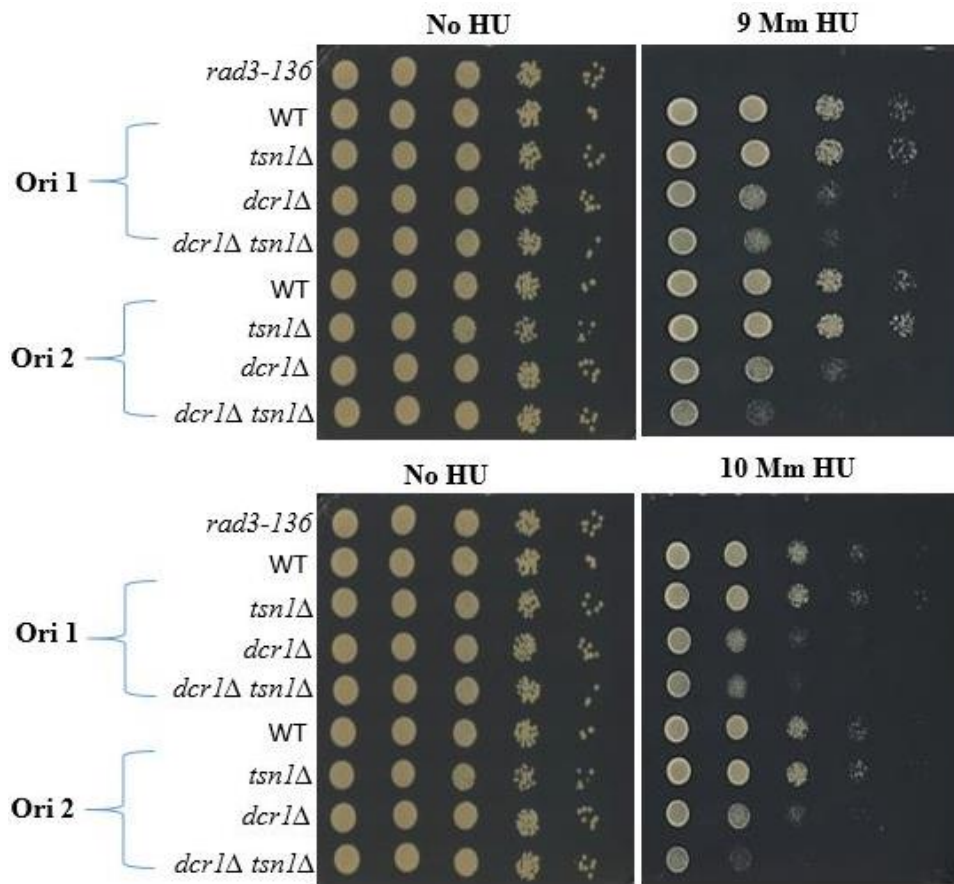


Figure 4.8 Spot assay of HU sensitivity spot assay that confirms the *dcr1Δ tsn1Δ* double mutants are hypersensitivity in orientations 2. 10-fold serial dilutions of all appropriated *S. pombe* strains were spotted onto YEA. Mutant strains have been exposed to HU in two range of concentration (9 mM-10 mM). The plates have been incubated for around 3 days at 30°C. The positive control was *rad3-136* cells, which is a checkpoint control gene. The *dcr1Δ tsn1Δ* double mutants in *tRNA^{GLU}* orientations (2) showed hypersensitivity to HU relative to the *dcr1Δ* single mutants, although it is less apparent in orientation 1.

4.2.3. Recombination frequency analysis for the *tsn1*Δ, *dcr1*Δ single mutants and the *tsn1*Δ *dcr1*Δ double mutants at tRNA genes.

Based on the experimental findings discussed above, we further explored whether the hypersensitivity of the *dcr1*Δ *tsn1*Δ double mutant towards damaging agents, such as HU and phleomycin, is associated to increased recombination frequency at (RFB). In order to assess this, mutations in strains carrying both orientations of the tRNA RFB in *S. pombe* were assessed for recombination frequency using the plasmid-by-chromosome recombination assay (Figure 4.1) (Pryce et al. 2009). The fluctuation analysis was used to measure adenine prototrophs generated per 10⁶ cells (Section 2.13).

Since the *tRNA^{GLU}* gene was introduced in two orientations into *ade6* locus both orientations were assessed for recombination frequency. In this assay, *swi1*Δ mutants were used as positive control because increased elevated recombination has been shown in *swi1*Δ cells (Pryce et al., 2009). Fluctuation tests for orientation 1 of the *ade6:: tRNA^{GLU}* strains showed there is no increased significantly in the frequency of recombination in *dcr1*Δ and *tsn1*Δ single mutants relative to the WT (Figure 4.9). This also suggests that there is no increase in formation of recombination simulating lesions on the *dcr1*Δ mutants in orientation 1. Whereas in orientation 2, it was seen that in the deficient of Tsn1 there was no statistically significant increase in the recombination frequency relative to the WT strain. However, in the *dcr1*Δ single mutant there was a small, marked increase in recombination frequency relative to the WT for *tRNA^{GLU}* orientation 2. This surprising result points towards a strict orientation effect of the tRNA gene, such that increase in frequency of recombination only occurs in orientation 2. Moreover, it was found that the increased recombination frequency was elevated further, when the *tsn1* gene was mutated in the *dcr1*Δ background (Figure 4.10). This result is statically meaningful and is an increase in *dcr1*Δ *tsn1*Δ double mutant of approximately 2- fold compared to WT. An interesting insight to draw from these results is that hypersensitivity of the mutated gene towards damaging agents such as HU and phleomycin showed in the *dcr1*Δ *tsn1*Δ double mutant, compared to the *dcr1*Δ single mutant is related to orientation- specific increase recombination at replication fork barrier RFB.

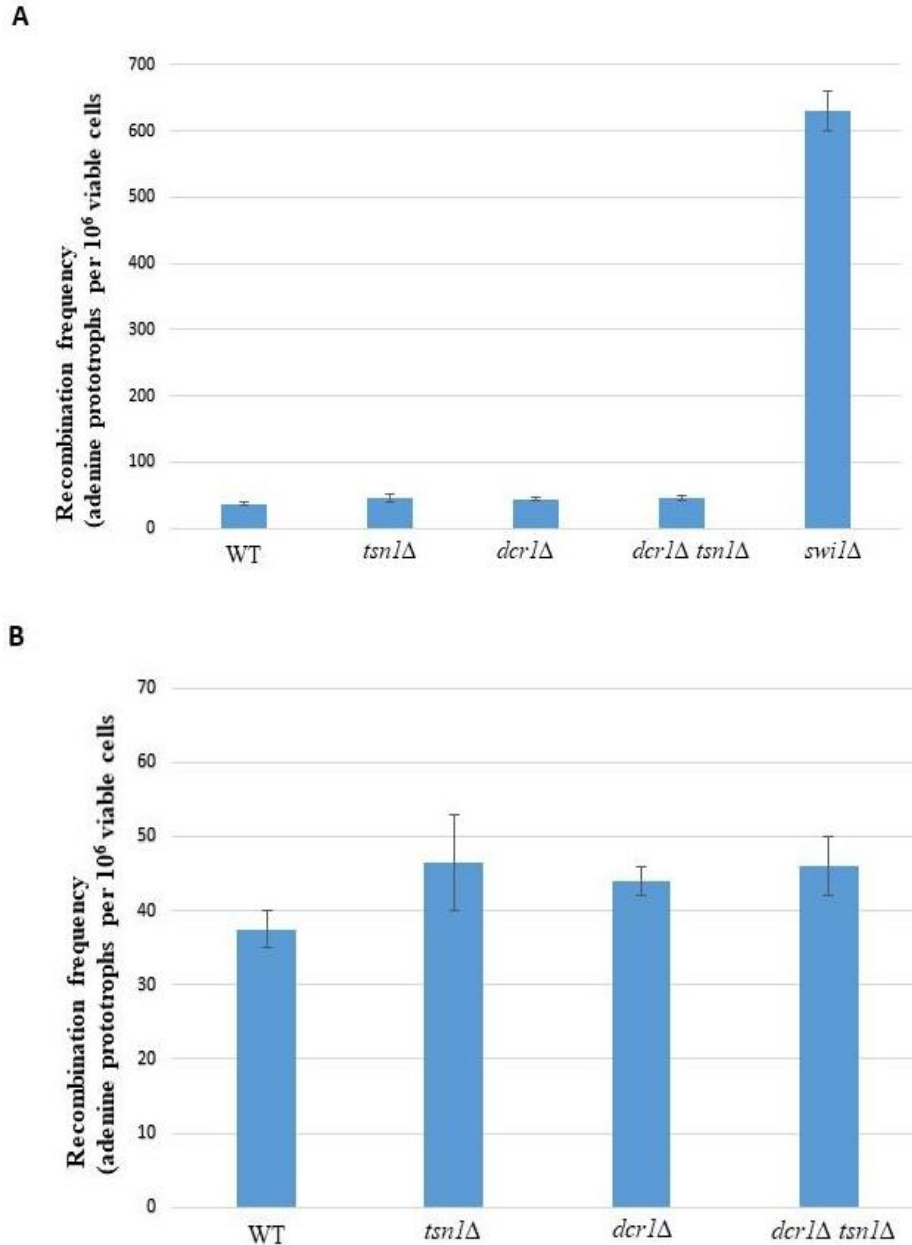


Figure 4.9 Recombination test for the *ade6::tRNA^{GLU}*–orientation 1 strains. **A.**

This bar chart shows the mean values obtained from three median values derived from fluctuation analysis. This data displayed there is no increased significantly in the frequency of recombination in *dcr1*Δ and *tsn1*Δ single mutants, compared to WT strain. The positive control was *swi1*Δ mutant and it is known from previous works that this mutant shows a recombination elevation at *ade6::tRNA^{GLU}*. **B** similar data but with the *swi1*Δ (positive control) data removed. The standard deviation is shown in the error bars. Pairwise students t-test were carried out to identify the p-value between the WT and *tsn1*Δ, *dcr1*Δ, *dcr1*Δ *tsn1*Δ double mutants. All p-values were > 0.05 except *swi1*Δ vs WT is less than 0.0001

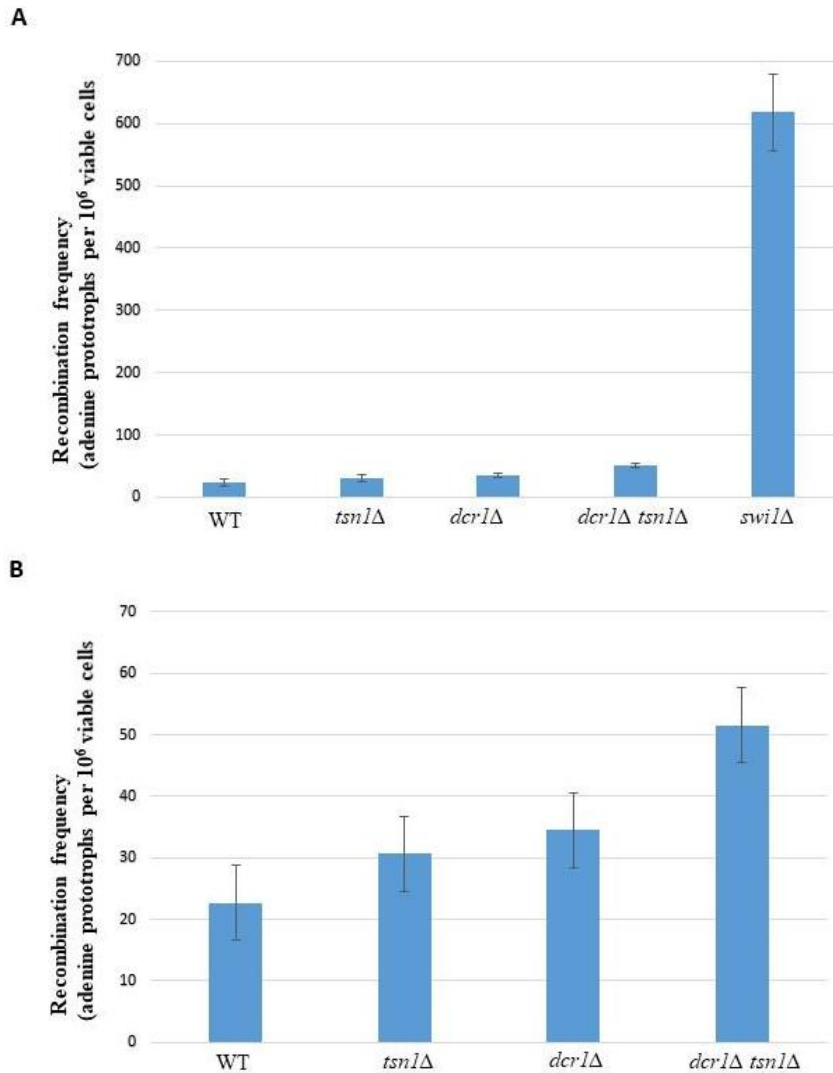


Figure 4.10 Construction of *tfx1*, *dcr1* single mutants and *tfx1 dcr1* double mutants.

In order to find out whether Tfx1 has a role in recombination regulation. The parent strains with *tRNA^{GLU}* has been used to deleted both *tfx1* and *dcr1* genes from both orientations (BP1478 and BP1508). We obtained three isolates of *tfx1*Δ from orientation 1 (BP3389, BP3390 and BP3393) and for *tfx1*Δ in orientation 2 we obtained two isolates (BP3392 and BP3393), *dcr1*Δ in orientation 1 (BP3313) and *dcr1*Δ in orientation 2 (BP3343) (Figures 4.3 and 4.4). In generating *tfx1*Δ *dcr1*Δ double mutants in orientation 1 (BP3395 and BP3397) and orientation 2 (BP3399 and BP3400) *tfx1*Δ background single mutant (BP3389 and BP3392) was used to delete *dcr1* (note: each mutant has two isolates as minimum). Plasmids with antibiotic-resistant selectable markers were derived from *Escherichia coli* (Table 2.3). The *kanMX6* (kanomycin-resistance) was used for the *tfx1*Δ mutants (Figure 4.11) and *natMX6* (nourseothricin-resistance) was used for the *dcr1*Δ (Figure 4.12).

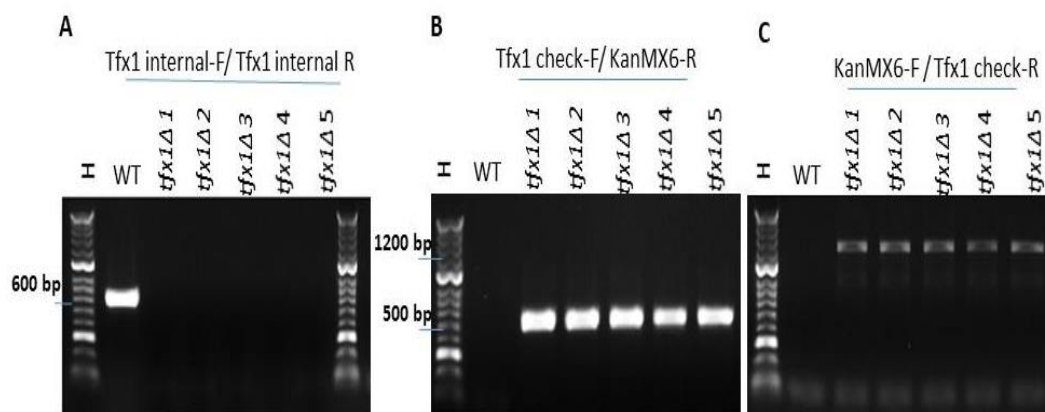


Figure 4.11 PCR screening for the efficient construction of *tfx1*Δ mutant. **A.** Agarose gel image shows products of PCR for the wild-type along with *tfx1*Δ1 and *tfx1*Δ2 and *tfx1*Δ3 in *tRNA^{GLU}* orientation 1 and *tfx1*Δ4 and *tfx1*Δ5 in *tRNA^{GLU}* orientation 2 using the the Tfx1-int-F and Tfx1-int-R primers. The *tfx1* PCR product is close to expected sizes of 626 bp. The gel image does not show bands for correct deletion of *tfx1*Δ strains. **B.** products of PCR for the WT and *tfx1*Δ strains were obtained utilities primers Tfx1 check-F and KanMX6-R. The *tfx1*Δ PCR products had PCR products close to the expected sizes of 523 bp, but not in the *tfx1*⁺ strains (WT). **C.** the *tfx1*Δ and WT candidate strains were amplified by using KanMX6-F and Tfx1 check-R primers. The *tfx1*Δ strains were present close to the expected sizes of 1244 bp. However, nothing was seen in the *tfx1*⁺ strains (WT). H = Hyper ladder

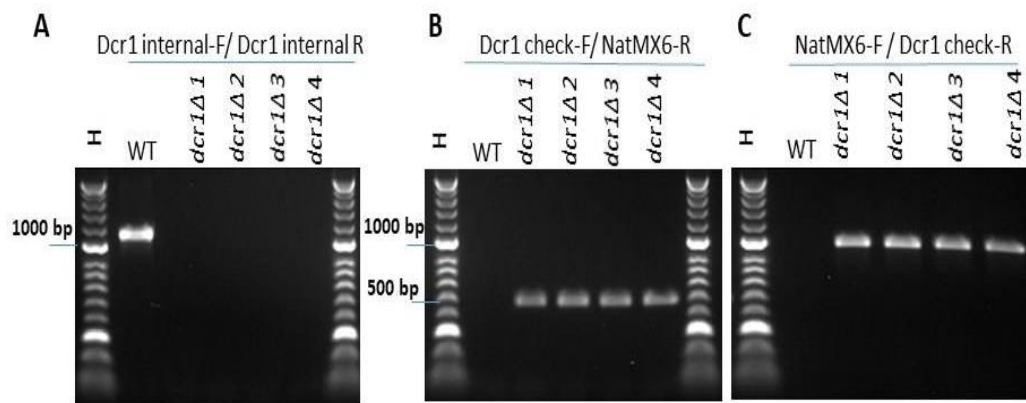


Figure 4.12 PCR screening for the efficient construction of *dcr1Δ tfx1Δ* mutants.

A. Agarose gel image shows products of PCR for the wild-type along with *dcr1Δ1* and *dcr1Δ2* in *tRNA^{GLU}* orientation 1 *dcr1Δ3* and *dcr1Δ4* in *tRNA^{GLU}* orientation 2 using the the Dcr1-int-F and Dcr1-int-R primers. The expected sizes of *dcr1* was seen in 1139 bp. The gel image does not show PCR products for correct deletion of *dcr1Δ* strains. **B.** products of PCR for the WT and *dcr1Δ* strains were obtained using Dcr1 check-F and NatMX6-R primers. The *dcr1Δ* PCR products were seen close to the expected sizes of 478 bp, but not in the *dcr1⁺* strains (WT). **C.** the *dcr1Δ* and WT candidate strains were amplified by using NatMX6-F and Dcr1 check-R primers. The *dcr1Δ* strains were present close to expected sizes of 969 bp However, nothing was seen in the *dcr1⁺* strains (WT). H = Hyper ladder

4.2.5. Sensitivity essay of TBZ and DNA damaging agent for *tfx1Δ*, *dcr1Δ* single mutant and *dcr1Δ tfx1Δ* double mutants.

We repeat the experiment here with new knockout strains with mutation of the *ade6::tRNA^{GLU}* strains, which are *tfx1Δ*, *dcr1Δ* single mutants and *dcr1Δ tfx1Δ* double mutant. It has been shown that the *dcr1Δ* single mutant was supersensitive to TBZ, phelomycin and HU relative to WT. The positive control was *rad3-136* cells. As we expected no measurable increased sensitivity was seen in *dcr1Δ tfx1Δ* double mutant relative to *dcr1Δ* single mutant. This result is consistent with our pervious finding, that the *dcr1Δ tfx1Δ* double mutant exhibited no increase in sensetivity in response to DNA damage relative to the *dcr1Δ* single mutant. Collectively, the findings verify that Tfx1 is not required in response of the DNA damage recovery in Dcr1 absence.

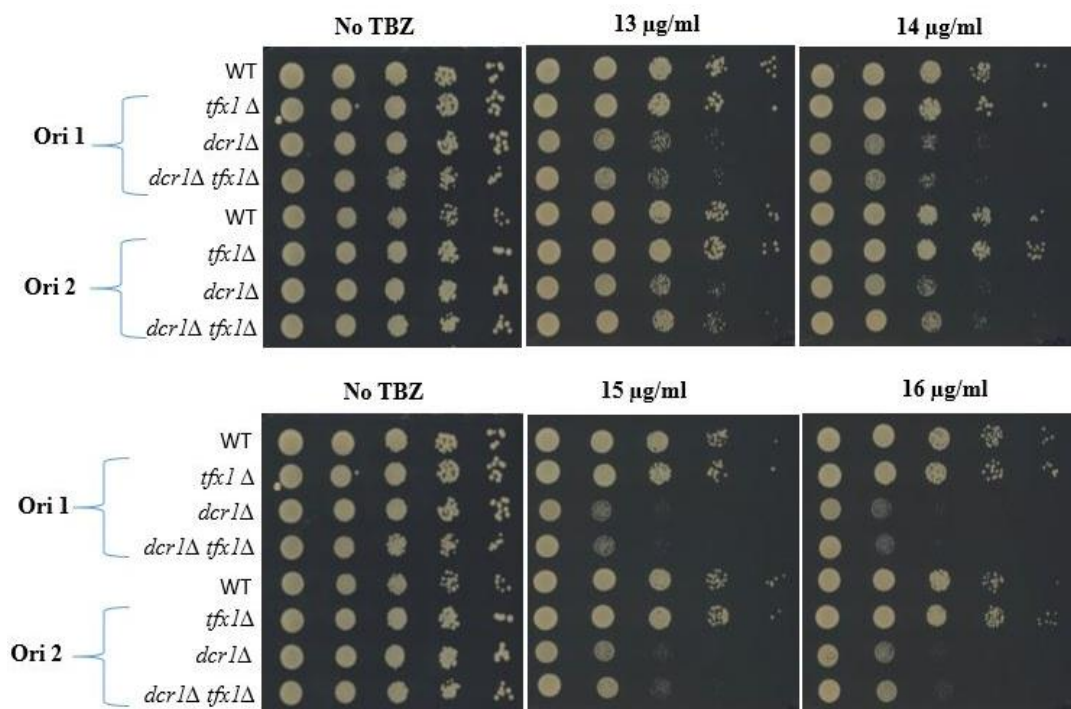


Figure 4.13 Mutation of *dcr1Δ* produces in equal suppression of *dcr1Δ tfx1Δ* double mutant of TBZ sensitivity only *tRNA^{GLU}* orientations 2. 10-fold serial dilutions of all appropriate *S. pombe* strains have been spotted onto YEA. Mutant strains were exposed to the TBZ in to TBZ in different range of concentration. The plates have been incubated for 3 days at 30°C. The data showed no increase sensitivity was observed between between the *dcr1Δ* and *dcr1Δ tfx1Δ* double mutants in *tRNA^{GLU}* orientations (1) but more suppression in orientations 2 to TBZ sensitivity.

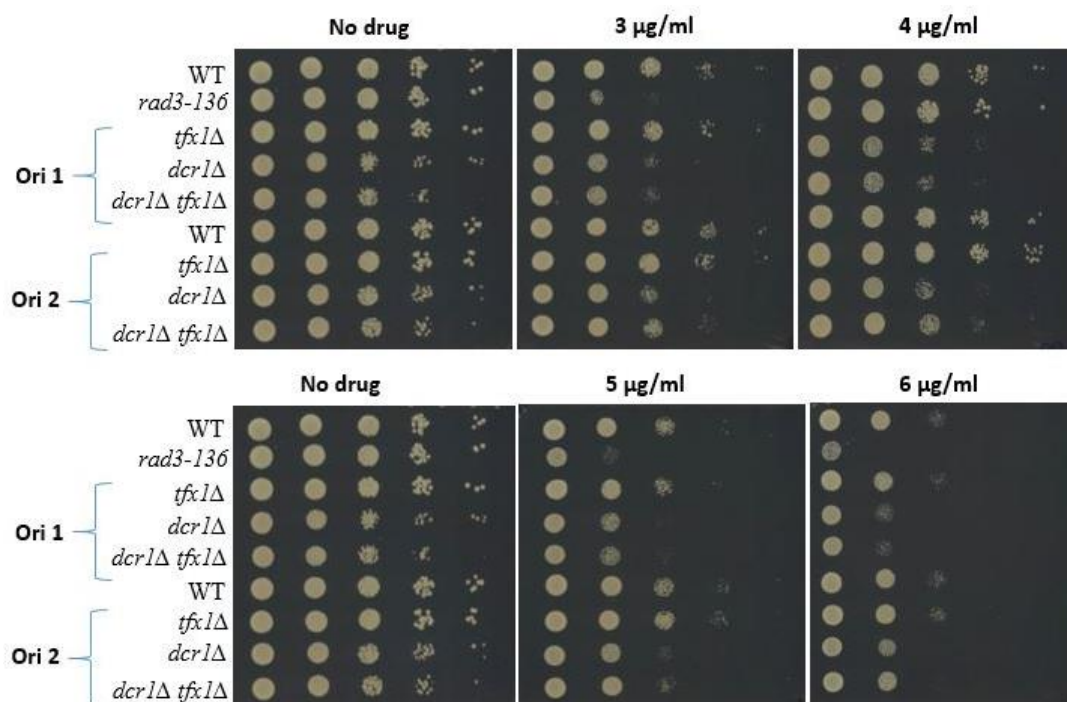


Figure 4.14 Mutation of *dcr1Δ tfx1Δ* genes in *tRNA^{GLU}* orientations one results in phelomycin sensitivity to have the same levels observed in the *dcr1Δ* single mutant. 10-fold serial dilutions of all appropriate *S. pombe* strains were spotted onto YAE. Mutant strains were exposed to the phelomycin in different range of concentration. The plates had been incubated for approximately 3 days at 30°C. The positive control was *rad3-136* cells. No measureable increase in phelomycin sensitivity was shown between the *dcr1Δ* and the *dcr1Δ tfx1Δ* double mutants. The *tfx1Δ* single mutant was already observed to exhibit no sensitivity to phelomycin in comparison with the WT.

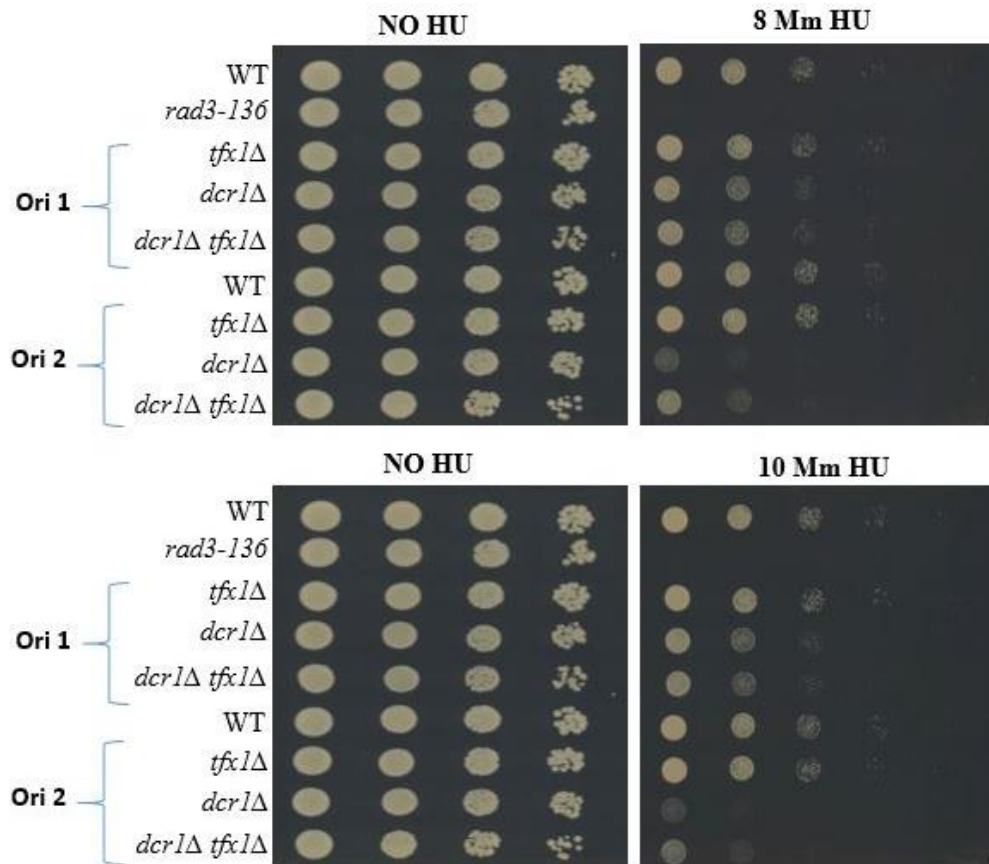


Figure 4.15 Mutation of the *dcr1Δ* results in a similar suppression of *dcr1Δ tfx1Δ* double mutant of HU sensitivity. 10-fold serial dilutions of all appropriated *S. pombe* strains were spotted onto YAE. Mutant strains were exposed to the HU in two different range of concentrations (8 mM -10 mM). The plates have been incubated for around 3 days at 30°C. The positive control was *rad3-136* cells. The data showed slight suppression in the *dcr1Δ tfx1Δ* double in HU sensitivity only in *tRNA^{GLU}* orientations two in compared with the *dcr1Δ* single mutant.

4.2.6. Recombination frequencies analysis for the *tfx1* Δ , *dcr1* Δ single mutants and the *tfx1* Δ *dcr1* Δ double mutants at tRNA genes.

We wished to establish whether the *dcr1* Δ *tfx1* Δ double mutant exhibited increases in replication at a tRNA RFB, as was observed for the *dcr1* Δ *tsn1* Δ double mutant in an orientation-dependent fashion. We hypothesised this would not be the case as the *dcr1* Δ *tfx1* Δ double mutant does not exhibit hypersensitivity to DNA replication disruption agents. Fluctuation assay were carried out on newly constructed mutants *tfx1* Δ , *dcr1* Δ and *dcr1* Δ *tfx1* Δ and wild-type strains using the plasmid pSRS5 to assess adenine prototrophs generated per 10^6 cells.

In *tRNA^{GLU}* orientation 1 for *tfx1* Δ , *dcr1* Δ and *dcr1* Δ *tfx1* Δ strains, the fluctuation assays showed no increase in the recombination frequency between WT and *tfx1* Δ or *dcr1* Δ and *dcr1* Δ *tfx1* Δ (Figure 4.16). In this assay the positive control was *swi1* Δ mutant. However, the *dcr1* Δ single mutant showed increased recombination relative to the WT and *dcr1* Δ *tfx1* Δ had a significant increase of approximately 2-fold when compared to WT (Figure 4.16). In orientation 2 the fluctuation test data indicate that the *dcr1* Δ resulted a roughly double increase in the rate of recombination compared to WT strain. The *dcr1* Δ *tfx1* Δ double mutant was statically significant increased in comparison with both WT strain and *tfx1* Δ . However, no statically significant has been showed between WT and *tfx1* Δ or *dcr1* Δ *tfx1* Δ double mutant and *dcr1* Δ (Figure 4.17). Overall, the data confirm that the Tfx1 lose dose not induce recombinogenic lesions in the deficient of Dcr1 for both orientations. In this expermint see the *dcr1* Δ single mutant appears to cause an orientation-independent increase in recombination. This was not observing in the first mutants for the *dcr1* Δ *tsn1* Δ double mutants set. The reason for that discrepancy is unclear, but it suggests a condition-dependent difference. It is unknown what these condition differences are, but clearly future experimental investigation is needed.

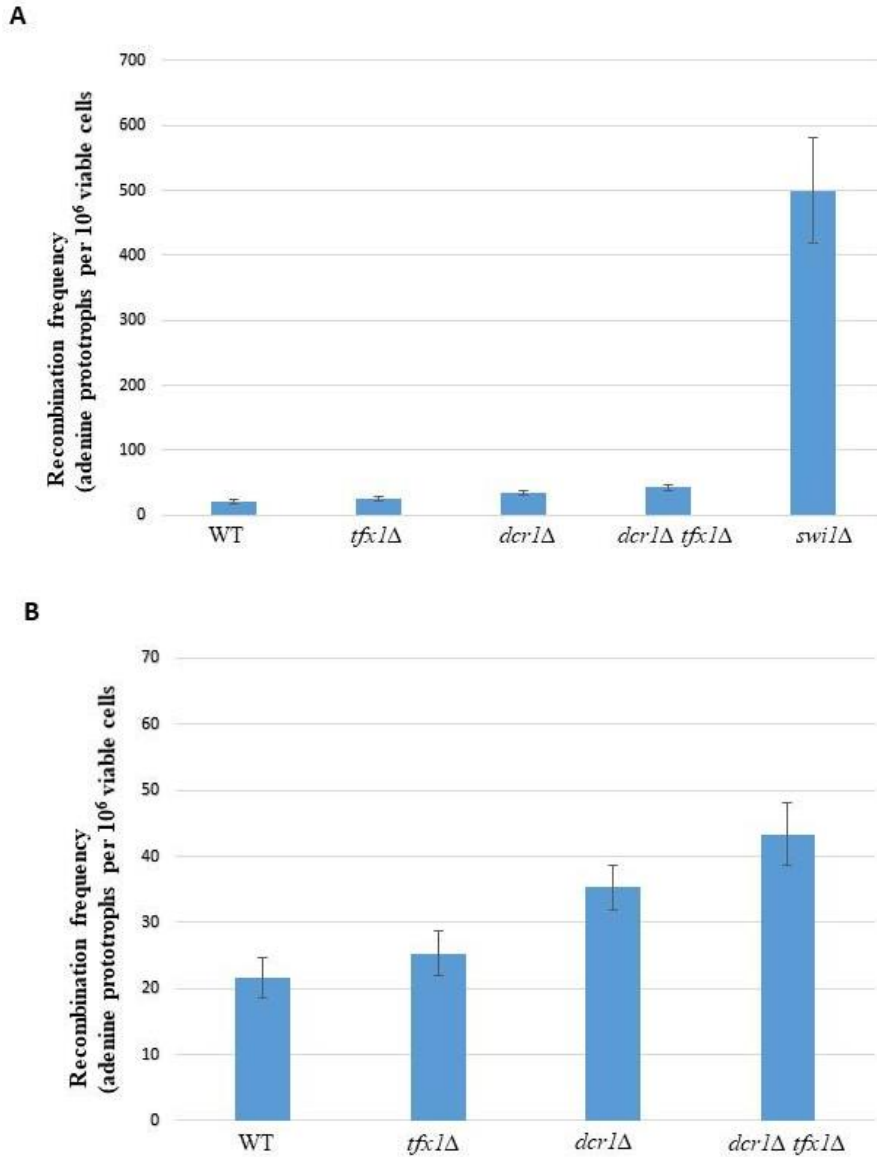


Figure 4.16 Recombination test for the *ade6::tRNA^{GLU}*–orientation 1 strains.

A. This bar chart shows the mean values obtained from three median values derived from the fluctuation analysis. This data displayed that the *dcr1Δ* lead to a roughly double increase in recombination frequency compared to WT strain. The *dcr1Δ tfx1Δ* double was statically significant in comparison with both WT strain and *tfx1Δ*. However, no statically significant has been observed between *dcr1Δ* and *dcr1Δ tfx1Δ* double mutant. **B.** similar data but with the *swi1Δ* (positive control) data removed. The standard deviation is shown in the error bars. Pairwise students t-test were carried out to identify the p-value of WT vs. *dcr1Δ*, $p < 0.01$; WT vs. *dcr1Δ tfx1Δ*, $p < 0.01$; and *dcr1Δ* vs. *dcr1Δ tfx1Δ*, $p > 0.05$ except *swi1Δ* vs WT is less than 0.0001.

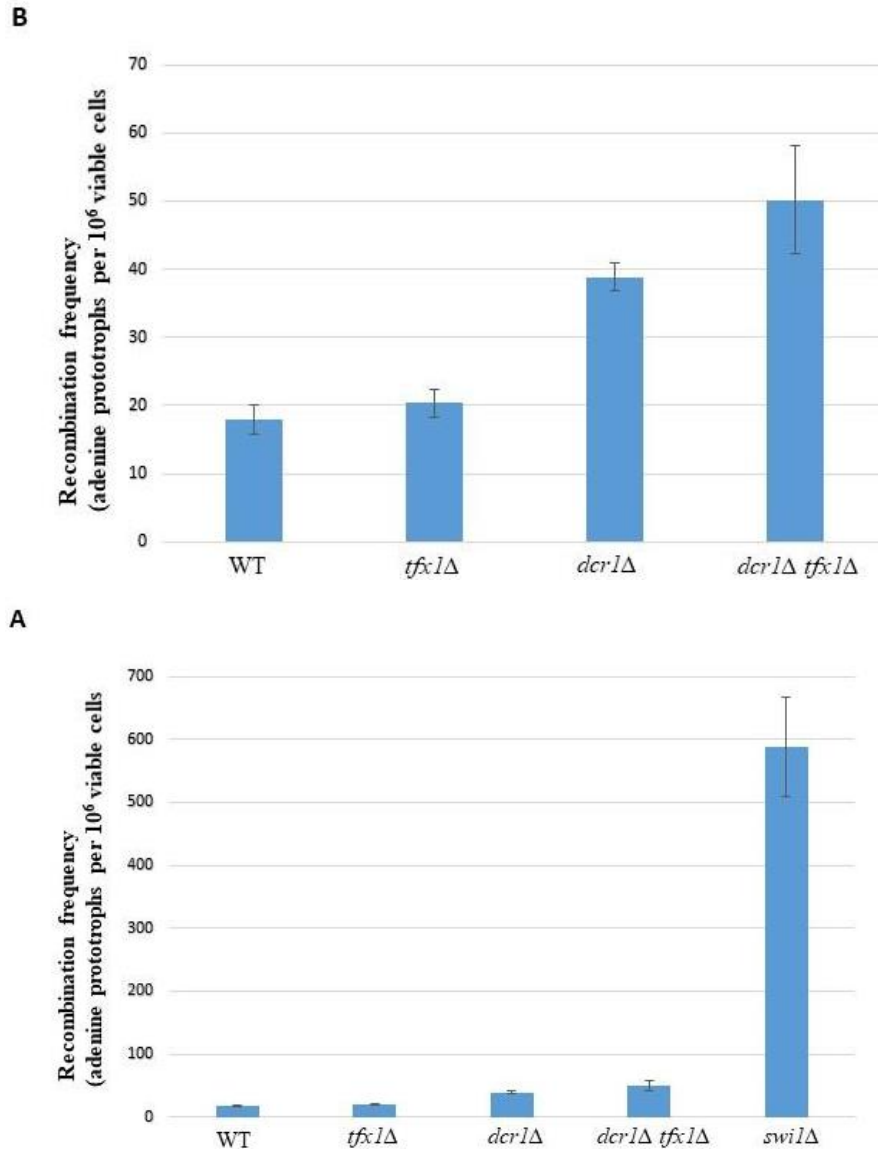


Figure 4.17 Recombination test for the *ade6::tRNA^{GLU}*–orientation 2 strains. **A.** This bar chart shows the mean values obtained from three median values obtained from the fluctuation analysis. This data displayed that the *dcr1Δ* lead to a roughly double elevate in the frequency of recombination compared to WT strain. The *dcr1Δ tfx1Δ* double mutant was statically significantly increased in comparison with both WT strain and *tfx1Δ*. However, no statically significant has been showed between WT and *tfx1Δ* or *dcr1Δ* and *dcr1Δ tfx1Δ* double mutant. **B.** similar data but with the *swi1Δ* (positive control) data removed. The standared deviation is shown in the error bars. Pairwise students t-test were carried out to identify the p-value of WT vs. *dcr1Δ*, $p < 0.01$; WT vs. *dcr1Δ tfx1Δ*, $p < 0.01$; and *dcr1Δ* vs. *dcr1Δ tfx1Δ*, $p > 0.05$ except *swi1Δ* vs WT is less than 0.0001.

4.3 Discussion

4.3.1 Tsn1, but not Tfx1, suppress recombination in the absence of Dcr1

In Chapter 3 of this study, we observed that *dcr1Δ tsn1Δ* double mutant in a *dcr1Δ* background is hypersensitive to TBZ. Moreover, loss of Tsn1 in a *dcr1Δ* mutant causes increased sensitivity to DNA damaging agents such as HU and phleomycin. In light of these findings, we hypothesised that Tsn1 was needed for recombination repair. To test this, we used an RFB-associated recombination reporter system previously established in the McFarlane group. Interestingly, in the new set of experiments, the *dcr1Δ tsn1Δ* double mutant at in both *tRNA^{GLU}* orientations displayed a slight higher level of sensitivity to some of DNA damage agents such as HU and phleomycin than the original *dcr1Δ tsn1Δ* double mutant, which was constructed from the BP90 strain background. This indicates that different background strains could have minor effect on this phenomenon. The results from the new strains confirm the *dcr1Δ tsn1Δ* double mutants but not *dcr1Δ tfx1Δ* might has an increase in replication-associated lesions initiating recombination.

A cause of DNA damage is the accumulation of RNA:DNA hybrids, because these hybrids inhibit and block DNA replication fork progression, and potentially cause fork collapse, resulting in genomic instability (Aguilera & Gómez-González, 2017; Ohle et al., 2016; Felipe-Abrio et al., 2015). Furthermore, highly recombinogenic RNA: DNA hybrids stabilise collision sites between DNA replication and transcription. If they are not processed correctly, chromosome rearrangement might occur, such as translocation (Castel et al., 2014; Brambati et al., 2015). Dcr1 has recently been demonstrated to remove RNA: DNA hybrids from potential collision sites, such as tRNA genes and the rDNA locus. This helps to prevent collisions between replication and transcription and preserve genome stability (Ren et al., 2015).

In the absence of Dcr1, there is an increase in RNA: DNA hybrids at the transcription (Castel et al., 2014). This finding could explain the sensitivity of the *dcr1Δ* single mutant to chromosome-breaking phleomycin and DNA replication pausing HU. Surprisingly, hypersensitive increases following an additional *tsn1Δ* mutation but not *tfx1Δ*, which appears to show these two genes function separately in this process.

Chapter 4: Results

In accordance with the original role suggesting Translin plays a great role in initiation of translocation of chromosomes (Aoki et al., 1995), and it is found to have higher affinity for targeting RNA molecules (Gomez-Escobar et al., 2016; Jaendling & Mcfarlane, 2010). We hypothesize that Tsn1 but not Tfx1 might be important in reducing the stability of the RNA: DNA hybrids in the absence of Dcr1 and limiting formation of recombinogenic lesions. If this is correct, *tsn1Δ* but not *tfx1Δ* in the *dcr1Δ* background might result in RNA:DNA hybrids level, which could be associated with an increase in recombination frequency. In a parallel biochemical, experiment in our lab it was found that in parallel molecular analyses in the group level of RNA:DNA hybrids were assessed in various mutant backgrounds. Previously, it had been demonstrated that *S. pombe dcr1Δ* mutants had elevated level of RNA:DNA hybrids throughout the genome, including the rDNA locus and tRNA genes (Castel et al., 2014). The *tsn1Δ* and *tfx1Δ* mutants surprisingly demonstrated that in both mutants RNA:DNA hybrids at the rDNA locus and tRNA genes were elevated to levels similar to those seen in *dcr1Δ* mutant. If increased RNA:DNA hybrids were sufficient to cause sensitivity to DNA replication inhibiting agents such HU, then the *tsn1Δ* and *tfx1Δ* mutants should exhibit sensitivity to HU, which they do not. Interestingly, *dcr1Δ tsn1Δ* double mutants does appear to have elevated RNA:DNA hybrids relative to the *dcr1Δ* mutants (Gomez-Escobar; data not shown). If this is correct, these finding could indicate lose of both Tsn1 and Tfx1 results in RNA:DNA hybrids increases, which Dcr1 can process, so Dcr1 is the key primary regulator.

Castel and co-workers (2014) had not only demonstrated requirement for Dcr1 in genome stability maintenance, they also found that RNA Pol II, as well as RNA Pol III was acting at tRNA genes. This was proposed to be due to RNA polymerase II transcribing the opposite strand to the strand transcribed by RNA Pol III. Here, in the recombination monitoring system developed in the McFarlane group, we observed a polarity in recombination. In orientation 1, RNA Pol III is predicted to cause head-to-head collision with DNA replication (Figure 4.1). Both the *dcr1Δ tsn1Δ* and *dcr1Δ tfx1Δ* were observed no statically elevated recombination in comparison to the *dcr1Δ* strain (Figure 4.9 and 4.16). So, we speculated that in this orientation that RNA Pol II might be transcribed the same direction of replication fork. If that was the case it indicates that head-to-tail conflict between RNA Pol II and DNA replication fork would not produce recombination substrates (RNA:DNA hybrids).

Chapter 4: Results

Whereas, in orientation 2, RNA Pol III is predicted to give a head-to-tail collision with DNA replication (Pryce et al., 2009). In fluctuation test data, the *dcr1Δ* single mutant showed that roughly double increase in the rate of recombination compared to WT strain (Figure 4.10). Moreover, deletion of *tsn1* but not *tfx1* in *dcr1Δ* background resulted in further statically significantly increased in comparison with the *dcr1Δ* strain mutant. If this correct, this assumes that a head-to-head collision between the replication fork and RNA Pol II could generate substrates for recombination. This also consisting with result of increased sensitivity to DNA damaging agents in *dcr1Δ tsn1Δ* but not *dcr1Δ tfx1Δ* in *tRNA^{GLU}* orientation 2 (Figure 4.9 and 4.11). These results might be due to elevated recombination initiating genome lesions, or a malfunction to process lesions accurately. The data from our experiment confirm that there is an orientation-dependent effect of the *dcr1Δ* mutant on recombination at *ade6::tRNA^{GLU}* which further increased in *dcr1Δ tsn1Δ* double mutant.

The findings from our data are in line with those of Castel et al. (2014), who posited that transcription by RNA Pol II occurs at some tRNA genes. However, it is still up for debate whether RNA Pol II transcription acts as an inhibitor to DNA replication process that promotes recombination in the *dcr1Δ* mutants at this specific site, *ade6::tRNA^{GLU}*. Whether RNA Pol II/III transcription occurs at this specific tRNA gene. One assumption is that RNA Pol III acts as a barrier, by binding with the elements itself; another assumption is that RNA Pol III binds with the DNA sequence without any other transcription and this inhibits the process. At this time, it not possible to determine whether transcription acts as a barrier that promotes recombination in the absence of Dcr1. Surprisingly, in this experiment we noticed that the *dcr1Δ* single mutant in *tRNA^{GLU}* orientation 1 seems to cause an orientation-independent elevatetion in one experimental set, but not the other. The reason for this difference is unclear, but it could be suggested that a condition-dependent different. It might be due to the growth phase of the yeast strains at the stage of samples harvest.

Chapter 4: Results

In conclusion, the results from our experiment suggest that in the lack of Dcr1, Tsn1, but not Tfx1, plays an important role in lowering the stability of the RNA: DNA hybrids. The lowering of stability leads to suppressions of the recombination process that occurs during DNA transcription and replication process. Despite being able to maintain the chromosomal stability, Tsn1 is unable to compensate for the actual loss caused by the absence of Dcr1 because the single mutant *dcr1Δ* exhibits hypersensitivity towards DNA damaging agents such as HU and phloemycin. Together all of these findings offer insight into why Translin was implicated for chromosomal translocations, cancer initiation and genetic diseases.

Chapter 5: Results

Analysis of the role of Tsn1 and Tfx1 in Double-Strand break repair.

5.1 Introduction

The conflict between replication and transcription machineries is an example of a natural impediment that might blocked and stalled DNA replication forks potentially leading to genomic instability (Chang & Stirling, 2017, Aguilera & García-Muse, 2013, Fragkos & Naim, 2017, Ren, Castel & Martienssen, 2015, Brambati, et al, 2015a). Many studies have been conducted on both prokaryotes and eukaryotes demonstrate a main internal cause of DNA damage is the accumulation of RNA:DNA hybrids and that their influence threatens genome stability (Gómez-González & Aguilera, 2019; Belotserkovskii, et al, 2018; Ohle, et al, 2016; Brambati, et al, 2015; Felipe-Abrio, et al, 2015). R-loops are structures of nucleic acid that are created when an RNA strand displaces a DNA strand in a double-stranded DNA duplex. Crick-Watson can be produced RNA-DNA hybrid and replace the non-hybridized strand as (ssDNA). R-loops are involved in several physiological processes, but they also block progression of DNA replication and transcription machinery and eventually lead to DNA damage and or DSB formation (Zhao, X., et al, 2017; Kojima, et al, 2018; Ohle, et al, 2016; Castel, et al, 2014). Moreover, highly recombinogenic structures at specific replication-transcription collision sites which accumulate hybrids. These results in recruitment of homologous recombination factors and R-loop misregulation potentially promotes genetic changes that drive cancer initiation and progression (Crossley, Bocek & Cimprich, 2019, Belotserkovskii, et al, 2018, Brambati, et al, 2015b, Castel, et al, 2014, Lin & Pasero, 2012).

One of the endogenous enzymes classes that is important for resolving R-loops are RNase Hs (Moelling K, 2017). RNase H activity is ubiquitous in cells and can be found in both nucleus and cytoplasm. On function of RNase H activity is to delete RNA primers during DNA replication from Okazaki fragment and although the precise mechanism of RNase H cleavage is unknown, RNase H can bind to the RNA moiety of DNA-RNA hybrids in a sequence independent manner and can degrade the RNA fragments and maintain genome stability (Kojima, et al, 2018; Zhao, et al, 2018; Fragkos & Naim, 2017; Cerritelli, 2009).

Chapter 5: Results

There are two different types of RNase H enzymes in Eukaryotic cells which are RNase H1 and RNase H2. RNase H1, coded via the gene of *RNH1* in *Saccharomyces cerevisiae*, is a monomeric protein the overexpression of which is usually used as a tool to enhance R-loop degradation (Lockhart, et al, 2019; Wahba et al., 2011). RNase H1 comprises of the hybrid-binding domain N-terminal (HBD) and the endonuclease motif C-terminal, which interacts with with four following molecules of ribose in the 2'-OH group for subsequent RNA moiety cleavage. RNase H1 is involved to hybrids by direct interaction with replication protein A (RPA) that binds and coats the displaced DNA strand of an R-loop to prevent degradation or mis-hybridization (Petzold, 2015). As in humans, yeast RNase H2 is a heterotrimeric complex and similar to RNase H1 to have the ability to degrade the RNA in R-loops. However, in addition, RNase H2 can also perform ribonucleotide excision repair (RER), through which misincorporated rNMPs (ribonucleotide monophosphate) are removed from DSB and subsequently the residual nick is repaired by other DNA damage repair machinery (Cerritelli & Crouch, 2016).

Recent evidences from Ohle and co-workers 2016 has indicated that formation of RNA:DNA hybrids regulate DNA damage respond in yeast using specific site of DSB system. They were able to show that RNA:DNA hybrids are formed around the DSB site which are involved in regulation of process of strand resection and RPA complex recruitment around DSB sites. Subsequently, RNase H comes into play in order to reduce the RNA:DNA intermediates and enable to complete the DSB repair process. In this study, we have been found that *tsn1*Δ and *tfx1*Δ single mutants appear to be more resistance in belomycin, which encourage us to extend the findings of Ohle and co-workers 2016. They demonstrated that RNase H activity is essential in the DSB repair process. Given the intend role for Tsn1 and Tfx1 in RNA:DNA hybrids we directly address the question of whether Tsn1 and Tfx1 function in DSB repair in *S. pombe* by monitoring DNA double strand break repair in a site-specific DSB system.

5.1.2 An overview of the induction of using I-PpoI in specific DSB system.

Previously, Ohle and co-workers observed that mutation both Rnh1 and Rnh201 in *S. pombe* are hypersensitive to DNA DSBs and cannot repair DSBs when treated with DNA damaging agents such as Hydroxyurea or camptothecin. Fission yeast (*S. pombe*) normally only has I-PpoI restriction sites in the rDNA repeats (~150 repeats). I-PpoI is endonuclease from *Physarum polycephalum*. Ohle and co-workers 2016 introduced individual I-PpoI site in Chromosome 2 to ease of DSB detection and repair monitoring. Following a similar experimental setup as Ohle et al., 2016. The tetracycline-inducible site- system of specific DSB was generated using the I-PpoI endonuclease (Figure 5.1). Within the rDNA in chromosome III, *S. pombe* has a number of I-PpoI cleavage site. Being harder to track the break in the repeated endogenous site, moreover to the normal cleavage sites, a single artificial cleavage site was used at chromosome II (Figure 5.1). We induce DSBs by expressing I-PpoI restriction enzyme for 2 hours and monitor repair by qPCR with primers flanking the unique I-PpoI site. They confirmed that only 10% of the *rnh1* Δ *rnh2* Δ double mutant strains repair the DSB. Interestingly, by utilizing the S9.6 monoclonal antibody to do a Drip-qPCR, they show RNA:DNA hybrids accumulation at the break site. Surprisingly, an attempt to recover the DNA damage by overexpressing Rnh1 did not work leading to a poor survival. More analysis showed that in the absence of RNase H activity, accumulation of RNA:DNA hybrids increased close to the break sites and also a delayed and reduced RPA loading in the ssDNA. When *rnh1* is overexpressed, the efficiency of RPA loading was higher close to the break. These observations indicated that R-loops are either regulating end resection for subsequent DSB repair or the availability of the resection of DNA to RPA. An obvious and extremely intriguing follow up of this study is to elucidate other accessory factors necessary for this RNaseH/ R-loop mediated DSB repair. The goal of our study was to address whether Tsn1 and/or Tfx1 are required. We have successfully shown that *tsn1* Δ and *tfx1* Δ mutants are more resistant than WT to some type of DNA damage repair, upon being exposed to belomycin response, so possibly lose of double mutants Tsn1 and Tfx1 cause increase RNA:DNA hybrids and thus increase the efficiency of DSB repair.

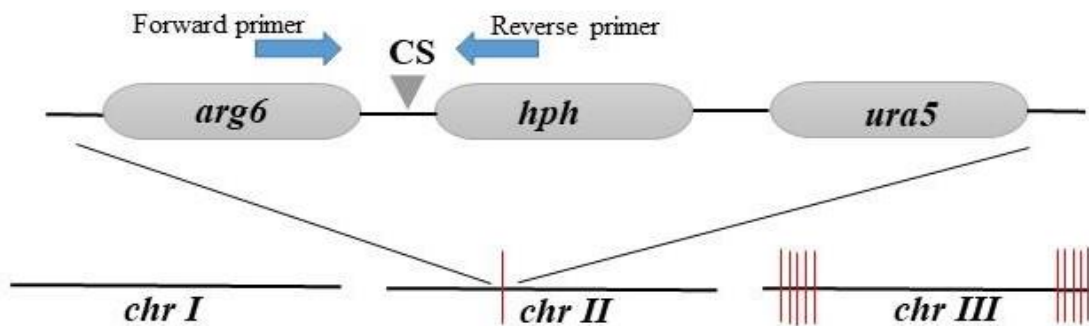


Figure 5.1 Schematic diagram depicting the I-PpoI cleavage sites within the *S. pombe* genome indicated by the red lines. The location of endogenous cleavage sites through the rDNA repeats (~150 repeats) at the ends of Chromosome III (multiple vertical red lines). CS indicates the location of the artificially integrated cleavage site is at Chromosome II that has been used for the qPCR assays. Blue arrows represent the position of primer flanking the DSB site (CS) for use in qPCR monitoring of the break (Figure adapted from Ohle et al. 2016).

5.2 Results

5.2.1 Construction of *tsn1*Δ and *tfx1*Δ single mutants in the I-PpoI background.

As mentioned previously, the strains of *S. pombe* were constructed using methods for targeting gene based on PCR, whereby they were replaced with antibiotic-resistant cassettes (see Section 2.3). The parent strains I-PpoI parent strain has been used to deleted both *tsn1* and *tfx1* genes. We obtained four isolates of *tsn1*Δ (BP3376, BP3378, BP3379 and BP3380) and for *tfx1*Δ, we obtained just one isolate (BP3381). Plasmids with antibiotic-resistant selectable markers were derived from *Escherichia coli* (Table 2.3). *natMX6* (nourseothricin-resistance) was used for the *tsn1*Δ and *tfx1*Δ (Figure 5.2 and Figure 5.3). The purified PCR product has been transformed chemically into the indicated *S. pombe* strains. To verify the gene deletion *tsn1*Δ and *tfx1*Δ candidates were checked by PCR (Figure 5.2 and Figure 5.3) using three primer sets.

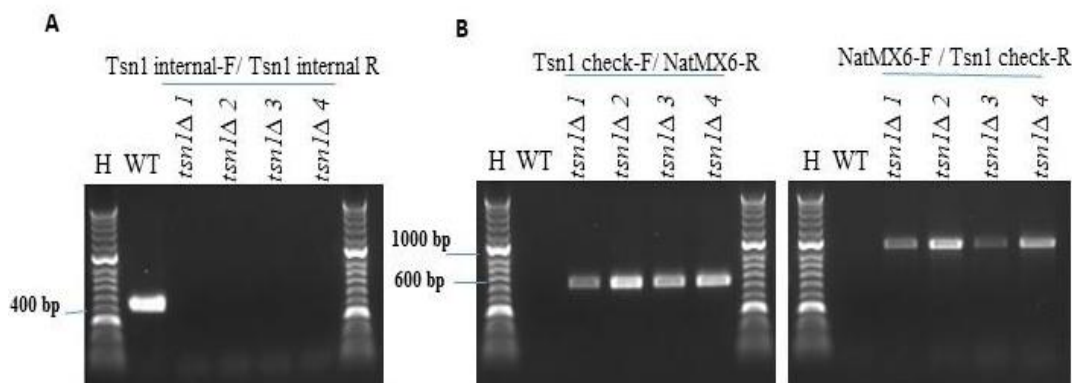


Figure 5.2 PCR screening for the efficient construction of *tsn1Δ* mutants in I-PpoI background. **A.** Agarose gel image shows products of PCR for the WT and *tsn1Δ1* along with *tsn1Δ2* *tsn1Δ3* and *tsn1Δ4* in 1-PpoI strain background using the the Tsn1-int-F and Tsn1-int-R primers. The *tsn1* PCR products was seen close to the expected sizes of 450 bp. **B.** products of PCR for the *tsn1Δ* and WT candidate strains were obtained using primers Tsn1 check-F and NatMX6-R. The *tsn1Δ* strains give PCR products close to the expected sizes of 680 bp, but not in the WT (the *tsn1*⁺ strains) **C.** the *tsn1Δ* and WT candidate strains were amplified by using NatMX6-F and Tsn1 check-R primers. The *tsn1Δ* strains give PCR products close to the expected sizes of 1000 bp. However, nothing was seen in the *tsn1*⁺ strains (WT). H = Hyper ladder.

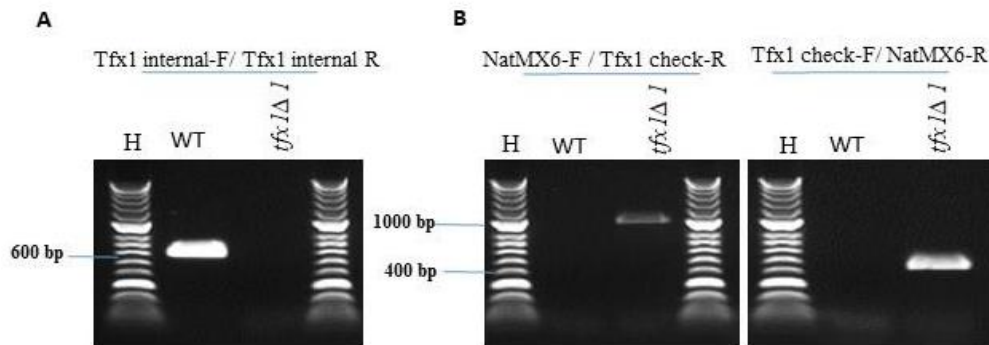


Figure 5.3 PCR screening for the efficient construction of *tfx1*Δ mutant mutants in I-PpoI background. **A.** Agarose gel image shows products of PCR for the wild-type along with *tfx1*ΔI using the the Tfx1-int-F and Tfx1-int-R primers. The *tfx1* PCR product is close to expected sizes of 626 bp. **B.** the *tfx1*ΔI and WT candidate strains were amplified by using NatMX6-F and Tfx1 check-R primers. The *tfx1*ΔI strains were present close to the expected sizes of 1100 bp. Products of PCR for the WT and *tfx1*ΔI strains were obtained utilities primers Tfx1 check-F and NatMX6-R. The *tfx1*ΔI PCR products had PCR products close to the expected sizes of 490 bp, but not in the *tfx1*⁺ strains (WT). However, nothing was seen in the *tfx1*⁺ strains (WT). H = Hyper ladder

5.2.2. Sensitivity assay of DNA damaging agent for *tsn1Δ* and *tfx1Δ* single mutants in the I-PpoI background.

We repeated the DNA damage response experiments with I-PpoI strains and BP90 background for *tsn1Δ* and *tfx1Δ* single mutants. Here, no sensitivity has been shown in *tsn1Δ* and *tfx1Δ* single mutants for both backgrounds to phelomycin and HU relative to WT (Figure 5.4 - 5.6). The positive control was *rad3-136* cells. Interestingly, *rnh1Δ rnh201Δ* exhibited hypersensitive similar to *rad3-136* cells and confirming the crucial role of RNase H in DNA damage response (Figure 5.5). Unexpectedly, the *tsn1Δ*, but not *tfx1Δ*, single mutants for the I-PpoI background were slight more sensitive to bleomycin relative to the isogenic WT control (Figure 5.5). This was not the case in the BP90 background. Collectively, as we did see it previously, both the *tsn1Δ* and *tfx1Δ* single mutant exhibited no increase in sensitivity in response to DNA damage in comparison to the WT in response to phelomycin and HU. The findings verify that Tfx1 and Tsn1 alone are not required for DNA damage recovery. With the exception of the mild increase in sensitivity observed in the *tsn1Δ* mutants in the I-PpoI background. We did observed the hyper resistance of the *tsn1Δ* and *tfx1Δ* single mutants to belomycin but not phelomycin in the BP90 background. Connectively, these finding indicate that different background could effect in strain sensitivity.

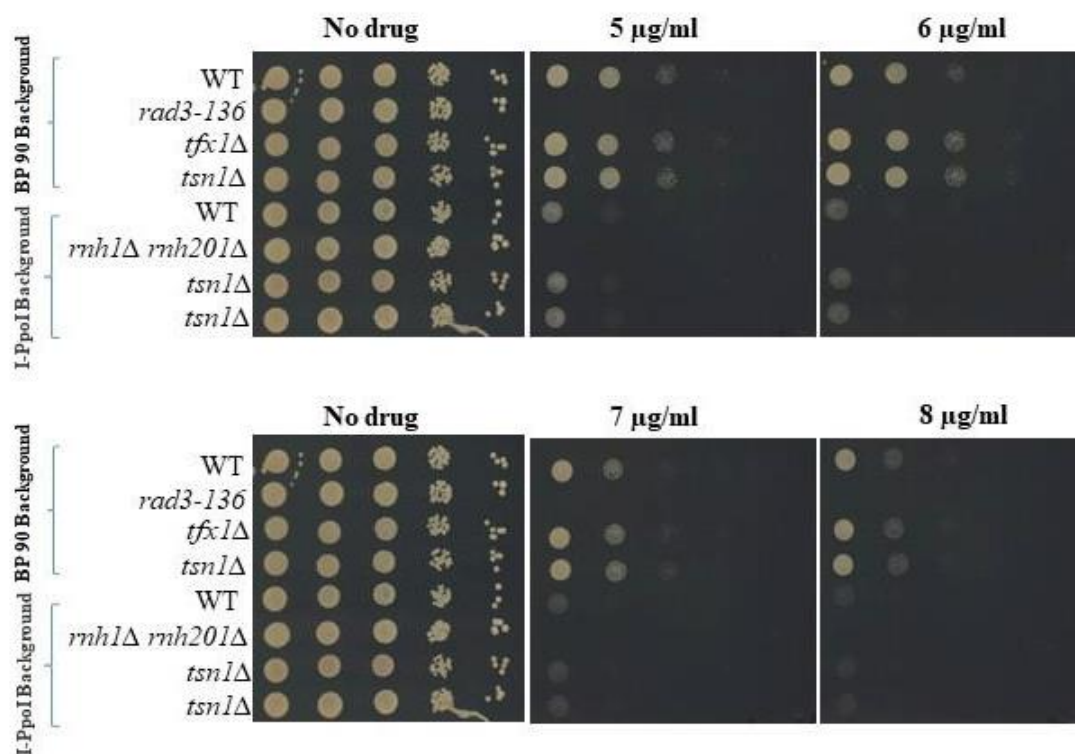


Figure 5.4 Mutation of *tsn1Δ* and *tfx1Δ* genes in both BP90 and I-PpoI backgrounds results in phleomycin sensitivity similar the WT. 10-fold serial dilutions of all appropriate *S. pombe* strains were spotted onto YAE. Several mutant strains have been exposed to phleomycin in different range of concentrations. The plates have been incubated for roughly 3 days at 30°C. The positive control was *rad3-136* cells. *rnh1Δ rnh201Δ* displayed strong sensitive, as *rad3-136* cells. No real change increase in phleomycin sensitivity was shown between the *tsn1Δ* and the *tfx1Δ* single mutants in both (BP90 and I-PpoI) backgrounds relative to WT control.

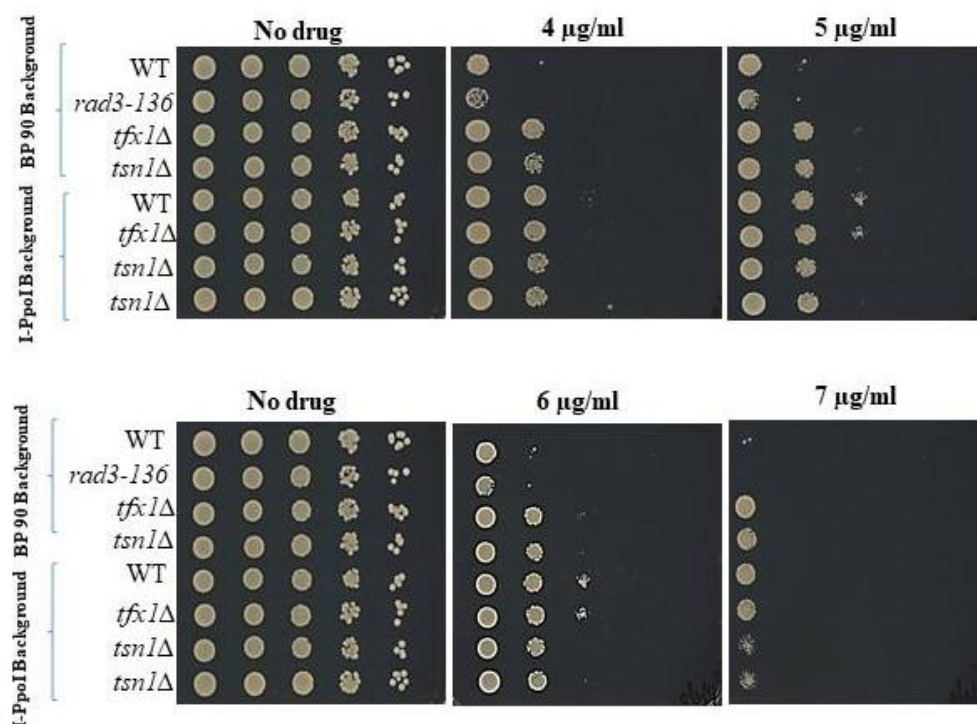


Figure 5.5 Mutation of *tsn1Δ* and *tfx1Δ* genes in both BP90 and I-PpoI backgrounds results distinct to bleomycin response. 10-fold serial dilutions of all appropriate *S. pombe* strains were spotted onto YAE. Mutant strains were exposed to the phelomycin in different range of concentrations. The plates have been incubated for roughly 3 days at 30°C. The positive control was *rad3-136* cells. The *tsn1Δ*, but not *tfx1Δ*, single mutant were observed to exhibit sensitivity to belomycine in comparison with the WT in the I-PpoI background but both *tsn1Δ* and *tfx1Δ* are more resistance in BP90 background.

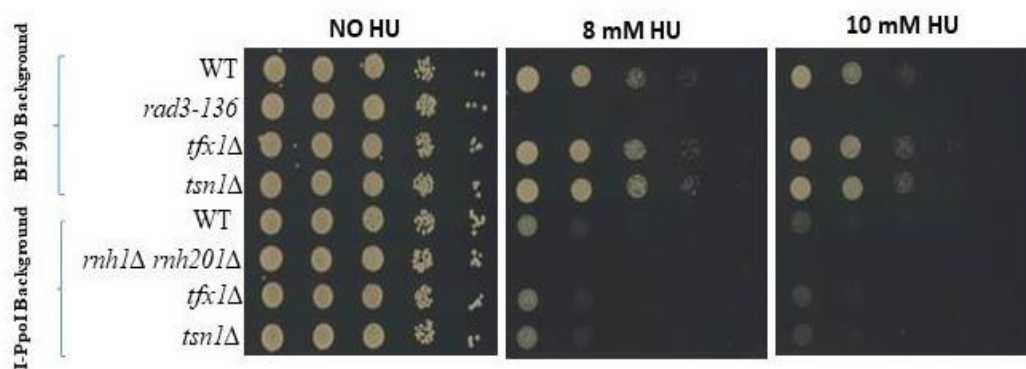


Figure 5.6 Mutation of the *tsn1Δ* and *tfx1Δ* result in a similar response to HU in both BP90 and I-PpoI backgrounds. 10-fold serial dilutions of all appropriated *S. pombe* strains were spotted onto YAE. Mutant strains were exposed to the HU at two different concentrations (8 mM and 10 mM). The plates have been incubated for around 3 days at 30°C. The positive control was *rad3-136* cells. The data showed no increased sensitivity in the *tsn1Δ* and *tfx1Δ* single in HU sensitivity compared with the WT. for both genetic backgrounds, although the I-PpoI background appears to confer greater sensitivity for all strains.

5.2.2 Analysis of I-PpoI induction.

We induced I-PpoI expression for 2 hours (TET-ON) in indicated mutant strains (WT, *rnh1Δ*, *rnh201Δ*, *tsn1Δ* and *tfx11Δ*). Uninduced cultured were used as controls (TET-OFF). Followed by the 2 hours induction in the present of tetracycline. The cells were grow in (YEL) without tetracycline in which I-PpoII protein production was repressed. Cells were collected at 2, 4 and 8-hours time points to monitor gradual loss of the endonuclease. To enable DSB generation and recovery to be monitored correctly, I-PpoI must be turned off to prevent renewed DSB formation. Western blotting was performed with Flag antibody to detect the Flag-I-PpoI induced protien level. After taking the cells out from the tetracyclin induction, in WT a minimal amount of I-PpoI level was seen at 2 hours and 4 hours followed by negligible to no protein level of I-PpoI at the 8 hours time point (Figure 5.7). In *rnh1Δ rnh201Δ* double mutants, The I-PpoI signal was detected just at 2 hours time point but not detected thereafter (Figure 5.8). The *tsn1Δ*, *tfx11Δ* single mutant had I-PpoI detected at both 4 and 6 hours (Figure 5.9 and 5.10). The Beta-Actin was used as positive loading control and result showed that the signals was detected at 42 kDa. In addition, notably the expression of I-PpoI has been induced in all indicated strains. This validated that our tetracycline inducible I-PpoI system worked well and I-PpoI enzyme in this system was lost after 8 hours time, point of the recovery stage.

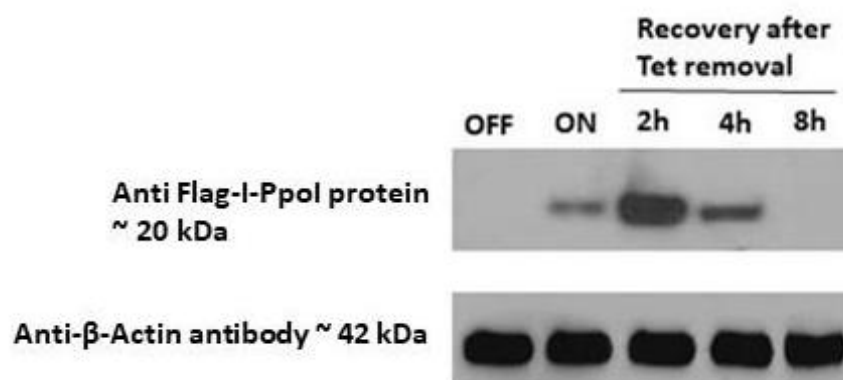


Figure 5.7 Western blotting showing the detection of I-PpoI protein levels in WT. Anti-Flag antibody was utilized to determine anti Flag-I-PpoI protein and result showed that signal at approximately of 20 kDa. The anti-β-Actin antibody was used as a positive control to exam loading at approximately of 42 kDa. I-PpoI was not induced (untreated cells or No TET induction) subsequently, tetracycline treatment was added in WT and I-PpoI induction has been stopped via tetracycline removal (t = 0 hr). The level of Flag- I-PpoII was assessed at the specified time-points (2 hr, 4 hr and 8 hr).

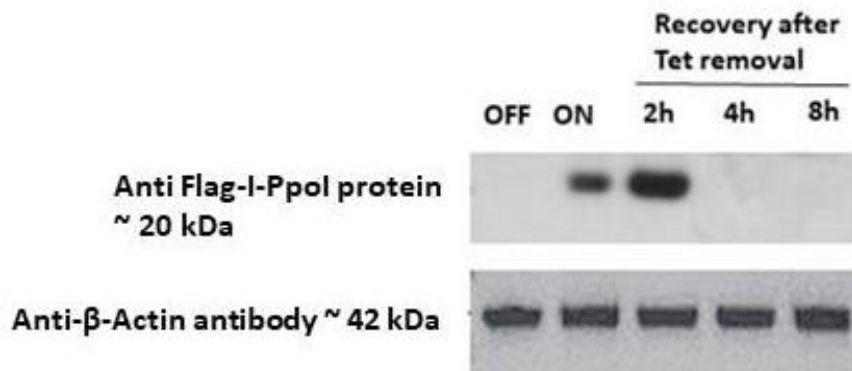


Figure 5.8 Western blotting showing the detection of I-PpoI protein levels in *rnh1Δ rnh201Δ*. Anti-Flag antibody was utilized to determine anti Flag-I-PpoI protein and result showed that signal at approximately of 20 kDa. The anti-β-Actin antibody was used as a positive control to exam loading at approximately of 42 kDa. I-PpoI was not induced (untreated cells or No TET induction) subsequently, tetracycline treatment was added in *rnh1Δ rnh201Δ* and I-PpoI induction has been stopped via tetracycline removal (t = 0 hr). The Flag- I-PpoI level was assessed at the specified time-points (2 hr, 4 hr and 8 hr).

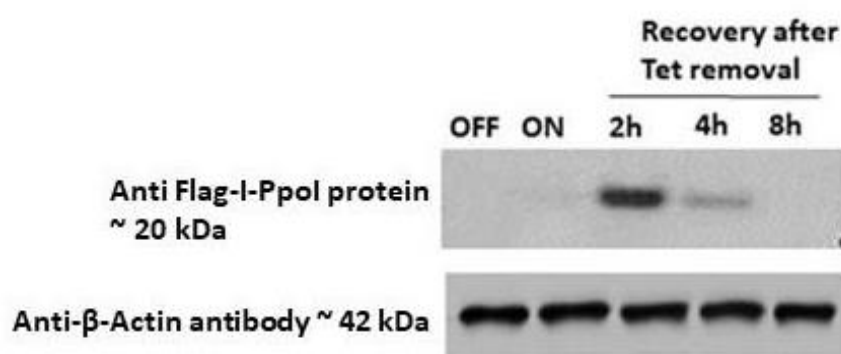


Figure 5.9 Western blotting showing the detection of I-PpoI protein levels in *tsn1Δ*. Anti-Flag antibody was utilized to determine anti Flag-I-PpoI protein and result showed that signal at approximately of 20 kDa. The anti-β-Actin antibody was used as a positive control to exam loading at approximately of 42 kDa. I-PpoI was not induced (untreated cells or No TET induction) subsequently, tetracycline treatment was added in *tsn1Δ* and I-PpoII induction has been stopped via tetracycline removal (t = 0 hr). The Flag- I-PpoI level was assessed at the specified time-points (2 hr, 4 hr and 8 hr).

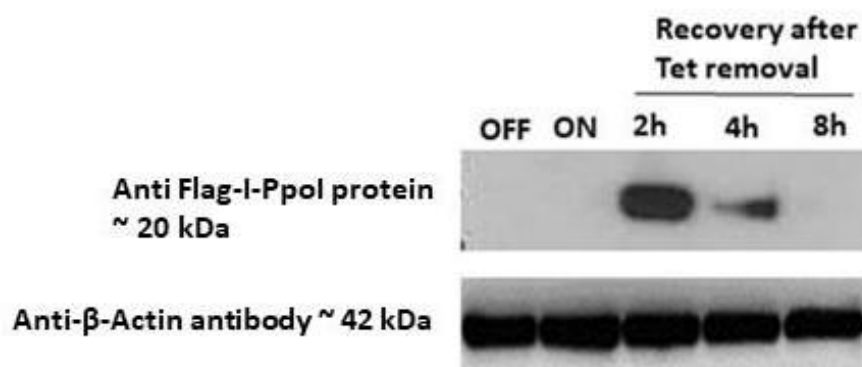


Figure 5.10 Western blotting showing the detection of I-PpoI protein levels in *tfx1Δ*. Anti-Flag antibody was utilized to determine anti Flag-I-PpoI protein and result showed that signal at approximately of 20 kDa. The anti-β-Actin antibody was used as a positive control to exam loading at approximately of 42 kDa. I-PpoI was not induced (untreated cells or No TET induction) subsequently, tetracycline treatment was added in *tfx1Δ* and I-PpoI induction has been stopped via tetracycline removal (t = 0hr). The Flag- I-PpoI level was assessed at the specified time-points (2 hr, 4 hr and 8 hr).

5.2.3 RNase H activity, but not Tsn1 or Tfx1 are needed for DSB repair.

To monitor the DNA DSB repair efficiency in the individual mutant strains compared to the WT, we performed a qPCR using site-specific primers spanning the I-PpoII induced break sites (CS in figure 5.1). We collected untreated cells (no tetracycline induction), cells at 0 hour time point (2 hours of tetracycline induction), and at 4 or 8 hours time points of recovery after taking them out from the tetracycline induction. We used the WT strain as a control. We performed qPCR on WT and all indicated mutant strains which are *rnh1Δ rnh201Δ*, *tsn1Δ* and *tfx1Δ* under similar conditions with three biological repeat to validate our findings. We also had primers against the house keeping gene acts as control. We calculated the fold change/ the repaired break site intensity in each case compared to the untreated sample and measured the P-values derived from the unpaired t-test to measure the significance of the DSB repair. We showed high level of the DSB site in the *rnh1Δ rnh201Δ* double mutant at the 0 hour time point very low level during the recovery period of 2, 6 and 8 hours time points. Our results suggest about 50-70% break induced by tetracycline and even at the 8 hours time point. The *rnh1Δ rnh201Δ* strain fails to repair the DSB damage, which supports the results from Ohle et al. (2016). On the other hand, neither *tsn1Δ* nor the *tfx1Δ* mutants affected the recovery process. The p-value for *tsn1Δ* and *tfx1Δ* indicate not statistically significant difference from wild-type. This indicates that lack of *tsn1Δ* and *tfx1Δ* single mutant do not negatively or positively affect the DSB recovery process.

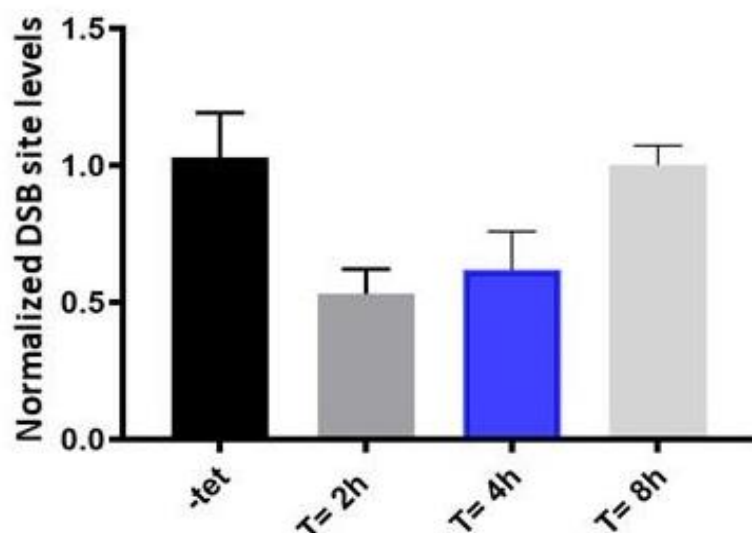


Figure 5.11 Bar graph showing qPCR analysis of the break site in the WT strain. The four bars indicate different time points as mentioned in the bottom of the figure. Pairwise Student's t-test were carried out to identify the p-value of WT. This data displayed no statically significant when you compared between –tet and 8hr (P value > 0.05).

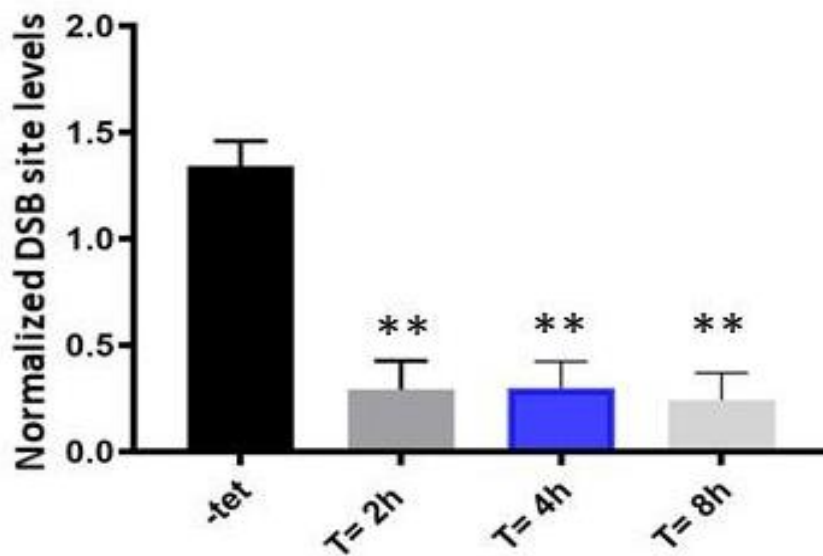


Figure 5.12 Bar graph showing qPCR analysis at the break site in the *rnh1Δ rnh201Δ* double mutant strain. The four bars indicate different time points as mentioned in the bottom of the figure. Clearly, *rnh1Δ rnh201Δ* showed statically significant increased and fails to repair the DSB as efficiently as WT, by a comparison with Figure 5.11. Pairwise Student's t-test were carried out to identify the p-value of *rnh1Δ rnh201Δ* (** P value < 0.001).

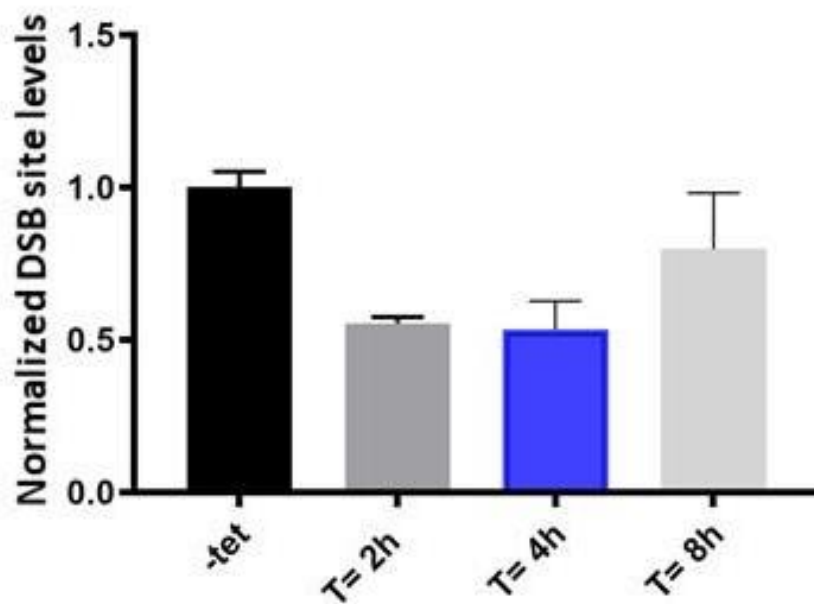


Figure 5.13 Bar graph showing qPCR analysis of the break site in the *tsn1*Δ single mutant strain. The four bars indicate different treatment or timepoints as mentioned in the bottom of the figure. *tsn1*Δ single mutant repairs the DSB with similar efficiency as WT. Pairwise Student's t-test were carried out to identify the p-value of WT. This data displayed no statically significant when you compared between -tet and 8hr (P value > 0.05).

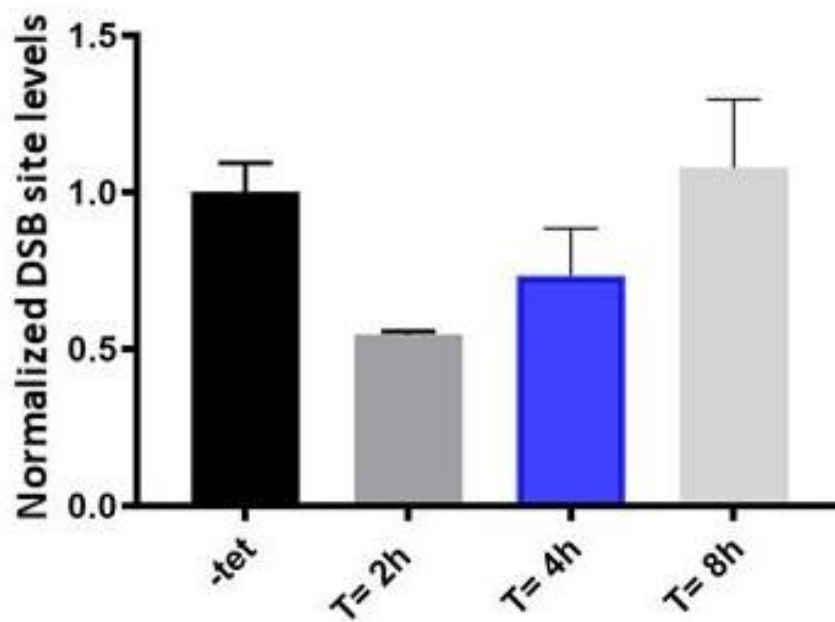


Figure 5.14 Bar graph showing qPCR analysis of the break site in the *tfx1Δ* single mutant strain. The four bars indicate different treatment or time points as mentioned in the bottom of the figure. *tfx1Δ* single mutant repairs the DSB with similar efficiency as WT. Pairwise Student's t-test were carried out to identify the p-value of WT. This result showed no statically significant when you compared between –tet and 8 hr (P value > 0.05).

5.3 Discussion

Genomic DNA integrity is constantly challenged by various external and internal factors such as ionizing radiation, UV light, or other DNA-damaging agents, within the cells and replication- or transcription-related events. One important endogenous factor leading to genomic instability is R-loops since they can stall replication machinery progression (Vasquez, 2014). These events may lead to transcription-replication conflicts (TRCs) may produce stalling of DNA replication-fork, and eventually DSBs and DNA recombination. There are several factors regulating R-loops and one such important factor is RNase H, which has been the primary focus of the study of Ohle, et al, (2016).

We proceeded to test if Translin and/or TRAX have role to participate in DNA damage recovery from some other genotoxic agents such as phleomycin, bleomycin and hydroxyurea (HU) in distinct I-PpoI background. We started with high concentrations with hydroxyurea (HU) and phleomycin, because the lab works have not observed any sensitivity in low concentrations. The result showed both the *tsn1Δ* and *tfx1Δ* single mutant exhibited no increase in sensitivity in response to DNA damage in comparison to the WT to phleomycin and HU. This indicate Tsn1 and Tfx1 alone are not involved to DNA damage recovery. We observed unexpectedly result that *tsn1Δ* single mutants were the hyper resistance to belomycin but not phelomycin in the BP90 background in compassion to WT. However, *tsn1Δ* single mutants were slight sensitive in I-PpoI background. This observations slightly different from pervious expermintis and could be coming from experimental differences. This could be due to the growth phase of the cells at the stage of the drug exposure. Cells in the log phase undergoes more division and hence replication which gets affected by addition of HU, leading to higher cell death. On contrary cells in stationary phase are metabolically less active, are enriched in a carbohydrate reservoir and causes changes in gene replication and transcription. Therefore, cells plated at stationary phase might not respond to the drugs in the same way as a cell plated in or before log phase, which could be the case for *tsn1Δ* strain or *tfx1Δ* strain under the current experimental condition.

Chapter 5: Results

A higher sensitivity in the I-PpoI strains background compared to the BP90 strain background indicates a complex change in the DNA damage response networks. Use of multiple gene markers could affect the normal DNA repair machinery. It can also indicate a potential increase in transcription-replication conflicts TRCs and TRC mediated damages. Here we present evidence to showing that in the fission yeast, loss of Trax or Translin function alone does not result in large-scale phenotypic abnormalities in HU and phelomycin. In fact, loss of TRAX or Translin function alone seem to have no negative effect on fission yeast cells (Jaendling et al., 2008). This suggest that Tsn1 and Tfx1 do not participate in the main function of fission yeast genome stability, but they might play function in redundant or secondary pathways (Jaendling et al., 2010). Mutation of *tsn1* and *tfx1* did not affect the DSB recovery process. This definitely needs further analysis carrying a double knockout as this could be interpreted in couple of different ways. One simplified interpretation would be that none of these two proteins plays an important role in DNA DSBs. Another interpretation would be that loss of these two proteins could be compensated for each other and do not affect the DNA DSB on an individual basis. The results from pervious chapter suggest that in the lack of Dcr1, Tsn1, but Tfx1, plays an important role in the stability of RNA: DNA hybrids. The lowering of stability of these hybrids by Tsn1 leads to suppressions of the recombination process that occurs during DNA transcription and replication process. This could indicate a role for Tsn1 in repairing DSBs in the absence of Dcr1. This study indicate that the instability of chromosome noticed in the case of the *dcr1Δ tsn1Δ* double mutants could be caused by the inability of the cell to repair or respond to DNA damage. These results also show that it is the Tsn1, and not Tfx1, which is needed by the cells to respond to DNA damages when Dcr1 is not present which indicates a separation of function between these Tsn1/and Tfx1.

rnh1Δ rnh201Δ exhibited hypersensitive similar to *rad3-136* cells under DNA damage agent and qPCR that indicates confirming the importance of RNase H activity in DNA damage repair. It is consist with finding of Ohle, et al, (2016).

Chapter 6: Results

Tsn1, but not Tfx1, functions in an RNase H pathway

6.1 Introduction

Correct replication of DNA is of crucial importance for cellular proliferation. Accordingly, cellular evolution has come up with several mechanisms for making sure that the DNA is copied precisely during division of cell (Kang, et al, 2018; Williams, Lujan & Kunkel, 2016; Potenski & Klein, 2014). Fidelity of replication generally means that the nucleotide sequence in the daughter cells remains the same as that of the parent cell. Still, structure and chemical composition of DNA can be changed by endogenous or exogenous agents (Bouwman & Crosetto, 2018; Kang, et al, 2018; Parker, Botchan & Berger, 2017). If left unrepaired, these change may potentially have serious mutagenic and/or cytotoxic for the cell. Genomic stability is usually threatened by a number of DNA abnormalities and amongst them, the most common is the existence of ribonucleotides in the backbone of DNA. Owing to the existence of reactive 2'-OH on the sugar moiety, polynucleotides can be easily cleaved and show hypersensitive in the presence of alkali, provide an effective screening tool for the presence of ribonucleotides in genomic DNA (Williams, Lujan & Kunkel, 2016; Vaisman, et al, 2013). Sometimes single and tandem ribonucleotides (rNMPs) and strands of RNA can get temporarily linked transiently to chromosomal DNA (Santos-Pereira & Aguilera, 2015; Cornelio, et al, 2017; Williams, Lujan & Kunkel, 2016). For instance, during transcription nascent mRNA molecule may continue to be linked with the DNA template strand as RNA:DNA hybrid duplex (R-loops). Replicative polymerases add considerable number of single rNMPs in the newly formed DNA during replication, failure or delay in removing tandem rNMPs used for the synthesis of prime lagging strand can cause the structures to persist. More importantly, RNA-DNA associations can impede normal genomic phenomena such as DNA relication leading to chromosomal destabilization (Santos-Pereira & Aguilera, 2015; Cornelio, et al, 2017). A primary source of rNMPs in DNA is RNA primers which are formed at the lagging-strand during the initiation of Okazaki fragment replication. For that reason, excision of these primers must occur before Okazaki fragments join to form full lagging strand (Zheng & Shen, 2011; Vaisman et al., 2013).

Chapter 6: Results

A number of nucleases have been involved in removal of deleterious rNMPs and/or RNA:DNA hybrids (Fragkos & Naim, 2017; Brambati, et al, 2015; Ohle, et al, 2016; Vaisman et al., 2013). These enzymes include the ones that are responsible for specific hydrolyzation of the phosphodiester bond present between ribonucleotides and deoxyribonucleotides.

These are ribonucleases HI and HII (RNase H) and ribonucleotide-specific endonucleases, which have major contribution in removal of RNA primers. Many researchers have recently demonstrated the role of ribonucleases from *Escherichia coli* and fission yeast *S. pombe* in ribonucleotide excision repair (RER) (Hyjek, Figiel and Nowotny, 2019; Vaisman, et al, 2013, Sparks, et al, 2012).

In both organisms, the removal of rNMPs is mainly initiated by RNase H2 enzyme. In prokaryotic cells, *rnhB* encodes the RNase HII while in *S. pombe* cells, *rnh201* encodes the RNase H2 enzyme. Wide range cleavage specificity is demonstrated by these ribonucleases, which cause hydrolysis of phosphodiester bonds found at the junction of RNA and DNA on DNA templates carrying the RNA fragments. They also act on phosphodiester bonds formed by isolated rNMPs which embed into the DNA double stranded molecules (Lockhart, et al, 2019; Hyjek, Figiel and Nowotny; 2019) Kojima, et al, 2018; Cornelio, et al, 2017; Williams, Lujan & Kunkel, 2016).

The type I ribonucleases, on the other hand, need a fragment of at least four ribonucleotides present one after another in the DNA strand for the cleavage activity. In prokaryotic cells, *rnhA* encodes the RNase HI enzyme while in eukaryotic cells, RNase H1 is encoded by *rnh1* (Lockhart, et al, 2019; Hyjek, Figiel and Nowotny, 2019; Kojima, et al, 2018; Cornelio, et al, 2017; Williams, Lujan & Kunkel, 2016). In this study, we wanted to determine if Tfx1 and/or Tsn1 have role in RNA:DNA hybrid control and preserving genome stability in the absence of RNase H activity

6.2 Results

6.2.1 Determination of *tsn1*Δ mutant responses to DNA damage in absence of RNase H activity.

Relative to the observations from the *dcr1*Δ background (more details in Chapter 3), analysis of the roles of both *tsn1* and *tfx1* function in the background of *dcr1*Δ showed that *tsn1*Δ but not *tfx1*Δ mutation increased chromosomal instability in the absence of Dcr1 for most of DNA damage agent. To prevent unscheduled RNA:DNA hybrid generation, many mechanism have developed in eukaryotic cells to degrade these hybrids such as RNase H1 and RNase H2 a class of protein enzymes which removes the RNA moiety of RNA:DNA hybrids (Kojima, et al, 2018; Zhao, et al, 2018; Fragkos & Naim, 2017; Brambati, et al, 2015; Ohle, et al, 2016). This led us to examine whether *tsn1* and *tfx1* are necessary or have redundant role for the pathway of DNA damage response in an RNase H activity (*rnh1* and *rnh201*). To address this question, the appropriate double mutant strains of *S. pombe* have been assessed and exposed to several DNA-damaging drugs with analyzed for their corresponding response to various pathways of repairing DNA damage. The DNA damaging agents include phleomycin (Figure 6.1), hydroxyurea (HU; Figure 6.2), ultraviolet irradiation (UV; Figure 6.3), camptothecin (CPT; Figure 6.4) and methyl methane sulfonate (MMS Figure 6.5). *rad3-136* cells were used as positive control in all DNA damage agent (checkpoint control genes) and the *rnh1*Δ *rnh201*Δ double mutants also, showed hypersensitive as positive control. No sensitivity has been observed in *rnh1*Δ and *rnh201*Δ single mutant relative to WT. Remarkably, we observed that the *tsn1*Δ *rnh201*Δ but not the *tsn1*Δ *rnh201*Δ double mutants was hypersensitivity to HU when compared to the *rnh201*Δ single mutant and WT. Also, the *tsn1*Δ *rnh201*Δ but not *tsn1*Δ *rnh1*Δ double mutants was slight sensitive to phelomycine in comparison of WT. Together these findings confirm the notion that in the absence of Rnh201, it is important to have Tsn1 in the DNA damage recovery response. These findings also support the proposed Tsn1 has a role in maintain genome stability and it could be to degraded RNA:DNA hybrids.

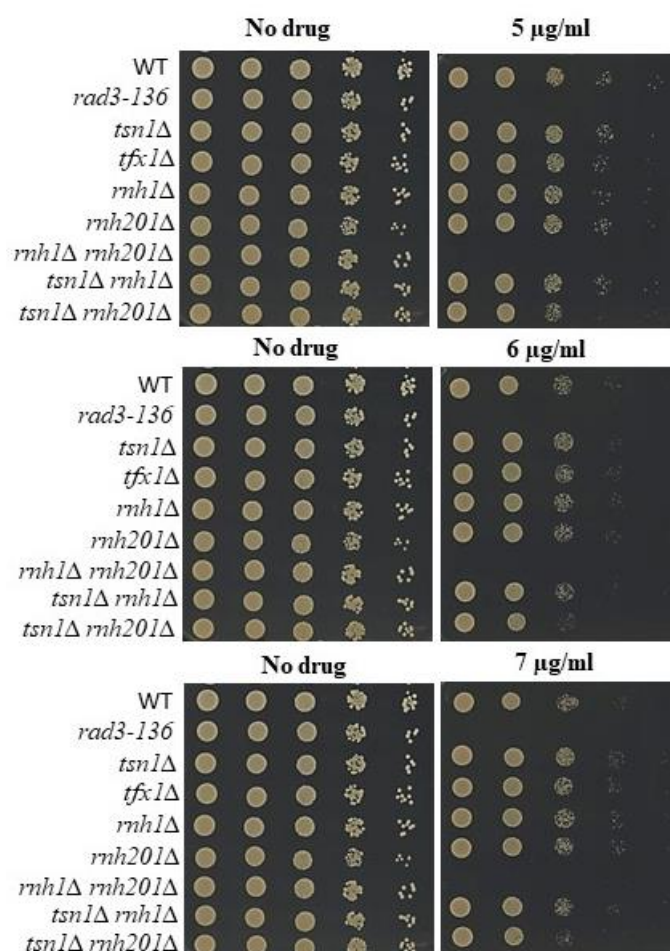


Figure 6.1 The *tsn1Δ rnh201Δ* mutant showed mild, elevated sensitivity to Phleomycin. 10-fold serial dilutions of all appropriated *S. pombe* strains were spotted onto YAE. Mutant strains were exposed to a different range of Phleomycin concentration. The plates have been incubated for around 3 days at 30°C. The positive control was *rad3-136* cells. The *rnh1Δ rnh201Δ* double mutant displayed hypersensitive as positive control. The data showed slight sensitive in the *tsn1Δ rnh201Δ* double mutants in phelomycine sensitivity compared with *tsn1Δ rnh1Δ* double mutants and the *rnh201Δ* single mutant.

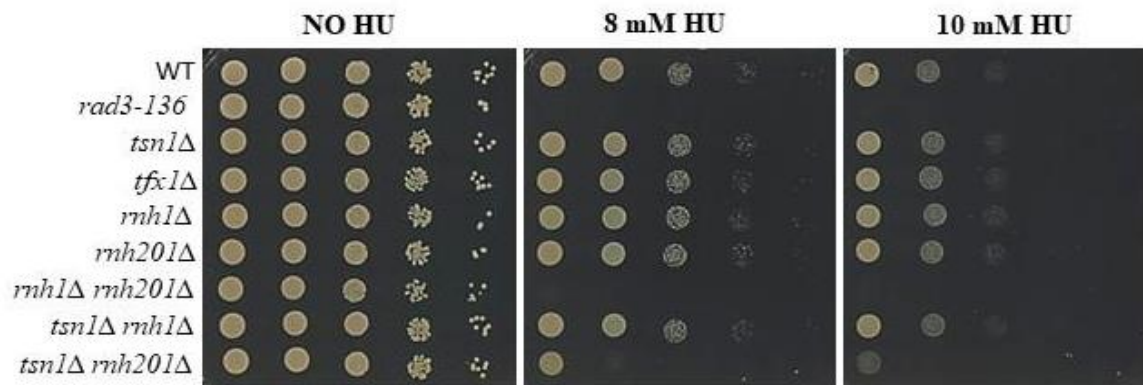


Figure 6.2 The *tsn1Δ rnh201Δ* mutant exhibits hypersensitivity to hydroxyurea (HU) sensitivity. 10-fold serial dilutions of all appropriated *S. pombe* strains were spotted onto YAE. Mutant strains were exposed to the HU in two different range of concentration (8 mM-10 mM). The plates have been incubated for around 3 days at 30°C. The positive control was *rad3-136* cells and *rnh1Δ rnh201Δ* double mutant showed hypersensitive as positive control. The result shows that the *tsn1Δ rnh201Δ* double mutants displayed an increased sensitivity in HU.

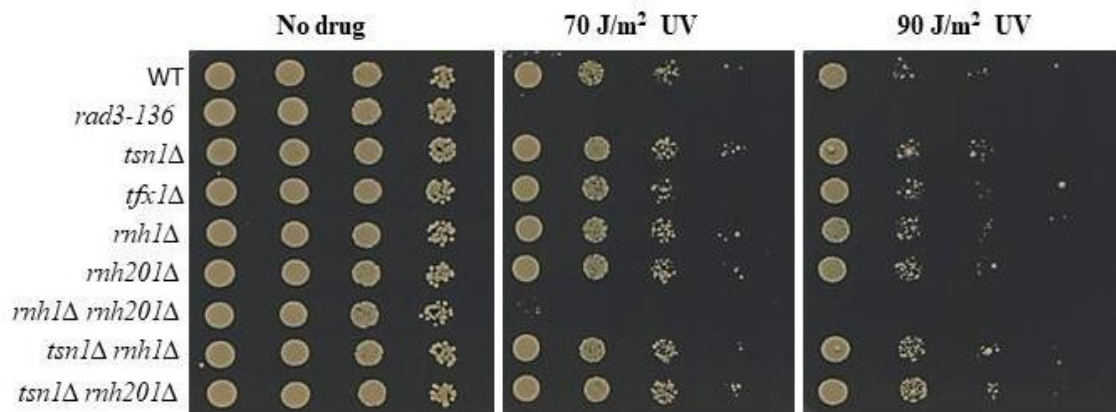


Figure 6.3 Sensitivity spot test of ultraviolet (UV) for several of *S. pombe* mutants. 10-fold serial dilutions of the indicated *S. pombe* strains were spotted onto YAE. Mutant Strains have been exposed to different doses of ultraviolet (UV). The plates were then incubated for approximately 3 days at 30°C. The positive control was *rad3-136* cells. The *rnh1*Δ *rnh201*Δ double mutants showed hypersensitive as positive control. The data showed no increase sensitivity was shown in both *tsn1*Δ *rnh201*Δ and *tsn1*Δ *rnh1*Δ double mutant in comparison to WT.

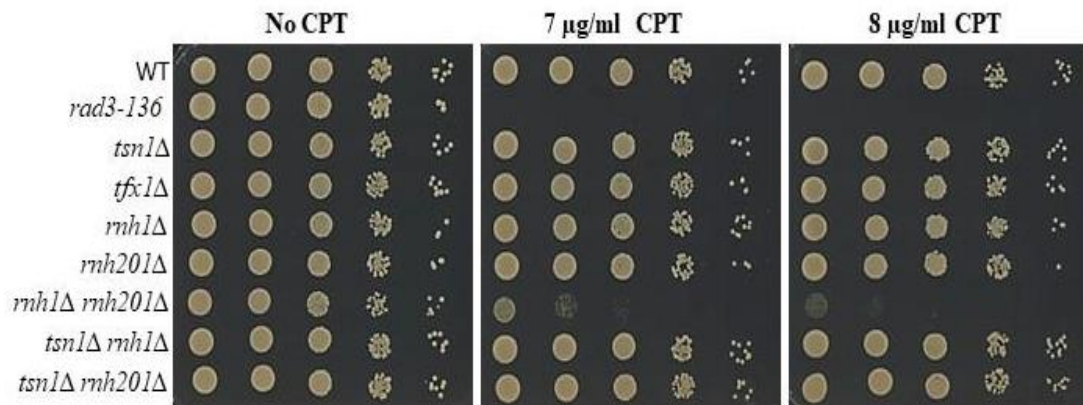


Figure 6.4 The *tsn1Δ rnh201Δ* double mutant is not sensitive to camptothecin (CPT). 10-fold serial dilutions of all appropriated *S. pombe* strains were spotted onto YAE. Mutant strains have been exposed to different concentration of camptothecin (CPT). The plates were then incubated for approximately 3 days at 30°C. The positive control was *rad3-136* (checkpoint control genes). The *rnh1Δ rnh201Δ* double mutant showed hypersensitive as positive control. The data showed no increase sensitivity was observed between the *tsn1Δ rnh201Δ* double mutant and *tsn1Δ rnh1Δ* double mutant.

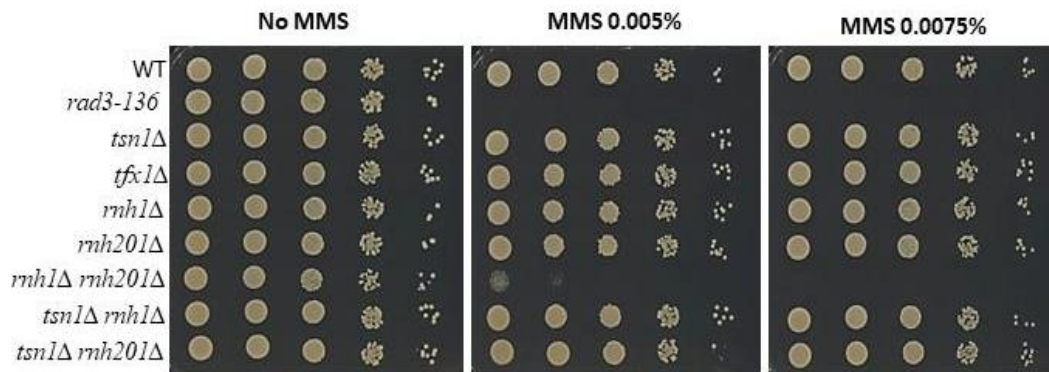


Figure 6.5 Sensitivity spot test of Methyl methane sulfonate (MMS) for several of *S. pombe* mutants. 10-fold serial dilutions of all appropriated *S. pombe* strains were spotted onto YAE. Mutant strains have been exposed to two different concentrations of MMS. The plates were then incubated for approximately 3 days at 30°C. The positive control was *rad3-136* cells (checkpoint control genes). The *rnh1Δ rnh201Δ* double mutants showed hypersensitive as positive control. The data showed no increased sensitivity was shown in both *tsn1Δ rnh201Δ* and *tsn1Δ rnh1Δ* double mutant in comparison to WT.

Chapter 6: Results

6.2.2 Determination of *tfx1*Δ mutant responses to DNA damage in absence of RNase H activity.

We repeated these experiment here with new knockout strains with mutation of Tfx1 in place of Tsn1 indicated strains, which are *tfx1*Δ, *rnh1*Δ, *rnh210*Δ single mutant and *tfx1*Δ *rnh1*Δ, *tfx1*Δ *rnh201*Δ double mutants. It has been shown that all *tfx1*Δ, *rnh1*Δ, *rnh210*Δ single mutant were not sensitive to Phelomycin and HU relative to WT. *rad3-136* cells were used as positive control in all experiments (checkpoint control genes). As we expected no measurable increased sensitivity was seen in *tfx1*Δ *rnh1*Δ and *tfx1*Δ *rnh201*Δ double mutants relative to both *rnh1*Δ and *rnh201*Δ single mutant as well as WT. Taken together, these results confirm that Tfx1 is not required in the DNA damage recovery respond and/ or the degradation of RNA:DNA hybrids.

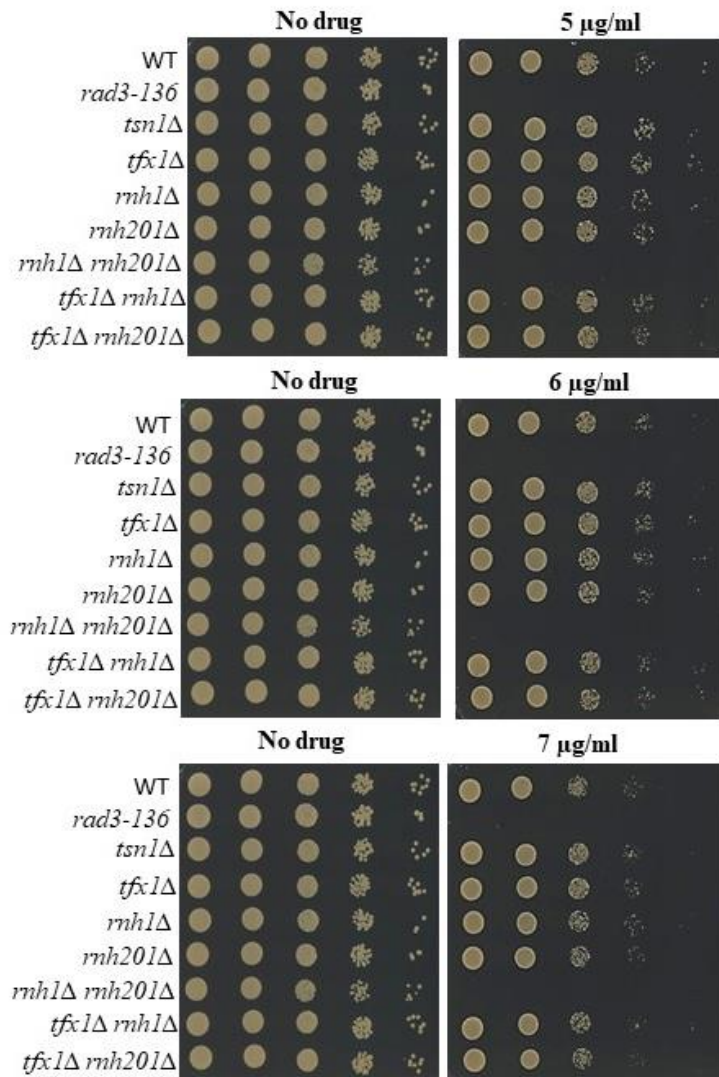


Figure 6.6 Mutation of *tfx1Δ rnh1Δ* and *tfx1Δ rnh201Δ* double mutants exhibit no elevated sensitivity to phleomycin. 10-fold serial dilutions of all appropriated *S. pombe* strains were spotted onto YAE. Mutant strains were exposed to different range of Phleomycin concentration. The plates had been incubated for around 3 days at 30°C. The positive control was *rad3-136* cells and *rnh1Δ rnh201Δ* double mutant also shown hypersensitive as positive control. The data showed no sensitive in the *tfx1Δ rnh1Δ* and *tfx1Δ rnh201Δ* double mutants to phleomycine sensitivity compared with *rnh1Δ* single mutant and WT.

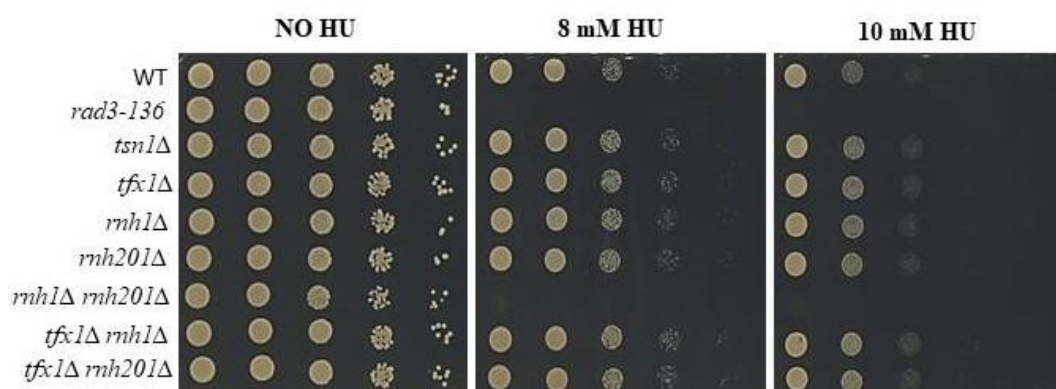


Figure 6.7 Tfx1 is not required from HU in the absence of RNase H activity. 10-fold serial dilutions of all appropriated *S. pombe* strains were spotted onto YAE. Mutant strains were exposed to the HU at two different range of concentrations (8 mM -10 mM). The plates have been incubated for around 3 days at 30°C. The positive control was *rad3-136* cells and *rnh1Δ rnh201Δ* double mutants showed hypersensitive as positive control. The result shows that no increased sensitivity has been shown between the *tfx1Δ* single mutant and *tfx1Δ rnh201Δ* double mutants in HU sensitivity.

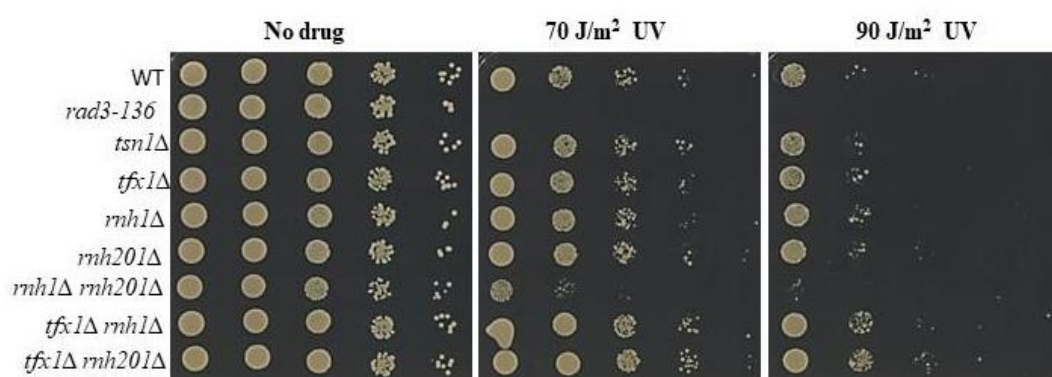


Figure 6.8 Sensitivity spot test of ultraviolet (UV) for several of *S. pombe* mutants. 10-fold serial dilutions of the indicated *S. pombe* strains were spotted onto YAE. Mutant Strains have been exposed to different doses of ultraviolet (UV). The plates were then incubated for approximately 3 days at 30°C. The positive control was *rad3-136* cells. The *rnh1*Δ *rnh201*Δ double mutant showed hypersensitive as positive control. No sensitivity has been shown shown in both *tsn1*Δ *rnh201*Δ and *tsn1*Δ *rnh1*Δ double mutant in comparison to WT.

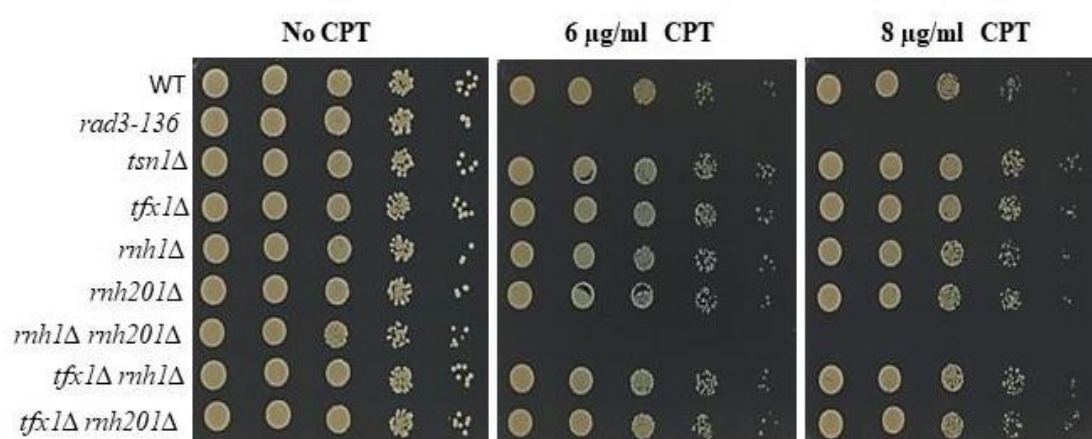


Figure 6.9 Sensitivity spot test of to camptothecin (CPT) for several of *S. pombe* mutants. 10-fold serial dilutions of all appropriated *S. pombe* strains were spotted onto YAE. Mutant strains have been exposed to different concentration of camptothecin (CPT). The plates were then incubated for approximately 3 days at 30°C. The positive control was *rad3-136* cells. The *rnh1* Δ *rnh201* Δ double mutants showed hypersensitive as a positive control. The data showed no increase sensitivity was observed in the *tfx1* Δ *rnh201* Δ double mutant relative to the *tfx1* Δ *rnh1* Δ double mutant.

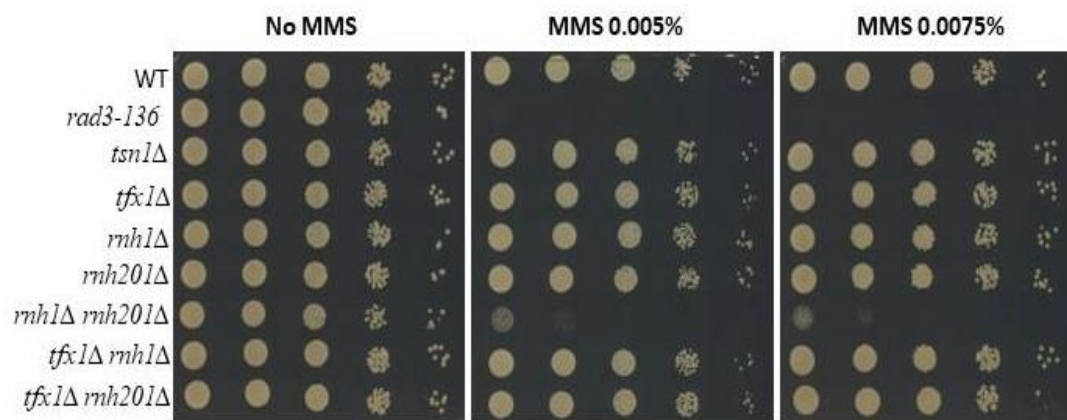


Figure 6.10 Sensitivity spot test of Methyl methane sulfonate (MMS) for several of *S. pombe* mutants. 10-fold serial dilutions of all appropriated *S. pombe* strains were spotted onto YAE. Mutant Strains have been exposed to two different consternations of MMS. The plates were then incubated for approximately 3 days at 30°C. The positive control was *rad3-136* cells. The *rnh1Δ rnh201Δ* double mutants showed hypersensitive as positive control. The data showed no increase sensitivity was shown in both *tfx1Δ rnh201Δ* and *tfx1Δ rnh1Δ* double mutant in comparison to WT.

6.3 Discussion

Cells carrying gene deletions encoding H-class ribonucleases show high levels of chromosome instability. The function of these enzymes is to remove RNA-DNA hybrids (R-loops), which are created through transcription and ribonucleotides incorporated into DNA through replication. RNases H1 and H2 can degrade the RNA component of R-loops, but only RNase H2 can initiate accurate ribonucleotide excision repair (RER) (Zhao et al., 2018; Kojima et al., 2018; Cornelio et al., 2017; Santos-Pereira and Aguilera, 2015; Williams, Lujan & Kunkel, 2016; Cerritelli & Crouch, 2016). In this study, we used *S. pombe* to analyse the role of Tsn1 and/or Tfx1 in protecting genome integrity in the absence of RNase H activity. From these experiments, we found that no increased sensitivity was observed in both the *tsn1Δ* and *tfx1Δ* single mutant or *rnh201Δ* and *rnh1Δ* single mutant to most of the DNA damage agents in comparison to the WT. This suggested that Tsn1 and Tfx1 alone are not involved to DNA damage recovery and are not usually required to repair DSBs. However, there was increased sensitivity in the *rnh1Δ rnh201Δ* mutant to most of the DNA damage agents. These finding indicate that the loss of *rnh1Δ* and *rnh201Δ* results in an increase in RNA:DNA hybrids and that the presence of both *rnh1* and *rnh201* are required to maintain the genome stability. We observed unexpectedly that *tsn1Δ rnh201Δ* mutant but not the *tsn1Δ rnh1Δ* was hypersensitive to HU, which could elevate ribonucleotide incorporation into DNA (Figure 6.2). Additionally, these was a slight sensitive in phelomycin in compassion to WT. One interpretation would be that Rnh201 and Tsn1 both have a role in helping to remove Okazaki primers on the lagging strand during DNA replication. It has been shown that the main alternative pathway that catalyses the removal ribonucleotides from DNA in the absence of RNase H2 enzymes fails to excise rNMPs from DNA and leads to stress on replication, increased mutation rates, and increased genome instability (Sparks et al., 2012b; Reijns et al., 2012). Another interpretation would be that the loss of Rnh201 and Tsn1, but not Tfx1 plays an important role in the stability of RNA:DNA hybrids. The lowering of the stability of these hybrids by Tsn1 could lead to suppression of the recombination process that occurs during DNA transcription and replication process.

Chapter 6: Results

This study indicates that RNase H1 and RNase H201 in *S. pombe* play redundant roles with Tsn1, but not Tfx1, possibly in the degradation of R-loops and/or tandem rNMPs in DNA. This could explain why *tsn1Δ rnh201Δ* is sensitive to HU the increased incorporation of ribonucleotides into DNA associated with the RER defect mechanism, RNA:DNA hybrid processing, and RNA prime removal. However, the spot assay results confirm that Rnh201 and Tsn1 are likely to play a greater role in replication rather than RNA:DNA hybrid formation.

Chapter 7: Final Discussion

7.1 Introduction

Translin is a novel nucleic acid binding protein which was discovered through an analysis of factors that bind to the breakpoint junctions of chromosomal translocation in lymphoid tumours in humans (Gupta et al., 2019; Aoki et al., 1995). Translin is a DNA and RNA binding protein and is found at elevated levels in the brain, testis and certain human cancers. It has proven to be extremely conserved (Gupta et al., 2019). Researchers later found that this protein binds with the translocation breakpoint junctions in a number of other genetic disorders and range of cancer (Jaendling and McFarlane, 2010), suggesting a role in genome stability control. Crystallographic studies have found that Trax and Translin can form a 2:6 barrel-like octamer that was recently recognized as C3PO the complex required for RNAi passenger strand removal (Park, et al, 2017; Ye, et al, 2011; Parizotto, Lowe & Parker, 2013; Zhang, J., et al, 2016). The Translin and Trax heterooctamer complex can act as an RNase, the activity of which depends on the Trax subunit (Weng, et al, 2018; Kasai, et al, 2018; Yang & Hecht, 2004; Jaendling & Mcfarlane, 2008). The amino acid sequence of Trax is paralogous to the Translin amino acid sequence (Aoki et al., 1997). This suggests a possible association between Trax and Translin proteins. In addition, Trax stability depends on the stability of Translin (Yang & Hecht, 2004; Jaendling, et al, 2008). This phenomenon highlights the close functional association between the two binding partners. Moreover, it has been demonstrated that both Translin and Trax orthologues should be found together in all eukaryotes (Claußen, et al, 2006; Jaendling, et al, 2008; Jaendling & McFarlane, 2010). Although *Archaea* appear to only have one orthologue. Translin appears control to levels of Trax at the post-transcriptional level. This observation was identified by mutation of the *tsn1* gene in *S. pombe* and mice followed by comparison of the level of *tfx1* mRNA and protein. The deletion resulted in a significant reduction of levels of Trax protein but no alteration to mRNA levels (Kasai, et al, 2018). Translin and Trax have been postulated to be involved in several distinct biological processes, including genome stability, response to DNA damage, cell growth, RNAi, mRNA transport, translation, telomere transcript control and the microRNA degradation in the process of oncogenesis.

Chapter 7: Discussion

The latter resulting in the suggestion that both proteins Translin/Trax could be druggable oncology targets (Gomez-Escobar, et al, 2016; Jaendling & McFarlane, 2010; Laufman, et al, 2005; Martienssen, Zaratiegui & Goto, 2005).

The reduction of mature miRNAs and accumulation of pre-miRNAs have been identified in many human cancer tissues (Gurtner et al., 2016; Kasai, et al, 2018). Moreover, the complete loss of the miRNA generating enzyme Dicer is fatal for cells and heterozygosity leads to tumour formation and progression (Kumar, et al, 2009; Asada, Canestrari & Paroo, 2016) . Some cancers show Dicer1 haploinsufficiency, and some have shown that mutation of Dicer can directly cause miRNA depletion, with their tumour suppressor activities being also lost as a result (Asada et al., 2014; Fu et al., 2016; Hata & Kashima, 2016). It has been revealed that the Translin and Trax (TN/TX) complex functions as an RNase enzyme by degrading pre-miRNAs in Dicer1 haploinsufficiency. Inhibition of TN/TX activity using small molecules in Dicer haploinsufficient tumours lead to both miRNA and tumour suppression restoration (Fu et al., 2016; Hata & Kashima, 2016; Kasai, et al., 2018). This has led to the speculated that these two proteins could act as therapeutic targets for proper functioning of the miRNA (Asada, et al, 2014; Asada, Canestrari & Paroo, 2016). If we are to therapeutically target Translin and/or Trax, then it is important to understand all cellular functions. This study addressed an important question about Trax and Translin proteins i.e. whether these proteins are required for DNA damage repair or chromosomal translocation and how this role links with other roles played by these proteins. These findings must be considered in drug design, which has an aim of targeting oncogenic role and not tumour suppressing roles.

7.2 Tsn1, but not Tfx1, suppress recombination in the Dcr1 deficient.

The initiation of cancer and its progression is caused by genetic alteration including chromosomal translocations (Nambiar & Raghavan, 2011; Roukos & Misteli, 2014; Harewood & Fraser, 2014; Zheng, 2013). Earlier researchers proposed that Translin could be involved in chromosome translations. However, the literature contains very little evidences supporting a role in repair of DNA damage (Jaendling and McFarlane, 2010). However, Trax has been shown to play an essential role in DNA damage repair through its interaction with Ataxia Telangiectasia Mutated (ATM)-mediated pathway, which is essential for the MRN complex at DSBs (Chern, et al, 2019; Wang, et al, 2016). It was further shown that a dysfunctional Trax can lead to ATM-inactivation (Wang et al., 2016). In an analysis of the *tsn1Δ* and *tfx1Δ* null mutants in *S. pombe*, the works of Jaendling et al. (2008) showed no detectable defects in DNA repair processes such chromosomal recombination. Before this particular study, the role of Translin as a redundant factor in DNA repair processes and recombination had not been tested, which might account for a potential cancer-initiation and progression activity (Jaendling & McFarlane, 2010). In addition, the complex of Translin-Trax (C3PO) plays a key role in RNAi pathways. Dcr1 has recently been postulated to remove RNA: DNA hybrids from potential DNA replication to transcription collision sites, preserving genome stability (Ren et al., 2015).

In the absence of Dcr1, there is an increase in RNA: DNA hybrids at some transcription sites (Castel et al., 2014). This finding could explain the sensitivity of the *dcr1Δ* single mutant to chromosome-breaking phleomycin and DNA replication pausing HU. Surprisingly, hypersensitive increases following an additional *tsn1Δ* mutation, but not *tfx1Δ*, which appears to show these two genes function separately in this process. In accordance with the original suggestion that Translin plays a great role in initiation of translocation of chromosomes (Aoki et al., 1995). We propose that Tsn1, but not Tfx1, might be important in reducing the stability of the RNA:DNA hybrids in the absence of Dcr1 and limiting the formation of recombinogenic lesions. If this is correct, *tsn1Δ* but not *tfx1Δ* in the *dcr1Δ* background might result in elevated RNA:DNA hybrid levels, which could be associated with an increase in recombination frequency.

Chapter 7: Discussion

In a parallel biochemical, experiment in our lab RNA:DNA hybrids were assessed in various mutant backgrounds. Previously, it had been demonstrated that *S. pombe dcr1Δ* mutants had elevated level of RNA:DNA hybrids throughout the genome, including the rDNA locus and tRNA genes (Castel et al., 2014). Surprisingly, the *tsn1Δ* and *tfx1Δ* single mutants also, demonstrated when RNA:DNA hybrid levels at the rDNA locus and tRNA genes elevated to levels similar to those seen in the *dcr1Δ* mutant. If increased RNA:DNA hybrids alone was sufficient to cause sensitivity to DNA replication inhibiting agents such HU, then the *tsn1Δ* and *tfx1Δ* mutants should exhibit sensitivity to HU similar to the *dcr1Δ*, which they do not. Interestingly, *dcr1Δ tsn1Δ* double mutants do not appear to have elevated RNA:DNA hybrids relative to the *dcr1Δ* mutant (Gomez-Escobar; data not shown). If this is correct, these finding could indicate lose of both Tsn1 and Tfx1 results in RNA:DNA hybrid increases, which Dcr1 can process, so Dcr1 is the key primary regulator. Castel and co-workers (2014) had not only demonstrated requirement for Dcr1 in genome stability maintenance, they also found that RNA Pol II, as well as RNA Pol III was acting at tRNA genes. This was proposed to be due to RNA polymerase II transcribing the opposite strand to the strand transcribed by RNA Pol III. Here, in the recombination monitoring system developed in the McFarlane group, we observed a polarity in recombination, suggesting of a model in which Tsn1 is required to overcome RNA Pol II -DNA replication collision at tRNA sites.

Collectively, the results from our experiments might appear to indicate that when Dcr1 is loss, Tsn1, but not Tfx1, plays a primary role in reducing the stability of the RNA: DNA hybrids. Over expression of *rnh1* (RNase H1) does not soppress the sensitivity of the *tsn1Δ dcr1Δ* double mutant to HU (McFarlane lab, date not shown). This appears to indicate Dcr1 and /or Tsn1 are not acting as RNase H activity providing, and a double-stranded RNase activity is more likely, givin what is known about both Dcr1 and Tsn1.

The decreasing of RNA:DNA hybrid stability leads to suppressions of the recombination process that occurs during DNA transcription and replication process. Despite being able to maintain the chromosomal stability, Tsn1 is unable to compensate for the actual loss caused by the loss of Dcr1 because the single mutant *dcr1Δ* exhibits hypersensitivity towards DNA damaging agents such as HU and phloemycin.

Chapter 7: Discussion

However, Dcr1 is an RNase III (double strand RNase) and Translin does have RNase activity (RNase H activity has not been demonstrated). This could suggest an RNase III (dsRNA) degradation step is critical, importantly. All of these findings offer insight into why Translin was implicated for chromosomal translocations, cancer initiation and genetic diseases.

7.3 Tsn1, but not Tfx1, functions in the RNases H pathways

Translin and Trax have been found to be involved in a number of biological phenomena that call for RNA regulation instead of DNA. This role is consistent with the fact that Tsn1 is capable of binding with nucleic acid and can demonstrate RNase activity (Jaendling and McFarlane, 2010). Many studies have been conducted on both prokaryotes and eukaryotes demonstrate a major internal cause of DNA damage is the accumulation of RNA:DNA hybrids and that their influence threatens genome stability (Gómez-González & Aguilera, 2019; Belotserkovskii, et al, 2018; Ohle, et al, 2016; Brambati, et al, 2015). RNase H1 and RNase H2 are the two suppressors of RNA-DNA hybrids, which prevent the development of stable RNA-DNA hybrids. They cause degradation of the RNA moiety for eliminating the RNA-DNA hybrids (García-Muse & Aguilera, 2019). According to Lockhart et al., (2019), RNases Hs make a substantial contribution to checking genome instability as well as in preventing genome transcription replication conflicts. Ohle et al., (2016) reported the essential involvement of RNases H1 and H2 in repairing of DSBs effectively in *S. pombe*. Accordingly, deletions of genes encoding these two enzymes causes impairment in DNA damage repair. Hence, it has been proposed that mechanisms involving RNases H are unavoidable for DSB repair process. Zimmer & Koshland et al., 2016 demonstrated that elimination of RNA-DNA hybrids is needed for DNA DSB repair. So, RNA:DNA hybrids can both cause DNA damage and are required for DSB repair.

In this study, it has been shown that Tsn1, not Tfx1, can play a role in mechanisms involving RNase H1. Findings of this research imply that Tsn1, not Tfx1, is involved in repairing of DNA damage caused by DNA replicative stress agents and genotoxic agents. Moreover, loss of both Tsn1 as well as RNase H2 (but not RNase H1) results in more marked phenotype of genome instability. Hence, we proposed that Tsn1 is involved in repair of DNA damage via an RNase H1-associated pathway.

Chapter 7: Discussion

It has been shown that the main alternative pathway that catalyses the removal of ribonucleotides from DNA in the absence of RNase H2 enzymes fails to excise rNMPs from DNA and leads to stress on replication, increased mutation rates, and increased genome instability (Sparks et al., 2012b; Reijns et al., 2012).

7.4 Closing remarks

Translin and Trax (C3PO) were identified approximately 25 years ago. Many functions have been associated with C3PO and it has been suggested that they have separate functions and specific tissue activity on nucleic acids. Up to now, most studies that revealed Translin and Trax have shown that the conserved proteins are sharing close relationship function. In this study, the model system, fission yeast, was used to provide better understanding of the function of these essential proteins. Firstly, in deficiency of Dcr1, the DNA damage recovery response needs Tsn1 but not Tfx1. Evidence is put forward in order to present a new primary role for Tsn1 but not Tfx1, in suppressing replication-associated recombination when Dcr1 is absent. That could clarify the original proposed role in the development of chromosome translocation through human cancers. Secondly, Tsn1, but not Tfx1, functions in an RNase H pathway.

This study has addressed two fundamentally important issues. Firstly, it reveals an explanation for the long-standing question of how Translin function might be linked to chromosome translocations. Secondly, it provides more understanding of the normal function of a possible oncological drug target. If targeting of Translin and/or Trax does prove to be important, then targeting oncogenic functions, but not genome stability maintaining functions will be important, to avoid drugs driving tumour evolution.

Chapter 7: Discussion

Lastly, the facile nature of the fission yeast and the highly conserved nature of Translin, made gaining insight into the genome stability control mechanisms in eukaryotes possible. Unpublished work from the McFarlane group demonstrate the *S. pombe tsn1Δ* defects (in *dcr1Δ* background) can be suppressed by over expressing the human *TSN* gene. This clearly indicates functional conservation, and the *S. pombe* system can be used to understand the mechanisms of action of this complex human protein. However, future studies should also focus on analysis of TSN (Translin) and TSNAX (Trax) in controlling genome stability in distinct human cells and tissues in both normal and disease setting.

References:

- Abeyasinghe, S.S., Chuzhanova, N., Krawczak, M., Ball, E.V. & Cooper, D.N. 2003. Translocation and gross deletion breakpoints in human inherited disease and cancer I: Nucleotide composition and recombination-associated motifs. *Human mutation*, 22 (3), pp. 229-244.
- Admire, A., Shanks, L., Danzl, N., Wang, M., Weier, U., Stevens, W., Hunt, E. & Weinert, T. 2006. Cycles of chromosome instability are associated with a fragile site and are increased by defects in DNA replication and checkpoint controls in yeast. *Genes & development*, 20 (2), pp. 159-173.
- Aguilera, A. & García-Muse, T. 2013. Causes of genome instability. *Annual Review of Genetics*, 47 pp. 1-32.
- Aguilera, A. & Gómez-González, B. 2008. Genome instability: a mechanistic view of its causes and consequences. *Nature Reviews Genetics*, 9 (3), pp. 204.
- Alessa Jaendling & Ramsay J McFarlane (eds). 2010. Biological roles of translin and translin-associated factor-X: RNA metabolism comes to the fore. England: .
- Alper, B.J., Lowe, B.R. & Partridge, J.F. 2012. Centromeric heterochromatin assembly in fission yeast—balancing transcription, RNA interference and chromatin modification. *Chromosome research*, 20 (5), pp. 521-534.
- Alzu, A., Bermejo, R., Begnis, M., Lucca, C., Piccini, D., Carotenuto, W., Saponaro, M., Brambati, A., Cocito, A. & Foiani, M. 2012. Senataxin associates with replication forks to protect fork integrity across RNA-polymerase-II-transcribed genes. *Cell*, 151 (4), pp. 835-846.
- Amon, J.D. & Koshland, D. 2016. RNase H enables efficient repair of R-loop induced DNA damage. *Elife*, 5 pp. e20533.
- Aoki, K., Suzuki, K., Sugano, T., Tasaka, T., Nakahara, K., Kuge, O., Omori, A. & Kasai, M. 1995a. A novel gene, Translin, encodes a recombination hotspot binding protein associated with chromosomal translocations. *Nature genetics*, 10 (2), pp. 167.
- Arezi, B. & Kuchta, R.D. 2000. Eukaryotic DNA primase. *Trends in biochemical sciences*, 25 (11), pp. 572-576.
- Aronica, L., Kasperek, T., Ruchman, D., Marquez, Y., Cipak, L., Cipakova, I., Anrather, D., Mikolaskova, B., Radtke, M. & Sarkar, S. 2015. The spliceosome-associated protein Nrl1 suppresses homologous recombination-dependent R-loop formation in fission yeast. *Nucleic acids research*, 44 (4), pp. 1703-1717.
- Asada, K., Canestrari, E. & Paroo, Z. 2016. A druggable target for rescuing microRNA defects. *Bioorganic & medicinal chemistry letters*, 26 (20), pp. 4942-4946.
- Asada, K., Canestrari, E., Fu, X., Li, Z., Makowski, E., Wu, Y., Mito, J.K., Kirsch, D.G., Baraban, J. & Paroo, Z. 2014. Rescuing dicer defects via inhibition of an anti-dicing nuclease. *Cell reports*, 9 (4), pp. 1471-1481.
- Asakawa, H., Haraguchi, T. & Hiraoka, Y. 2007. Reconstruction of the kinetochore: a prelude to meiosis. *Cell division*, 2 (1), pp. 17.

References

- Atlas, M., Head, D., Behm, F., Schmidt, E., Zeleznik-Le, N.J., Roe, B.A., Burian, D. & Domer, P.H. 1998. Cloning and sequence analysis of four t (9; 11) therapy-related leukemia breakpoints. *Leukemia*, 12 (12), pp. 1895.
- Baraban, J.M., Shah, A. & Fu, X. 2018. Multiple pathways mediate microRNA degradation: focus on the translin/trax RNase complex. In: Anon *Advances in Pharmacology*. Elsevier. pp. 1-20.
- Barlow, J.H. & Rothstein, R. 2010. Timing is everything: cell cycle control of Rad52. *Cell division*, 5 (1), pp. 7.
- Bartel, D.P. 2004. MicroRNAs: genomics, biogenesis, mechanism, and function. *Cell*, 116 (2), pp. 281-297.
- Beard, W. A., Horton, J. K., Prasad, R. and Wilson, S. H. (2019) ‘Eukaryotic Base Excision Repair: New Approaches Shine Light on Mechanism’, *Annual Review of Biochemistry*, 88(1), pp. 137–162. doi: 10.1146/annurev-biochem-013118-111315.
- Belotserkovskii, B.P., Tornaletti, S., D’Souza, A.D. & Hanawalt, P.C. 2018a. R-loop generation during transcription: Formation, processing and cellular outcomes. *DNA repair*, 71 pp. 69-81.
- Bermejo, R., Lai, M.S. & Foiani, M. 2012. Preventing replication stress to maintain genome stability: resolving conflicts between replication and transcription. *Molecular cell*, 45 (6), pp. 710-718.
- Berti, M. & Vindigni, A. 2016. Replication stress: getting back on track. *Nature structural & molecular biology*, 23 (2), pp. 103.
- Boboila, C., Alt, F.W. & Schwer, B. 2012. Classical and alternative end-joining pathways for repair of lymphocyte-specific and general DNA double-strand breaks. In: Anon *Advances in immunology*. Elsevier. pp. 1-49.
- Boulianne, B. & Feldhahn, N. 2018. Transcribing malignancy: transcription-associated genomic instability in cancer. *Oncogene*, 37 (8), pp. 971-981.
- Bouwman, B.A. & Crosetto, N. 2018. Endogenous DNA double-strand breaks during DNA transactions: emerging insights and methods for genome-wide profiling. *Genes*, 9 (12), pp. 632.
- Brambati, A., Colosio, A., Zardoni, L., Galanti, L. & Liberi, G. 2015. Replication and transcription on a collision course: eukaryotic regulation mechanisms and implications for DNA stability. *Frontiers in genetics*, 6 pp. 166.
- Branzei, D. & Foiani, M. 2007. Interplay of replication checkpoints and repair proteins at stalled replication forks. *DNA repair*, 6 (7), pp. 994-1003.
- Brouwers, N., Martinez, N.M. & Vernos, I. 2017. Role of Kif15 and its novel mitotic partner KBP in K-fiber dynamics and chromosome alignment. *PloS one*, 12 (4), pp. e0174819.
- Brugmans, L., Kanaar, R. & Essers, J. 2007. Analysis of DNA double-strand break repair pathways in mice. *Mutation Research/Fundamental and Molecular Mechanisms of Mutagenesis*, 614 (1-2), pp. 95-108.
- Bühler, M. & Gasser, S.M. 2009. Silent chromatin at the middle and ends: lessons from yeasts. *The EMBO journal*, 28 (15), pp. 2149-2161.

References

- Burgers, P.M. & Kunkel, T.A. 2017. Eukaryotic DNA replication fork. *Annual Review of Biochemistry*, 86 pp. 417-438.
- Burrell, R.A., McClelland, S.E., Endesfelder, D., Groth, P., Weller, M., Shaikh, N., Domingo, E., Kanu, N., Dewhurst, S.M. & Gronroos, E. 2013. Replication stress links structural and numerical cancer chromosomal instability. *Nature*, 494 (7438), pp. 492.
- Castel, S.E. & Martienssen, R.A. 2013. RNA interference in the nucleus: roles for small RNAs in transcription, epigenetics and beyond. *Nature Reviews Genetics*, 14 (2), pp. 100.
- Castel, S.E., Ren, J., Bhattacharjee, S., Chang, A., Sánchez, M., Valbuena, A., Antequera, F. & Martienssen, R.A. 2014. Dicer promotes transcription termination at sites of replication stress to maintain genome stability. *Cell*, 159 (3), pp. 572-583.
- Cerritelli, S.M. & Crouch, R.J. 2016a. The balancing act of ribonucleotides in DNA. *Trends in biochemical sciences*, 41 (5), pp. 434-445.
- Cha, R.S. & Kleckner, N. 2002. ATR homolog Mec1 promotes fork progression, thus averting breaks in replication slow zones. *Science*, 297 (5581), pp. 602-606.
- Chang, E. & Stirling, P. 2017. Replication fork protection factors controlling R-loop bypass and suppression. *Genes*, 8 (1), pp. 33.
- Chang, H.H., Pannunzio, N.R., Adachi, N. & Lieber, M.R. 2017. Non-homologous DNA end joining and alternative pathways to double-strand break repair. *Nature reviews Molecular cell biology*, 18 (8), pp. 495.
- Chang, Y., Wang, P., Li, W.H., Chen, L., Chang, C., Sung, P., Yang, M., Cheng, L., Lai, Y. & Cheng, Y. 2013. Balanced and unbalanced reciprocal translocation: an overview of a 30-year experience in a single tertiary medical center in Taiwan. *Journal of the Chinese Medical Association*, 76 (3), pp. 153-157.
- Chatterjee, N. and Walker, G. C. (2017) 'Mechanisms of DNA damage, repair, and mutagenesis', *Environmental and Molecular Mutagenesis*, 58(5), pp. 235–263. doi: 10.1002/em.22087.
- Chen, X., Mangala, L.S., Rodriguez-Aguayo, C., Kong, X., Lopez-Berestein, G. & Sood, A.K. 2018. RNA interference-based therapy and its delivery systems. *Cancer and metastasis reviews*, 37 (1), pp. 107-124.
- Chennathukuzhi, V., Stein, J.M., Abel, T., Donlon, S., Yang, S., Miller, J.P., Allman, D.M., Simmons, R.A. & Hecht, N.B. 2003. Mice deficient for testis-brain RNA-binding protein exhibit a coordinate loss of TRAX, reduced fertility, altered gene expression in the brain, and behavioral changes. *Molecular and cellular biology*, 23 (18), pp. 6419-6434.
- Chern, Y., Chien, T., Fu, X., Shah, A.P., Abel, T. & Baraban, J.M. 2019. Trax: A versatile signaling protein plays key roles in synaptic plasticity and DNA repair. *Neurobiology of learning and memory*, 159 pp. 46-51.
- Chiaruttini, C., Vicario, A., Li, Z., Baj, G., Braiuca, P., Wu, Y., Lee, F.S., Gardossi, L., Baraban, J.M. & Tongiorgi, E. 2009. Dendritic trafficking of BDNF mRNA is mediated by translin and blocked by the G196A (Val66Met) mutation. *Proceedings of the National Academy of Sciences*, 106 (38), pp. 16481-16486.

References

- Chien, T., Weng, Y., Chang, S., Lai, H., Chiu, F., Kuo, H., Chuang, D. & Chern, Y. 2018. GSK3 β negatively regulates TRAX, a scaffold protein implicated in mental disorders, for NHEJ-mediated DNA repair in neurons. *Molecular psychiatry*, 23 (12), pp. 2375.
- Choi, J.D. & Lee, J. 2013. Interplay between epigenetics and genetics in cancer. *Genomics & informatics*, 11 (4), pp. 164.
- Claußen, M., Koch, R., Jin, Z. & Suter, B. 2006. Functional characterization of Drosophila Translin and TRAX. *Genetics*, 174 (3), pp. 1337-1347.
- Cohen, S., Puget, N., Lin, Y., Clouaire, T., Aguirrebengoa, M., Rocher, V., Pasero, P., Canitrot, Y. & Legube, G. 2018. Senataxin resolves RNA: DNA hybrids forming at DNA double-strand breaks to prevent translocations. *Nature communications*, 9 (1), pp. 533.
- Cornelio, D.A., Sedam, H.N., Ferrarezi, J.A., Sampaio, N.M. & Argueso, J.L. 2017. Both R-loop removal and ribonucleotide excision repair activities of RNase H2 contribute substantially to chromosome stability. *DNA repair*, 52 pp. 110-114.
- Cottenet, C. 2017a. Scanned with CamScanner. *Temps Noir*, (20), pp. 4-19.
- Crossley, M.P., Bocek, M. & Cimprich, K.A. 2019. R-Loops as Cellular Regulators and Genomic Threats. *Molecular cell*, 73 (3), pp. 398-411.
- Daley, J.M., Palmbo, P.L., Wu, D. & Wilson, T.E. 2005. Nonhomologous end joining in yeast. *Annu.Rev.Genet.*, 39 pp. 431-451.
- Davis, A.J. & Chen, D.J. 2013a. DNA double strand break repair via non-homologous end-joining. *Translational cancer research*, 2 (3), pp. 130.
- Druker, B.J. 2008. Translation of the Philadelphia chromosome into therapy for CML. *Blood*, 112 (13), pp. 4808-4817.
- Duff, B.J., Macritchie, K.A., Moorhead, T.W., Lawrie, S.M. & Blackwood, D.H. 2013. Human brain imaging studies of DISC1 in schizophrenia, bipolar disorder and depression: a systematic review. *Schizophrenia research*, 147 (1), pp. 1-13.
- Durkin, S.G. & Glover, T.W. 2007. Chromosome fragile sites. *Annu.Rev.Genet.*, 41 pp. 169-192.
- Duzdevich, D., Warner, M.D., Tica, S., Ivica, N.A., Bell, S.P. & Greene, E.C. 2015. The dynamics of eukaryotic replication initiation: origin specificity, licensing, and firing at the single-molecule level. *Molecular cell*, 58 (3), pp. 483-494.
- Egan, E.D., Braun, C.R., Gygi, S.P. & Moazed, D. 2014. Post-transcriptional regulation of meiotic genes by a nuclear RNA silencing complex. *Rna*, 20 (6), pp. 867-881.
- Eliash, E., Litovco, P., Yosef, R.B., Bendalak, K., Ziv, T. & Manor, H. 2014. Identification of proteins that form specific complexes with the highly conserved protein Translin in *Schizosaccharomyces pombe*. *Biochimica et Biophysica Acta (BBA)-Proteins and Proteomics*, 1844 (4), pp. 767-777.
- Erdemir, T., Bilican, B., Cagatay, T., Goding, C.R. & Yavuz, U. 2002. *Saccharomyces cerevisiae* C1D is implicated in both non-homologous DNA end joining and homologous recombination. *Molecular microbiology*, 46 (4), pp. 947-957.

References

- Espejel, S., Franco, S., Rodríguez-Perales, S., Bouffler, S.D., Cigudosa, J.C. & Blasco, M.A. 2002. Mammalian Ku86 mediates chromosomal fusions and apoptosis caused by critically short telomeres. *The EMBO journal*, 21 (9), pp. 2207-2219.
- Essani, K., Glieder, A. & Geier, M. 2015. Combinatorial pathway assembly in yeast. *AIMS Bioengineering*, 2 pp. 423-436.
- Evrin, C., Clarke, P., Zech, J., Lurz, R., Sun, J., Uhle, S., Li, H., Stillman, B. & Speck, C. 2009. A double-hexameric MCM2-7 complex is loaded onto origin DNA during licensing of eukaryotic DNA replication. *Proceedings of the National Academy of Sciences*, 106 (48), pp. 20240-20245.
- Faggioli, F., Vijg, J. & Montagna, C. 2011. Chromosomal aneuploidy in the aging brain. *Mechanisms of ageing and development*, 132 (8-9), pp. 429-436.
- Felipe-Abrio, I., Lafuente-Barquero, J., García-Rubio, M.L. & Aguilera, A. 2015. RNA polymerase II contributes to preventing transcription-mediated replication fork stalls. *The EMBO journal*, 34 (2), pp. 236-250.
- Fell, V.L. & Schild-Poulter, C. 2015. The Ku heterodimer: function in DNA repair and beyond. *Mutation Research/Reviews in Mutation Research*, 763 pp. 15-29.
- Ferguson, L.R., Chen, H., Collins, A.R., Connell, M., Damia, G., Dasgupta, S., Malhotra, M., Meeker, A.K., Amedei, A. & Amin, A. 2015. Genomic instability in human cancer: Molecular insights and opportunities for therapeutic attack and prevention through diet and nutrition. *Seminars in cancer biology*. Elsevier. pp. S5.
- Fragkos, M. & Naim, V. 2017. Rescue from replication stress during mitosis. *Cell Cycle*, 16 (7), pp. 613-633.
- Fu, X., Shah, A. & Baraban, J.M. 2016. Rapid reversal of translational silencing: Emerging role of microRNA degradation pathways in neuronal plasticity. *Neurobiology of learning and memory*, 133 pp. 225-232.
- Fukuda, Y., Ishida, R., Aoki, K., Nakahara, K., Takashi, T., Mochida, K., Suzuki, O., Matsuda, J. & Kasai, M. 2008. Contribution of Translin to hematopoietic regeneration after sublethal ionizing irradiation. *Biological and Pharmaceutical Bulletin*, 31 (2), pp. 207-211.
- Gadaleta, M. & Noguchi, E. 2017a. Regulation of DNA replication through natural impediments in the eukaryotic genome. *Genes*, 8 (3), pp. 98.
- Gajecka, M., Pavlicek, A., Glotzbach, C.D., Ballif, B.C., Jarmuz, M., Jurka, J. & Shaffer, L.G. 2006a. Identification of sequence motifs at the breakpoint junctions in three t (1; 9)(p36. 3; q34) and delineation of mechanisms involved in generating balanced translocations. *Human genetics*, 120 (4), pp. 519-526.
- Geigl, J.B., Obenauf, A.C., Schwarzbraun, T. & Speicher, M.R. 2008. Defining ‘chromosomal instability’. *Trends in Genetics*, 24 (2), pp. 64-69.
- Gelot, C. & Lopez, B. 2015. Replication stress in Mammalian cells and its consequences for mitosis. *Genes*, 6 (2), pp. 267-298.
- Gollin, S.M. 2007. Mechanisms leading to nonrandom, nonhomologous chromosomal translocations in leukemia. *Seminars in cancer biology*. Elsevier. pp. 74.

References

- Gomez-Escobar, N., Almobadel, N., Alzahrani, O., Feichtinger, J., Planells-Palop, V., Alshehri, Z., Thallinger, G.G., Wakeman, J.A. & McFarlane, R.J. 2016. Translin and Trax differentially regulate telomere-associated transcript homeostasis. *Oncotarget*, 7 (23), pp. 33809.
- Gomez-Escobar, N., Almobadel, N., Alzahrani, O., Feichtinger, J., Planells-Palop, V., Alshehri, Z., Thallinger, G. G., Wakeman, J. A. and McFarlane, R. J. (2016) ‘Translin and Trax differentially regulate telomere-associated transcript homeostasis’, *Oncotarget*, 7(23), pp. 33809–33820. doi: 10.18632/oncotarget.9278.
- Gómez-González, B. & Aguilera, A. 2019. Transcription-mediated replication hindrance: a major driver of genome instability. *Genes & development*, .
- Gordon, D.J., Resio, B. & Pellman, D. 2012a. Causes and consequences of aneuploidy in cancer. *Nature Reviews Genetics*, 13 (3), pp. 189.
- Gou, K., Liu, J., Feng, X., Li, H., Yuan, Y. and Xing, C. (2018) ‘Expression of Minichromosome Maintenance Proteins (MCM) and Cancer Prognosis: A meta-analysis’, *Journal of Cancer*, 9(8), pp. 1518–1526. doi: 10.7150/jca.22691.
- Grierson, P.M., Lillard, K., Behbehani, G.K., Combs, K.A., Bhattacharyya, S., Acharya, S. & Groden, J. 2011. BLM helicase facilitates RNA polymerase I-mediated ribosomal RNA transcription. *Human molecular genetics*, 21 (5), pp. 1172-1183.
- Gupta, A., Pillai, V. S. and Chittela, R. K. (2019) ‘Role of amino acid residues important for nucleic acid binding in human Translin’, *The International Journal of Biochemistry & Cell Biology*, 115, p. 105593. doi: 10.1016/j.biocel.2019.105593.
- Gupta, A., Pillai, V.S. & Chittela, R.K. 2019. Translin: A multifunctional protein involved in nucleic acid metabolism. *Journal of Biosciences*, 44 (6), pp. 139.
- Gupta, G.D. & Kumar, V. 2012. Identification of nucleic acid binding sites on translin-associated factor X (TRAX) protein. *PloS one*, 7 (3), pp. e33035.
- Gurtner, A., Falcone, E., Garibaldi, F. & Piaggio, G. 2016. Dysregulation of microRNA biogenesis in cancer: the impact of mutant p53 on Drosha complex activity. *Journal of Experimental & Clinical Cancer Research*, 35 (1), pp. 45.
- Hamperl, S. & Cimprich, K.A. 2016. Conflict Resolution in the Genome: How Transcription and Replication Make It Work. *Cell*, 167 (6), pp. 1455-1467.
- Hamperl, S., Bocek, M.J., Saldivar, J.C., Swigut, T. & Cimprich, K.A. 2017a. Transcription-replication conflict orientation modulates R-loop levels and activates distinct DNA damage responses. *Cell*, 170 (4), pp. 774-786. e19.
- Han, J., Gu, W. & Hecht, N.B. 1995. Testis-brain RNA-binding protein, a testicular translational regulatory RNA-binding protein, is present in the brain and binds to the 3' untranslated regions of transported brain mRNAs. *Biology of reproduction*, 53 (3), pp. 707-717.
- Hanahan, D. & Weinberg, R.A. 2011a. Hallmarks of cancer: the next generation. *Cell*, 144 (5), pp. 646-674.
- Harewood, L. & Fraser, P. 2014. The impact of chromosomal rearrangements on regulation of gene expression. *Human molecular genetics*, 23 (R1), pp. R76-R82.

References

- HASEGAWA, T., Hengyi, X., HAMAJIMA, F. & ISOBE, K. 2000. Interaction between DNA-damage protein GADD34 and a new member of the Hsp40 family of heat shock proteins that is induced by a DNA-damaging reagent. *Biochemical Journal*, 352 (3), pp. 795-800.
- Hastings, P.J., Lupski, J.R., Rosenberg, S.M. & Ira, G. 2009. Mechanisms of change in gene copy number. *Nature Reviews Genetics*, 10 (8), pp. 551.
- Hata, A. & Kashima, R. 2016. Dysregulation of microRNA biogenesis machinery in cancer. *Critical reviews in biochemistry and molecular biology*, 51 (3), pp. 121-134.
- He, Q., Au, B., Kulkarni, M., Shen, Y., Lim, K.J., Maimaiti, J., Wong, C.K., Luijten, M.N., Chong, H.C. & Lim, E.H. 2018. Chromosomal instability-induced senescence potentiates cell non-autonomous tumourigenic effects. *Oncogenesis*, 7 (8), pp. 62.
- Heyer, W., Ehmsen, K.T. & Liu, J. 2010a. Regulation of homologous recombination in eukaryotes. *Annual Review of Genetics*, 44 pp. 113-139.
- Hiller, B., Hoppe, A., Haase, C., Hiller, C., Schubert, N., Müller, W., Reijns, M. A. M., Jackson, A. P., Kunkel, T. A., Wenzel, J., Behrendt, R. and Roers, A. (2018) 'Ribonucleotide Excision Repair Is Essential to Prevent Squamous Cell Carcinoma of the Skin', *Cancer Research*, 78(20), pp. 5917–5926. doi: 10.1158/0008-5472.CAN-18-1099.
- Holoch, D. & Moazed, D. 2015. RNA-mediated epigenetic regulation of gene expression. *Nature Reviews Genetics*, 16 (2), pp. 71.
- Hosaka, T., Kanoe, H., Nakayama, T., Murakami, H., Yamamoto, H., Nakamata, T., Tsuboyama, T., Oka, M., Kasai, M. & Sasaki, M.S. 2000. Translin binds to the sequences adjacent to the breakpoints of the TLS and CHOP genes in liposarcomas with translocation t (12; 16). *Oncogene*, 19 (50), pp. 5821.
- Ishida, R., Okado, H., Sato, H., Shionoiri, C., Aoki, K. & Kasai, M. 2002. A role for the octameric ring protein, Translin, in mitotic cell division. *FEBS letters*, 525 (1-3), pp. 105-110.
- Jacob, E., Pucshansky, L., Zeruya, E., Baran, N. & Manor, H. 2004. The human protein translin specifically binds single-stranded microsatellite repeats, d (GT) n, and G-strand telomeric repeats, d (TTAGGG) n: a study of the binding parameters. *Journal of Molecular Biology*, 344 (4), pp. 939-950.
- Jaendling, A. & McFarlane, R.J. 2010. Biological roles of translin and translin-associated factor-X: RNA metabolism comes to the fore. *Biochemical Journal*, 429 (2), pp. 225-234.
- Jaendling, A., Ramayah, S., Pryce, D.W. & McFarlane, R.J. 2008a. Functional characterisation of the *Schizosaccharomyces pombe* homologue of the leukaemia-associated translocation breakpoint binding protein translin and its binding partner, TRAX. *Biochimica et Biophysica Acta (BBA)-Molecular Cell Research*, 1783 (2), pp. 203-213.
- Janssen, A., van der Burg, M., Szuhai, K., Kops, G.J. & Medema, R.H. 2011. Chromosome segregation errors as a cause of DNA damage and structural chromosome aberrations. *Science*, 333 (6051), pp. 1895-1898.
- Jeggo, P.A., Pearl, L.H. & Carr, A.M. 2016. DNA repair, genome stability and cancer: a historical perspective. *Nature Reviews Cancer*, 16 (1), pp. 35.
- Kalantari, R., Chiang, C. & Corey, D.R. 2015a. Regulation of mammalian transcription and splicing by nuclear RNAi. *Nucleic acids research*, 44 (2), pp. 524-537.

References

- Kang, S., Kang, M., Ryu, E. & Myung, K. 2018. Eukaryotic DNA replication: Orchestrated action of multi-subunit protein complexes. *Mutation Research/Fundamental and Molecular Mechanisms of Mutagenesis*, 809 pp. 58-69.
- Kang, Z., Liu, Y., Xu, L., Long, Z., Huang, D., Yang, Y., Liu, B., Feng, J., Pan, Y. & Yan, J. 2016. The Philadelphia chromosome in leukemogenesis. *Chinese journal of cancer*, 35 (1), pp. 48.
- Kanoe, H., Nakayama, T., Hosaka, T., Murakami, H., Yamamoto, H., Nakashima, Y., Tsuboyama, T., Nakamura, T., Ron, D. & Sasaki, M.S. 1999. Characteristics of genomic breakpoints in TLS-CHOP translocations in liposarcomas suggest the involvement of Translin and topoisomerase II in the process of translocation. *Oncogene*, 18 (3), pp. 721.
- Kasai, M., Ishida, R., Nakahara, K., Okumura, K. & Aoki, K. 2018. Mesenchymal cell differentiation and diseases: involvement of translin/TRAX complexes and associated proteins. *Annals of the New York Academy of Sciences*, 1421 (1), pp. 37-45.
- Kasai, M., Matsuzaki, T., Katayanagi, K., Omori, A., Maziarz, R.T., Strominger, J.L., Aoki, K. & Suzuki, K. 1997a. The translin ring specifically recognizes DNA ends at recombination hot spots in the human genome. *Journal of Biological Chemistry*, 272 (17), pp. 11402-11407.
- Kassavetis, G.A. & Kadonaga, J.T. 2014. The annealing helicase and branch migration activities of Drosophila HARP. *PLoS One*, 9 (5), pp. e98173.
- Katto, J. & Mahlknecht, U. 2011. Epigenetic regulation of cellular adhesion in cancer. *Carcinogenesis*, 32 (10), pp. 1414-1418.
- Keeney, S. & Neale, M.J. 2006. No title. *Initiation of meiotic recombination by formation of DNA double-strand breaks: mechanism and regulation*, .
- Khalil, H.S., Tummala, H. & Zhelev, N. 2012. ATM in focus: A damage sensor and cancer target. *Biodiscovery*, 5 pp. e8936.
- Knijnenburg, T.A., Wang, L., Zimmermann, M.T., Chambwe, N., Gao, G.F., Cherniack, A.D., Fan, H., Shen, H., Way, G.P. & Greene, C.S. 2018. Genomic and molecular landscape of DNA damage repair deficiency across The Cancer Genome Atlas. *Cell reports*, 23 (1), pp. 239-254. e6.
- Kojima, K., Baba, M., Tsukiashi, M., Nishimura, T. & Yasukawa, K. 2018. RNA/DNA structures recognized by RNase H2. *Briefings in functional genomics*, .
- Kolesar, P., Sarangi, P., Altmannova, V., Zhao, X. & Krejci, L. 2012. Dual roles of the SUMO-interacting motif in the regulation of Srs2 sumoylation. *Nucleic acids research*, 40 (16), pp. 7831-7843.
- Kramara, J., Osia, B. & Malkova, A. 2018. Break-induced replication: the where, the why, and the how. *Trends in Genetics*, 34 (7), pp. 518-531.
- Kumar, M.S., Pester, R.E., Chen, C.Y., Lane, K., Chin, C., Lu, J., Kirsch, D.G., Golub, T.R. & Jacks, T. 2009. Dicer1 functions as a haploinsufficient tumor suppressor. *Genes & development*, 23 (23), pp. 2700-2704.
- Labib, K. & Hodgson, B. 2007. Replication fork barriers: pausing for a break or stalling for time? *EMBO reports*, 8 (4), pp. 346-353.

References

- Laufman, O., Yosef, R. B., Adir, N. and Manor, H. (2005) 'Cloning and characterization of the *Schizosaccharomyces pombe* homologs of the human protein Translin and the Translin-associated protein TRAX', *Nucleic Acids Research*, 33(13), pp. 4128–4139. doi: 10.1093/nar/gki727.
- Laufman, O., Yosef, R.B., Adir, N. & Manor, H. 2005. Cloning and characterization of the *Schizosaccharomyces pombe* homologs of the human protein Translin and the Translin-associated protein TRAX. *Nucleic acids research*, 33 (13), pp. 4128-4139.
- Lei, M. 2005. The MCM complex: its role in DNA replication and implications for cancer therapy. *Current cancer drug targets*, 5 (5), pp. 365-380.
- Leman, A. & Noguchi, E. 2013a. The replication fork: understanding the eukaryotic replication machinery and the challenges to genome duplication. *Genes*, 4 (1), pp. 1-32.
- Li, J. & Xu, X. 2016. DNA double-strand break repair: a tale of pathway choices. *Acta biochimica et biophysica Sinica*, 48 (7), pp. 641-646.
- Li, L., Gu, W., Liang, C., Liu, Q., Mello, C.C. & Liu, Y. 2012. The translin–TRAX complex (C3PO) is a ribonuclease in tRNA processing. *Nature structural & molecular biology*, 19 (8), pp. 824.
- Li, X. & Heyer, W. 2008. Homologous recombination in DNA repair and DNA damage tolerance. *Cell research*, 18 (1), pp. 99.
- Li, Z., Wu, Y. & Baraban, J.M. 2008. The Translin/Trax RNA binding complex: clues to function in the nervous system. *Biochimica et Biophysica Acta (BBA)-Gene Regulatory Mechanisms*, 1779 (8), pp. 479-485.
- Lieber, M.R. 2010. The mechanism of double-strand DNA break repair by the nonhomologous DNA end-joining pathway. *Annual Review of Biochemistry*, 79 pp. 181-211.
- Lieber, M.R. 2016. Mechanisms of human lymphoid chromosomal translocations. *Nature Reviews Cancer*, 16 (6), pp. 387.
- Lin, Y.L. & Pasero, P. 2012. Interference between DNA replication and transcription as a cause of genomic instability. *Current Genomics*, 13 (1), pp. 65-73.
- Liu, P., Gan, W., Guo, C., Xie, A., Gao, D., Guo, J., Zhang, J., Willis, N., Su, A. & Asara, J.M. 2015. Akt-mediated phosphorylation of XLF impairs non-homologous end-joining DNA repair. *Molecular cell*, 57 (4), pp. 648-661.
- Liu, Y., Ye, X., Jiang, F., Liang, C., Chen, D., Peng, J., Kinch, L.N., Grishin, N.V. & Liu, Q. 2009. C3PO, an endoribonuclease that promotes RNAi by facilitating RISC activation. *Science*, 325 (5941), pp. 750-753.
- Llorente, B., Smith, C.E. & Symington, L.S. 2008. Break-induced replication: what is it and what is it for? *Cell cycle*, 7 (7), pp. 859-864.
- Lluis, M., Hoe, W., Schleit, J. & Robertus, J. 2010. Analysis of nucleic acid binding by a recombinant translin–trax complex. *Biochemical and biophysical research communications*, 396 (3), pp. 709-713.
- Lockhart, A., Pires, V.B., Bento, F., Kellner, V., Luke-Glaser, S. & Luke, B. 2019. RNase H1 and H2 are differentially regulated to eliminate RNA-DNA hybrids. *bioRxiv*, pp. 593152.

References

- Lord, C.J. & Ashworth, A. 2012. The DNA damage response and cancer therapy. *Nature*, 481 (7381), pp. 287.
- Lord, C.J. & Ashworth, A. 2016. BRCAness revisited. *Nature Reviews Cancer*, 16 (2), pp. 110.
- Lujan, S.A., Williams, J.S. & Kunkel, T.A. 2016. DNA polymerases divide the labor of genome replication. *Trends in cell biology*, 26 (9), pp. 640-654.
- Ly, P., Brunner, S.F., Shoshani, O., Kim, D.H., Lan, W., Pyntikova, T., Flanagan, A.M., Behjati, S., Page, D.C. & Campbell, P.J. 2019. Chromosome segregation errors generate a diverse spectrum of simple and complex genomic rearrangements. *Nature genetics*, pp. 1.
- Malkova, A. & Ira, G. 2013. Break-induced replication: functions and molecular mechanism. *Current opinion in genetics & development*, 23 (3), pp. 271-279.
- Martienssen, R.A., Zaratiegui, M. & Goto, D.B. 2005. RNA interference and heterochromatin in the fission yeast *Schizosaccharomyces pombe*. *TRENDS in Genetics*, 21 (8), pp. 450-456.
- Martinelli, G., Terragna, C., Amabile, M., Montefusco, V., Testoni, N., Ottaviani, E., De Vivo, A., Mianulli, A., Saglio, G. & Tura, S. 2000. Alu and transposon recognition site sequences flanking translocation sites in a novel type of chimeric bcr-abl transcript suggest a possible general mechanism for bcr-abl breakpoints. *Haematologica*, 85 (1), pp. 40-46.
- Matsui, M. & Corey, D.R. 2017. Non-coding RNAs as drug targets. *Nature reviews Drug discovery*, 16 (3), pp. 167.
- Mazina, O.M., Keskin, H., Hanamshet, K., Storici, F. & Mazin, A.V. 2017. Rad52 inverse strand exchange drives RNA-templated DNA double-strand break repair. *Molecular cell*, 67 (1), pp. 19-29. e3.
- McCaffrey, A.P., Meuse, L., Pham, T.T., Conklin, D.S., Hannon, G.J. & Kay, M.A. 2002. Gene expression: RNA interference in adult mice. *Nature*, 418 (6893), pp. 38.
- McFarlane, R. J. and Wakeman, J. A. (2020) 'Translin-Trax: Considerations for Oncological Therapeutic Targeting', *Trends in Cancer*, 6(6), pp. 450–453. doi: 10.1016/j.trecan.2020.02.014.
- McFarlane, R.J., Al-Zeer, K. & Dalgaard, J.Z. 2011. Eukaryote DNA replication and recombination: an intimate association. In: *AnonDNA Replication-Current Advances*. IntechOpen.
- Medeiros, M. H. G. and Medeiros, M. H. G. (2019) 'DNA Damage by Endogenous and Exogenous Aldehydes', *Journal of the Brazilian Chemical Society*. Brazilian Chemical Society, 30(10), pp. 2000–2009. doi: 10.21577/0103-5053.20190056.
- Mehta, A. & Haber, J.E. 2014. Sources of DNA double-strand breaks and models of recombinational DNA repair. *Cold Spring Harbor perspectives in biology*, 6 (9), pp. a016428.
- Mei, F., Kehui, X. & Wenming, X. 2016. Research advances of Dicer in regulating reproductive function. *Hereditas (Beijing)*, 38 (7), pp. 612-622.
- Meng, Z. & Lu, M. 2017. RNA Interference-induced innate immunity, off-target effect, or immune adjuvant? *Frontiers in immunology*, 8 pp. 331.

References

- Merrikh, H., Zhang, Y., Grossman, A.D. & Wang, J.D. 2012. Replication–transcription conflicts in bacteria. *Nature Reviews Microbiology*, 10 (7), pp. 449.
- Minocherhomji, S., Ying, S., Bjerregaard, V.A., Bursomanno, S., Aleliunaite, A., Wu, W., Mankouri, H.W., Shen, H., Liu, Y. & Hickson, I.D. 2015. Replication stress activates DNA repair synthesis in mitosis. *Nature*, 528 (7581), pp. 286.
- Mizuno, K., Miyabe, I., Schalbetter, S.A., Carr, A.M. & Murray, J.M. 2013. Recombination-restarted replication makes inverted chromosome fusions at inverted repeats. *Nature*, 493 (7431), pp. 246-249.
- Mladenov, E. & Iliakis, G. 2011a. Induction and repair of DNA double strand breaks: the increasing spectrum of non-homologous end joining pathways. *Mutation Research/Fundamental and Molecular Mechanisms of Mutagenesis*, 711 (1-2), pp. 61-72.
- Mladenov, E., Magin, S., Soni, A. & Iliakis, G. 2016. DNA double-strand-break repair in higher eukaryotes and its role in genomic instability and cancer: Cell cycle and proliferation-dependent regulation. *Seminars in cancer biology*, 37-38 pp. 51-64.
- Mladenov, E., Magin, S., Soni, A. & Iliakis, G. 2016. DNA double-strand-break repair in higher eukaryotes and its role in genomic instability and cancer: Cell cycle and proliferation-dependent regulation. *Seminars in cancer biology*. Elsevier. pp. 51.
- Moazed, D. 2009a. Small RNAs in transcriptional gene silencing and genome defence. *Nature*, 457 (7228), pp. 413.
- Najafi, M., Cheki, M., Rezapoor, S., Geraily, G., Motevaseli, E., Carnovale, C., Clementi, E. & Shirazi, A. 2018. Metformin: Prevention of genomic instability and cancer: A review. *Mutation Research/Genetic Toxicology and Environmental Mutagenesis*, 827 pp. 1-8.
- Nambiar, M. & Raghavan, S.C. 2011. How does DNA break during chromosomal translocations? *Nucleic acids research*, 39 (14), pp. 5813-5825.
- Nicolás, F. & Ruiz-Vázquez, R. 2013. Functional diversity of RNAi-associated sRNAs in fungi. *International journal of molecular sciences*, 14 (8), pp. 15348-15360.
- Nussenzweig, A. & Nussenzweig, M.C. 2010. Origin of chromosomal translocations in lymphoid cancer. *Cell*, 141 (1), pp. 27-38.
- Oestergaard, V.H. & Lisby, M. 2017. Transcription-replication conflicts at chromosomal fragile sites—consequences in M phase and beyond. *Chromosoma*, 126 (2), pp. 213-222.
- Ohle, C., Tesorero, R., Schermann, G., Dobrev, N., Sinning, I. & Fischer, T. 2016. Transient RNA-DNA hybrids are required for efficient double-strand break repair. *Cell*, 167 (4), pp. 1001-1013. e7.
- Paeschke, K., Capra, J.A. & Zakian, V.A. 2011. DNA replication through G-quadruplex motifs is promoted by the *Saccharomyces cerevisiae* Pif1 DNA helicase. *Cell*, 145 (5), pp. 678-691.
- Pannunzio, N.R., Watanabe, G. & Lieber, M.R. 2018. Nonhomologous DNA end-joining for repair of DNA double-strand breaks. *Journal of Biological Chemistry*, 293 (27), pp. 10512-10523.
- Parizotto, E.A., Lowe, E.D. & Parker, J.S. 2013. Structural basis for duplex RNA recognition and cleavage by *Archaeoglobus fulgidus* C3PO. *Nature structural & molecular biology*, 20 (3), pp. 380.

References

- Park, A.J., Havekes, R., Fu, X., Hansen, R., Tudor, J.C., Peixoto, L., Li, Z., Wu, Y., Poplawski, S.G. & Baraban, J.M. 2017. Learning induces the translin/trax RNase complex to express activin receptors for persistent memory. *Elife*, 6 pp. e27872.
- Parker, M.W., Botchan, M.R. & Berger, J.M. 2017a. Mechanisms and regulation of DNA replication initiation in eukaryotes. *Critical reviews in biochemistry and molecular biology*, 52 (2), pp. 107-144.
- Parker, M.W., Botchan, M.R. & Berger, J.M. 2017b. Mechanisms and regulation of DNA replication initiation in eukaryotes. *Critical reviews in biochemistry and molecular biology*, 52 (2), pp. 107-144.
- Patil, V.S., Zhou, R. & Rana, T.M. 2014. Gene regulation by non-coding RNAs. *Critical reviews in biochemistry and molecular biology*, 49 (1), pp. 16-32.
- Patterson, A.D., Hollander, M.C., Miller, G.F. & Fornace, A.J. 2006. Gadd34 requirement for normal hemoglobin synthesis. *Molecular and cellular biology*, 26 (5), pp. 1644-1653.
- Pellegrini, L. & Costa, A. 2016. New insights into the mechanism of DNA duplication by the eukaryotic replisome. *Trends in biochemical sciences*, 41 (10), pp. 859-871.
- Peng, G. & Lin, S. 2011. Exploiting the homologous recombination DNA repair network for targeted cancer therapy. *World journal of clinical oncology*, 2 (2), pp. 73.
- Petermann, E., Orta, M. L., Issaeva, N., Schultz, N. and Helleday, T. (2010) 'Hydroxyurea-Stalled Replication Forks Become Progressively Inactivated and Require Two Different RAD51-Mediated Pathways for Restart and Repair', *Molecular Cell*, 37(4), pp. 492–502. doi: 10.1016/j.molcel.2010.01.021.
- Petermann, E., Orta, M.L., Issaeva, N., Schultz, N. & Helleday, T. 2010. Hydroxyurea-stalled replication forks become progressively inactivated and require two different RAD51-mediated pathways for restart and repair. *Molecular cell*, 37 (4), pp. 492-502.
- Plosky, B.S. 2016. The good and bad of RNA: DNA hybrids in double-strand break repair. *Molecular cell*, 64 (4), pp. 643-644.
- Potenski, C.J. & Klein, H.L. 2014. How the misincorporation of ribonucleotides into genomic DNA can be both harmful and helpful to cells. *Nucleic acids research*, 42 (16), pp. 10226-10234.
- Prado, F. & Aguilera, A. 2005. Impairment of replication fork progression mediates RNA polII transcription-associated recombination. *The EMBO journal*, 24 (6), pp. 1267-1276.
- Pryce, D.W., Ramayah, S., Jaendling, A. & McFarlane, R.J. 2009. Recombination at DNA replication fork barriers is not universal and is differentially regulated by Swi1. *Proceedings of the National Academy of Sciences*, 106 (12), pp. 4770-4775.
- Raghavan, S.C. & Lieber, M.R. 2006. DNA structures at chromosomal translocation sites. *Bioessays*, 28 (5), pp. 480-494.
- Reijns, M.A., Rabe, B., Rigby, R.E., Mill, P., Astell, K.R., Lettice, L.A., Boyle, S., Leitch, A., Keighren, M. & Kilanowski, F. 2012. Enzymatic removal of ribonucleotides from DNA is essential for mammalian genome integrity and development. *Cell*, 149 (5), pp. 1008-1022.

References

- Remus, D. & Diffley, J.F. 2009. Eukaryotic DNA replication control: lock and load, then fire. *Current opinion in cell biology*, 21 (6), pp. 771-777.
- Ren, J., Castel, S.E. & Martienssen, R.A. 2015. Dicer in action at replication-transcription collisions. *Molecular & cellular oncology*, 2 (3), pp. e991224.
- Reyes-Turcu, F.E. & Grewal, S.I. 2012. Different means, same end—heterochromatin formation by RNAi and RNAi-independent RNA processing factors in fission yeast. *Current opinion in genetics & development*, 22 (2), pp. 156-163.
- Roukos, V. & Misteli, T. 2014. The biogenesis of chromosome translocations. *Nature cell biology*, 16 (4), pp. 293.
- Ruff, P., Donnianni, R.A., Glancy, E., Oh, J. & Symington, L.S. 2016. RPA stabilization of single-stranded DNA is critical for break-induced replication. *Cell reports*, 17 (12), pp. 3359-3368.
- Saada, A.A., Lambert, S.A. & Carr, A.M. 2018. Preserving replication fork integrity and competence via the homologous recombination pathway. *DNA repair*, 71 pp. 135-147.
- Sahu, S., Philip, F. & Scarlata, S. 2014. Hydrolysis rates of different small interfering RNAs (siRNAs) by the RNA silencing promoter complex, C3PO, determines their regulation by phospholipase C β . *Journal of Biological Chemistry*, 289 (8), pp. 5134-5144.
- Sakofsky, C.J. & Malkova, A. 2017a. Break induced replication in eukaryotes: mechanisms, functions, and consequences. *Critical reviews in biochemistry and molecular biology*, 52 (4), pp. 395-413.
- Sankar, T. S., Wastuwidyaningtyas, B. D., Dong, Y., Lewis, S. A. and Wang, J. D. (2016) ‘The nature of mutations induced by replication–transcription collisions’, *Nature*. Nature Publishing Group, 535(7610), pp. 178–181. doi: 10.1038/nature18316.
- Santos-Pereira, J.M. & Aguilera, A. 2015a. R loops: new modulators of genome dynamics and function. *Nature Reviews Genetics*, 16 (10), pp. 583.
- Seol, J.-H., Shim, E. Y. and Lee, S. E. (2018) ‘Microhomology-mediated end joining: Good, bad and ugly’, *Mutation Research/Fundamental and Molecular Mechanisms of Mutagenesis*, 809, pp. 81–87. doi: 10.1016/j.mrfmmm.2017.07.002.
- Shah, A.P., Johnson, M.D., Fu, X., Boersma, G.J., Shah, M., Wolfgang, M.J., Tamashiro, K.L. & Baraban, J.M. 2019a. Deletion of translin (Tsn) induces robust adiposity and hepatic steatosis without impairing glucose tolerance. *International journal of obesity*, pp. 1.
- Shah, A.P., Johnson, M.D., Fu, X., Boersma, G.J., Shah, M., Wolfgang, M.J., Tamashiro, K.L. & Baraban, J.M. 2019b. Deletion of translin (Tsn) induces robust adiposity and hepatic steatosis without impairing glucose tolerance. *International journal of obesity*, pp. 1.
- Singh, A. and Xu, Y.-J. (2016) ‘The Cell Killing Mechanisms of Hydroxyurea’, *Genes*. Multidisciplinary Digital Publishing Institute, 7(11), p. 99. doi: 10.3390/genes7110099.
- Sirbu, B.M. & Cortez, D. 2013a. DNA damage response: three levels of DNA repair regulation. *Cold Spring Harbor perspectives in biology*, 5 (8), pp. a012724.

References

- Sishc, B. & Davis, A. 2017a. The role of the core non-homologous end joining factors in carcinogenesis and cancer. *Cancers*, 9 (7), pp. 81.
- So, A., Le Guen, T., Lopez, B.S. & Guirouilh-Barbat, J. 2017a. Genomic rearrangements induced by unscheduled DNA double strand breaks in somatic mammalian cells. *The FEBS journal*, 284 (15), pp. 2324-2344.
- Son, H., Park, A.R., Lim, J.Y., Shin, C. & Lee, Y. 2017. Genome-wide exonic small interference RNA-mediated gene silencing regulates sexual reproduction in the homothallic fungus *Fusarium graminearum*. *PLoS genetics*, 13 (2), pp. e1006595.
- Song, M. & Rossi, J.J. 2017. Molecular mechanisms of Dicer: endonuclease and enzymatic activity. *Biochemical Journal*, 474 (10), pp. 1603-1618.
- Sotiriou, S.K., Kamileri, I., Lugli, N., Evangelou, K., Da-Ré, C., Huber, F., Padayachy, L., Tardy, S., Nicati, N.L. & Barriot, S. 2016. Mammalian RAD52 functions in break-induced replication repair of collapsed DNA replication forks. *Molecular cell*, 64 (6), pp. 1127-1134.
- Soultanas, P. 2011. The replication-transcription conflict. *Transcription*, 2 (3), pp. 140-144.
- Sparks, J.L., Chon, H., Cerritelli, S.M., Kunkel, T.A., Johansson, E., Crouch, R.J. & Burgers, P.M. 2012a. RNase H2-initiated ribonucleotide excision repair. *Molecular cell*, 47 (6), pp. 980-986.
- Stahl, B.A., Slocumb, M.E., Chaitin, H., DiAngelo, J.R. & Keene, A.C. 2017. Sleep-dependent modulation of metabolic rate in *Drosophila*. *Sleep*, 40 (8), .
- Stein, J.M., Bergman, W., Fang, Y., Davison, L., Brensinger, C., Robinson, M.B., Hecht, N.B. & Abel, T. 2006. Behavioral and neurochemical alterations in mice lacking the RNA-binding protein translin. *Journal of Neuroscience*, 26 (8), pp. 2184-2196.
- Stillman, B. 2008. DNA polymerases at the replication fork in eukaryotes. *Molecular cell*, 30 (3), pp. 259-260.
- Stokowa-Sołtys, K., Dzyhovskyi, V., Wieczorek, R. and Jeżowska-Bojczuk, M. (2019) 'Phleomycin complex – Coordination mode and in vitro cleavage of DNA', *Journal of Inorganic Biochemistry*, 195, pp. 71–82. doi: 10.1016/j.jinorgbio.2019.03.010.
- Sugasawa, K. (2016) 'Molecular mechanisms of DNA damage recognition for mammalian nucleotide excision repair', *DNA Repair*. (Cutting-edge Perspectives in Genomic Maintenance III), 44, pp. 110–117. doi: 10.1016/j.dnarep.2016.05.015.
- Sugitani, N., Sivley, R. M., Perry, K. E., Capra, J. A. and Chazin, W. J. (2016) 'XPA: A key scaffold for human nucleotide excision repair', *DNA Repair*. (Cutting-edge Perspectives in Genomic Maintenance III), 44, pp. 123–135. doi: 10.1016/j.dnarep.2016.05.018.
- Sugiyama, T., Kantake, N., Wu, Y. & Kowalczykowski, S.C. 2006. Rad52-mediated DNA annealing after Rad51-mediated DNA strand exchange promotes second ssDNA capture. *The EMBO journal*, 25 (23), pp. 5539-5548.
- Suseendranathan, K., Sengupta, K., Rikhy, R., D'Souza, J.S., Kokkanti, M., Kulkarni, M.G., Kamdar, R., Chagede, R., Sinha, R. & Subramanian, L. 2007. Expression pattern of *Drosophila* translin and behavioral analyses of the mutant. *European journal of cell biology*, 86 (3), pp. 173-186.

References

- Suwaki, N., Klare, K. & Tarsounas, M. 2011. RAD51 paralogs: roles in DNA damage signalling, recombinational repair and tumorigenesis. *Seminars in cell & developmental biology*. Elsevier. pp. 898.
- Svobodova, E., Kubikova, J. & Svoboda, P. 2016. Production of small RNAs by mammalian Dicer. *Pflügers Archiv-European Journal of Physiology*, 468 (6), pp. 1089-1102.
- Swarts, D.C., Makarova, K., Wang, Y., Nakanishi, K., Ketting, R.F., Koonin, E.V., Patel, D.J. & Van Der Oost, J. 2014. The evolutionary journey of Argonaute proteins. *Nature structural & molecular biology*, 21 (9), pp. 743.
- Tabarestani, S. & Movafagh, A. 2016. New developments in chronic myeloid leukemia: Implications for therapy. *Iranian journal of cancer prevention*, 9 (1), .
- Tadeo, X., Wang, J., Kallgren, S.P., Liu, J., Reddy, B.D., Qiao, F. & Jia, S. 2013. Elimination of shelterin components bypasses RNAi for pericentric heterochromatin assembly. *Genes & development*, 27 (22), pp. 2489-2499.
- Takagi, M. 2017a. DNA damage response and hematological malignancy. *International journal of hematology*, 106 (3), pp. 345-356.
- Takeuchi, Y., Horiuchi, T. & Kobayashi, T. 2003. Transcription-dependent recombination and the role of fork collision in yeast rDNA. *Genes & development*, 17 (12), pp. 1497-1506.
- Talens, F., Jalving, M., Gietema, J.A. & Van Vugt, M.A. 2017. Therapeutic targeting and patient selection for cancers with homologous recombination defects. *Expert opinion on drug discovery*, 12 (6), pp. 565-581.
- Tashiro, S., Asano, T., Kanoh, J. & Ishikawa, F. 2013. Transcription-induced chromatin association of RNA surveillance factors mediates facultative heterochromatin formation in fission yeast. *Genes to Cells*, 18 (4), pp. 327-339.
- Tatiparti, K., Sau, S., Kashaw, S. & Iyer, A. 2017. siRNA delivery strategies: a comprehensive review of recent developments. *Nanomaterials*, 7 (4), pp. 77.
- Tian, H., Gao, Z., Li, H., Zhang, B., Wang, G., Zhang, Q., Pei, D. & Zheng, J. 2015. DNA damage response—a double-edged sword in cancer prevention and cancer therapy. *Cancer letters*, 358 (1), pp. 8-16.
- Tian, Y., Simanshu, D.K., Ascano, M., Diaz-Avalos, R., Park, A.Y., Juranek, S.A., Rice, W.J., Yin, Q., Robinson, C.V. & Tuschl, T. 2011. Multimeric assembly and biochemical characterization of the Trax–translin endonuclease complex. *Nature structural & molecular biology*, 18 (6), pp. 658.
- Tubbs, A. & Nussenzweig, A. 2017a. Endogenous DNA damage as a source of genomic instability in cancer. *Cell*, 168 (4), pp. 644-656.
- Tubbs, A. & Nussenzweig, A. 2017b. Endogenous DNA damage as a source of genomic instability in cancer. *Cell*, 168 (4), pp. 644-656.
- Tubbs, A. and Nussenzweig, A. (2017) ‘Endogenous DNA Damage as a Source of Genomic Instability in Cancer’, *Cell*, 168(4), pp. 644–656. doi: 10.1016/j.cell.2017.01.002.
- Tucker, J.D. 2010. Chromosome translocations and assessing human exposure to adverse environmental agents. *Environmental and molecular mutagenesis*, 51 (8-9), pp. 815-824.

References

- Uckelmann, M. & Sixma, T.K. 2017. Histone ubiquitination in the DNA damage response. *DNA repair*, 56 pp. 92-101.
- Vaisman, A., McDonald, J.P., Huston, D., Kuban, W., Liu, L., Van Houten, B. & Woodgate, R. 2013. Removal of misincorporated ribonucleotides from prokaryotic genomes: an unexpected role for nucleotide excision repair. *PLoS genetics*, 9 (11), pp. e1003878.
- Valencia-Sanchez, M.A., Liu, J., Hannon, G.J. & Parker, R. 2006. Control of translation and mRNA degradation by miRNAs and siRNAs. *Genes & development*, 20 (5), pp. 515-524.
- VanLoock, M.S., Yu, X., Kasai, M. & Egelman, E.H. 2001. Electron microscopic studies of the translin octameric ring. *Journal of structural biology*, 135 (1), pp. 58-66.
- Vijg, J. & Montagna, C. 2017a. Genome instability and aging: Cause or effect? *Translational Medicine of Aging*, 1 pp. 5-11.
- Visser, R., Shimokawa, O., Harada, N., Kinoshita, A., Ohta, T., Niikawa, N. & Matsumoto, N. 2005. Identification of a 3.0-kb major recombination hotspot in patients with Sotos syndrome who carry a common 1.9-Mb microdeletion. *The American Journal of Human Genetics*, 76 (1), pp. 52-67.
- Voglova, K., Bezakova, J. & Herichova, I. 2016. Progress in micro RNA focused research in endocrinology. *Endocrine regulations*, 50 (2), pp. 83-105.
- Volpe, T. & Martienssen, R.A. 2011. RNA interference and heterochromatin assembly. *Cold Spring Harbor perspectives in biology*, 3 (9), pp. a003731.
- Wang, J.Y., Chen, S.Y., Sun, C.N., Chien, T. & Chern, Y. 2016a. A central role of TRAX in the ATM-mediated DNA repair. *Oncogene*, 35 (13), pp. 1657.
- Wei, Y., Sun, M., Nilsson, G., Dwight, T., Xie, Y., Wang, J., Hou, Y., Larsson, O., Larsson, C. & Zhu, X. 2003. Characteristic sequence motifs located at the genomic breakpoints of the translocation t (X; 18) in synovial sarcomas. *Oncogene*, 22 (14), pp. 2215.
- Weng, Y., Chien, T., Kuan, I.I. & Chern, Y. 2018. The TRAX, DISC1, and GSK3 complex in mental disorders and therapeutic interventions. *Journal of Biomedical Science*, 25 (1), pp. 71.
- Williams, J.S., Lujan, S.A. & Kunkel, T.A. 2016a. Processing ribonucleotides incorporated during eukaryotic DNA replication. *Nature reviews Molecular cell biology*, 17 (6), pp. 350.
- Woolcock, K.J. & Bühler, M. 2013. Nuclear organisation and RNAi in fission yeast. *Current opinion in cell biology*, 25 (3), pp. 372-377.
- Wu, X., Gu, W., Meng, X. & Hecht, N.B. 1997. The RNA-binding protein, TB-RBP, is the mouse homologue of translin, a recombination protein associated with chromosomal translocations. *Proceedings of the National Academy of Sciences*, 94 (11), pp. 5640-5645.
- Yang, K., Guo, R. & Xu, D. 2016a. Non-homologous end joining: advances and frontiers. *Acta biochimica et biophysica Sinica*, 48 (7), pp. 632-640.
- Yang, S. & Hecht, N.B. 2004. Translin associated protein X is essential for cellular proliferation. *FEBS letters*, 576 (1-2), pp. 221-225.
- Yang, S., Cho, Y.S., Chennathukuzhi, V.M., Underkoffler, L.A., Loomes, K. & Hecht, N.B. 2004. Translin-associated factor X is post-transcriptionally regulated by its partner protein TB-RBP,

References

- and both are essential for normal cell proliferation. *Journal of Biological Chemistry*, 279 (13), pp. 12605-12614.
- Yao, Y. & Dai, W. 2014. Genomic instability and cancer. *Journal of carcinogenesis & mutagenesis*, 5.
- Ye, X., Huang, N., Liu, Y., Paroo, Z., Huerta, C., Li, P., Chen, S., Liu, Q. & Zhang, H. 2011. Structure of C3PO and mechanism of human RISC activation. *Nature structural & molecular biology*, 18 (6), pp. 650.
- Yu, Y., Cui, Y., Niedernhofer, L. J. and Wang, Y. (2016) ‘Occurrence, Biological Consequences, and Human Health Relevance of Oxidative Stress-Induced DNA Damage’, *Chemical Research in Toxicology*, 29(12), pp. 2008–2039. doi: 10.1021/acs.chemrestox.6b00265.
- Yu, Z. & Hecht, N.B. 2008. The DNA/RNA-binding protein, translin, binds microRNA122a and increases its in vivo stability. *Journal of andrology*, 29 (5), pp. 572-579.
- Zaboikin, M., Zaboikina, T., Freter, C. & Srinivasakumar, N. 2017. Non-Homologous End Joining and Homology Directed DNA Repair Frequency of Double-Stranded Breaks Introduced by Genome Editing Reagents. *PloS one*, 12 (1), pp. e0169931.
- Zhang, B., Pan, X., Cobb, G.P. & Anderson, T.A. 2007. microRNAs as oncogenes and tumor suppressors. *Developmental biology*, 302 (1), pp. 1-12.
- Zhang, J., Liu, H., Yao, Q., Yu, X., Chen, Y., Cui, R., Wu, B., Zheng, L., Zuo, J. & Huang, Z. 2016. Structural basis for single-stranded RNA recognition and cleavage by C3PO. *Nucleic acids research*, 44 (19), pp. 9494-9504.
- Zhang, Y., Gostissa, M., Hildebrand, D.G., Becker, M.S., Boboila, C., Chiarle, R., Lewis, S. & Alt, F.W. 2010. The role of mechanistic factors in promoting chromosomal translocations found in lymphoid and other cancers. In: *AnonAdvances in immunology*. Elsevier. pp. 93-133.
- Zhao, H., Zhu, M., Limbo, O. & Russell, P. 2018. RNase H eliminates R-loops that disrupt DNA replication but is nonessential for efficient DSB repair. *EMBO reports*, 19 (5), pp. e45335.
- Zhao, X., Wei, C., Li, J., Xing, P., Li, J., Zheng, S. & Chen, X. 2017a. Cell cycle-dependent control of homologous recombination. *Acta biochimica et biophysica Sinica*, 49 (8), pp. 655-668.
- Zheng, J. 2013a. Oncogenic chromosomal translocations and human cancer. *Oncology reports*, 30 (5), pp. 2011-2019.
- Zheng, L. & Shen, B. 2011. Okazaki fragment maturation: nucleases take centre stage. *Journal of molecular cell biology*, 3 (1), pp. 23-30.
- Zocco, M., Marasovic, M., Pisacane, P., Bilokapic, S. & Halic, M. 2016. The Chp1 chromodomain binds the H3K9me tail and the nucleosome core to assemble heterochromatin. *Cell discovery*, 2 pp. 16004.